MECHANICAL STABILITY OF INTERMEDIATE MOISTURE STARCH-GLYCEROL SYSTEMS

By

Javier Enrione, BSc, MSc.

Thesis submitted to the University of Nottingham for the degree of
Doctor of Philosophy

September 2005

Division of Food Sciences
School of Biosciences
University of Nottingham
Sutton Bonington Campus
Loughborough, LE12 5RD
United Kingdom

ABSTRACT

There is conflicting information on the mechanical properties and ageing kinetics of starch-water-glycerol systems. This makes understanding the changes occurring on storage of edible products difficult to predict. The work described in this thesis looks at model systems consisting of thermomechanically extruded plasticized starches (waxy maize, rice and wheat) and commercial products. The objectives of the work were to evaluate how the presence of polyols effects glass transition temperature (Tg), sorption isotherms, diffusion rates and texture parameters and to create models that could be used to predict behaviour.

Very similar results were obtained for the starch samples except that monolayer (m_o) values were higher for the waxy maize starch than for the wheat and rice. The waxy maize also was more brittle at equivalent moisture content when compared to the other two starches.

Glycerol had a major impact on the water absorption. For RHs > 70% more water absorbed up by samples containing glycerol while the opposite occurred at RHs <60%. Monolayer values for GAB and BET confirmed this finding. The behaviour could be predicted if an interaction factor <1 was used in weight fraction models. Tg of the samples was measured by DSC and also by using predictive models, where the ten-Brinke Karas equation was found to give the best predictions. A value that was found to be most beneficial for the prediction of retrogradation was (storage temperature minus Tg). Change in texture was associate with (T-Tg), although the brittle ductile transition occurred 40°C below T-Tg=0. Diffusivity values increased with plasticizer level up to $8*10^{-13}$ m^2/s. There was an apparent fall in values when the samples were above Tg. However, it is suggested that this is due to sample geometry change rather than a change in diffusion mechanism.

The Tg values also were found to be a good predictor of the type of change occurring in the model systems and food products during storage. Below Tg physical aging (enthalpy relaxtion) could be seen in the samples and retrogradation of the starch occurred above Tg. The rates of retrogradation were not affected by glycerol content directly and knowledge of Tg and storage temperature were sufficient to predict the retrogradation.

Products became stiffer on storage and this was associated with molecular re association of the starchy component, but control of the moisture was also critical as water still dominated product behaviour even in the presence of glycerol.

ACKNOWLEDGEMENTS

First of all I would like to thank Dr. Imad Farhat for his generosity and friendship he has giving me over the last years both during my Master degree and PhD. I am also very grateful to Dr. Sandra Hill for her continuous supervision and unconditional support and Professor John Mitchell for his invaluable input during this project.

I would like to express my gratitude to Masterfoods, specially Dr. Phil McGenity and Dr. Charles Spears, for giving me the opportunity to participate in this project and to the University of Nottingham for its financial support.

My special gratitude to Dr. Bill MacNaughtan, Val Street, Mike Chapman, Phil Glover, Kath Brasnett, Lynne Moseley and Caroline Newton for their patience and support during my stay in the Division of Food Sciences.

Many thanks to all my friends; Asgar and his family, Abde, Celine, David, Marga, Fojan, Pepa, Rodrigo, Astrid, Sarai, Carlos, Nameeta, Nuno and many others for their friendship and generosity.

I also would like to thank my parents, my sister Paola and my brothers Daniel and Alfredo for their love and encouragement.

Above all, special thanks to my wife Macarena, to whom I will be in eternal gratitude for all her patience, support and unconditional love during all these years in UK.

TABLE OF CONTENTS

LIST OF FIGURES

LIST OF TABLES

LIST OF ABBREVIATIONS

p_w^θ	vapour pressure of pure water at the same temperature and pressure
$(1-\theta)$	fraction of the surface not covered.
a	sphere radius
a_T	shift factor expressed as the ratio between the viscosity of the polymer at a given temperature T and its viscosity at a reference temperature T_s
Aw	water activity
C	constant (related to the net heat of sorption)
C_d	concentration of diffusing substance
D	diffusion coefficient
d	diluent
%db	dry basis
E_1	heat of adsorption monolayer
E_b	heat of condensation of the bulk liquid
E_L	heat of condensation second and higher layers
F	rate of transfer per unit area section
G	free energy of the system, n_i.
$ierfc$	integrated complementary error function
K	constant (related to the heat of sorption of the multilayer)
k	constant incorporating characteristics of the molecular network system.
k_r	crystal growth rate
k_a, k_d	rate constant for adsorption and desorption respectively
k_o	entropic factor

M	moisture content (%db)
M_∞	mass at time infinity
M_{cal}	moisture content at specific water activity (Aw)
M_i	equilibrium moisture content (5db) of component i
m_o	monolayer value
M_t	mass at time t
n	diffusional exponent
N	diffusional geometry factor
n	Avrami coefficient
n_j	number of moles of component j
p	polymer
P	pressure
p/p_0	gas partial pressure, relative humidity in the case of water
p_i	pressure of the pure component
p_w	equilibrium water vapour pressure over the system
R	universal gas constant
RH_c	modulus inflection point relative humidity
s_1	first layer surface area covered
T	temperature
Tc, M_c, Aw_c	parameter defining modulus inflection point occurs
Tg_d	Tg of diluent
Tg_p	Tg of polymer
u	chemical potential of the component i,
$U(t)$	uncrystallised starch fraction at time t
w	weight fraction

W_i	individual component weight expressed on a dry basis
w_p and w_d	weight fractions of the polymer and diluent respectively
W_{Si},	mass fraction of the i^{th} component in the mixture
x	space coordinate measured normal to the section
$Y(RH)$	magnitudes of the mechanical parameter at a specific relative humidity
$Y(M)$	magnitude of any mechanical parameter at a specific moisture content
$Y(T)$	magnitude of any mechanical parameter at a specific temperature
Y_∞	value of physical parameter at time equal infinity
Y_o	value of physical parameter at time = 0
Y_s	magnitude of the mechanical parameter in the glassy state
Y_t	physical parameter describing the retrogradation dependency on time t
ΔCp_d	specific heat capacity of the diluent
ΔCp_p	specific heat capacity of the polymer
θ	fraction of the surface covered

1. INTRODUCTION

This dissertation focuses on the study of the mechanical and structural stability of commercial cereal based pet-care products. These materials are characterised by having a considerable amount of cereal starches and polyols in their formulations. It is believed that the addition of starch to these mixtures contributes to the formation of a structural matrix that holds and integrates other components in the formulation. Another important characteristic is their low water activity (Aw), which allows long shelf life without the need of refrigeration. This is achieved by the replacement of water in the system by polyols maintaining the products textural attributes.

Although the low Aw of these products makes them microbiologically safe to be consumed after long storage, changes in their texture have been reported. The mechanisms causing these changes in texture are not well understood, neither are the influence of storage variables such as temperature and relative humidity.

These changes in texture may affect the product digestibility increasing the risk of injuries to animals' teeth and the digestive track.

In order to minimise the kinetic of this change in quality, it is important to have a better understanding of the behaviour of the main components present in these formulations during storage. This would allow a better control over the stability of this material and a more efficient devolvement of new products.

One of the key points in this understanding is the functional effect (e.g. mechanical stability) of polyols on starchy materials.

Abundant information about the effect of plasticisers on starchy systems can be found in the literature. The limitation of this material is the difficulty to separate the individual effect of water and polyols. The hygroscopic nature of polyols can attract water from the environment and from within the products affecting the overall textural performance of these materials.

For this particular work, three models systems were prepared by thermomechnical extrusion. Common starches used in industry, such as rice and wheat, were extruded in the presence of different concentrations of

glycerol. Waxy maize starch was also extruded in order to compared the effect of amylose on the stability of these materials.

The first part of the experimental work presented in this dissertation includes sorption studies of extruded starch-glycerol systems. For this work a new analytical instrument received at the beginning of this project, was used. The dynamic vapour sorption (DVS) provided complete sorption isotherms for all the prepared model systems. The sorption kinetic for each of the equilibrating relative humidities was also obtained. In order to improve the understanding of sorption and diffusion, theoretical models were fitted to the obtained experimental data.

In the next section of this dissertation, the plasticising effect of glycerol on the glass transition temperature (Tg) is discussed. It was measured for all three starch-glycerol systems using differential scanning calorimetry (DSC). This Tg value was obtained at different moisture and glycerol contents. Similarly to the sorption studies, theoretical models used to predict Tg are presented and applied to the experimental data. These equations provide fundamental information about thermodynamic properties of the individual components and how these properties may change in presence of other compounds.

Is it well recognised that the addition of polyols have also an effect on the mechanical properties of these materials. The flexural modulus as a function of water and glycerol content was also evaluated using the three point bending (TPBT) method. An empirical model is used to numerically compare parameters such the inflexion point of the stiff to ductile transition. The obtained values were also plotted against (T-Tg) values to assess the effect of Tg on the mechanical properties of these systems.

Conflicting information is commonly found about to the effect of polyols on the ageing of starch based materials. The next section in this thesis focuses on the study of the increase in the hardness with storage time on one of the extruded starch-glycerol systems. Different analytical approaches such as DSC and DMTA were used to investigate these changes with storage time. The hypothesis relating the ageing kinetic with (T-Tg) is also discussed.

The final section of the work focuses on the characterisation of starch based pet-care products and their mechanical and structural stability during storage. The experimental approach is based on the work done on the starch-glycerol model systems. The application of theoretical and empirical models to predict moisture sorption, effect of moisture on texture and the kinetics of increase in hardening with time tested on the model systems is also discussed here.

It is important to consider that the better understanding gained from the study of the stability of starch-glycerol systems is not only relevant to this particular type of product, but also to many others intermediate moisture starch-polyol products commonly produced by food manufactures.

1.1 General Objectives

As mentioned before, the study of starch-water-glycerol systems during storage is very complex due to the hygroscopic nature of polyols affecting the overall moisture content of these systems and varying the water distribution between its main polymeric components.

Therefore, the general objectives set for this research project were: *(i)* assessment of the effect of glycerol on the sorption (kinetics and at equilibrium) of starch based systems when exposed to different relative humidities (RH); *(ii)* evaluate how these changes in plasticiser contents affect the mechanical properties of these systems; *(iii)* confirm if the changes in texture are related to phase transitions such as the glass transition temperature (Tg) of the polymer; *(iv)* determine if the compatibility of glycerol with starch can have a significant effect on the hardening kinetic during storage; *(v)* finally applying similar principles to complex formulation such as pet-care products, including the application of models to predict the textural behaviour of these materials during storage.

2 Literature Review

One of the common methods of reducing the risk of microbial growth in food products is by keeping a low molar fraction of the water available to microorganisms. This concept of available water has been associated with the term water activity (Aw), which is defined as the ratio of the partial water vapour in the product over water vapour of pure water. Keeping a low Aw has proved to be a very successful technique in extending food products shelf life. The drawback in this approach, especially in biopolymer containing products, is its effect on the texture attributes of these materials. To reduce this effect, other plasticisers such as glycerol, polyethylene glycol and sorbitol, are used to maintain the desired textural properties, whilst reducing the Aw.

An example of the industrial applications on this technology is in pet-care products. These materials are relatively dry but they are highly plasticized by low molecular weight compounds other than water. The formulation of these materials is characterised in having a higher proportion of cereals than common pet foods. The objective is not to fulfil the animal nutritional requirement but to obtain functional products with properties such as tooth cleaning.

The general hypothesis presented states that these starch based materials undergo ageing by a re-crystallisation process similar to the one identified for bread staling. In order to test these ideas, a fundamental understanding of the behaviour of these mixtures at a simpler level is very important. Therefore, the following review concentrates on the interaction of the three main compounds present in the formulations; starch, water and polyols.

Following the "the food polymer science approach" that emphasises fundamental similarities between the synthetic polymers and food, this review will focus on the current knowledge on molecular starch structure, phase transitions and stability, assuming a non-equilibrium state. Theoretical models used to predict these transitions on starch and more complex systems are also discussed. Finally a description of the extrusion processes applied to starch and pet-care products is presented.

2.1 Starch

The major constituents of the products being investigated are cereal grains, such as waxy maize, rice and wheat. Although the amount of starch contained in grains varies, it is generally between 60 and 75% of the weight of the grain providing 70–80% of the calories consumed by humans worldwide (AACC, 1999).

Starch occurs in the form of granules that are usually characterised by an irregular rounded shape, ranging in size from 2 to 150μm (Belitz et al., 2004; Coultate, 1996). A summary of the general characteristics of commerial staches is presented in table 2.1. Starch granules are composed of a mixture of minor components such as moisture (typically 12%), proteins (0.1 to 0.5%), lipids (0.1 to 0.8%), ash (<0.5%) plus major components; an essentially linear polysaccharide called amylose, and a highly branched polysaccharide known as amylopectin.

Based on X-Ray diffraction, native starch granules show a semi –crystalline structure that indicates a high degree of molecular orientation. About 70% of the mass of the starch granule is regarded as amorphous and 30% as crystalline (Belitz et al., 2004).

Table 2.1. General properties of starch granules variety modified from (Fennema 1996;Belitz et al. 2004)

	Corn starch	Waxy maize starch	High-amylose corn starch	Potato starch	Rice starch	Wheat starch
Granule size (diameter, μm)	2-30	2-30	2-24	5-100	3-8	2-55
Amylose (%)	28	< 2	50-70	21	14-32	28
Gelatinisation/pasting temperature (°C)[a]	62-80	63-72	66-170	58-65	61-78	52-85
Crystallinity %	--	39	20-25	25	38	36
Lipid (%db)	0.8	0.2	--	0.1	0.3-1.1	0.9
Protein (%db)	0.35	0.25	0.5	0.1	--	0.4
Phosphorous (%db)	0.0	0.0	0-0	0.08	--	0.0

[a]From the initial temperature of gelatinisation to complete pasting

2.1.1 Amylose

An amylose molecule is essentially a linear chain of (1→4)-linked α-D-glucopyranosyl units. The chain, given sufficient mobility could form a coil left-handed with six residues per turn helix (figure 2.1 B).

Enzyme hydrolysis of the chain is achieved by α-amylase, β-amylase and gluco-amylase. Often, β-amylase does not degrade the molecule completely into maltose, since a very low branching is found along the chain with α (1→ 6) linkages (Belitz et al., 2004). Takaya et al. (2000) working on corn estimated that branching can occur between 180-320 glucose units. The molecular weight of amylose has been estimated to be ~ 10^6 g/mol (Buléon et al., 1998).

Amylose chains can associate themselves to form parallel double-stranded helices, right or left handed packed in a cell unit (figure 2.1).

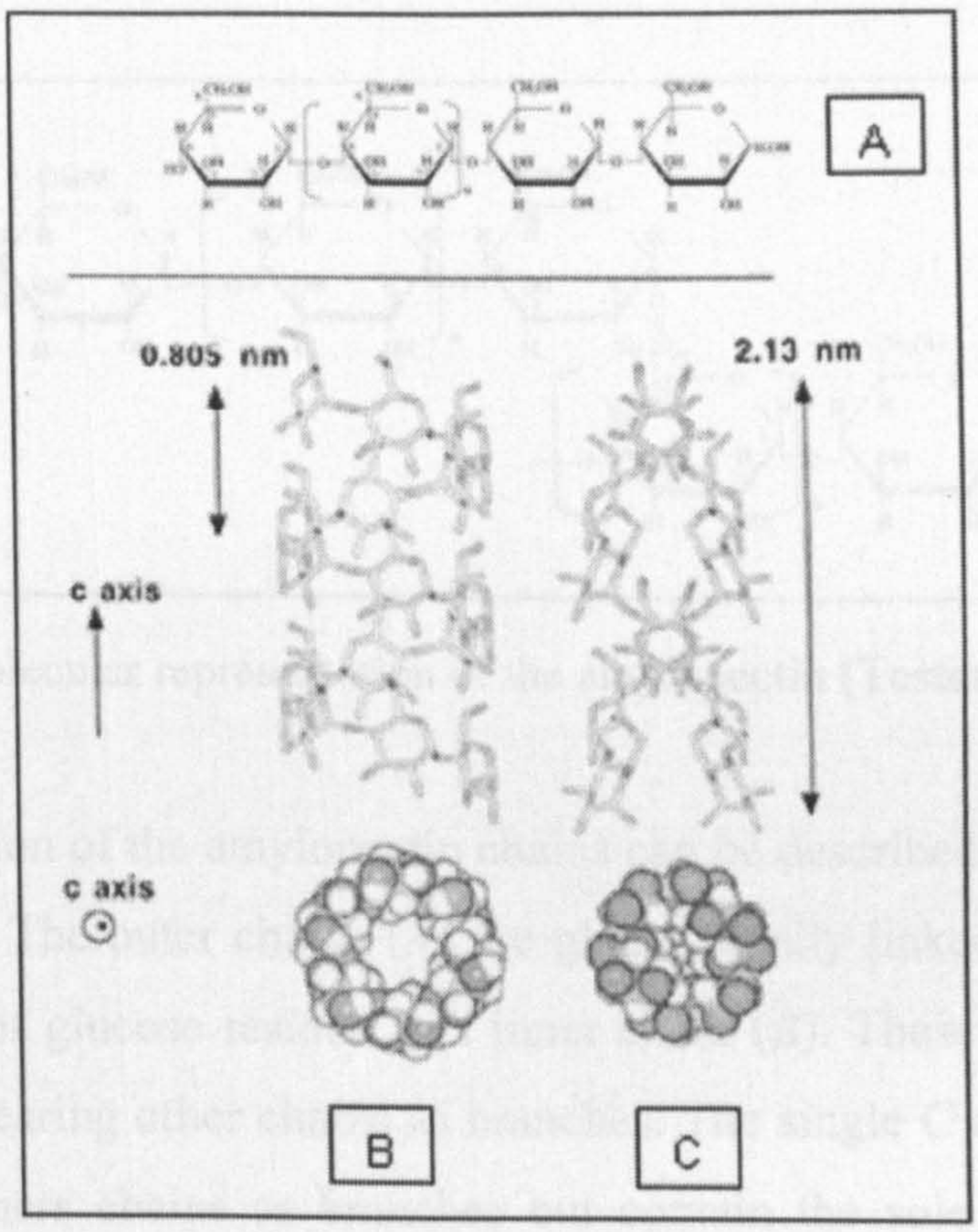

Figure 2.1. (A) Linear amylose chain (Tester et al. 2004). Helical conformations present in starch and starch components: (B) 6-fold single helix; (C) 6-fold left-handed double helix (modified from Buléon et al., 1998).

2.1.2 Amylopectin

Amylopectin is present in all starches, constituting about 75% of most common starches (see table 2.1). Some starches consist almost entirely of amylopectin (~ 95%) and are called waxy starches.

Potato amylopectin is unique in having phosphate ester groups with 60% attached at a O-6 position, with the other third at O-3 position (Fennema, 1996).

Amylopectin is a highly branched molecule, it is formed through chains of α-D-glucopyranisyl residues linked together mainly by (1→ 4) linkages but with (1→ 6) bonds at branch points (figure 2.2). The branches are short, with an average of 15-30 glucose units in length (Belitz et al., 2004). The amylopectin molecule is one of the biggest found in nature with an estimated molecular weight between 10^7 to $5x10^9$ g/mol (AACC, 1999; Belitz et al., 2004).

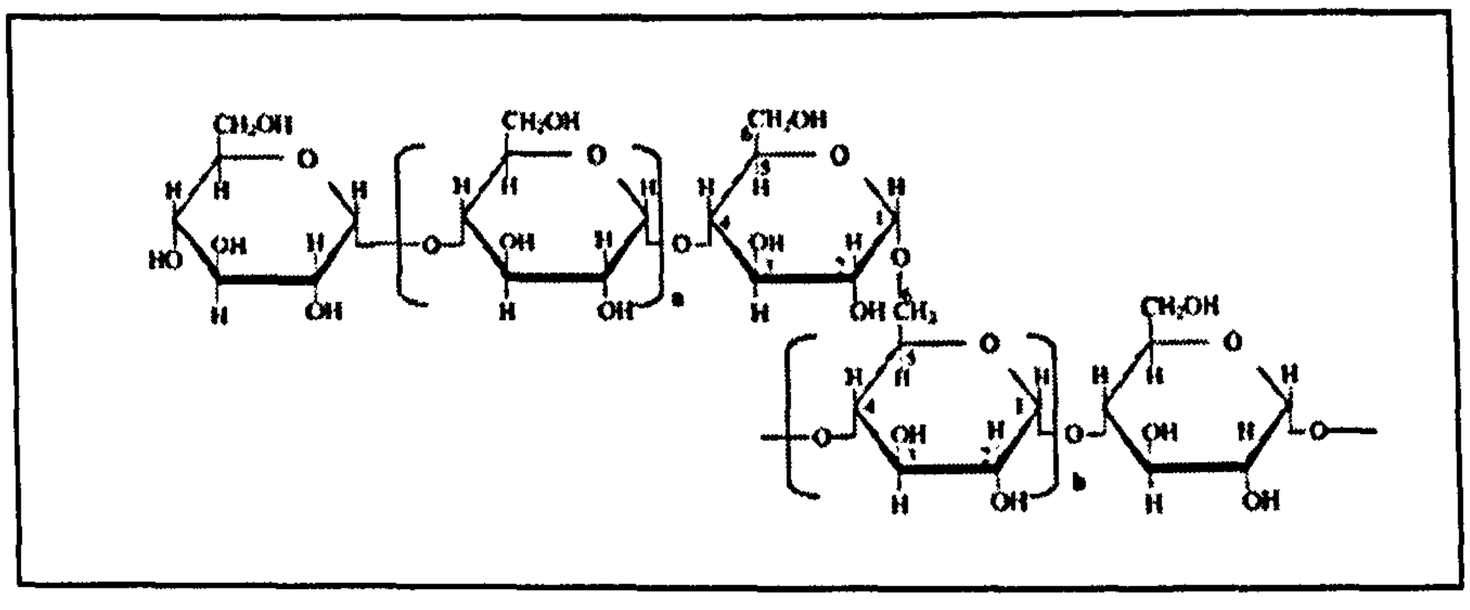

Figure 2.2. Molecular representation of the amylopectin (Tester et al. 2004).

The basic organisation of the amylopectin chains can be described in term of *A, B, C* chains (figure 2.5). The outer chains (*A*) are glycosidically linked at their reducing group through *C6* of glucose residue to a inner chain (*B*). These chains are in turn defined as chains bearing other chains as branches. The single *C* chain per molecule likewise carries others chains as branches but contain the sole reducing terminal residue (Buléon et al., 1998).

An important feature of amylopectin molecule is that *S*-chains (S- for short), *A* and *B* chains with a degree a polymerization (DP) 14-18, are associated in discrete clusters supported by *L* chains (L- for long) (DP 45-55) (figure 2.3).

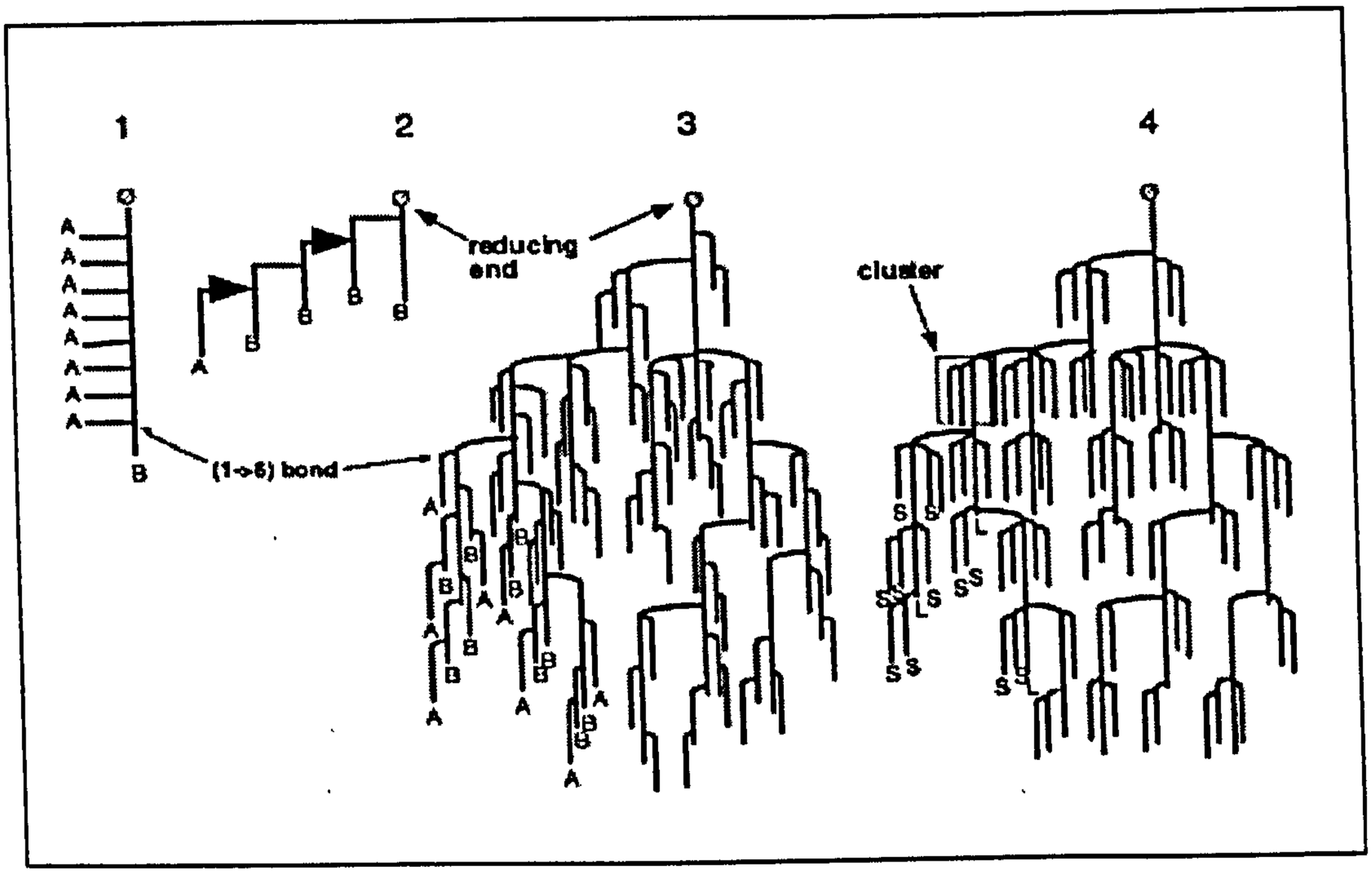

Figure 2.3. Molecular structure of amylopectin as proposed by (1) Haworth, (2) Staudinger, (3) Meyer and (4) Meyer redrawn as cluster-type architecture (Buléon et al., 1998).

2.1.3 Molecular Ordering of Starch Chains

It has been shown that double helices strands of amylose can form crystallites named A and B types (Buléon et al., 1998; Carvalho, 2001). In the A-type structure these double helices are packed closely leaving space for 8 water molecules per unit cell space. B-type structure is characterised by double helices packed in a hexagonal unit cell with 36 molecules of water per unit cell (figure 2.4).

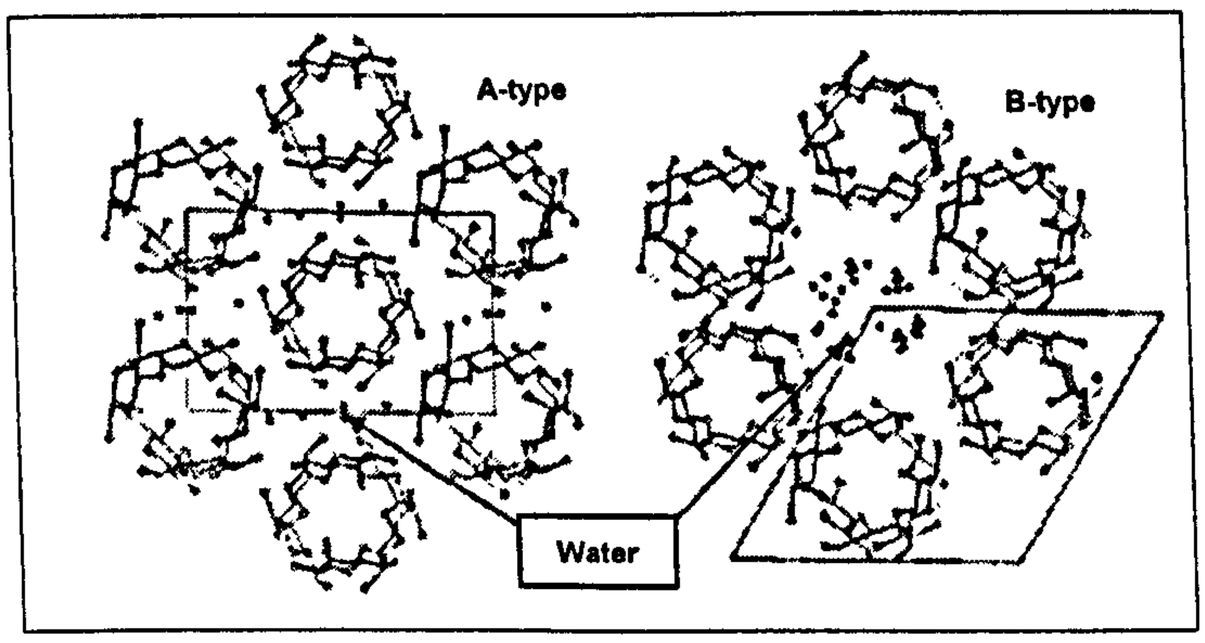

F igure 2.4. Crystalline packing of amylose double helices in A-type (*A*) and B-type (*B*) amylose. Projection of the structure onto the plane (Tester et al. 2004).

Single amylose helices can form a structure called V-type in the presence of linear alcohols and fatty acids. Since the internal helix is hydrophobic, the enclosed molecule has also to be lipophylic in nature (Buléon et al., 1998; Becker et al., 2001; Belitz et al., 2004). In the case of amylose-lipid complexes, it is assumed that the aliphatic part of the lipid lies inside the amylose helix (figure 2.5), while the polar group lies outside, being too large to be included (Buléon et al., 1998).

The presence of these "guest" molecules complexed with amylose can have a stabilising effect affecting the overall crystallisation process of the amylose molecule over time (Gelders et al., 2004).

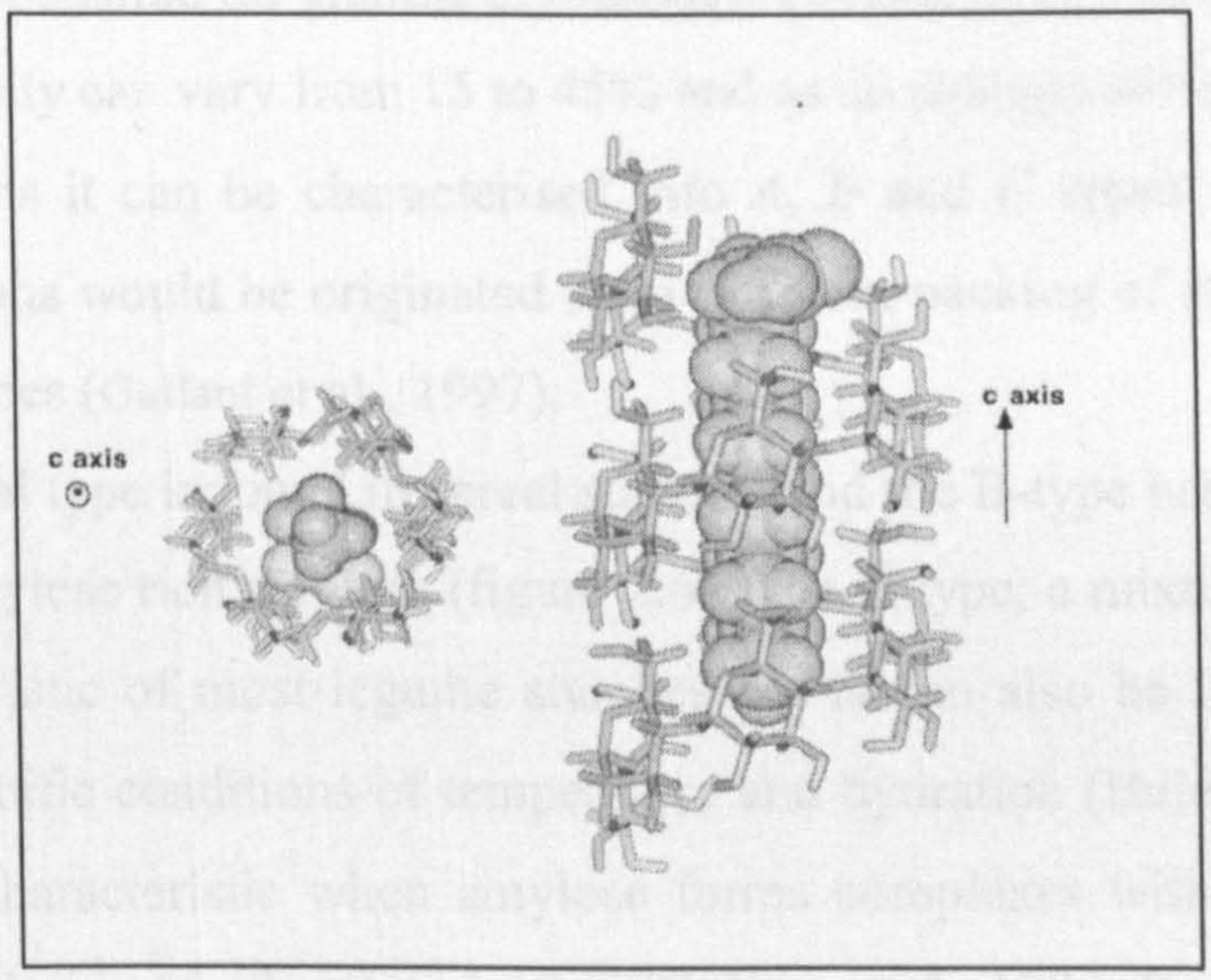

Figure 2.5. Molecular representation of amylose fatty acid complexes showing the inclusion of the aliphatic part (C12) of the fatty acid inside the hydrophobic cavity of the amylose single helix (Buléon et al., 1998).

The complexation between amylose and lipids can be followed by crystallisation. It has been suggested that at temperatures below 60°C, the nucleation rate is very high and the amylose helices "freeze" rapidly in a structure with low crystal order giving an "amorphous like" order (Gelders et al., 2004). This type of interaction has been named as "type I" amylose-lipid interaction having a relatively low dissociation temperature (<100°C). In contrast higher complexation temperatures (>91°C) a slow

nucleation is followed by a distinct crystal growth, yielding a "semi-crystalline" or "type II" amylose-lipids interaction (Gelders et al., 2004).

2.1.4 Granule Internal Organisation

The starch granule organisation is very complex which is also reflected in the existence of different shapes depending on the botanical origin.

When the starch granules are observed under polarised light, birefringence is produced which is characteristic for distorted spherocrystals (Buléon et al., 1998;Tester et al., 2004). It is widely accepted that the amylopectin polymer (which comprises around 75% of the granule composition in non-mutant starches) is predominantly responsible for granule crystallinity (Gallant et al., 1997).

Granule crystallinity can vary from 15 to 45% and as an analogy from amylose X-ray diffraction patterns it can be characterised into *A*, *B* and *C* types. These different crystals polymorphs would be originated from different packing of amylopectin sub-chain double helices (Gallant et al., 1997).

The A-type crystal type is found in cereal starches and the B-type has been identified on tubers and amylose rich starches (figure 2.6). The C-type, a mixture of A- and B-type, is characteristic of most legume starches but is can also be found on cereals grown under specific conditions of temperature and hydration (Buléon et al., 1998). The V-form is characteristic when amylose forms complexes with fatty acids and monoglycerides during starch gelatinisation (Buléon et al., 1998; Becker et al., 2001; Gelders et al., 2004).

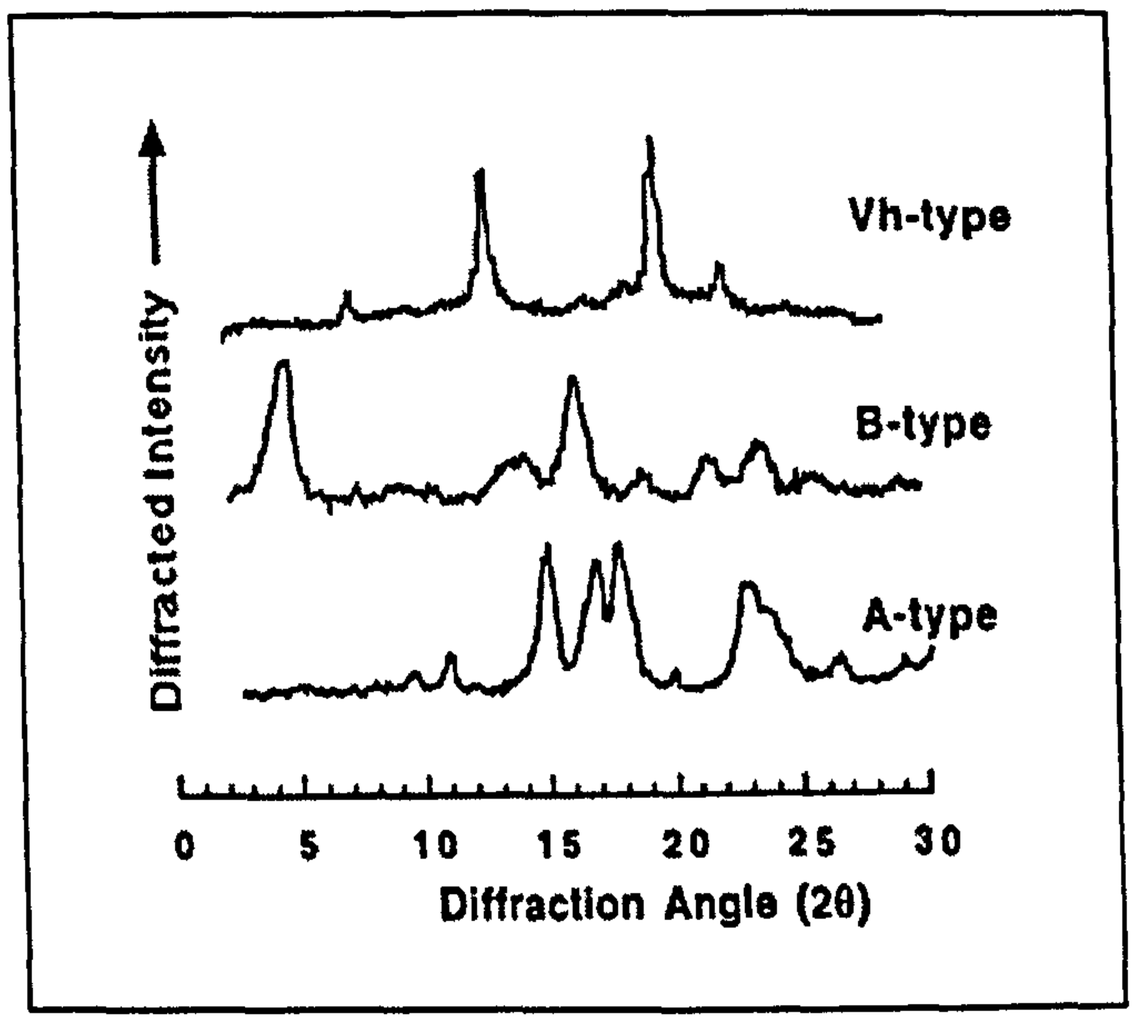

Figure 2.6. X-ray diffraction pattern for in A-type, B-type structure and Vh type for amylose-lipid complexes (Buléon et al., 1998).

It is believed that the clustered branches of amylopectin support the framework of the crystalline regions of the granules. These clusters are formed by packed double helices. It is the packing together of these double helical structures that forms the many small crystalline areas comprising the layers (lamellae) of starch granules that alternate with less dense amorphous layers (branching region). The thickness of these crystalline lamellae has been estimated in 9-10 nm (estimated length of the cluster) (Blanshard 1987; Gallant, Bouchet et al. 1997; Buléon, Colonna et al. 1998; Tester, Karkalas et al. 2004).

Results from new analytical techniques have suggested that the crystalline and the amorphous lamellae of the amylopectin are organised into larger, more or less spherical structures called "blocklets" (Gallant et al., 1997). This structures range in diameter from around 20 to 500nm depending of the starch botanical source and location of the granule.

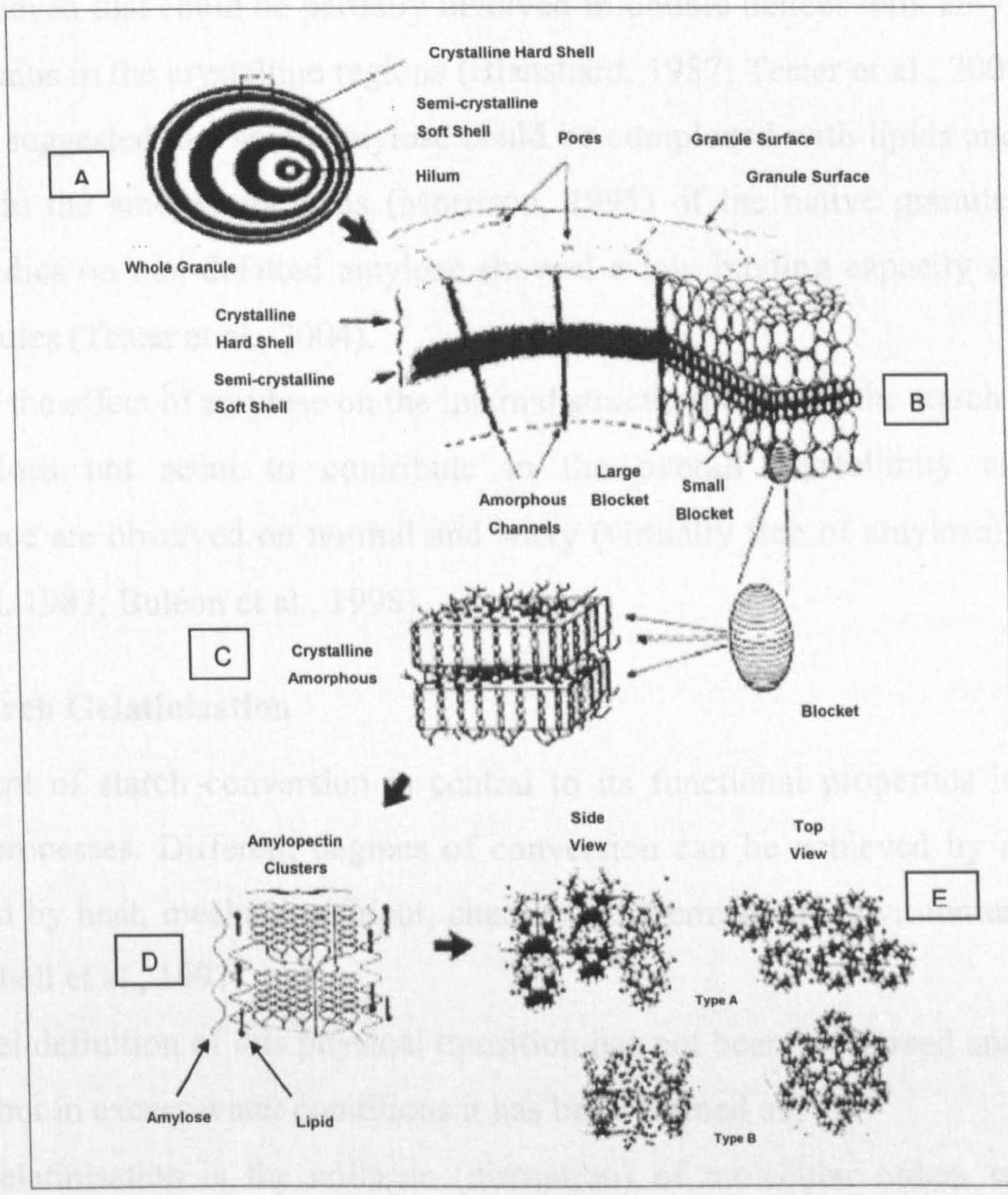

Figure 2.7. Overview of a starch granule structure (Gallant et al., 1997)

Figure 2.7 shows the starch granule model proposed by Gallant (1997). It starts with the highest level of granule organisation, showing the alternating crystalline and semi-crystalline shells (A). At a lower level of structure, the blocklets forming the crystalline hard shell are shown (B). The crystalline and amorphous lamellaes forming the blocklets are shown in the next diagram (C). The next figure (D) (Blanshard, 1987) represents the branched amylopectin polymer and the presence of linear amylose-lipid complexes. At the lowest level of organisation (E) the two different crystalline polymorphs for the starch polymers are described.

The positioning of amylose chains in the native starch granule is yet to be confirmed, but it is believed that could be partially involved in double helices with amylopectin polymer chains in the crystalline regions (Blanshard, 1987; Tester et al., 2004). Also it has been suggested that some amylose could be complexed with lipids and mono-glycerides in the amorphous areas (Morrison, 1995) of the native granule. Iodine binding studies on non-defatted amylose showed a low binding capacity on native starch granules (Tester et al., 2004).

In terms of the effect of amylose on the internal structural order of the starch granule, amylose does not seem to contribute to the overall crystallinity as strong birefringence are observed on normal and waxy (virtually free of amylose) starches (Blanshard, 1987; Buléon et al., 1998).

2.1.5 Starch Gelatinisation

The concept of starch conversion is central to its functional properties in a wide range of processes. Different degrees of conversion can be achieved by a process determined by heat, mechanical input, chemical and enzymatic environment (figure 2.8) (Mitchell et al., 1997).

A universal definition of this physical transition has not been yet agreed among food scientists but in excess water conditions it has been defined as:

"Starch gelatinisation is the collapse (disruption) of molecular orders within the starch granule manifested in irreversible changes in properties such as granular swelling, native crystalline melting, loss of birefringence, and starch solubilisation. The point of initial gelatinisation and the range over which it occurs is governed by temperature, starch concentration, method of observation, granular type, and heterogeneities within the granular population under observation" AACC (1999).

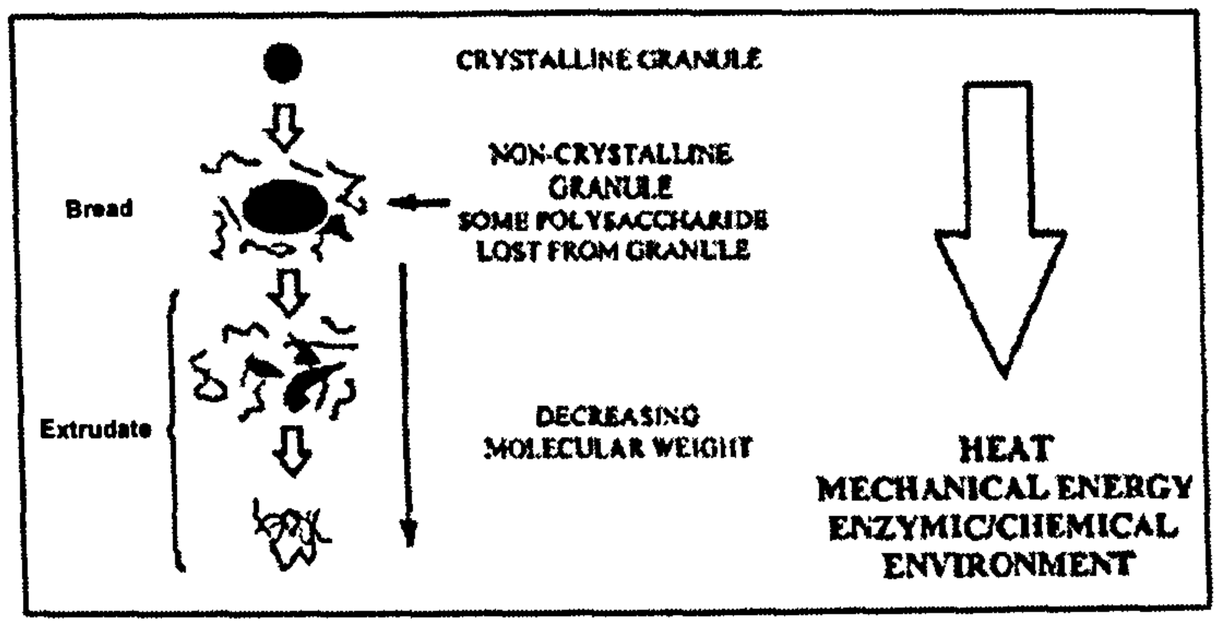

Figure 2.8. The behaviour of starch with increasing levels of conversion in excess water (Mitchell et al., 1997).

Using differential scanning calorimetry (DSC), this molecular disordering is often observed as an endothermic peak (Biliaderis, 1990). This peak seems to be associated to the disruption of the crystalline fraction of the amylopectin as the peak area increases when the concentration of this polymer increases. Amylose is not believed to exhibit a DSC gelatinisation peak, as it has not been systematically detected using this analytical technique (Russell, 1987). The evaluation of the disruption of the crystalline structure has been measured using other techniques such as X-Ray diffraction (Ottenhof, 2003). Although the data given by this technique correlates well with the DSC endotherm, it has been suggested that calorimetric analysis is able to measure early stages of molecular disruption (disruption of double helices structures) rather that the loss of crystalline order (Cooke and Gidley, 1992). The gelatinisation phenomenon can also be described by the changes in the rheology of a starch-water system. Figure 2.9 show viscosity and structural changes when wheat starch granules are heated in excess water using the Rapid Viscometer Analyser (RVA) (Ottenhof, 2003). At ambient temperatures starch granules are insoluble in cold water due to highly organised structure. This behaviour is represented by a constant low viscosity at the starting zone of the profile. As the temperature increases, the polymer chains held together by hydrogen bonding, become mobile allowing the ingress of water from its surroundings making the granules swell. Up to this stage, this process is considered to be fully reversible as the structure of the granule, although swollen, has not been degraded by the

temperature and shear.

This phenomenon is commonly detected as a sudden increase in viscosity shown on the RVA profile. Further increase in temperature would lead to greater swelling, which would allow amylose to leach out of the granule. Here the viscosity reaches a maximum point at which the gelatinisation temperature is reached. Over this point, granules begin to disintegrate by the combined effect of temperature and shear. This is represented by a marked decrease in the viscosity in the RVA profile.

During the cooling from 90°C to 50°C phase, solubilised amylose and amylopectin polymers begin to re-associate, process represented by another increase in viscosity at the end of the profile. This change in viscosity on cooling is also known as "paste set back" (AACC, 1999).

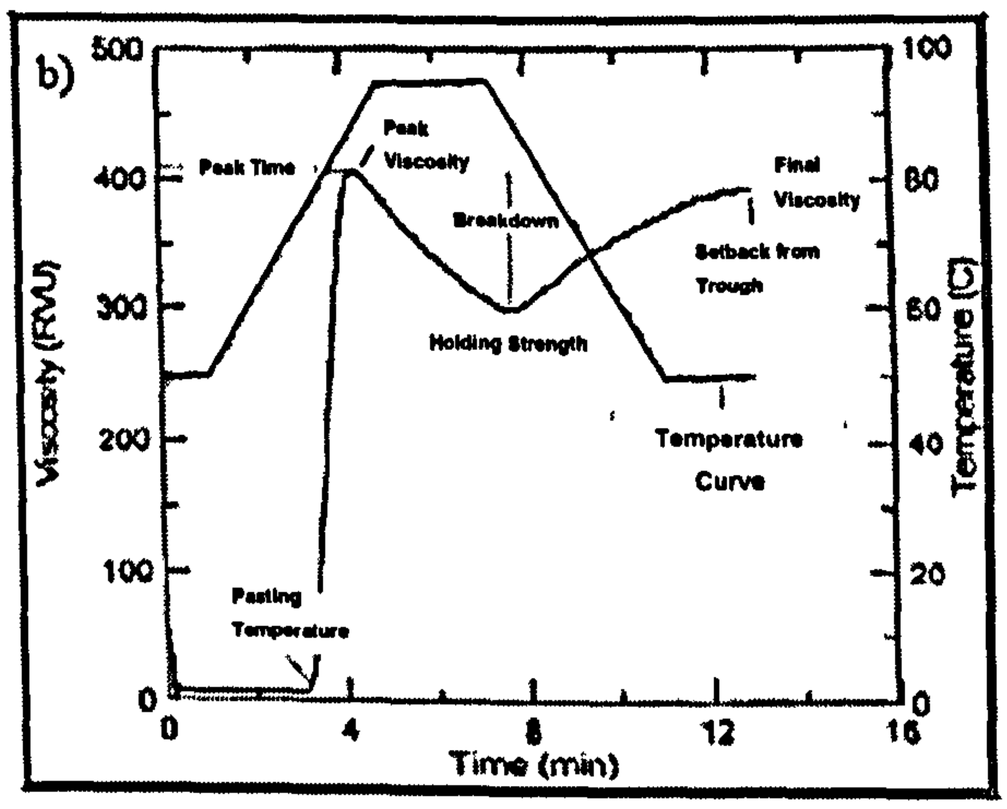

Figure 2.9. Schematic representation of granular changes in relationship to viscosity and temperature (Ottenhof, 2003).

It is known that increasing moisture content decreases the temperature and spread of the gelatinisation endotherm of native starch (figure 2.10). Donovan (1979) detected difference on the DSC endotherms of native potato starch for different moisture contents. Under excess water conditions (water mass fraction ~0.8), a well defined endotherm was obtained at a narrow temperature range (65 °C), suggesting that the starch granule has been homogeneously hydrated. When the moisture content is reduced to levels below 60% (wb) the hydration of the granule is incomplete. This behaviour is represented by the development of a shoulder at higher temperatures on

the DSC endotherm trace (water volume fraction 0.55) on figure 2.10. If the moisture content is reduced even further, the shoulder area increases and the temperature range at which molecular disruption occurs broaden. The gelatinisation phenomenon measured by DSC occurring in excess water conditions becomes a complex process under limited moisture condition, where the distribution of water within the starch determines the thermal event associated with the disruption of the crystalline fraction of the granule.

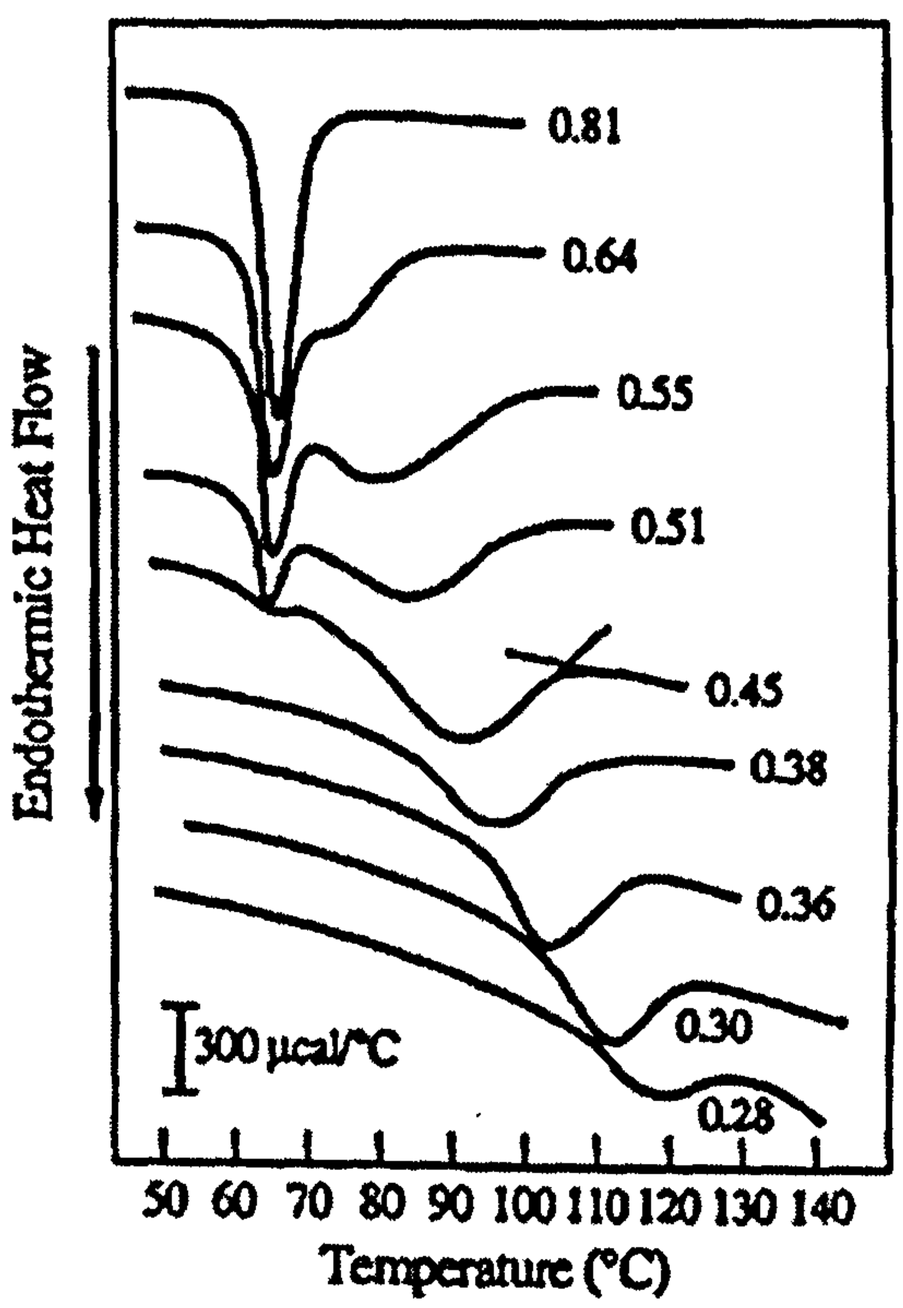

Figure 2.10. The process of potato starch gelatinisation with different volume fraction of water (Donovan, 1979).

The effect of water on the starch conversion temperature has been modelled using the Flory-Huggins approach (Biliaderis et al., 1986; Blanshard, 1987; Farhat and Blanshard, 1997).

According to this equation, the following relation holds between the melting point of a polymer and diluent's concentration:

$$\frac{1}{T_m} - \frac{1}{T_m^o} = \frac{R}{\Delta H_u}\frac{V_u}{V_1}(v_1 - x_1 v_1^2) \qquad \textit{Equation 2.1}$$

where:

ΔH_u : change in the enthalpy of fusion per repeating unit (glucose).

V_u/V_l: ratio of the molar volumes of the repeating units in the chain to that of water.

R: gas constant.

T_m: (in K) is the melting point of the polymer-diluent system.

T^o_m: true melting point of the undiluted polymer.

v_l: volume fraction of the diluent.

x_l: interaction parameter.

In an ideal solvent, the interaction parameter is 0 and consequently a plot $1/Tm$ against v_l gives a straight line with $1/T^o_m$ as intercept (Farhat and Blanshard, 1997).
This approach also led to extrapolated T^o_m.. Values for starch have been estimate at around 50-100°K above Tg^o (Mousia, 2000).

A common manufacturing process where cereals are processed under limited water conditions is extrusion cooking. At combination of thermal and mechanical energy are applied to the cereals, disrupting the integrity of its starch granules to the extent of obtaining an open amorphous structure that becomes available to other components. Further chain fragmentation and the formation amylose lipids complex are also expected during extrusion of cereals. More details about this process are discussed in section 2.2 of this review.

2.1.6 Starch Retrogradation

When amorphous starches are stored in their rubbery state, a molecular re-association will occur, leading to the formation of aggregates or crystallites. In the case of starchy materials this process is also known as retrogradation. This polymer re-association may be originated by two or more starch chains forming a simple junction zone point which then may develop into more extensively ordered regions, which under favourable conditions, would result in crystalline order (Atwell et al., 1988; Van Soest and Knooren, 1997).

This ageing phenomenon has important commercial implications as it is believe to be responsible for texture changes that take place during storage (Van Soest and Vliegenthart 1997; Farhat et al., 2000b). For example, it is generally accepted that starch retrogradation contributes to bread staling (Jagannath et al., 1998; Karim et al., 2000; Kulp and Ponte, 1981).

The retrogradation kinetics for each of the starch polymers follows different rates. Amylose re-association tends to occur rapidly due to its mostly linear structure, process that is even considered as time independent (Jagannath et al., 1998). In the case of amylopectin, its retrogradation rate seems to be lower due to its highly branched structure making the re-association process more difficult.

A description of the gelation and retrogradation of amylose is given by Goodfellow and Wilson (1990) on amylose-water solution (10%w/w) using Fourier Transform Infrared (FTIR). They suggested that for this polymer the molecular re-association was related to the formation of double helices followed by a phase separation which lead to the formation of a network, with subsequent aggregation of these double helices producing crystallinity (figure 2.11).

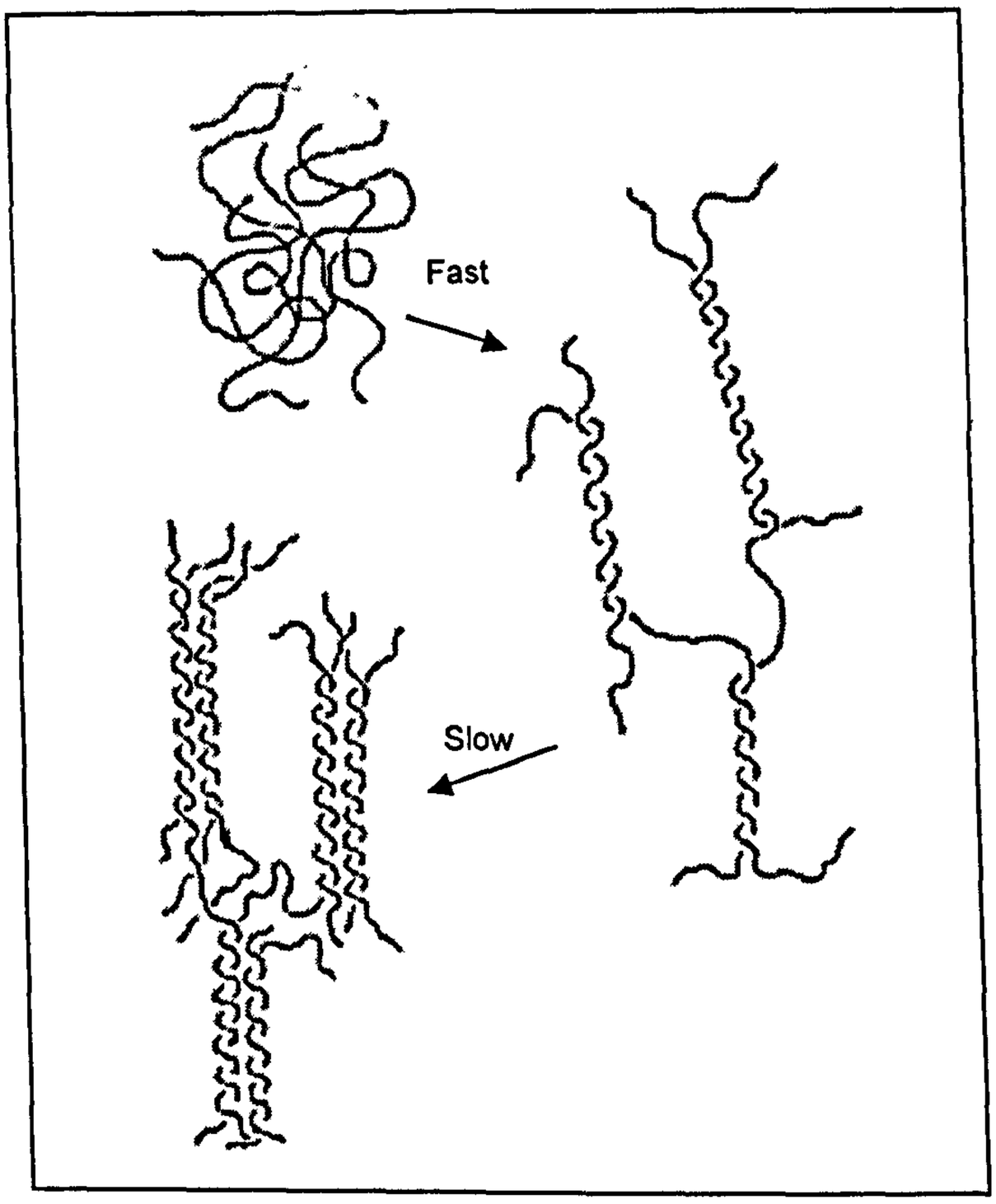

Figure 2.11. Schematic diagram showing the gelation and retrogradation of amylose (Goodfellow and Wilson, 1990)

Goodfellow and Wilson (1990) also suggested a mechanism to describe the retrogradation for amylopectin. The initial change involves a coil to helix transition of the side chains followed by a slower aggregation of these helices to produce crystallinity.

The kinetics of molecular re-association for each of the polymers forming the starch will depend on the molecular scale being examined. For short range ordering (random coil to helices conformation), both polymers undergo short rage ordering in a short time (for 10%w/w solutions) on cooling (Goodfellow and Wilson, 1990). This process is followed by polymer-rich and polymer-deficient phases formed by the aggregation of the helices. In the case of amylose this aggregation leads to the formation of a gel network, which is followed by an ordering of double helices forming crystalline region.

In the case of amylopectin, the double helices aggregation step would take much

longer due to its highly branched nature (figure 2.12).

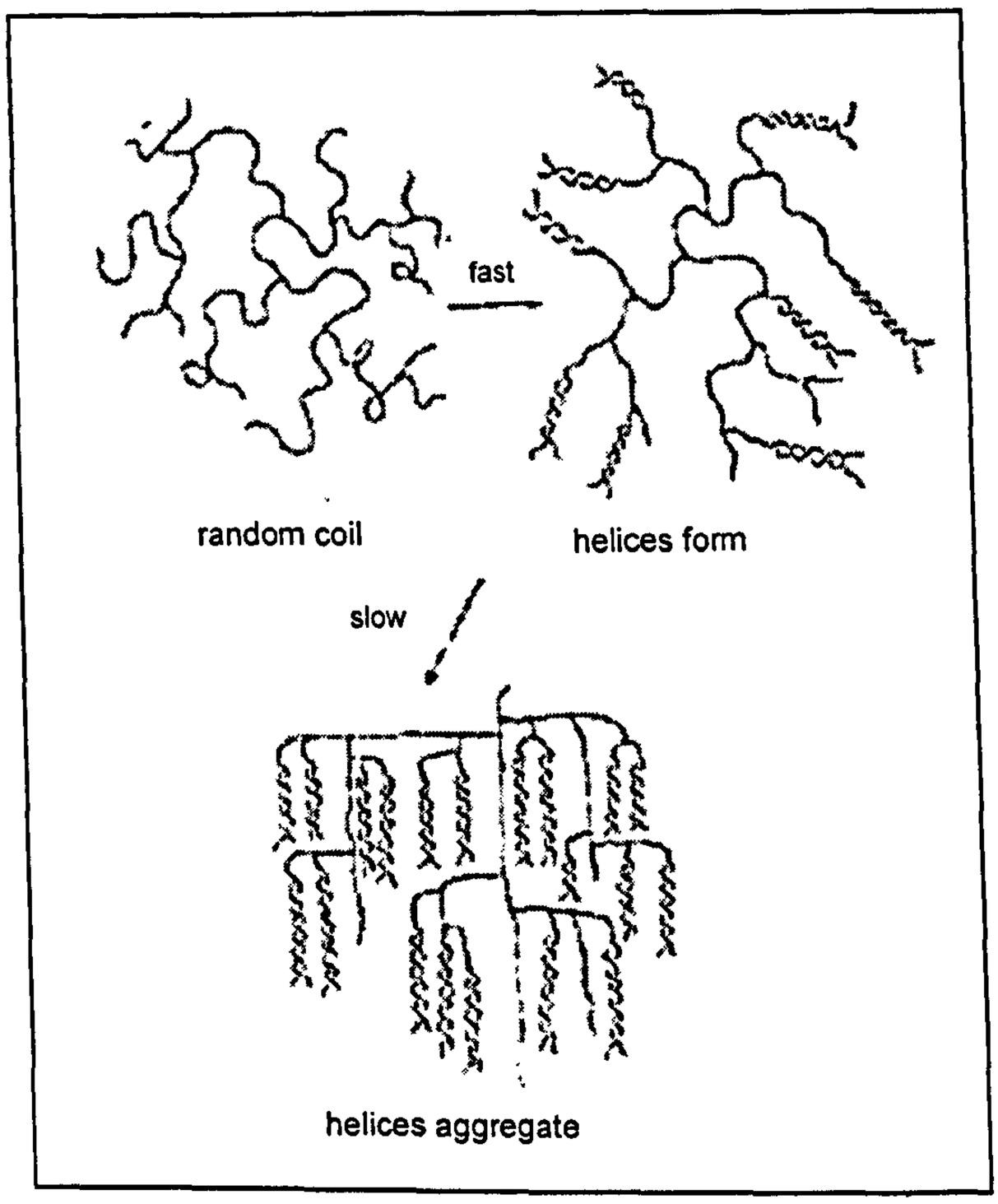

Figure 2.12. Schematic diagram showing the gelation and retrogradation of amylopectin (Goodfellow and Wilson, 1990)

Several theories have been developed to describe the kinetics of crystallisation, with the Avrami equation being the most widely used to describe this reordering process with time (Kulp and Ponte, 1981;Jouppila et al., 1998; Farhat et al., 2000b; Mousia, 2000; Takaya et al., 2000). A detailed description of this model is discussed in chapter 6 of this thesis.

2.1.7 Glass Transition in Starch

After the work by Slade and Levine (1988a, 1988b, 1991, 1993, 1995) the notion of the glass transition temperature and its relevance to food components has been widely accepted. It has contributed significantly to increase the understanding of how complex polymer mixtures such as food systems behave under specific processing

and storage conditions.

Amorphous materials are not easy to be classified in terms of their physical state. A fully amorphous and/or semi-crystalline materials (amorphous phase) can exist in the glassy state or in the viscous, super cooled, liquid state (Roos, 1995; Sperling, 1996). In the glassy state, amorphous materials behave as solids with an extremely high viscosity estimated in 10^{12} Pa s (Roos, 1995). Under these conditions molecular motions are restricted to vibrations and short-range rotational movements (Ward and Hardly, 1993). On warming, the polymer softens when the glass to rubber transition temperature (Tg) is reached. Sperling (1996) conveniently summarised the three main approaches (theories) to define the glass transition. They are not completely independent but they examine three aspects of the same phenomenon.

1. The free-volume theory

This approach introduces the free volume in the form of segment-size voids as a requirement for the onset of the coordinated molecular motion. This theory provides relationships between the coefficients of expansion below and above Tg and yields equations relating viscoelastic motion to the variables of time and temperature.

Williams et al. (1955) propose a model based theoretical approach by Doolittle (1951) to describe the viscosity on the basis of free volume (equation 2.2).

$$\log a_T = \log\left(\frac{\eta}{\eta_g}\right) = \left[\frac{-C_1(T - T_g)}{C_2(T - T_g)}\right] \qquad \textit{Equation 2.2}$$

Where a_T is a temperature shift factor, T is temperature, C_1 and C_2 are universal constant for all amorphous polymers with values of 17.44 and 51.6 respectively. η is the viscosity with η_g being the viscosity at Tg.

Fox and Flory suggested a model based on the notion that free volume *f*, in the glassy state is constant and it increases above Tg according to equation 2.3 where f_g is fractional free volume at Tg and α_f is the thermal expansion coefficient of free volume (Roos, 1995).

$$f = f_g + \alpha_f (T - Tg) \qquad \textit{Equation 2.3}$$

2. *The kinetic theory*

This theory defines Tg as the temperature at which the relaxation time for the segmental motions in the main polymer chain is of the same order of magnitude as the time scale of the experimental measurement. The kinetic theory is concern with the rate of approach to the equilibrium of the system, taking the respective motions of the holes and molecules into account. It also explains the temperature shift in Tg when the time scale of the experiment is changed by log cycle.

Roos (1995) summarised Sperling's theoretical description as: assuming that matter may have holes of molar mass v_h , or it may exist in a no hole state with molar excess energy ε_h, The activation energy for the disappearance of the holes is ε_j. The holes partition function is Q^h with its correspondent activated state Q^{Ξ} . The equilibrium number of holes N_h^*, is give by equation 2.4, where N_0 and v_0 are the number of moles of repeating units and the molar volume per repeating unit, respectively. The kinetics or relaxation time of the disappearance of holes, τ_h, is given by equation 2.5.

$$N_h^* = N_0 (v_0 / v_h) e^{-\varepsilon_h / RT} \qquad \textit{Equation 2.4}$$

$$\tau_h = \frac{h}{kT} \frac{Q^h}{Q^{\Xi}} e^{\varepsilon_j / RT} \qquad \textit{Equation 2.5}$$

3. *The thermodynamic theory*

This theory introduces the notion of equilibrium and the requirements for a true second-order transition, albeit at infinity long time experiments. The theory postulates the existence of a true second-order transition, which the glass transition approaches as a limit when the measurements are carried out more and more slowly. It successfully predicts the variation of Tg with

molecular weight and cross-link density, diluent content and other variables.

Unlike liquid to solid phase transitions (e.g. water freezing), the glass transition is represented by a continuity in the volume (V) and enthalpy (H) when the transition temperature is reached (figure 2.13 B). The first derivative on V and H, with respect to temperature at constant pressure, show a simple step change (figure 2.13 B) compared to the first derivative the first order transition (figure 2. 13 A). In this case, the derivative shows a peak generated from the heat released/absorbed from crystallisation/melting process (Allen, 1993).

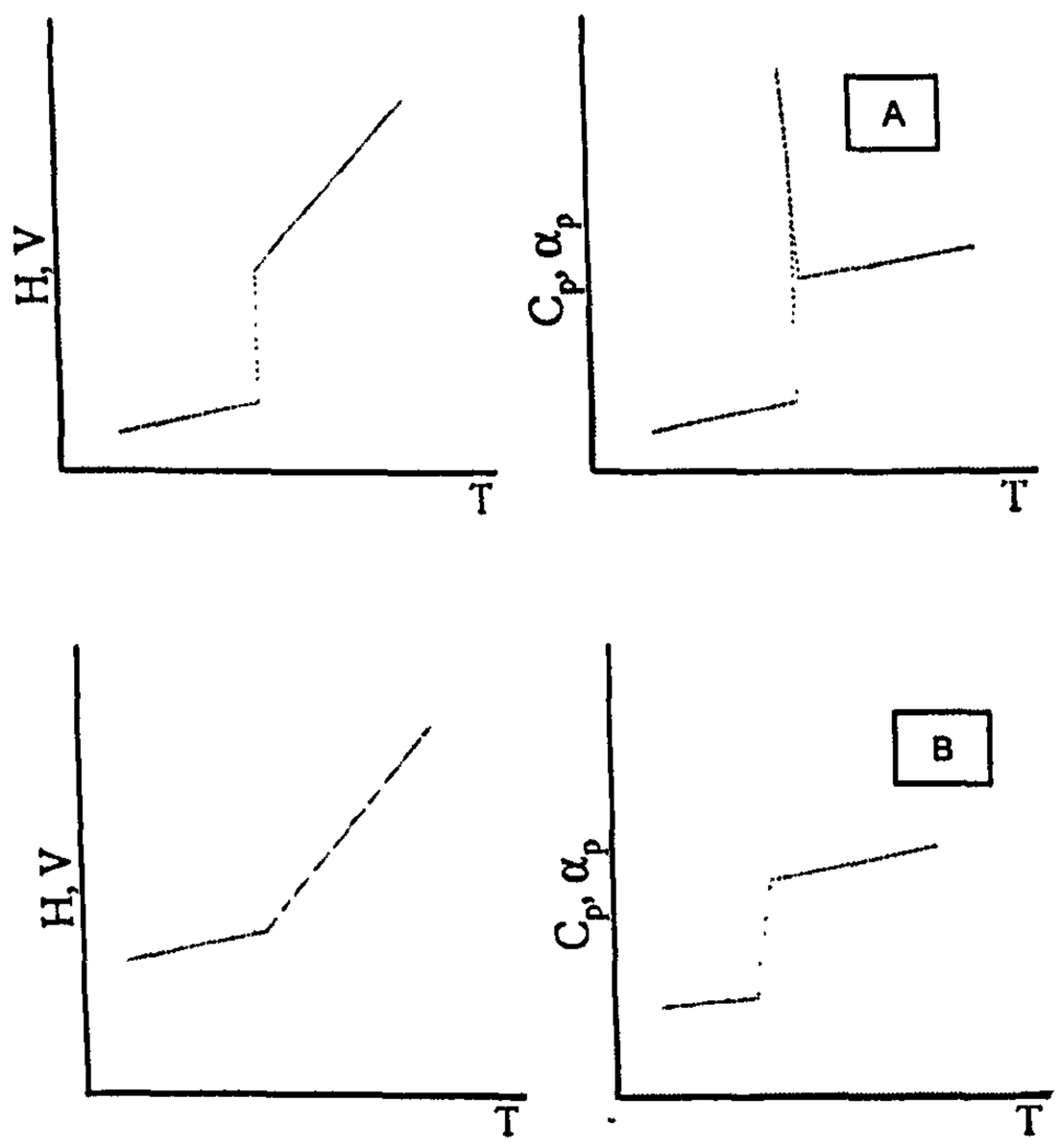

Figure 2.13. Representation of the change of enthalpy (H), volume (V) and its correspondent first derivatives, with respect to temperature at constant pressure, Cp and α_p for first (A) and second order (B) transitions (Allen, 1993).

This theoretical approach has been successfully used to rationalised phase transitions on starch systems (Arvanitoyannis et al., 1994; Baik et al., 1997; Bindzus et al., 2002; Graaf et al., 2003; Hallberg and Chinachoti, 1992; Jiugao et al., 1998; Jouppila et al., 1998; Kalichevsky, 1992; Lim, 2001; Liu, 2001; Mizuno et al., 1998; Nashed et al., 2003; Stading et al., 2001).

As it has been mentioned, starch occurs as partially crystalline, water-insoluble

granules which are disrupted through heating in the presence of a diluent, usually water, to give an amorphous polymer which is glassy when dry at room temperature (Moates et al., 2001). The estimation of glass transition temperature (Tg) of dry starches has not been experimentally measured due to thermal degradation. Extrapolation of the observed Tg values of dry malto-oligomers has given values of around 230°C for the high molecular limit of Tg (Orford et al., 1989). An extrapolation performed for dry waxy maize starch gave a Tg of around 285°C (Bizot et al., 1997).

2.1.7.1 Effect of Molecular Weight on Tg

Following the "free volume" theoretical definition of Tg, the decrease in the temperature of this phase transition can be related to an increase in the proportion of free volume in the polymeric system (Roos, 1995).

Early work by Fox and Flory (1950) on polystyrene reported that Tg increased rapidly with increasing average molecular weight (Mw), levelling off for Mw greater than 25000. They discovered a linear correlation between Tg and the inverse of Mw (Roos, 1995). From this work it was concluded that adding low molecular weight components to polymers would decrease the average Mw reducing the Tg.

Water Mw is very small in comparison with that of any polymer, influencing overall composition Tg. In the case of starch, water has a strong depressing effect on the Tg, addition of ~20% (wb) water depresses the Tg to room temperature (Zeleznak and Hoseney, 1987).

Similarly to water, other small molecules such as polyols can affect Tg. For example, the effect of glycerol on starch can be explained by its relatively small molecular weight, spacing out the molecules and reducing the interactions (Graaf et al., 2003). Other small Mw carbohydrates such as sucrose had also shown to have a plasticizing effect in similar systems (Kalichevsky, 1992).

A brief description of the structure and functionality of polyols commonly used in the foods products are presented in the following paragraphs.

Glycerol or glycerine (1, 2, 3-Propanetriol) has the formula $C_3H_8O_3$ with a molecular weight of 92.09 (NIST, 2005). It is a liquid, miscible with water, it has a sweet flavour and it is highly hygroscopic. Some of its main uses in the food industry are as solvent, humectant, plasticizer and sweetener for low calories products. As its chemical name suggests, it is formed by a propane backbone with one hydroxyl group bound to each carbon atom (figure 2.14).

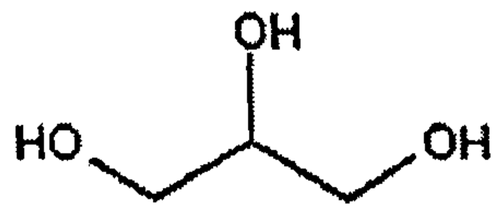

Figure 2.14. Chemical structure of glycerol (1, 2, 3-Propanetriol) (NIST, 2005).

Ethylene glycol (1, 2-Ethanediol) has the formula: $C_2H_6O_2$ with a molecular weight of 62.07 (NIST, 2005). Similarly to glycerol, it is a liquid, miscible in water and highly hygroscopic. The main limitation in the use of this compound is its high toxicity. The minimum lethal dose of undiluted EG is 1.4 mL/kg body wt in cats, 4.4 mL/kg body wt in dogs, 7-8 mL/kg body wt in poultry, and 2-10 mL/kg body wt in cattle (younger animals may be more susceptible) (MERCK, 2003). It is used as a solvent and plasticiser. Its chemical structure is based on a on hydroxyl groups bound to each carbon atom of the ethylene molecule (figure 2.15).

Figure 2.15. Chemical structure of ethylene glycol (1, 2-Ethanediol) (NIST, 2005).

Sorbitol is a much bigger molecule compared to glycerol and ethylene glycol. With chemical formula $C_6H_{14}O_6$ and a molecular weight of 182.17 (NIST 2005). It is available in liquid (solubilised in water) as in solid form. Sorbitol is used in low calorie candies and in many foods as both a sweetener and as a humectant. It also has extended application in pharmaceutical preparations sweetening agent and excipient.

Its structure is similar to glucose molecule with two added hydrogens on either side of what used to be the double bond connecting the oxygen to the carbon (figure 2.16).

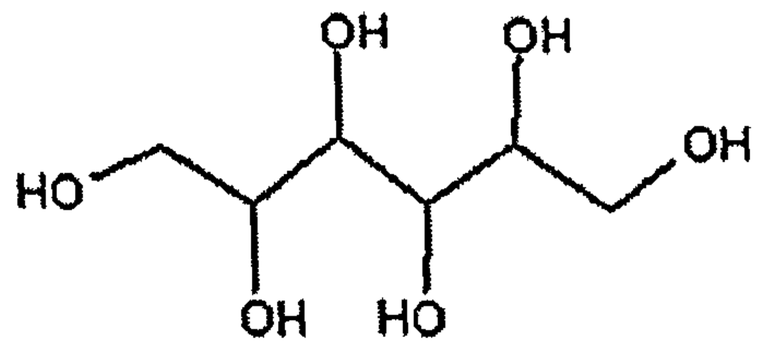

Figure 2.16. Chemical structure of Sorbitol (NIST, 2005).

Ideally, plasticizers should be non-volatile; reduce the sensitivity of the material properties of starch to changes in water content; and reduce the sensitivity of the material to ageing through crystallisation {Sperling, 1996; Moates et al. 200).

The ability of predicting the effect of plasticisers on Tg has tremendous significance in terms of the understanding of the functional and organoleptic properties of foods. One of the approaches used on mixtures is that developed by Couchman and Karasz (1978). They based their model (equation 2.6) on the thermodynamics of the system, relating Tg of binary blends of miscible polymers to composition (Roos, 1995).

$$Tg = \frac{x_1 Tg_1 + \left(\frac{\Delta Cp_1}{\Delta Cp_2}\right) x_2 Tg_2}{x_1 + \left(\frac{\Delta Cp_1}{\Delta Cp_2}\right) x_2} \qquad \textit{Equation 2.6}$$

where:

x_1 and x_2: mole fraction of components 1 and 2.

Tg_1 and Tg_2: glass transition temperatures of components 1 and 2.

ΔCp_1 and ΔCp_2: differences in heat capacities of components 1 and 2 below and above Tg

It has been suggested that this model could be expanded to more than two components. Kalichevsky and Blanshard (1992) modified the equation to tertiary mixtures in order to predict plasticisation effect of water on a mixture of amylopectin and casein.

A more detailed discussion of this equation and other models is presented on chapter 5 of this thesis.

2.1.7.2 Effect of Tg on Retrogradation Kinetics

Literature suggests that the glass transition temperature (Tg) can have a significant effect on retrogradation kinetics (Farhat et al., 2000b). At temperatures near the (Tg), the rate of nucleation is high but the rate propagation is low due to a dramatic increase in viscosity. At higher temperatures the increase in molecular mobility leads to an increase in crystal growth. For temperatures near melting (Tm), the rate of propagation is increased but the rate of nucleation is low. Over Tm, crystal nucleation and propagation would cease. Therefore, the maximum rate of crystallisation occurs at intermediate levels of supercooling (Roos, 1995; Slade and Levine, 1988). The next figure shows a representation of the effect of temperature on the crystallisation rate.

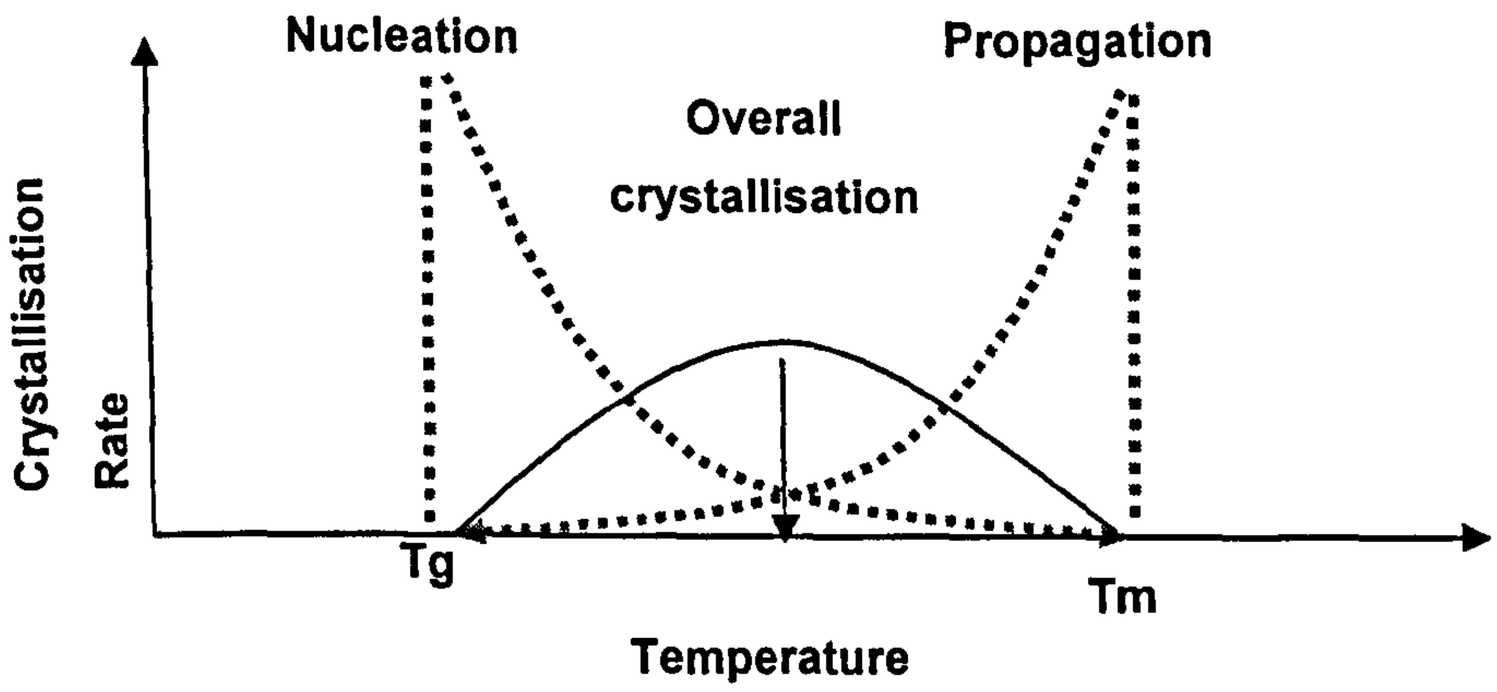

Figure 2.17. Diagram showing the polymer crystallisation kinetics (modified from Slade and Levine, 1988b).

Several theories exist to describe the effect of the temperature on the kinetics of polymer crystallisation. The Lauritzen-Hoffman (Lauritzen and Hoffman, 1973) theory based on the growth of chain-folded polymer crystals by deposition of the polymer chains on an existing crystal subtract is viewed as a secondary nucleation (Mousia, 2000). The crystallisation rate as a function of time is given by the following equation:

$$G(T) = G_o \exp\left[-\frac{U^*}{R(T - T_\infty)}\right]\exp\left[-\frac{K_g}{T\Delta Tf}\right] \qquad \textit{Equation 2.7}$$

where:

T : is the crystallisation temperature

U^* : activation energy

R : the gas constant

ΔT : the undercooling $\Delta T = Tm - T$, Tm being the melting temperature

f : factor accounting for the change in the heat of fusion with temperature

K_g : contant.

$$f = \frac{2T}{Tm + T} \qquad T_\infty = T_g - \delta T \qquad \textit{Equation 2.8}$$

T_∞ is a hypothetical temperature at which viscous flow is supposed to cease. It is related to Tg. For most synthetic polymer, $\delta T = 30K$ and $U^* \approx 6$ kJmol^{-1}.

Plasticisers can also affect the crystallisation kinetic by their influence on Tg and Tm. Figure 2.18 shows the effect of plasticizers on the rate of crystallisation. In this example, Tg and Tm are shifted to a lower temperature by the addition of a plasticiser (e.g. water, sugars, polyols). The rate of crystallisation will increase or decrease depending on the temperature at which the material is being stored (Farhat

et al., 2000a).

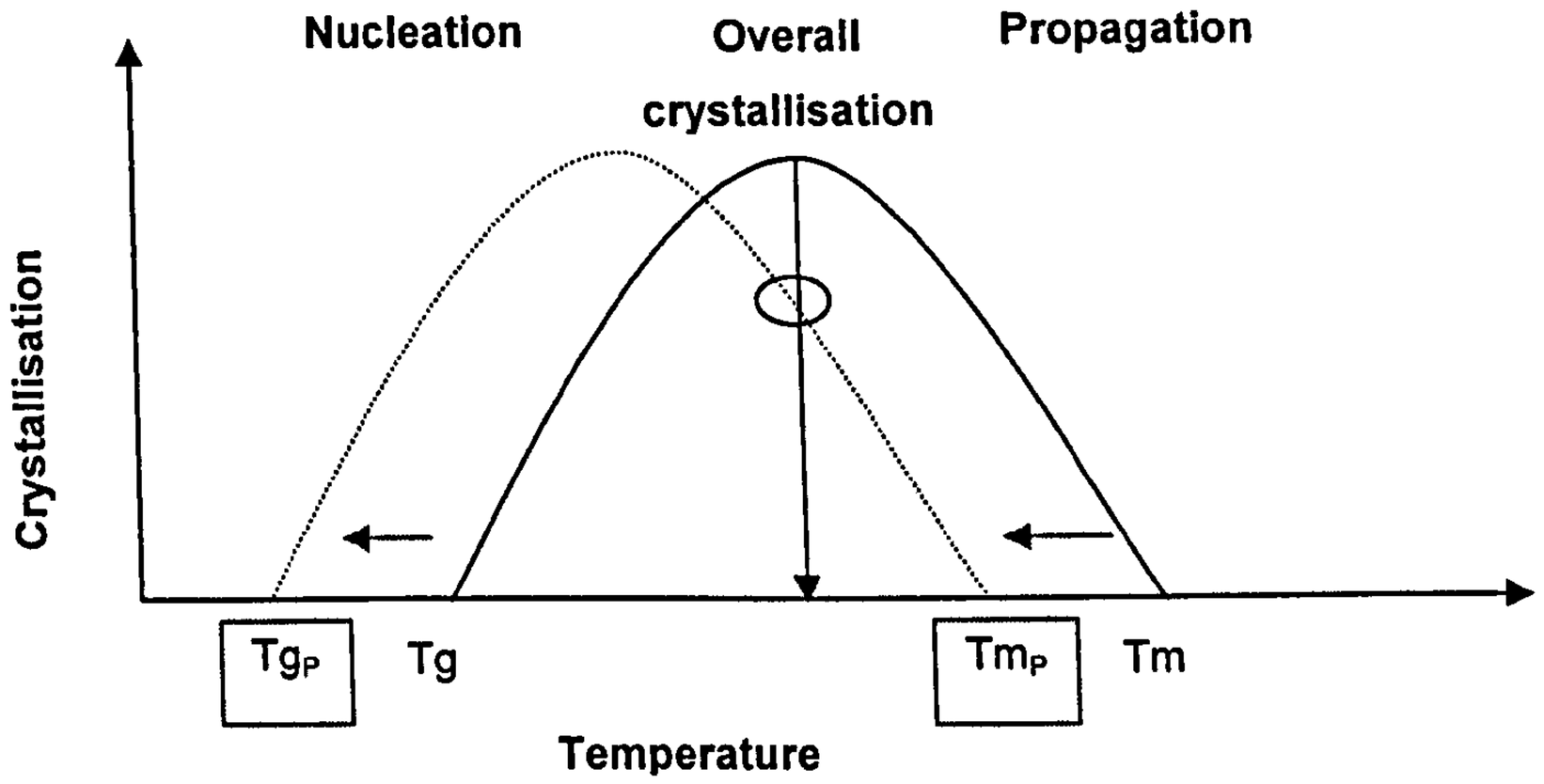

Figure 2.18. Effect of the addition of a plasticizers on Tg and Tm, in this example, decreasing the rate of retrogradation (Farhat et al., 2000a).

It has to be considered that the behaviour of starch based materials would also depend on the structural configuration, which would be mainly influenced by the manufacturing process.

The next paragraphs describe extrusion cooking as the common method of manufacturing starch based products. This description includes the extrusion process, types of extrusions, the main factors affecting this process and its effects on starch based materials.

2.2 Extrusion Cooking

Extrusion has been used in food industry for the last eighty-five years. Its first applications started in the early 1930s, where it was just limited to convey the food mixture through a die. Neither heat nor substantial mechanical energy was applied on early applications (Carvalho, 2001).

Nowadays extrusion cooking has become increasingly important. Very diverse applications ranging from confectionery processing to caseinate production, from solid fat manufacture to development of flavours (Kokini, Ho et al. 1992). The flexibility of the extrusion process allows the used of different raw materials to produce many different food products.

Proteins are commonly "texturised" during extrusion to produce "meat extenders" and "meat analogs", which are considered very similar in appearance, texture and mouthfeel to meats (Kearns et al., 2004). In the case of cereals many starch-based products are produced by extrusion such breakfast cereals, snacks, pasta products (Gomez and Aguilera, 1984), pet foods (Heldman and Hartel, 1997), degradable plastics (Blanche and Sun, 2004), nano-composites (Kalambur, 2004).

2.2.1 Extrusion Process

Definitions of the extrusion process includes general descriptions such as "an operation of producing rods, tubes and various solids and hollow sections, by forcing suitable material through a die by means of a ram for which a screw-drive is frequently used (Walker, 1995). Accordingly, food extrusion has been defined as "a technique for continuously forming a food product from a number of raw ingredient, which are conveyed forward by the extruder screw or screws" (Fletcher et al., 1985) or simply "forcing a pumpable product through a small opening to shape materials in a designed fashion" (Heldman and Hartel, 1997).

Extrusion cooking is considered as a high temperature short process or HTSP capable of generating high temperatures up to 180°C, high pressures ~ 7 Atm, and relatively high shear rates of 10 to 200s^{-1} (Carvalho, 2001).

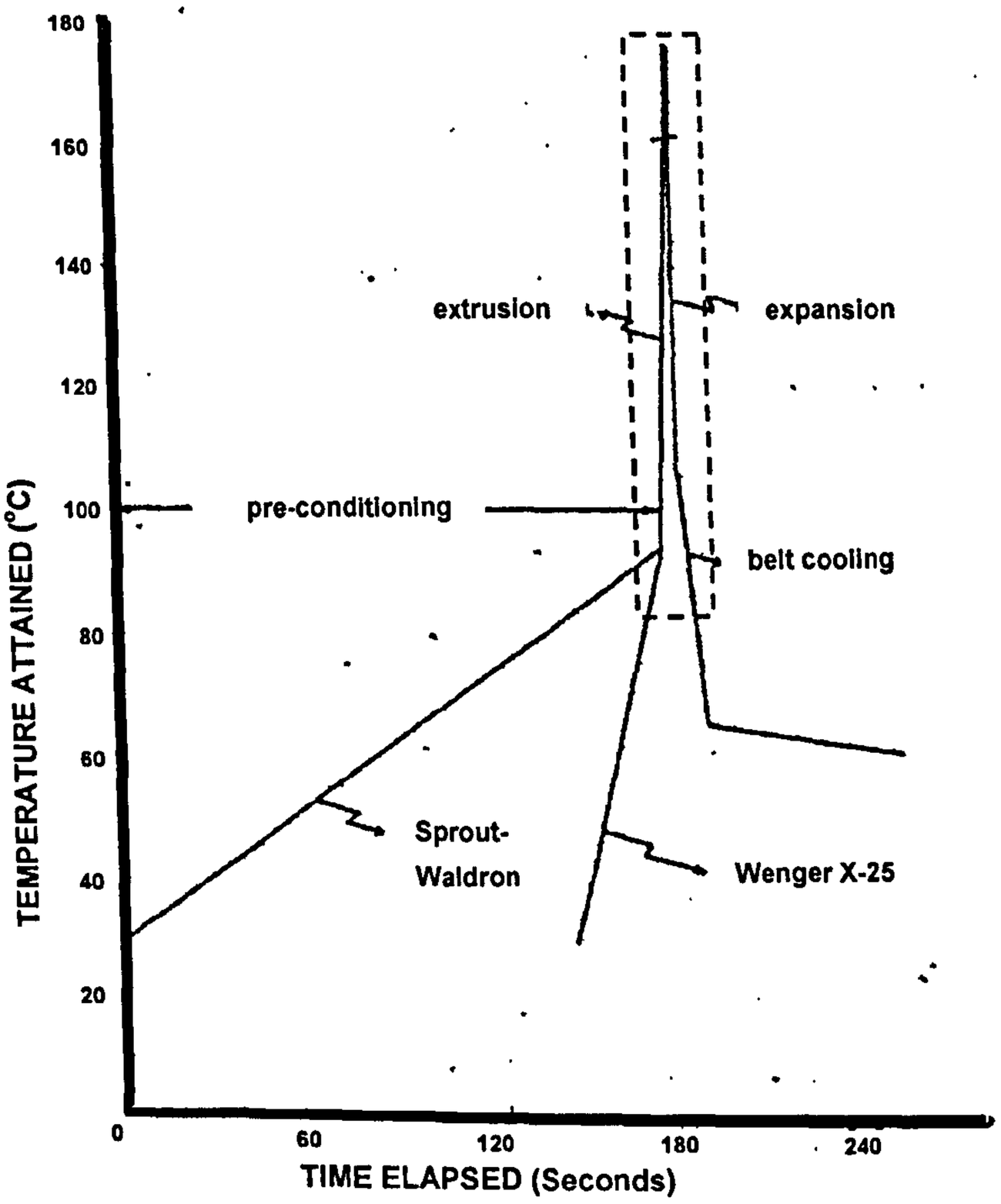

Figure 2.19. Temperature-time relationship for a complete extrusion process. Adapted from de Muelenaere, H. J. H. and Buzzardm J. L. (1969).

Figure 2.19 shows an example of a time-temperature relationship for the whole food extrusion process. It is clear that the actual extrusion step (dotted line) is very short compared with the preconditioning and post extrusion cooling.

Thermo-mechanical extrusion is a continuous process in which a rotating screw is used to force the food material through the barrel of the machine and out through a narrow die opening. In this process the food is simultaneously transported, mixed, shaped, stretched and sheared under elevated temperature and pressure.

To better characterise the effect of some of these parameters on the final product, the specific mechanical energy (SME) was defined (Van Lengerich, 1990):

$$SME = \frac{M_d \omega n}{m} \qquad \textit{Equation 2.9}$$

where:

SME = specific mechanical energy (Wh/kg)

M_d = torque (Nm)

ω = rotational speed of screw (h^{-1})

m = mass flow rate (kg/h)

n = number of screws

The SME is commonly used to evaluate the effect of energy input on raw materials and its impact on the final products.

2.2.2 Type of Extruders

In the food industry there are two types of extruders commonly used; single and twin screw. The choice will depend mainly on the physicochemical characteristics of the raw materials to be processed and the required specification of the final product.

2.2.2.1 Single Screw Extruder

Single screw extrusion is one of the core operations in polymer processing and is also a key component in many other processing operations. The foremost goal of a single screw extrusion process is to build pressure in a polymer melt so that it can be extruded through a die or injected into a mould.

According to Harper (1992), the screw can be divided into three sections: feed, transition and metering (figure 2.20). The feed zone receives and conveys the food materials into the extruder along the barrel. The significant volume difference between the screw and the barrel allows an efficient mixing. The transition section is the location where the compression ratio increases and most of the mechanical energy is transferred to the food mixture increasing its temperature. It is in this section where the actual cooking starts, the different ingredients (usually in the powder form) begin to melt forming a viscous liquid.

Lopez (2003) mentioned three possible mechanisms of heat transfer to the dough: viscous dissipation of mechanical energy, heat transfer from steam or electrical heaters surrounding the barrel or direct injection of steam in the extruder barrel.

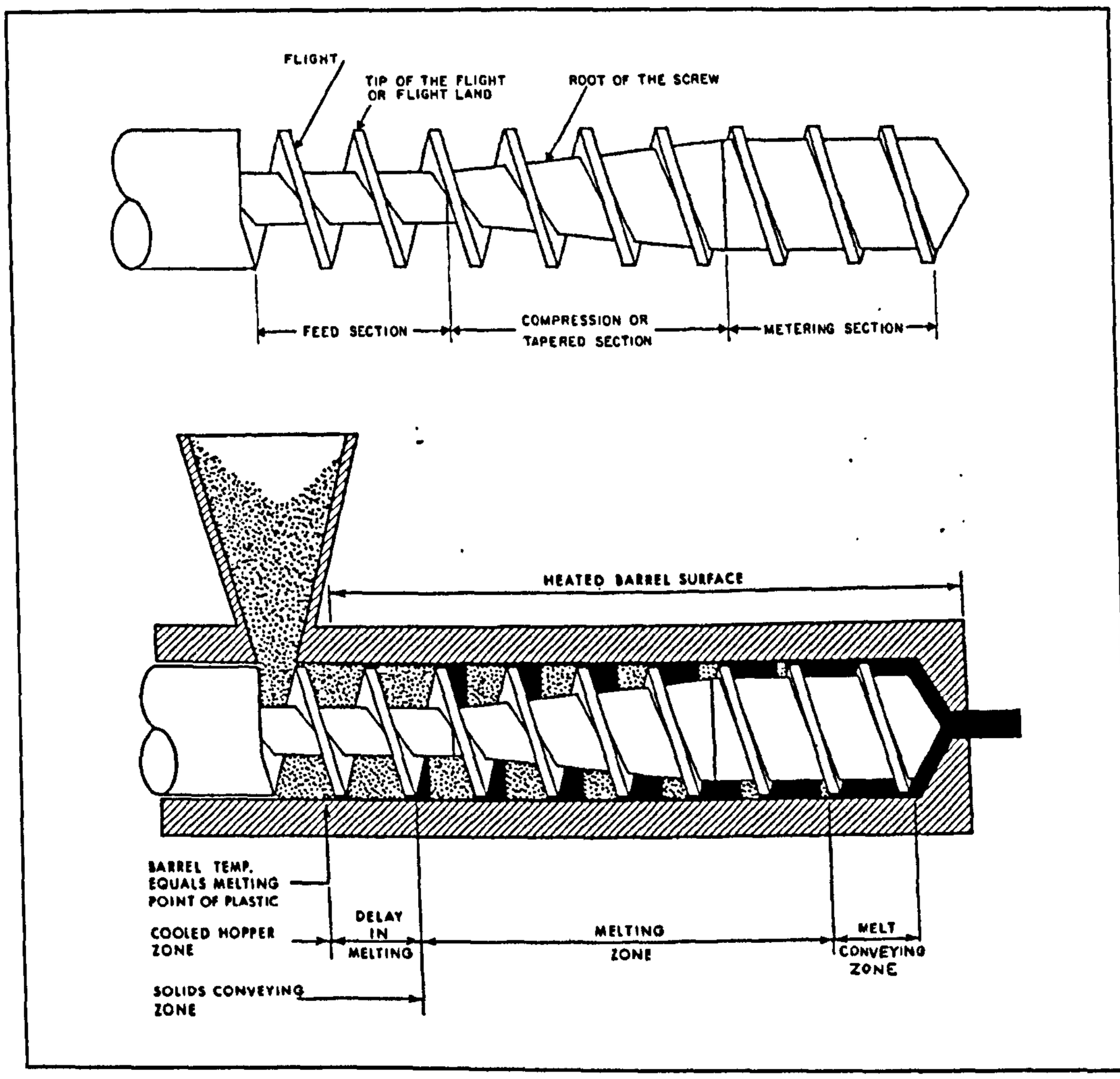

Figure 2.20. Schematic representation of a cooking extruder (modified from Tadmor and Klein, 1970).

Some of the drawbacks of using a single screw extruder include: low mechanical efficiency, since a large part of the energy supplied by the shaft is dissipated as heat and its limited use because of its inability to transport sticky and gummy materials. For example for some raw materials containing a high lipid content, the barrel wall produces insufficient resistance to prevent the product from slipping thus spinning with the screw instead of being conveyed (Carvalho, 2001). The reason is that the transport mechanism is based of frictional forces between the material and the barrel

walls (Lopez, 2003). It has also been mentioned that the mixing capabilities of this type of extruders are limited due to its flows conditions usually being laminar (Carvalho, 2001).

The mixture flow inside the barrel has been described as a combination of drag and pressure flows (Harper, 1981). The drag flow is created from the pumping action of the edge of the screw, forcing the fluid adhering to the barrel wall and slipping freely from the root of the screw.

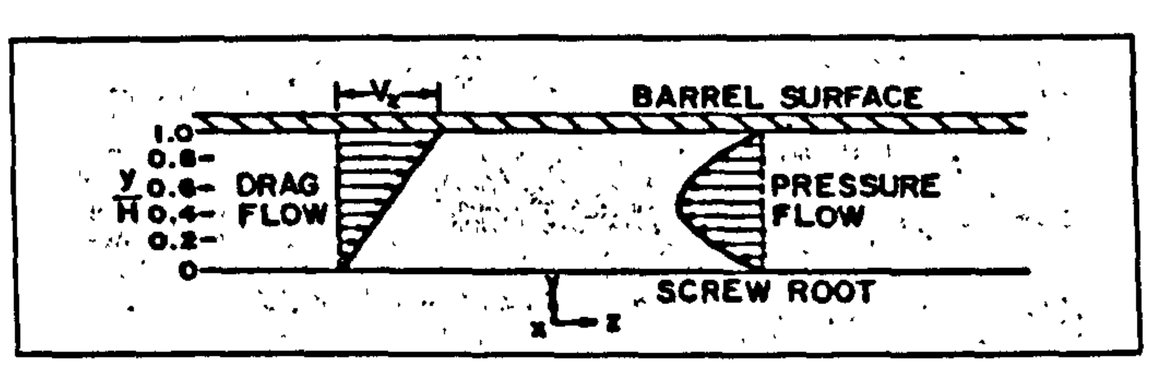

Figure 2.21. Velocity profile in a single screw extruder (modified from Harper, 1981)

2.2.2.2 Twin Screw Extruder

Twin screw extrusion is used extensively for mixing and compounding polymeric materials. The flexibility of twin screw extrusion equipment allows this operation to be designed specifically for the formulation being processed. For example, the two screws may be co-rotating or counter-rotating, intermeshing or non-intermeshing (Table 2.22). In addition, the configurations of the screws themselves may be varied using forward conveying elements, reverse conveying elements, kneading blocks, and other designs in order to achieve particular mixing characteristics (Harper, 1992).

The co-rotating configuration allows the material to be transferred from the channel of one screw to the other producing a self-cleaning action preventing material from sticking to the screw preventing heat sensible material from degradation. This configuration also contributes to the efficient mixing of individual components improving the end product homogeneity (Lopez, 2003).

Table 2.22. Twin screw extruder configurations (Harper, 1992).

SCREW ENGAGEMENT		SYSTEM	COUNTERROTATING	COROTATING
INTERMESHING	FULLY INTERMESHING	LENGTHWISE AND CROSSWISE CLOSED	1 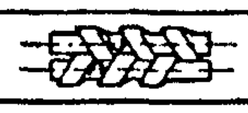	2 THEORETICALLY NOT POSSIBLE
		LENGTHWISE OPEN AND CROSSWISE CLOSED	3 THEORETICALLY NOT POSSIBLE	Screws 4 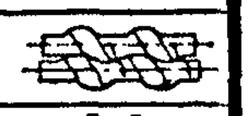
		LENGTHWISE AND CROSSWISE OPEN	5 THEORETICALLY POSSIBLE BUT PRACTICALLY NOT REALIZED	Kneading disc 6 
	PARTIALLY INTERMESHING	LENGTHWISE OPEN AND CROSSWISE CLOSED	7 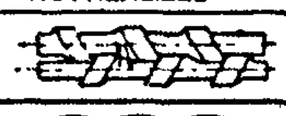	8 THEORETICALLY NOT POSSIBLE
		LENGTHWISE AND CROSSWISE OPEN	9A 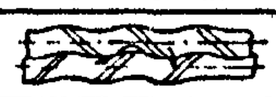	10A 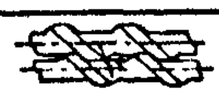
			9B 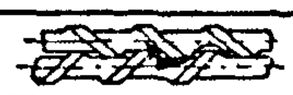	10B 
NOT INTERMESHING	NOT INTERMESHING	LENGTHWISE AND CROSSWISE OPEN	11 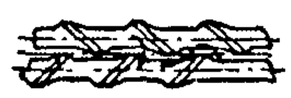	12 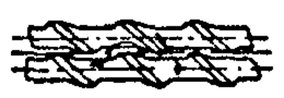

2.2.3 Factors Affecting Food Extrusion

2.2.3.1 Material Feeding

2.2.3.1.1 Moisture level

Variations in water feed rate will have a direct effect on the mixture viscosity and process throughput influencing the overall SME. This change in energy input would have a significant effect on the processability of the raw material.

In the case of starch extrusion, changes in moisture will affect gelatinisation. This is mainly caused by the plasticizing effect of water, reducing the glass transition and melting temperatures of the polymer (Blanche and Sun, 2004). This change on the Tg can have a significant impact on the expansion of the product at the exit of the die. Carvalho (2001) and Lopez (2003) reported increasing in the maize extrudate bulk density when Tg increased.

2.2.3.1.2 Type of feed materials

The type of feed material such as protein, starch, lipid, and moisture plays a significant role on the nature of extruded products. Each of these components will have different viscosities affecting the mechanical performance of the mixture during the extrusion process. This will have a significant effect on the end product internal structure. For example, adding whey proteins to grain-type extruded products will significantly alter the gel structure during extrusion cooking, hence a different

product will be produced (Tattiyakul, 2004).

2.2.3.1.3 pH of ingredients

Changes on the feed materials pH can have an effect on some of the components such as proteins that can undergo conformational changes. Other effects from the change of this parameter include change in texture, colour and nutritional value of the final extrudate (Heldman and Hartel, 1997; Tattiyakul, 2004).

When using an extruder as a bioreactor, an optimum pH range needs to be carefully chosen. For example, in production of maltodextrin from starch using enzyme alpha-amylase, an optimum pH for the enzyme would be 5.0-8.0. Lowering pH value in this case will inhibit the enzyme activity.

2.2.3.1.4 Particle size of feed materials

Particle size distribution of the feed materials can have a significant effect on the paste properties during extrusion (Carvalho, 2001; Chen et al., 2000; Garber et al., 1997; Lopez, 2003).

Is has been found for rice flour that expansion of the extrudates is reduced when the particle size decreased. The mechanism is thought to be related to a more uniform internal cell distribution (Ryu and Lee, 1988). A decrease in starch conversion has also been observed for large particle size at relatively high moisture contents (20%wb) from the changes in rate of water diffusion (Garber et al., 1997).

2.2.3.1.5 Other ingredients

Ingredients such as oil and emulsifier may also be added to the feed material to decrease viscosity of the raw material reducing the amount of viscous heat dissipation (Tattiyakul, 2004). These compounds would also have a lubrication effect on the extrusion process affecting the shear effect on the polymeric structure of the polymer.

2.2.3.2 Extruder operating parameters

2.2.3.2.1 Feed rate

The effect of feed rate on the extrusion performance seems to be related to a change

in the SME. When the feed rate is increased, the average residence time is decreased reducing the total energy input. This would have an antagonist effect on the material transformation. Despite the logic of this rationale some experimental work has shown the opposite behaviour (Carvalho et al., 2003).

2.2.3.2.2 Screw speed

Screw speed affects the degree of fill within the screw, residence time distribution of product flowing through the extruder, heat transfer rates, mechanical energy input in the extruder, and the shear forces exerted on the materials. The normal minimum screw speed range is 70-100 rpm. Below this, the volumetric capacity would be severely limited and make the majority of food extrusion products costly to manufacturers (Tattiyakul, 2004).

2.2.3.2.3 Barrel temperature

Most extruders operate with temperature control. The pressure differentials and shear stress forces influence reaction rates and generate frictional heat. Barrel heating generates conductive and convective heat in the filled and partially filled zones. The effect of the generated heat will depends on the physical and rheological properties of the feed (e.g., specific heat, phase transition temperature, moisture content, density, particle size and gelatinisation enthalpy), the barrel temperature profile and the available motor power (Tattiyakul, 2004).

2.2.4 Effect of Extrusion on Starch

Extrusion is a very complex process where design factors (e.g. screw geometry, die size/shape, dimension of the barrel) and controllable variable (e.g. temperature, screw speed, feed rate, water rate added) can have a significant effect on the final product quality.

2.2.4.1 Starch Conversion During Extrusion

During extrusion, starches are subjected to relatively high pressure (up to 70 Atm), heat and mechanical shear forces (Lai and Kokini, 1990).

The major changes occurring to starch during extrusion are the disruption of the

crystalline regions in the granule followed by a loss of granule integrity, formation of amylose-lipid complexes (Mitchell and Areas, 1992) and polymer fragmentation (Lai and Kokini, 1991).

Surface response designs have shown that the interaction between the variables temperature and moisture content is an important factor affecting conversion of starch on a twin extruder (Owasu-Ansah et al., 1983). This interaction is not a simple one, Lai and Kokini (1991) showed that at low temperatures (65 and 75°C) moisture alone did not affect starch transformation but it enhanced its conversion at higher temperatures (95 and 110°C).

Lai and Kokini (1990) demonstrated that if the moisture present in the barrel is increased even further, the conversion of high amylopectin extruded corn starch decreased. These results support the importance of the shear force factor on this process especially at lower temperatures. This parameter has been considered the main factor affecting the starch fragmentation during extrusion (Mitchell and Areas, 1992).

2.2.4.2 Starch Fragmentation

The fragmentation of the starch amylopectin and amylose is a product of the high shear forces in the extruder screws and barrel. This fragmentation has been detected as a "complete destruction of the crystalline structure of the native granule" measured by X-ray diffraction and visualised using scanning electron microscopy (SEM) (Chinnaswamy et al., 1989).

A change in molecular size has also been detected by a decrease in viscosity, an increase in starch solubility (Colonna et al., 1984) and a change in elution profiles using gel-permeation chromatography (GPC) after extrusion (Chinnaswamy et al., 1989; Colonna and Mercier, 1983). It is believed that this fragmentation can lead to further partial hydrolysis or drextrinization of the starch molecules (Lai and Kokini, 1991).

Gomez and Aguilera (1983) studied the physicochemical changes of the corn starch fraction during extrution. They showed that when the moisture content decreased during extrusion there was an increase in water solubility (WSI), enzyme

susceptibility (ES), degree of gelanisation (DG) and blue value (BV), while water absorption index (WAI) and water insoluble carbohydrate decreased (table 2.2). The changes of these parameters suggest a decreased in the molecular size or fragmentation of the biopolymer by increasing the shear due to friction generated in the extruder.

Table 2.2. Physicochemical properties of corn extrudates (Gomez and Aguilera, 1983).

	EMC[b] (%)	ES[c] (g maltose/100g)	DG[d] %	BV[e]	WIC[f] (%)	WSI[g] (%)	WAI[h] (g/g)
Raw	–	0.43 ± 0.1	0.00	0.00	74.62 ± 2.0	4.23 ± 0.1	1.73 ± 0.00
E1	23.7	7.68 ± 0.2	33.96 ± 2.0	8.60 ± 0.4	51.69 ± 1.5	16.17 ± 2.1	7.22 ± 0.06
E2	18.5	8.39 ± 0.2	48.00 ± 2.0	10.10 ± 0.3	37.05 ± 2.0	27.07 ± 1.2	6.57 ± 0.10
E3	15.4	9.07 ± 0.2	68.63 ± 1.5	9.73 ± 0.3	31.78 ± 2.0	30.20 ± 2.3	5.34 ± 0.12
E4	13.9	9.01 ± 0.1	70.37 ± 2.0	10.64 ± 0.4	26.70 ± 1.5	35.94 ± 0.3	5.79 ± 0.11
E5	7.6	10.13 ± 0.2	96.36 ± 2.0	11.03 ± 0.4	21.43 ± 1.5	46.00 ± 1.5	42.5 ± 0.10

(a) The data are averages of two determinations. Values are listed as means with confidence intervals with 95% confidence.
(b) Moisture content before extrusion.
(c) Enzyme susceptibility.
(d) Degree of gelatinization
[e]Blue value.
[f]Water insoluble carbohydrate.
[g]Water solubility index.
[h]Water absorption index.

Measureing ES and WSI from surface response statistical design, Gomez and Aguilera (1983) suggested that the obtained extrudates were a composite of gelatinised and dextrinized starch. This was also supported by SEM analysis on the different mixtures. Later work (Gomez and Aguilera, 1984), showed that reducing extrusion moisture content resulted in a progressive change from gelatinised-like to destrinized-like extrudates. Maximum gelatinisation was observed at about 29% moisture. Below 20% moisture, dextrinization becomes predominant during high-shear cooking-extrusion.

The mechanism of fragmentation suggested is in the form of limited debranching in the amylopectin, which causes significant decreases in the molecular size without changing the percentage of the 1→6 bonds as analysed by the relative number of reducing end groups (Lai and Kokini, 1991). In the case of amylose, fragmentation is thought to be in the form of random chain splitting (Colonna et al., 1984). This structural change seems to affect amylopectin more than amylose. Colonna et al (1984) calculated the reduction in the average molecular weight of amylopectin and amylose by a factor 15 and 1.5 respectively.

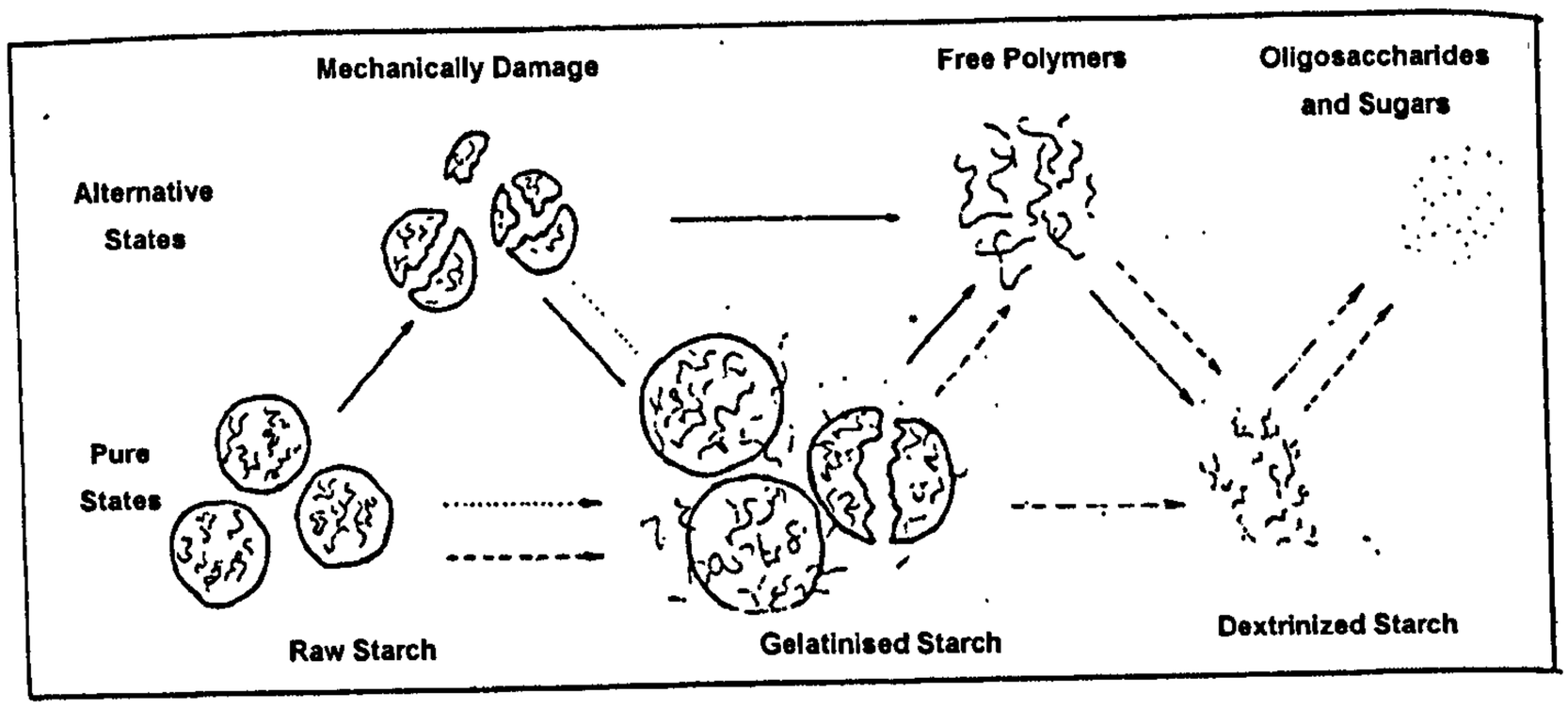

Figure 2.23. Proposed model of starch degradation during extrusion: ⟶ Shear; -----► Heat; ·····► Moisture (Gomez and Aguilera, 1984).

2.2.4.3 Amylose-Lipid Complex Formation

Amylose-lipid complexation occurs when lipids form an inclusion compound with amylose, with the hydrocarbon portion of the lipid located with helical cavity of amylose (Kaur and Singh, 2000).

The formation of this complex can have important effects on the functional properties of starchy materials. Seneviratne and Biliaderis (1991) reported a decrease in the water solubility and susceptibility of starches to alpha amylase digestion. Other starch physicochemical properties such as swelling power has also been reported as affected when amylose-lipid complexes are formed (Hoover and Hadziyev, 1981). Importantly a decrease in starch retrogradation has been reported when amylose has been complexed with oleic acid or linoleic acid (Mercier et al., 1980).

It is believed that in the kneading zone of the extruder, the raw ingredients are transformed into a dough like mass under effect of mixing and mild shear forces with heat generation. The increase in mixing at the final cooking zone, where the product moves in opposing direction, with the maximum generation of heat due to the friction generated (Guzman et al., 1992). This combination of high energy mixing and temperature provides sufficient energy for the interaction amylose-lipid complex to be formed

Other factors such as different concentrations of moisture in the extruder barrel have been observed to have a significant effect on the extent of the complexation (Ho and Izzo, 1992).

2.2.5 Extrusion of Pet-care Products

Extrusion cooking of pet foods can be regarded as the cooking, shaping and cutting of raw ingredients into a specific shape and size in a very short space of time, while simultaneously destroying detrimental micro-organisms. For this type of products, extrusion cooking presents some advantages over other dry food technologies for the following reasons: (a) it is a high productive operation unit as it allows a continuous production of different sizes and shapes of product without delay in production; (b) it is able to process a larger variety of foods by enabling different combinations of ingredients.

A general description of the manufacturing process is presented on figure 2.24. The ingredients are mixed into an homogenous dough which is cooked in the extruder barrel. Then, the material is forced through a specially designed die plate under pressure and high heat. This causes rapid cooking of the cereals in the mixture within the product improving the product digestibility. After cooking, the semi-finished products are then allowed to cool, before being sprayed with a coating that includes liquid fat and proteins, to enhance appeal and add protein and fat to the food. Hot air drying then reduces the total moisture content to 10% or less.

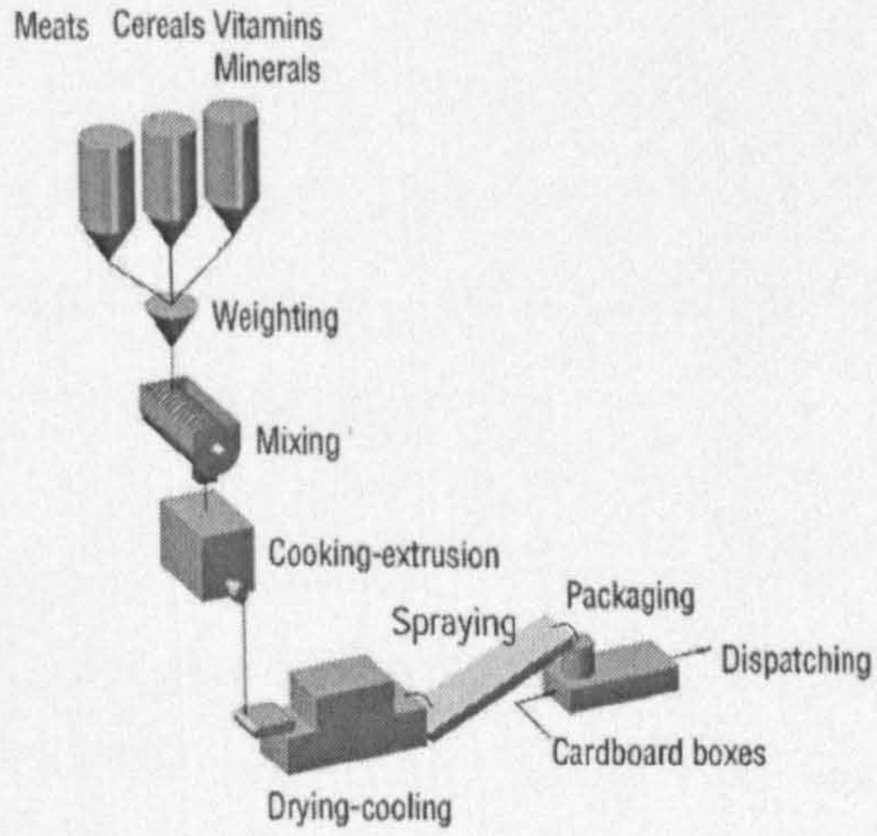

Figure 2.24. General diagram describing the pet-food extrusion process

In general, pet food formulations aim to provide optimum nutritional balance. To achieve this, proteins and cereals are present in an important proportion of the total

mixture mass. But in the particular case of pet-care product or "treats", the aim is to produce products with properties other than nutritional. For example products with a long lasting texture to clean the animal teeth and gums or long lasting artificial bones for entertainment. The formulation for these materials is characterised in having a higher proportion of cereals than normal pet foods.

A more detail discussion of the formulations of these products and its manufacturing is presented in chapter 8.

3 Materials and Methods

Material science applied to food systems is an innovative approach that emphasizes the fundamental and generic similarities between synthetic polymers and food molecules. On this basis, the functional properties of food materials during processing and product storage can be explained and often predicted. Following this rationale, analytical techniques traditionally used in the synthetic polymer world are now applied to food components. The following paragraphs give a brief description of such techniques used during the work described in this thesis. The systems analysed were extruded starches from different botanical sources which were processed in the presence of water and different concentrations of glycerol. Starch-based products were also characterised using similar approach.

3.1 Materials

The materials used were wheat starch (WS)-13%MC (wb), obtained from Avebe, Holland, waxy maize starch (WMS)-13%MC (wb) variety Amioca, obtained from National Starch and Chemical Co. UK, rice starch (RS)-10%MC (wb) obtain from Sigma UK, and Glycerol (99% purity) from Merck UK,.
A detailed description of the pet-care product is presented in chapter 8.

3.2 Equipment

Starch-glycerol samples were prepared by thermo-mechanical cooking. This method of cooking starch is typical of many food products and it is also used in the manufacture of commercial pet-care products.

3.2.1 Extruder

A Clextral BC-21 (Firminy, France) twin screw, co-rotating extruder was used to prepare the samples. The 400 mm barrel has a 1:16 length to diameter ratio and consists of four modules each 100 mm long.
The extruder was equipped with a slit die dimension of 1 mm in height, 30 mm in width and 14.5 mm in length. The schematic diagram of the extruder is shown in figure 3.1. A volumetric feeder (K-tron T20 Niederlenz, Schweiz, Switzerland) was used to

feed the material (powder) into the extruder. Distilled water was continuously added using a DKM-Clextral (type: TO/2 Firminy, France) volumetric pump. Both, the feeder and the water pump were calibrated prior the extrusion in order to give the desired formulation.

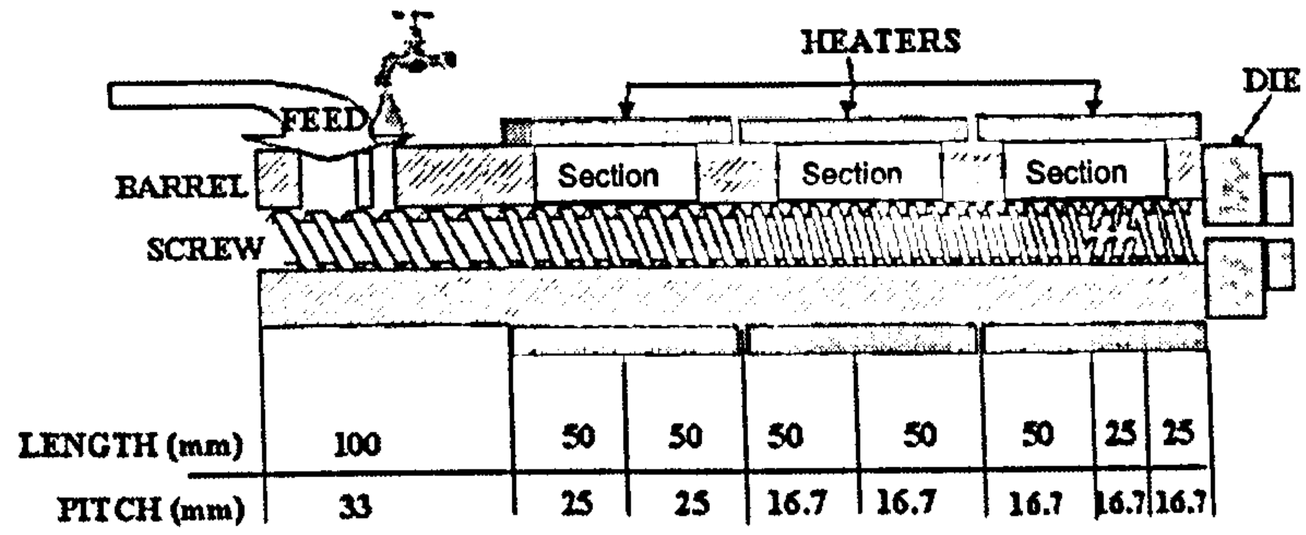

Figure 3.1. Schematic diagram of the Clextral BC-21 twin extruder. (Norton, C. 1998).

Glycerol was added by a syringe pump (Harvard Apparatus Model 55-5920 USA) using a syringe with an internal diameter of 35mm. The glycerol was directed added into the extruder barrel.

3.2.2 Other Equipment

Other equipment used for the sample preparation is listed in table 3.1.

Table 3.1. Other equipment used in sample preparation.

Equipment	Brand/Model
Balance	Sartorious 1518. Germany
Oven (105°C)	Gallenkamp oven 300 plus series. UK
Oven (70°C)	Thomas Collins & Co. (Bristol) Ltd. UK
Vacuum oven (70°C)	Gallenkamp. UK.
Freezer (-80°C)	Denley. UK
Infrared drier	Sartorius Thermo Control YTC 01L. Germany
Planetary mixer	Kenwood –Peerless, Peerless and Ericsson Ltd. UK
Shaker AS200	Retsch, Haan. Germany
Knifetec mill	Foss Tecator. Model 1095, Sweden
Freeze Drier	Dryer Super Modulyo, Edwards Pirani 1001, UK
Optical microscope	Enrst Leitz Wetzlar GmbH. Germany

3.2.3 Sample Preparation

3.2.3.1 Extrusion

Waxy maize (WMS), rice (RS) and wheat starches (WS) were fed into the extruder barrel in native form (powder). Distilled water and glycerol were directly pumped into section 1 of the extruder (figure 3.1). The glycerol concentration in the final products was 0 (control), 5, 10, 15 and 20% (db). The feeding rate of the solid (starch) and liquids (water and glycerol) was adjusted in order to obtain a fully translucent ribbon at the exit of the extruder die keeping a similar specific mechanical energy (SME) for the different mixtures. In general the final moisture concentration obtained was ~35% (wb). Table 3.2 shows the extruder setting, the material feed rate and the calculated specific mechanical energy (SME) for the different starch-glycerol formulations.

For all the starch-glycerol mixtures the SME was calculated using the relationship described by:

$$\text{SME}\,(\text{W.h.kg}^{-1}) = \frac{\text{screw torque}\,(\text{N.m}) \times \text{screw speed}(\text{r.p.m.}) \times 2 \times \pi \times \text{number of screws}}{\text{mass flow rate}\,(\text{kg.h}^{-1}) \times 60}$$

Table 3.2. Extruder settings and SME for waxy maize starch-glycerol mixtures.

	Control	**5% Glycerol**	**10% Glycerol**	**15% Glycerol**	**20% Glycerol**
Barrel Thermal Profile (*)	*Section 2*: 90°C *Section 3*: 150°C *Section 4*: 91°C	*Section 2*: 90°C *Section 3*: 150°C *Section 4*: 90°C	*Section 2*: 90°C *Section 3*: 150°C *Section 4*: 90°C	*Section 2*: 90°C *Section 3*: 150°C *Section 4*: 91°C	*Section 2*: 88°C *Section 3*: 150°C *Section 4*: 89°C
Mat. Feed Rate	4 kg/h	4 kg/h	4 kg/h	4 kg/h	4 kg/h
Water Feed Rate	1.4 kg/h	1.3 kg/h	1.1 kg/h	1.1 kg/h	0.9 kg/h
Glycerol Feed Rate	0.0 kg/h	0.18 kg/h	0.35 kg/h	0.53 kg/h	0.70 kg/h
SME	**54 Wh/kg**	**49 Wh/kg**	**50 Wh/kg**	**48 Wh/kg**	**45 Wh/kg**

Table.3.3. Extruder settings and SME for rice starch-glycerol mixtures.

	Control	**5% Glycerol**	**10% Glycerol**	**15%Glycerol**	**20% Glycerol**
Barrel Thermal Profile (*)	*Section 2*: 90°C *Section 3*: 90°C *Section 4*: 70°C	*Section 2*: 90°C *Section 3*: 90°C *Section 4*: 70°C	*Section 2*: 90°C *Section 3*: 90°C *Section 4*: 70°C	*Section 2*: 90°C *Section 3*: 90°C *Section 4*: 70°C	*Section 2*: 90°C *Section 3*: 90°C *Section 4*: 70°C
Mat. Feed Rate	5 kg/h	5 kg/h	5 kg/h	5 kg/h	5 kg/h
Water Feed Rate	2.0 kg/h	1.9 kg/h	1.6 kg/h	1.6 kg/h	1.5 kg/h
Glycerol Feed Rate	0.0 kg/h	0.22 kg/h	0.44 kg/h	0.66 kg/h	0.88 kg/h
SME	**68 Wh/kg**	**64 Wh/kg**	**66 Wh/kg**	**63 Wh/kg**	**61 Wh/kg**

Table.3.4. Extruder settings and SME for wheat starch-glycerol mixtures.

	Control	5% Glycerol	10% Glycerol	15%Glycerol	20% Glycerol
Barrel Thermal Profile (*)	*Section 2*: 82°C *Section 3*: 80°C *Section 4*: 60°C	*Section 2*: 83°C *Section 3*: 80°C *Section 4*: 60°C	*Section 2*: 83°C *Section 3*: 80°C *Section 4*: 60°C	*Section 2*: 85°C *Section 3*: 80°C *Section 4*: 60°C	*Section 2*: 84°C *Section 3*: 80°C *Section 4*: 60°C
Mat. Feed Rate	3.5 kg/h	3.5 kg/h	3.5 kg/h	3.5 kg/h	3.5 kg/h
Water Feed Rate	2.5 kg/h	2.3 kg/h	2.1 kg/h	2.0 kg/h	1.8 kg/h
Glycerol Feed Rate	0.00 kg/h	0.15 kg/h	0.30 kg/h	0.50 kg/h	0.60 kg/h
SME	**52 Wh/kg**	**53 Wh/kg**	**53 Wh/kg**	**53 Wh/kg**	**53 Wh/kg**

(*) The first section is not temperature controlled.

After extrusion, the ribbons (~15cm long) were hermetically packed, quenched under liquid nitrogen (N_2) and stored at -80°C.

Further sample preparation was tailored (e.g. geometry) depending of the type of analysis and analytical technique used.

The nomenclature for each starch type after extrusion was WMSE for waxy maize starch extrudates; RSE for rice starch extrudates and WSE for wheat starch extrudates.

Next section describes the analytical techniques and methods used in the analysis of the starch-glycerol extrudates. A brief description of the fundamental theory and applications examples for starch based materials are also presented.

3.3 Analytical Techniques

The analyses of the model systems (starch-glycerol extrudates) were carried out to establish the following:

a) The uptake and loss of water at different relative humidities (sorption isotherms) and the rate associated to this change of moisture content.
b) The glass transition temperature by mechanical spectroscopy and calorimetry.
c) The degree of molecular order by DSC and wide angle WAXS.

Theory related to these techniques is given, followed by the specific methodology used for each experiment including a description of the sample preparation.

3.3.1 Dynamic Vapour Sorption (DVS)

Traditionally, sorption isotherms of materials have been obtained from water vapour equilibration over solutions in hermetically sealed containers. Different relative humidities can be created by materials whose affinity for water regulates the water vapour pressure in the atmosphere surrounding the material. Among the more readily controllable materials are salt solutions (saturated) and acid solutions (Labuza 1994). Numerous lists of the humidities created by various salts and acid concentrations appear in the literature (Martin 1962, Iglesias and Chirife 1982)

The main advantages of using these substances are the low costs involved in their use and the relative high accuracy in producing a determined relative humidity. Nevertheless in order to obtained reproducible results, controlled experimental conditions are needed. Labuza (1994) stated that stable relative humidities would depend on purity of salts, purity of water, the preparation of the salt solution, the water vapour equilibrium rate between the liquid and vapour, equilibrium temperature between the liquid and vapour and by the presence of hygroscopic materials within the vapour space. Another disadvantage related to this method is its discrete nature. Frequent weight measurements are needed before reaching equilibrium. This would bring changes in the relative humidity each time the container is opened to weigh the material thus affecting the surroundings of the sample. Moreover, physical phenomenon that may occur during equilibration (crystalline-amorphous transitions) may be undetected.

Instrumental techniques have been developed to improve accuracy during sorption/desorption experiments. Two methods commonly used are based on gravimetric and barometric changes during the equilibration. For the gravimetric method, the rate of change in weight of a polymer sample is recorded, while barometric techniques record the rate of change in pressure in a sorption cell. Other methods of determining sorption rates include measurement of the change in volume on an isobaric sorption cell and the penetration depth of a swelling front (Felder and Huvard 1980).

Due to its simplicity and sensitivity, gravimetric techniques are generally preferred over barometric. The gravimetric technique includes a set of different components

such as a microbalance, an incubator, a relative humidity controller and an electronic logger (PC). This type of method can be also used to measure diffusivity, where the kinetics of sorption/desorption can be easily obtained after recording the changes in weight at specific time intervals.

The analytical instrument used for the sorption studies presented is this work is the Dynamic Vapour Sorption or DVS (Surface Microsystems London, UK). It is a gravimetric technique based on a continuous determination of changes in weight when materials are exposed to different partial vapour pressures (water vapour in this case). It is also classified as a dynamic method as continuous flow of a gas is flown over the sample.

This instrument was acquired at the time this project started, thus significant time was dedicated to the validation of the methodology. Experimental data from sorption isotherms for different starches equilibrated over saturated salt solutions were compared with DVS data. Results were comparable to the validation experiment obtained by Surface Microsystems validation experiments using (e.g. microcrystalline cellulose, RM 302) (table 3.5).

Table.3.5. Sorption data comparison (equilibration over saturated salt solutions) and DVS (Levoguer and Booth).

Relative Humidity (%)	Mean % H_2O Content COST 90	Mean % H_2O Content DVS-1	Standard Deviation DVS-1
11.05	2.13 ± 0.11	2.45	0.026
22.45	3.24 ± 0.12	3.59	0.041
33.00	4.15 ± 0.09	4.40	0.029
42.76	5.16 ± 0.09	5.02	0.027
52.86	5.97 ± 0.14	5.89	0.026
57.70	6.48 ± 0.15	6.43	0.029
70.83	8.25 ± 0.17	8.29	0.060
75.28	8.90 ± 0.24	8.84	0.081
84.26	11.00 ± 0.33	10.98	0.071
90.19	13.27 ± 0.43	12.82	0.160

The main feature that differentiates this gravimetric technique from others is the way the vapour pressure is obtained. The flow of a dry gas (e. g. nitrogen) is split into two equal flows. One goes directly into a humidifier (bottle filled with distilled water) where the dry gas gets saturated by bubbling through water. Then, the desired equilibrating relative humidity or partial pressure is obtained by varying the ratio of the vapour saturated and dry gas flows.

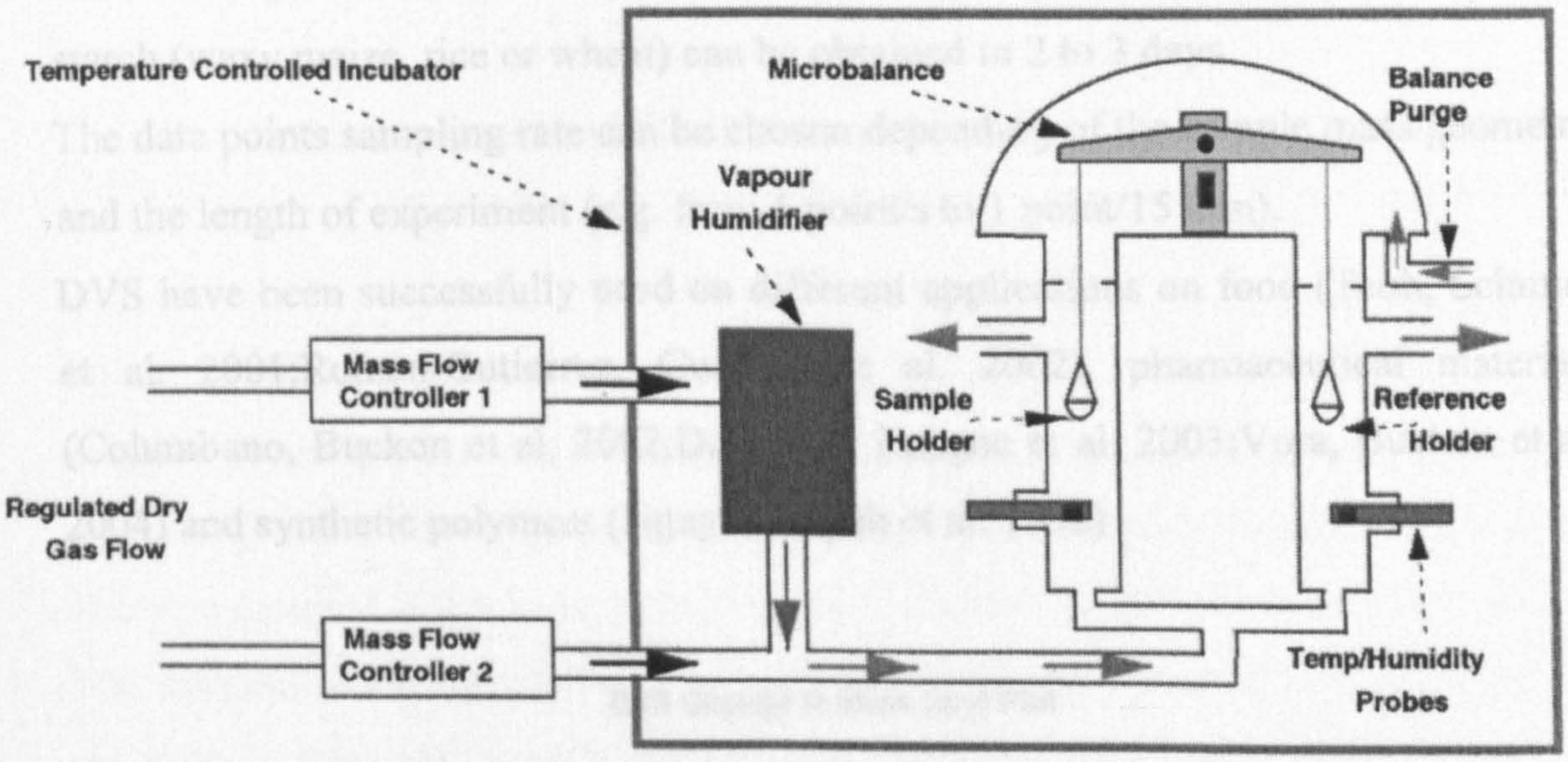

Figure 3.2. Dynamic Vapour Sorption (DVS) (Surface-Measurement-Systems 2000).

The working relative humidity range recommended by the manufacturer is from 0% to 95%. Higher values may cause condensation on the electronics of the microbalance. The instrument is housed in a controlled incubator with a range of working temperature from 5 to 45°C. The flow rate can be set up from 10 to 200 cm^3/min, and the load weight recommended is from 2.0 mg to 100 mg (including the mass absorbed by the sample). Another the advantages of this technique is its automation and relatively rapid equilibration times. The DVS is fully controlled by a dedicated PC compatible computer. The full sorption-desorption curves (figure 3.3), sorption/desorption isotherms (figure 3.4), and information related to modelling can be automatically obtained by running Excel macros included in DVS software package (Standard and Advanced Analysis Macros for Excel 2.0, Surface Measurement Systems, UK). In terms of automation during the experiment, the

DVS software allows the definition of the sorption/desorption equilibrium conditions. By setting the parameter dm%/dt (changes in percentage of mass per minute) it is possible for the software to have complete control over the experiment. In case the "equilibrium state" is never reached on the time scale needed, the dm%/dt parameter will be automatically changed to a pre-defined length of time for any or all of the relative humidities steps in the run.

Based on experience, a full sorption-desorption cycle for 3 mg of ground particles of starch (waxy maize, rice or wheat) can be obtained in 2 to 3 days.

The data points sampling rate can be chosen depending of the sample mass/geometry and the length of experiment (e.g. from 1 point/s to 1 point/15 min).

DVS have been successfully used on different applications on food (Teoh, Schmidt et al. 2001;Roman-Gutierrez, Guilbert et al. 2002), pharmaceutical materials (Columbano, Buckon et al. 2002;Davidson, Langne et al. 2003;Vora, Buckon et al. 2004) and synthetic polymers (Nguyen, Sipek et al. 1992)

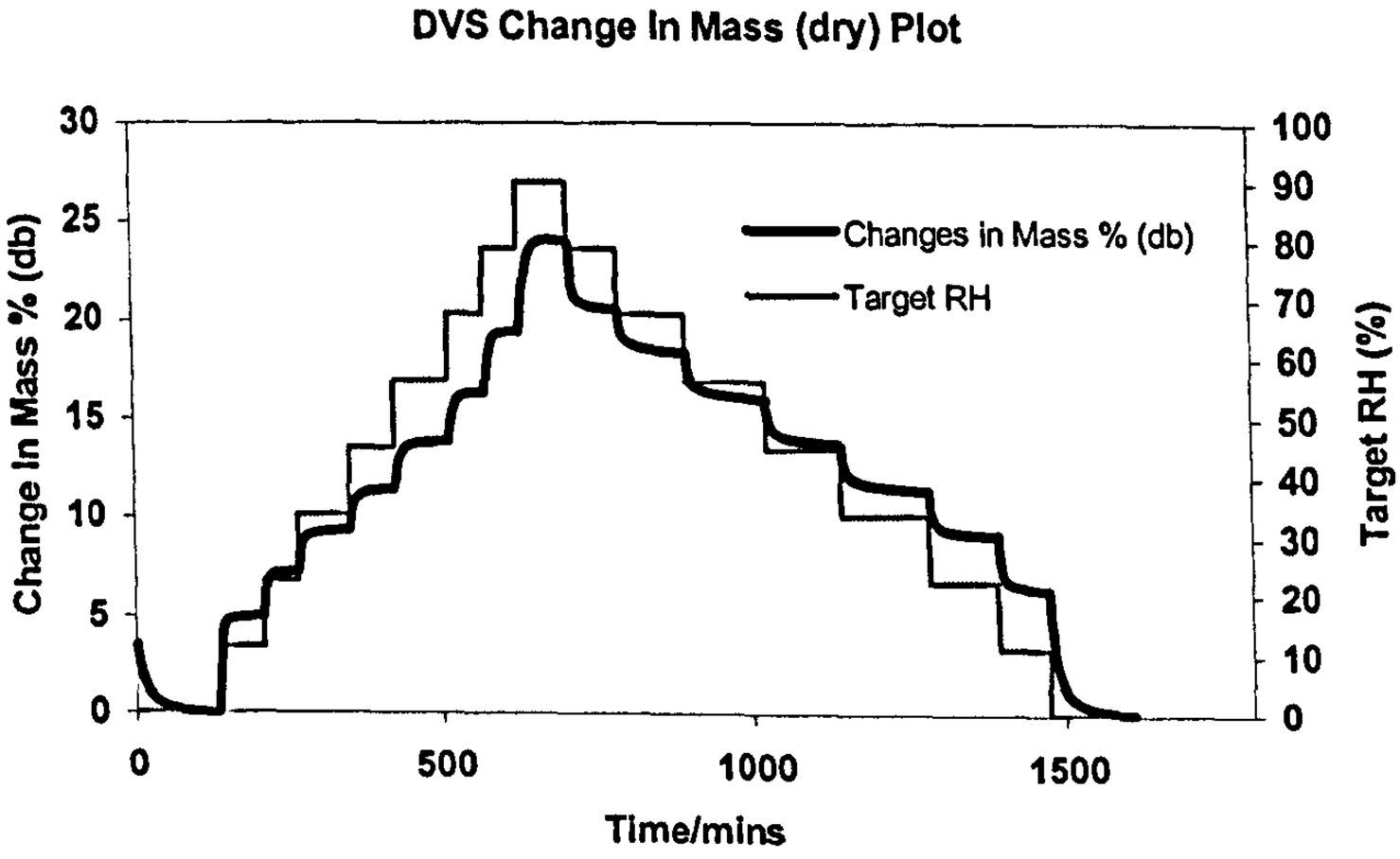

Figure 3.3. Moisture sorption-desorption full cycle on gelatinised wheat starch at 25°C.

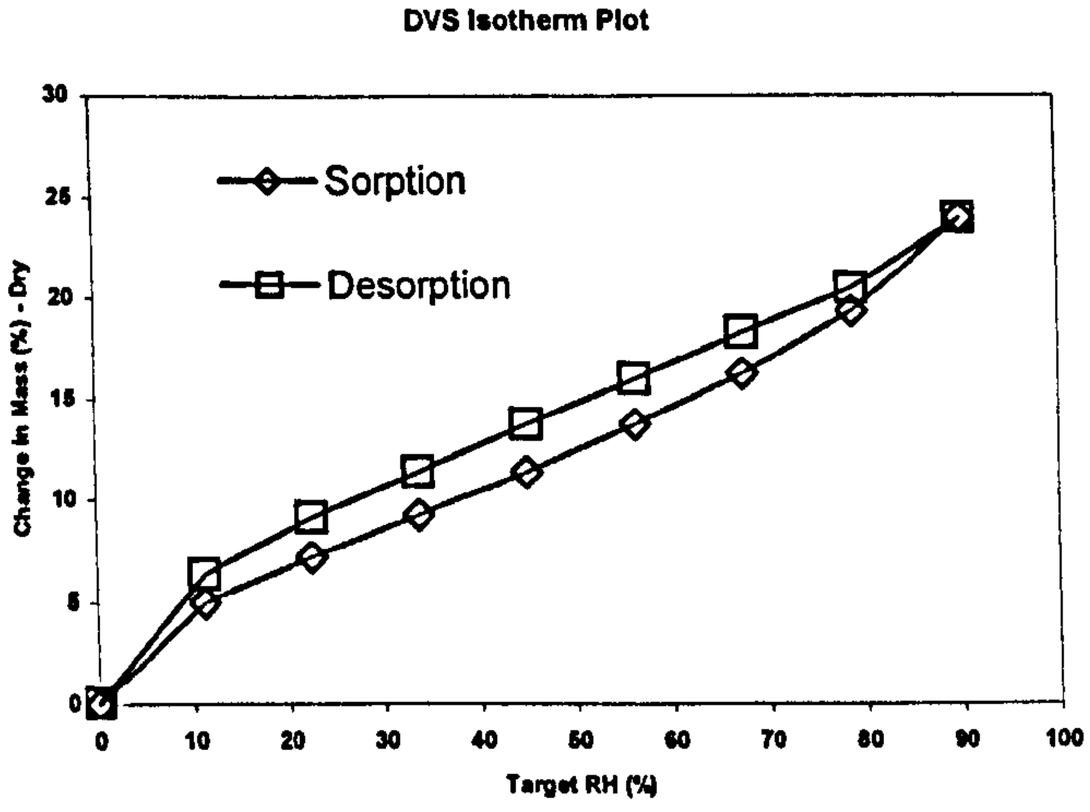

Figure 3.4. Moisture sorption-desorption isotherm for gelatinised wheat starch at 25°C.

3.3.1.1 Methodology

Sorption isotherms for waxy maize, wheat and rice starch-glycerol extrudates with different glycerol contents were obtained from DVS-1 (Surface Measurements, UK). The programmed RH's were from 0 to 90% divided in 10% increments (9 points). The samples were considered at equilibrium when the value dm/dt (slope of the changing in mass with time) was set to less than 0.002 (m%/min).

It has been observed, especially at the low end of RHs, that sorption does not reach equilibrium within the maximum time length specified for each step (6 h in this case). For these particular sorption steps, a simple exponential model was used to extrapolate the experimental data to the final moisture at equilibrium (Roman-Gutierrez, Guilbert et al. 2002). The moisture content obtained from this methodology were used in the sorption isotherms curves and diffusivities studies.

3.3.1.2 TSample Preparation

Prior the analysis, the extruded ribbons were freeze dried, ground under cryogenic conditions and sieved to the particle diameter fraction 150μm < *d* <212μm (~ 180 μm). The sorption studies of the powders were done after further drying over P_2O_5 for 12 hours with the objective of shorting the initial drying period within the DVS.

3.3.2 Texture Analyser (TA)

The effect of moisture and glycerol content on the flexural properties of the three

different starches was studied by the three point bending test method (TPBT). This technique has been commonly used to characterise the mechanical properties of different starches (Kirby, Clark et al. 1993, Nicholls, Appelqvist et al. 1995).

The advantage of evaluating the flexural properties over other fundamental techniques is that for a given force, the deflections are generally much larger than the amount of extension or compression making measurement easier (Dobraszczyk and Vincent 1999).

The major disadvantage of the bending is that it does not produce a uniform stress; different parts of the sample undergo different strains. The inner curve surface will be in compression and the outer surface will be in tension. Tensile stress is at a maximum at the outer curved surface, and compressive stress is maximum on the inner surface (Dobraszczyk and Vincent 1999). Also, a regular specimen geometry is required in order to reduce the variance between replicates (Dobraszczyk and Vincent 1999, Valles 2000). A general description of the three point bending test (TPBT) set-up is shown in the next diagram.

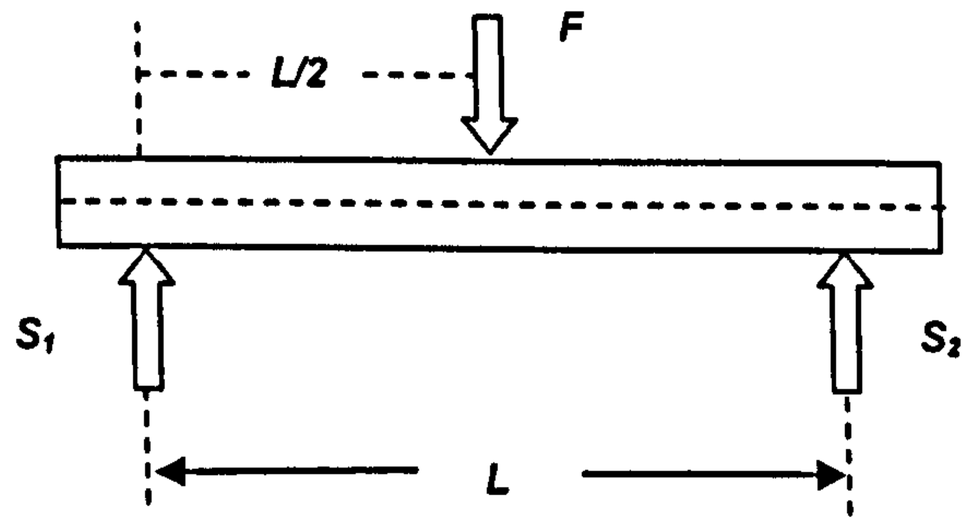

Figure 3.5. Schematic representation of the Three Point Bend Test (TPBT)

Where F is the force applied on the material, S_1 and S_2 are the supports where the sample is placed and L is the distance between them.

Taking values from the linear relation of the force-distance curve the stress and strain were calculated using the following relationship (BS EN ISO 178: 1997):

Where:

$$Stress(\delta) = \frac{3FL}{2bh^2} \qquad \textit{Equation 3.1}$$

δ: is the stress, force applied in a unit area (N/cm^2)

F: is the applied force (N)

L: is the span (cm)

b: is the width of the sample (cm)

h: is the thickness of the sample (cm)

$$Strain\ (\varepsilon) = \frac{6Dh}{L^2} \qquad Equation\ 3.2$$

Where:

ε: is the strain, change in length per unit of the original length (cm/cm)

D: is the deflection (cm)

L: is the span (cm)

h: is the thickness of the sample (cm)

The flexural modulus (E_f) was calculated from the initial portion of the stress-strain curve, between points where follows Hooke's law (dotted line). Here, the stress applied to the material is proportional to the obtained strain (figure 3.6). In other words E_f is equivalent to the slope of the linear portion of the viscoelastic curve.

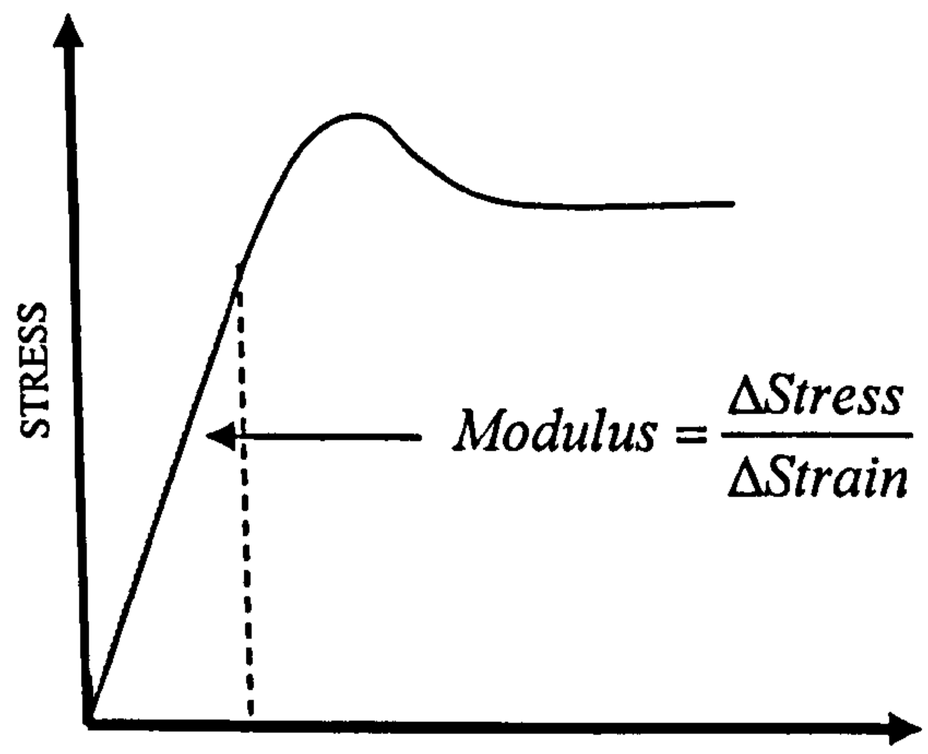

Figure 3.6. Typical stress-strain curve (modified from Dobraszczyk and Vincent 1999).

Following this rationale the flexural modulus (E_f) is obtained by relating 3.1 and 3.2 into the equation:

$$E_f = \frac{(\delta_2 - \delta_1)}{(\varepsilon_2 - \varepsilon_1)} \qquad \textit{Equation 3.3}$$

Where:

E_f: *Elastic Modulus (MPa)*

3.3.2.1 Methodology

The instrument employed was the Texture Analyser XT 2 Plus (Stable Micro Systems, UK) fitted with a 30 kg load cell. Before each measurement the cell was calibrated using a standard 5 kg weight.

The span (distance between supports) was 6 cm; the probe speed was 0.2 mm/s. The force needed to deform the sample 1 mm was recorded. These values were automatically logged by the purpose built macro using the Texture Analyser XT 2 Plus software.

3.3.2.2 Samples Preparation

A regular geometry (width and length) of the extruded ribbons was obtained by cutting the wet samples (35%MC) using a customised cutter (stainless steel) device with a dimension of 2.5 cm width and 10 cm in length (see figure 3.7). The thicknesses of the ribbons were typically 1.5 mm thick.

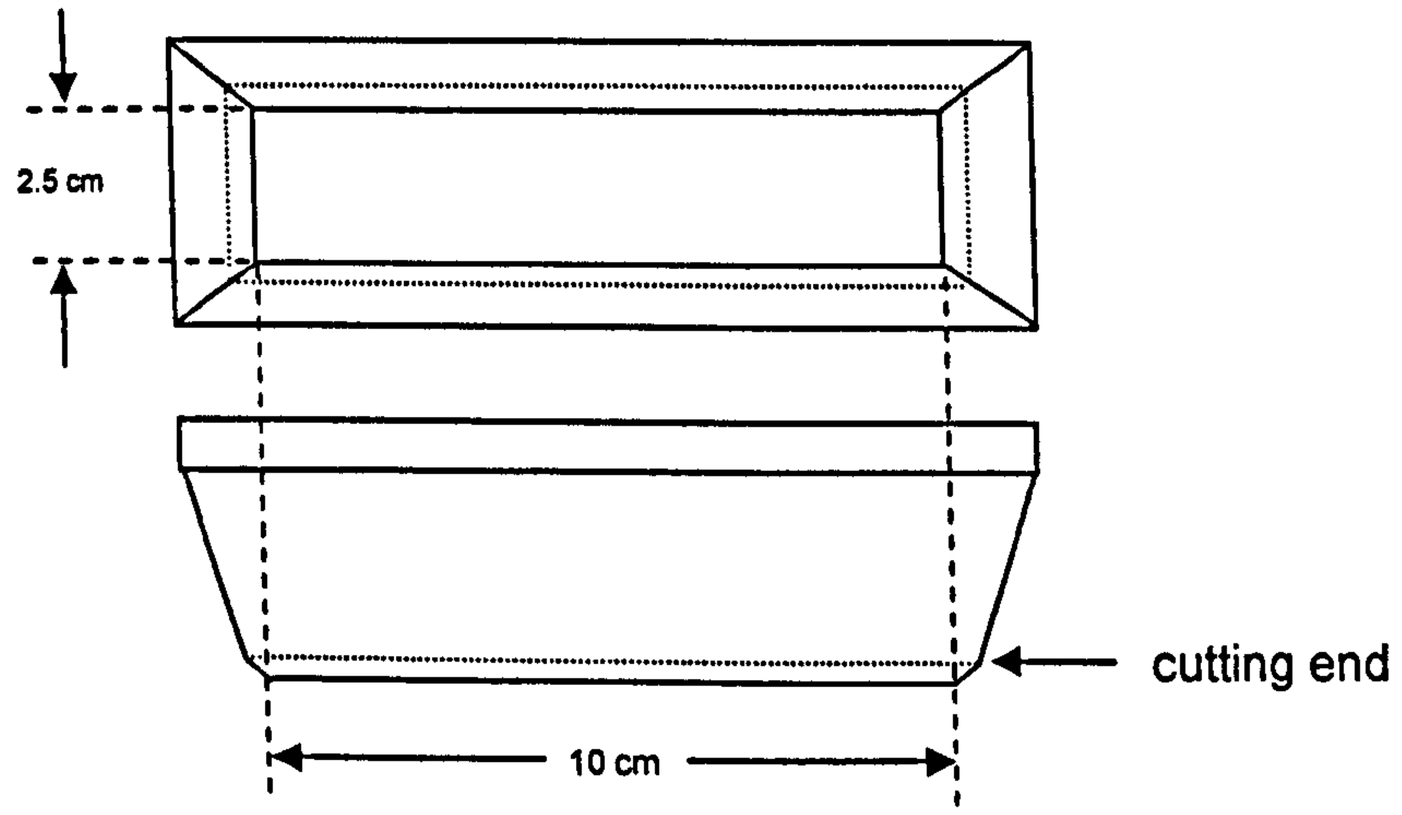

Figure 3.7. Schematic diagram describing the cutting device

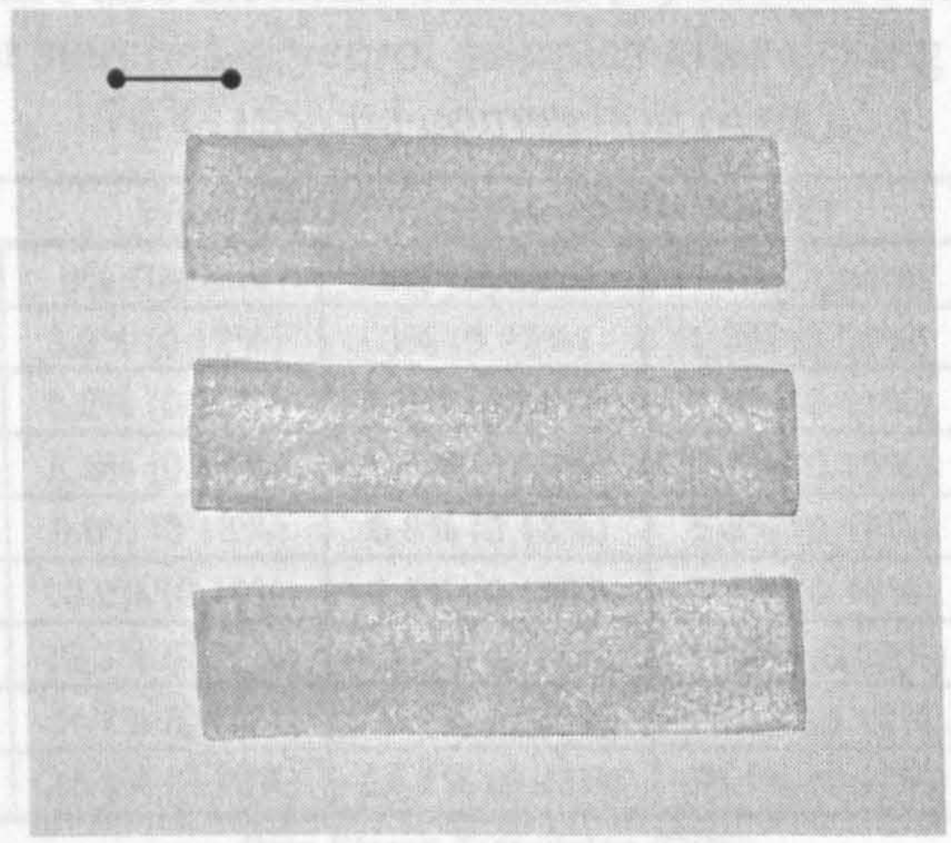

Figure 3.8. Example of extruded ribbons (wheat starch) after cutting.

It is known that retrogradation may occur when a starch based material is equilibrated under different RH to obtain a range of moisture contents. To minimise this ageing process, different moisture contents were obtained by placing the shaped ribbons under forced convection conditions at 70°C for different times (Gallenkamp, UK).

The next table presents the obtained moisture content (%wb) after drying for waxy maize, rice and wheat starches and different glycerol concentrations.

Table 3.6. Drying times and moisture content (*) obtained for the extruded waxy maize, rice and wheat starches-glycerol samples after drying for different times at 70°C (forced convection oven).

Waxy Maize Starch Extrudates (WMSE)				
Drying Time (h)	0% Glycerol	5% Glycerol	10% Glycerol	20% Glycerol
22.0	3.2% (0.12%)	3% (0.17%)	1.8% (0.05%)	1.3% (0.10%)
10.0	5.2% (0.20%)	4.5% (0.21%)	1.9% (0.11%)	2.4% (0.11%)
8.0	6.5% (0.14%)	5.4% (0.19%)	2.7% (0.15%)	4.5% (0.17%)
6.0	9.0% (0.18%)	6.8% (0.13%)	5.8% (0.18%)	6.2% (0.15%)
3.5	10.2% (0.12%)	8.5% (0.18%)	7.4% (0.14%)	8.6% (0.13%)
2.5	12.3% (0.21%)	13.6% (0.18%)	12.9% (0.13%)	13% (0.18%)
1.3	14.7% (0.22%)	15.9% (0.23%)	16.3% (0.17%)	18.4% (0.17%)
0.7	25.9% (0.19%)	25.7% (0.23%)	28.1% (0.22%)	32.6% (0.25%)
Rice Starch Extrudates (RSE)				
Drying Time (h)	0% Glycerol	5% Glycerol	10% Glycerol	20% Glycerol
19.0	2.0% (0.09%)	1.8% (0.09%)	1.3% (0.09%)	1.3% (0.07%)
6.0	5.4% (0.15%)	4.6% (0.13%)	4.3% (0.13%)	3.2% (0.16%)
5.0	6.8% (0.13%)	5.5% (0.16%)	5.1% (0.12%)	3.9% (0.12%)
4.0	8.7% (0.16%)	7.3% (0.14%)	6.3% (0.15%)	5.5% (0.17%)
3.0	10.2% (0.23%)	8.7% (0.18%)	7.8% (0.17%)	8.0% (0.19%)
2.0	11.5% (0.18%)	10.7% (0.19%)	12% (0.16%)	12.0% (0.16%)
1.3	13.3% (0.22%)	13.7% (0.17%)	18.5% (0.19%)	17.2% (0.15%)
0.7	23.7% (0.23%)	25.2% (0.20%)	29.9% (0.22%)	31.4% (0.26%)
Wheat Starch Extrudates (WSE)				
Drying Time (h)	0% Glycerol	5% Glycerol	10% Glycerol	20% Glycerol
19.0	5.2% (0.19%)	5.3% (0.11%)	4.3% (0.08%)	3.1% (0.11%)
6.0	6.1% (0.11%)	5.8% (0.12%)	4.8% (0.11%)	3.9% (0.13%)
5.0	7.4% (0.12%)	6.7% (0.21%)	5.2% (0.16%)	4.8% (0.17%)
4.0	9.9% (0.14%)	7.5% (0.18%)	6.0% (0.15%)	5.9% (0.15%)
3.0	11.7% (0.21%)	9.5% (0.15%)	7.2% (0.16%)	8.5% (0.18%)
2.0	13.3% (0.17%)	12% (0.16%)	13.9% (0.18%)	16.0% (0.19%)
1.3	15.5% (0.19%)	15.4% (0.22%)	19.1% (0.19%)	23% (0.20%)
0.7	22.5% (0.21%)	25.7% (0.23%)	31.3% (0.24%)	37.1% (0.28%)

(*) Moisture content was determined in duplicates by vacuum oven at 70°C overnight. Values in brackets are the arithmetic differences between duplicates

In order to reduce the bending of the material during drying, the extrudates were placed between two aluminium meshes (sandwiched by screws). After drying, the extrudates were hermetically packed and stored in –80°C freezer (Denley, UK). The moisture content of the different samples was measured by drying under vacuum (-1 Atm) at 70°C for 24 h (Gallenkamp, UK.).

The degree of retrogradation of these samples are presented in section 3.3.5.2 where diffractograms of the high and low end of moisture contents samples are presented.

The same set of samples were also used for the determination of the effect of glycerol on the glass transition temperature (Tg) of these systems.

3.3.3 Dynamic Mechanical Thermal Analysis (DMTA)

DMTA is concerned with the measurement of the mechanical properties (mechanical modulus or stiffness and damping), under different oscillation frequencies, of a specimen as a function of temperature (Price 2002).

This dynamic analytical technique has been used extensively in the synthetic polymer world for many years. It has given information about amorphous single phase and multi-face polymers and semi-crystalline polymers. Due to its dynamic oscillation feature, a range of frequencies have been used to study parameters such as relaxation time and to predict other viscoelastic properties (Wetton 1986).

Applications of this technique on foods components (e. g. starches, gelatine) have included; molecular relaxations measurements (Hallberg and Chinachoti 1992, Kalichevsky 1992, Arvanitoyannis, Kalichevsky et al. 1994, Lourdin, Bizot et al. 1997, Biliaderis, Lazaridou et al. 1999, Gaudin, Lourdin et al. 1999, Graaf, Karman et al. 2003), ageing (Mizuno, Mitsuiki et al. 1998, Chung and Lim 2004) and phase separation in multi-components mixtures (Mousia, Farhat et al. 2000).

Figure 3.9 shows a general diagram of a DMTA including the drive-shaft, linear variable displacement transducer (LVDT), Pt100 thermometer and heating-cooling jacket.

The sample is fixed onto the instrument (test fixture used will depend on the sample stiffness, geometry and type of measurement) and it is subjected to a determined force by a drive-shaft at a certain frequency. The temperature range used, heating rate and frequencies are set depending on the mechanical characteristics of the material to be analysed.

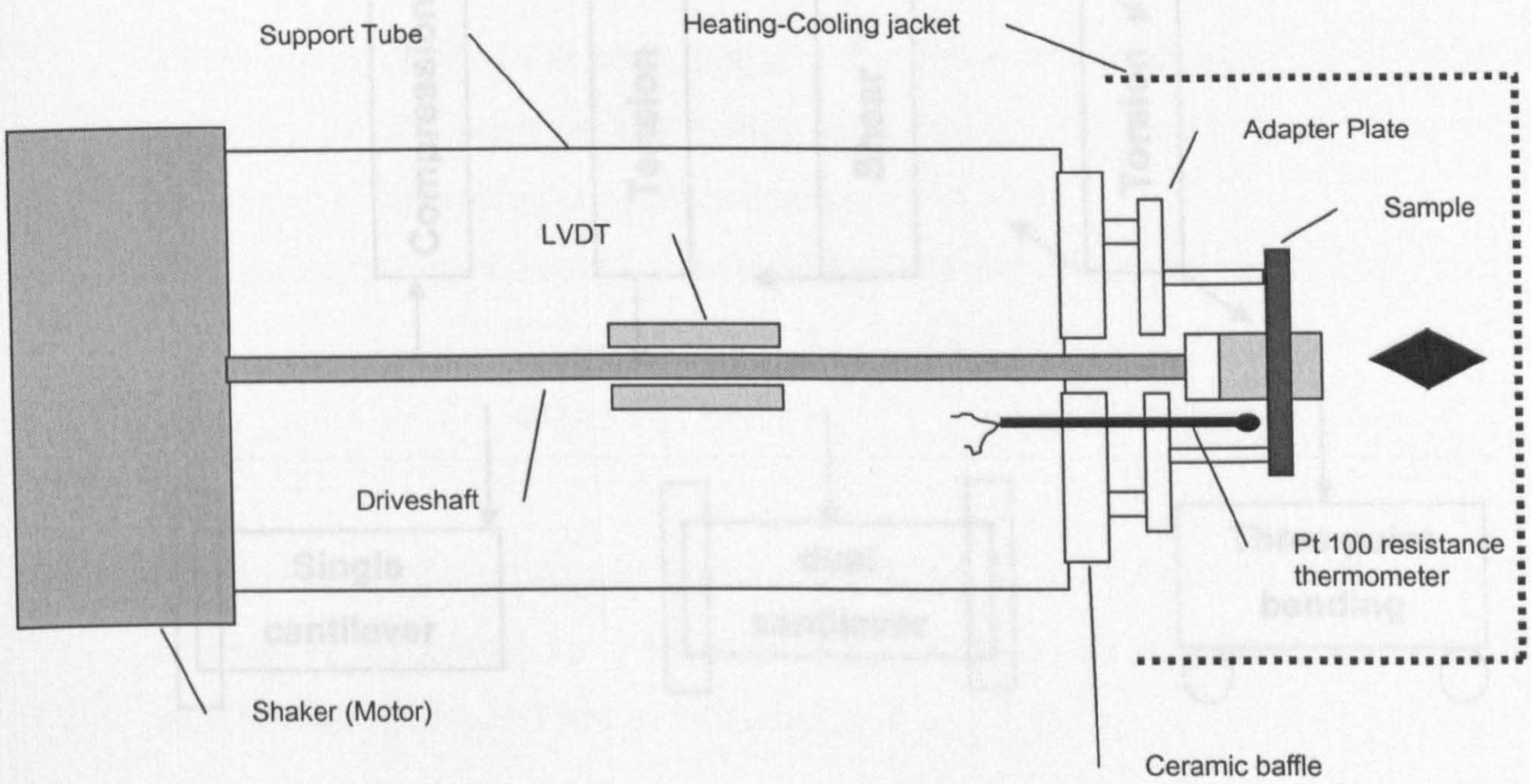

Figure 3.9. Schematic diagram of a DMTA head. (Triton-Technology 2003)

The following paragraphs present brief introduction to the theory behind the development of this analytical technique.

The stress (σ) is defined as the ratio of the mechanical force applied (F) divided by the area over its acts (A):

$$\sigma = \frac{F}{A} \qquad \textit{Equation 3.4}$$

The stress is usually applied in compression or tension, but it may also be applied in shear, torsion, or in some other bending mode as shown in next figure.

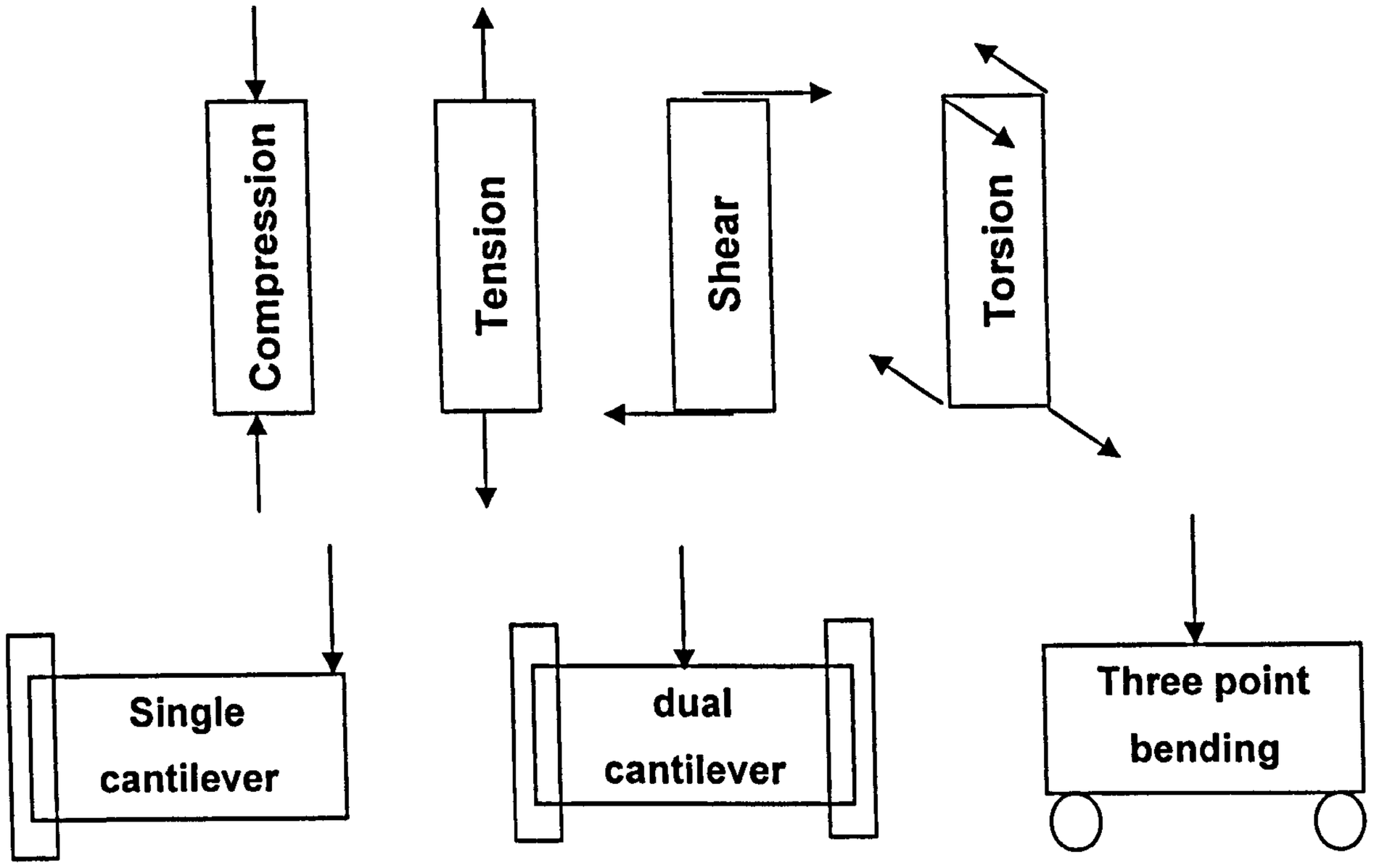

Figure 3.10. Common mechanical formation modes; compression, tension, shear, torsion, bending (single cantilever, dual cantilever, three point bending) (Price 2002).

The applied stress produces a corresponding deformation or strain (ε) defined by:

$$\varepsilon = \frac{\Delta l}{l_o} \qquad \textit{Equation 3.5}$$

Where Δl is the change in dimension and l_o is the original dimension. The strain is dimensionless, but usually expressed in percentage *(%)*.

The definition given above for modulus does not take time into account. For materials that exhibit time-invariant deformation, for example metals and ceramics at room temperature, any measurement of strain will lead to constant modulus. However for materials that exhibit time-dependent deformation, such as polymers, the quoted modulus must include the time variable to be valid. For this type of measurement the material is subjected to an oscillating stress, following a sinusoidal waveform:

$$\sigma(t) = \alpha_{max} \sin \omega t \qquad \textit{Equation 3.6}$$

Where $\sigma(t)$ is the stress at time t, σ_{max} is the maximum stress and ω is the angular frequency of oscillation usually measured in radians per second. It is important to note that $\omega = 2\pi f$ where f is the frequency in Hertz (Hz).

Responding the applied stress, a sinusoidal strain is obtained, represented by:

$$\varepsilon(t) = \varepsilon_{max} \sin(\omega t) \qquad \textit{Equation 3.7}$$

Where ε_{max} is the amplitude and ω frequency in radians per second. Since the material is viscoelastic the stress resulting from the strain will not be in phase. The shift between stress and strain is denoted by δ.

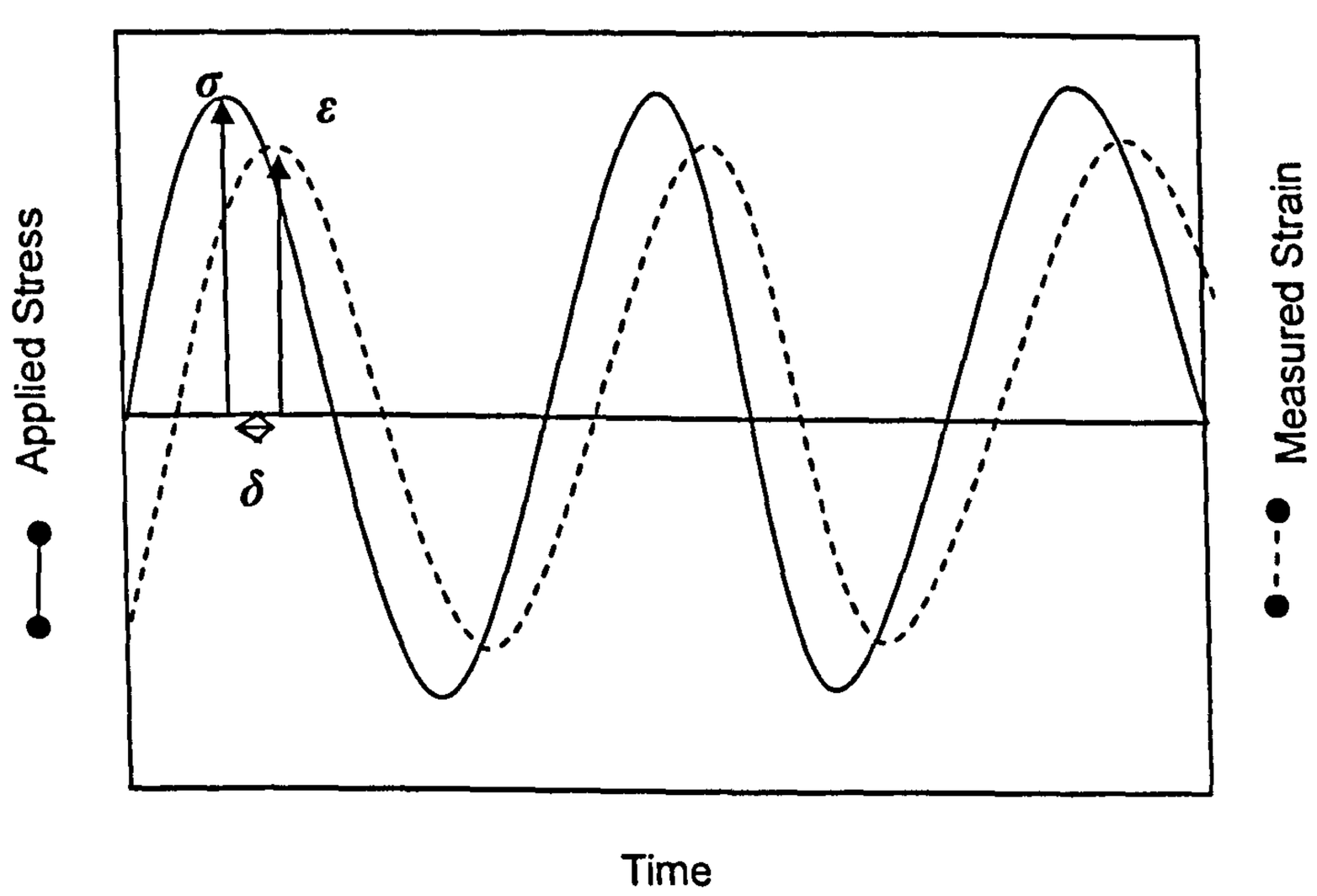

Figure 3.11. Relationship between stress (σ) and strain (ε) during a dynamic mechanical test (Price 2002).

The ratio of the peak stress to peak strain gives the complex modulus (E^*) which consists of an in-phase component or storage modulus (E') (elastic component) and a 90° out-out phase component or loss modulus (E'') (viscous component).

The ratio between the loss and the storage modulus (E''/E') gives a useful value known as the mechanical damping factor ($tan\ \delta$) which is the amount of deformation energy that is dissipated as heat during each cycle.

The relationship between these quantities can be illustrated using the Argand diagram (Figure 3.12) used to represent complex numbers. Here, the complex modulus is a vector quantity characterised by a magnitude (E^*) and angle (δ). E' and E'' represent the real and imaginary components of the vector. Therefore:

$$E^* = E' + iE'' = \sqrt{(E''^2 + E'^2)} \qquad \textit{Equation 3.8}$$

So that:

$$E' = E^* \cos \delta \qquad \textit{Equation 3.9}$$

$$E'' = E^* \sin \delta \qquad \textit{Equation 3.10}$$

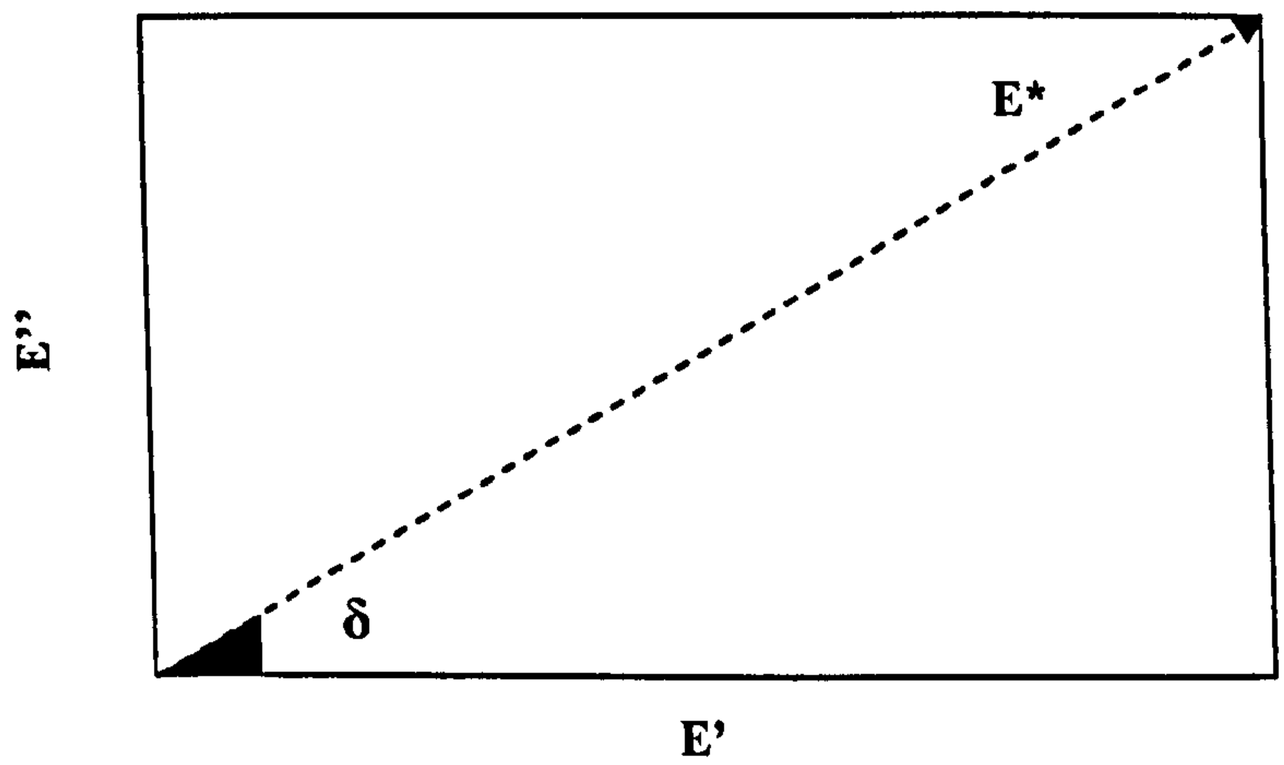

Figure 3.12. Argand diagram illustrates the relationship between complex modulus (E^*) and its components E' and E'' (Wetton 1986)

The most common DMTA experiment is to measure the storage modulus (E') and the mechanical damping factor ($tan\ \delta$) against temperature at a single oscillation frequency (Figure 3.13).

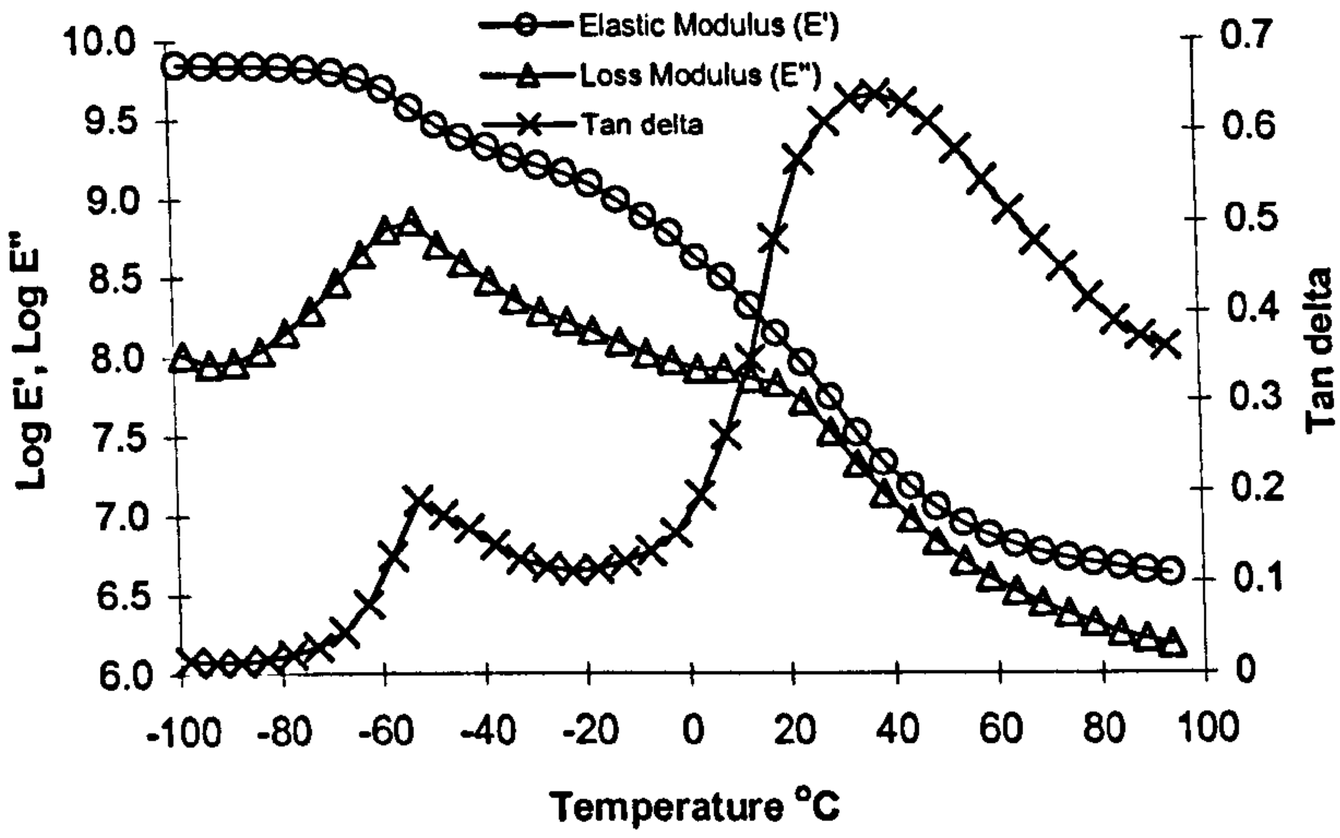

Figure 3.13. Example of a typical DMTA profile. Wheat starch extrudate, ~18 % moisture and 10%glycerol run at 2 Hz.

Figure 3.13 shows *E'* having two reductions in its value, a small transition from -60 to -50°C and a significant one from –0 to 40°C. The *tan δ* curve shows two peaks at similar temperatures compared to the *E'* modulus drops. It is a generally accepted that main reduction in *E'* (main *tan δ* peak) is related to the main relaxation of the polymer, usually called α-transition or glass transition temperature (Tg). The reduction in *E'* (lower *tan δ* peaks) at sub-Tg temperatures are described as secondary relaxations normally known as β-transitions.

As mentioned before, the dynamic nature of this technique allows measurements at different frequencies (time scales) at a different temperatures. Figure 3.14 depicts the dependency of *E''*, *E'* and tan *δ* on frequencies.

This approach can be useful to describe the glass-rubber transition as a simple thermally activated phenomenon (Arrhenius equation) and when it is described by cooperative mechanism using time-temperature superimposition (Price 2002).

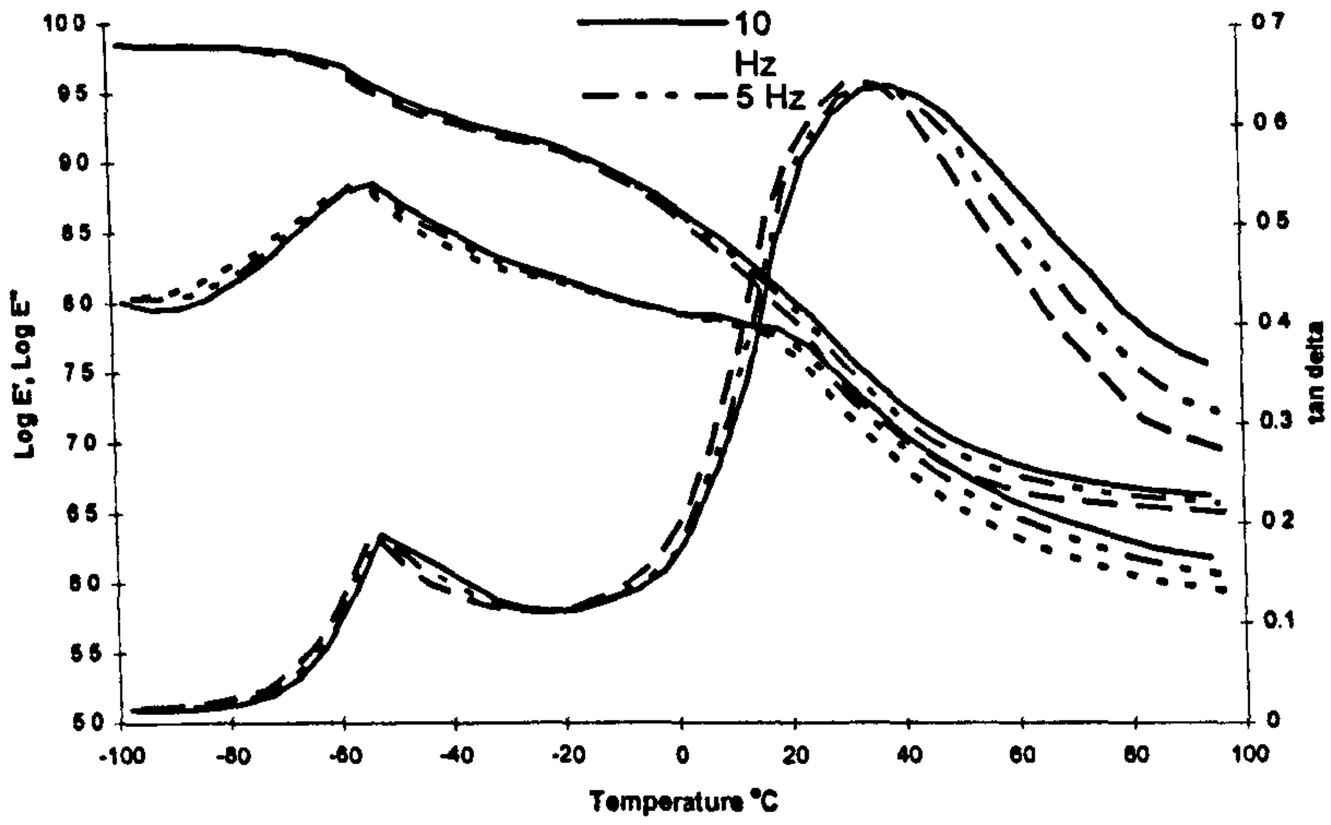

Figure 3.14. Example of frequency dependency for *E'*, *E''* and tan δ. DMTA profile for wheat starch extrudate and 10%glycerol run at 2, 5, 10 Hz.

3.3.3.1 TMethodology

The DMTA (Rheometric Scientific Mk, III, Loughborough, UK) experimental settings were: single cantilever (one end of samples fixed to the frame and the other to the oscillating drive-shaft), temperature range from -100°C to ~150°C (the end temperature was set depending on the expected value for Tg), heating rate of 3°C/min and a strain x4 (62 μm amplitude). This strain was set in order to make sure the measurements were done on the initial linear zone of the stress-strain viscoelastic curve. The frequencies used on the analysis were arbitrary set to 2, 5 and 10 Hz.

The parameters considered were the storage modulus (*E'*), the loss modulus (*E''*) and tan δ. For determination of Tg the peak of the *E''* curve after the main decrease in *E'* (3 to 4 orders of magnitude) was considered (figure 3.15).

Each sample run was analysed in triplicate.

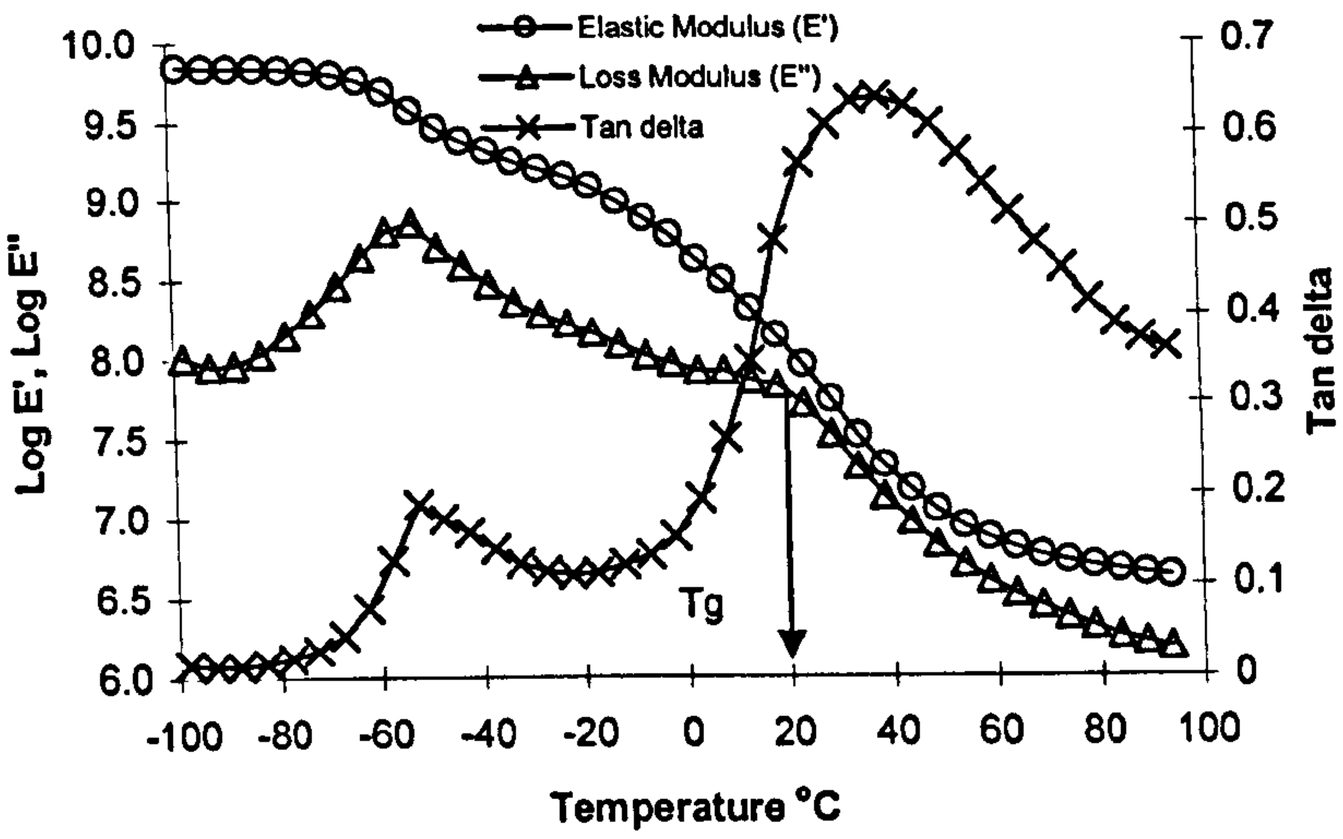

Figure 3.15.Example of Tg measurements. DMTA profile for wheat starch extrudate, 18% moisture and 10%glycerol run at 2 Hz.

3.3.3.2 Sample Preparation

The same set of samples prepared for the flexural modulus measured by TA (different moisture contents) were analysed by DMTA. These samples were cut to the required geometry. Reformation of samples was avoided as the integrity of these materials can be affected by this procedure. The dimensions for each sample were typically ~10 mm length, ~7 mm width and ~1.5 mm thickness. If the samples were rubbery they were cut with a sharp object. If in a glass, they were cut using a metal saw. The shaping of the samples was done in shortest time possible to avoid exchange of moisture with the environment. Samples were covered with silicon oil to reduce moisture loss during the analysis.

3.3.4 Differential Scanning Calorimetry (DSC)

The definition for differential scanning calorimetry (DSC), given by the International Confederation of Thermal Analysis (ICTA) is:

"A technique for recording the energy necessary to establish a zero temperature difference between a substance and a reference material against either time or temperature, as the two specimens are subjected to identical temperature regimes in a environment heated or cooled at a controlled rate" (Schenz and Davis 1998).

Following this definition, it is clear that the sample and the reference cell must have different heating flows in order to keep same temperatures during heating (Nielsen 1998).

The following diagram shows the DSC furnace system:

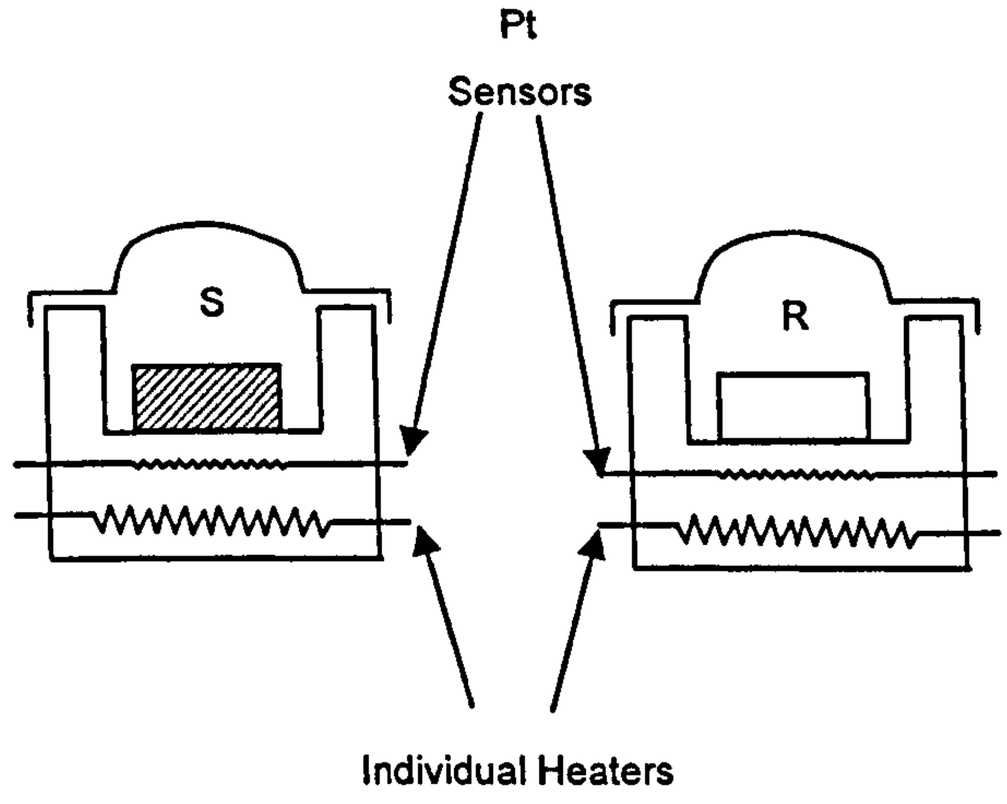

Figure 3.16. Schematic of a typical differential thermal analyser (Nielsen 1998).

As mentioned above, DSC is a form of calorimetry and as such it is concerned with measuring the heat of a reaction or process. At constant pressure, enthalpy (ΔH) is defined by the internal energy (U) and the work done on the system by the variations in volume ($P\Delta V$):

$$\Delta H = U + P\Delta V \qquad \textit{Equation 3.11}$$

Heat added to raise the temperature at constant pressure is given as:

$$dH = dq_p = CpdT \qquad \textit{Equation 3.12}$$

where, Cp is the heat capacity of the system at constant temperature. If the temperature changes from T_o to T_1, the enthalpy of the reaction (ΔH) is:

$$\Delta H = \int_{T_o}^{T_1} CpdT \qquad \textit{Equation 3.13}$$

When ΔT is small, Cp is independent of the temperature between T_1 and T_o. The integral thus is reduced to:

$$\Delta H = Cp(T_1 - T_2) = Cp\Delta T \qquad \textit{Equation 3.14}$$

Second order transitions, such as the glass transition (Tg), are shown as a discrete change in the Cp. First order transitions, such as melting or crystallisation, will appear as a peak. The area under the peak will be the heat released or absorbed during the transition. This information will give, for example, the heat of fusion, ΔH_f, or the heat of crystallisation, ΔH_c:

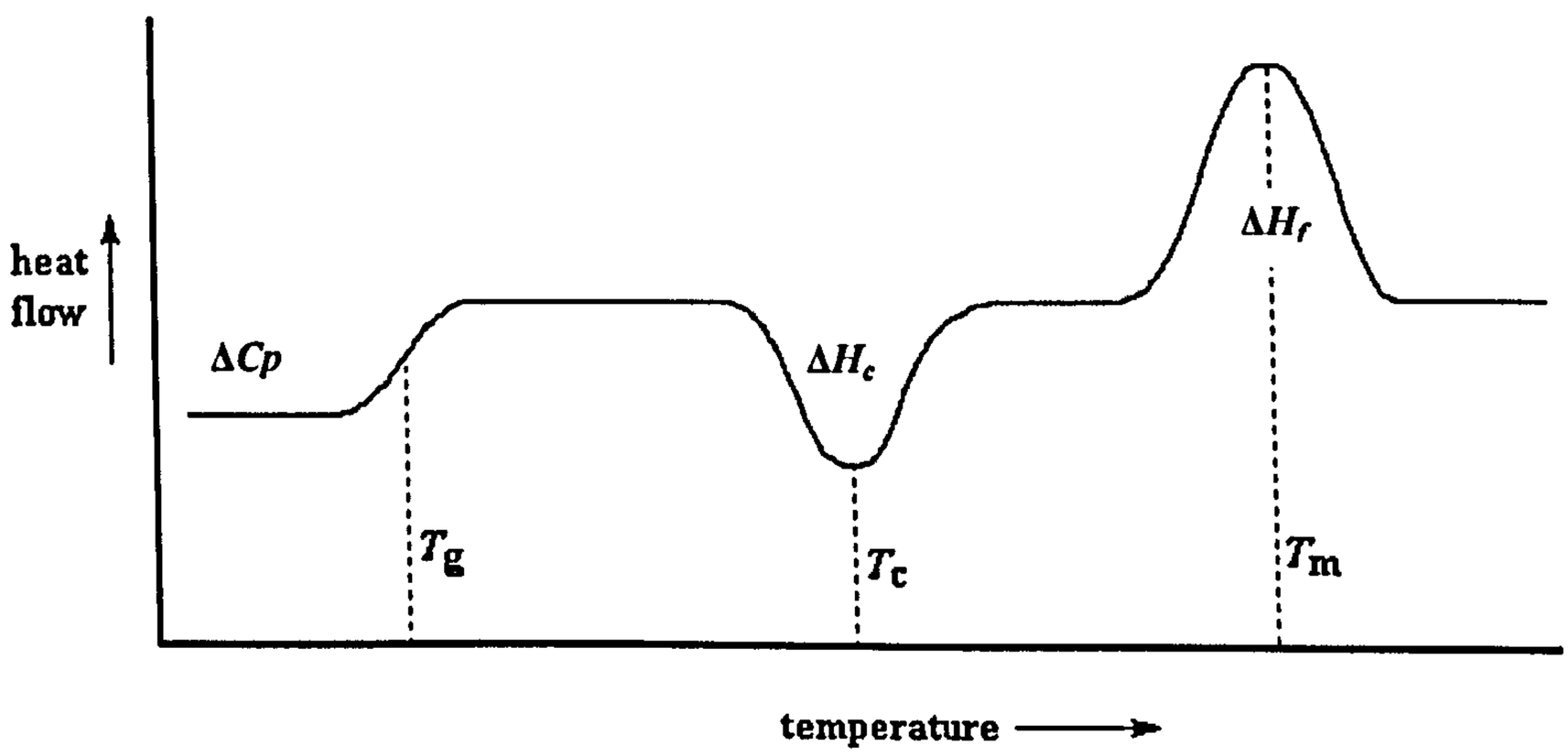

Figure 3.17. Set of thermal transitions as they may appear when a material is heated (Nielsen 1998)

3.3.4.1 Methodology

The *DSC 7* and *Diamond Pyris* (Perkin Elmer, USA) instruments were calibrated for temperature (heating rate 10°C/min), from the melting point of indium (156.6°C) and

cyclohexane (7.0°C). The heat flow was calibrated from the heat of melting of indium (28.45 J/g), and the calibration for heat capacity was checked against a sapphire standard.

For glass transition temperature (Tg) measurements the experimental settings were typically, heating from -30 to 140°C (run and re-run) at a heating rate of 10°C/min. The information obtained was Tg (temperature at half value in the step change in heat capacity), onset temperature (Tg_o) and the differences in heat capacity below and above Tg (ΔCp).

In case of evaluation of the presence of ordered structures, the samples were analysed under excess water conditions typically from 5 to 140°C (run and re-run) at a heating rate of 10°C/min. The parameters considered were the onset temperature (T_o), the peak temperature (T_p) and the enthalpy of the transition (ΔH) (peak area).

The obtained curves, first and second runs, were corrected by subtracted a base line (empty pan run). The numerical analysis was performed using the software package from Pyris software version 3.52 (Perkin Elmer, USA).

The analysis for all the samples (model systems and commercial products) was done in triplicate.

3.3.4.2 Sample Preparation

For Tg determination, the set of samples prepared for flexural modulus and DMTA were loaded (solid or ground) into stainless steel pans. Using these pans it was possible to analyse at high temperatures (140°C) while reducing the risk of pan bursting inside the DSC oven. The weight for all the samples was typically 50mg.

For the determination of native or retrograded starchy structures and amylo-lipid complexes the samples were prepared in excess water (distilled). The ratio solid material:water was 1:3. This mixtures ware also loaded in stainless steel pans, allowing safe measurements at temperatures higher than water boiling point.

3.3.5 Wide Angle X-Ray Diffraction (WAXS)

X-ray scattering involves exposing a material to X-ray radiation, which energises the electrons present in the atoms, making them secondary emitters of X-ray radiation. When X-rays of wavelength (λ) and incidence angle (θ) strike a crystalline sample (ordered molecular structure) formed by lattices of a certain distance (d) such that the scattered rays are able to constructively interfere, the resulting X-ray beam will be of high intensity if the differences between wavelength is an integer n.

Bragg's Law refers to the simple equation:

$$n\lambda = 2d\sin\theta \qquad \textit{Equation 3.15}$$

Derived by the English physicists Sir W.H. Bragg and his son Sir W.L. Bragg in 1913 to explain why the cleavage faces of crystals appear to reflect X-ray beams at certain angles of incidence (theta, θ). The variable d is the distance between atomic layers in a crystal, and the variable lambda λ is the wavelength of the incident X-ray beam and n is an integer

Bragg's Law can easily be derived by considering the conditions necessary to make the phases of the beams coincide when the incident angle equals the reflecting angle. X-rays of the incident beam are always in phase and parallel up to the point at which the top beam strikes the top layer at atom z (Figure 3.19). The second beam continues to the next layer where it is scattered by atom B (constructive interference). The second beam must travel the extra distance AB + BC if the two beams are to continue travelling adjacent and parallel. This extra distance must be an integral (n) multiple of the wavelength (λ) for the phases of the two beams to be the same (in phase) (Schields 2002):

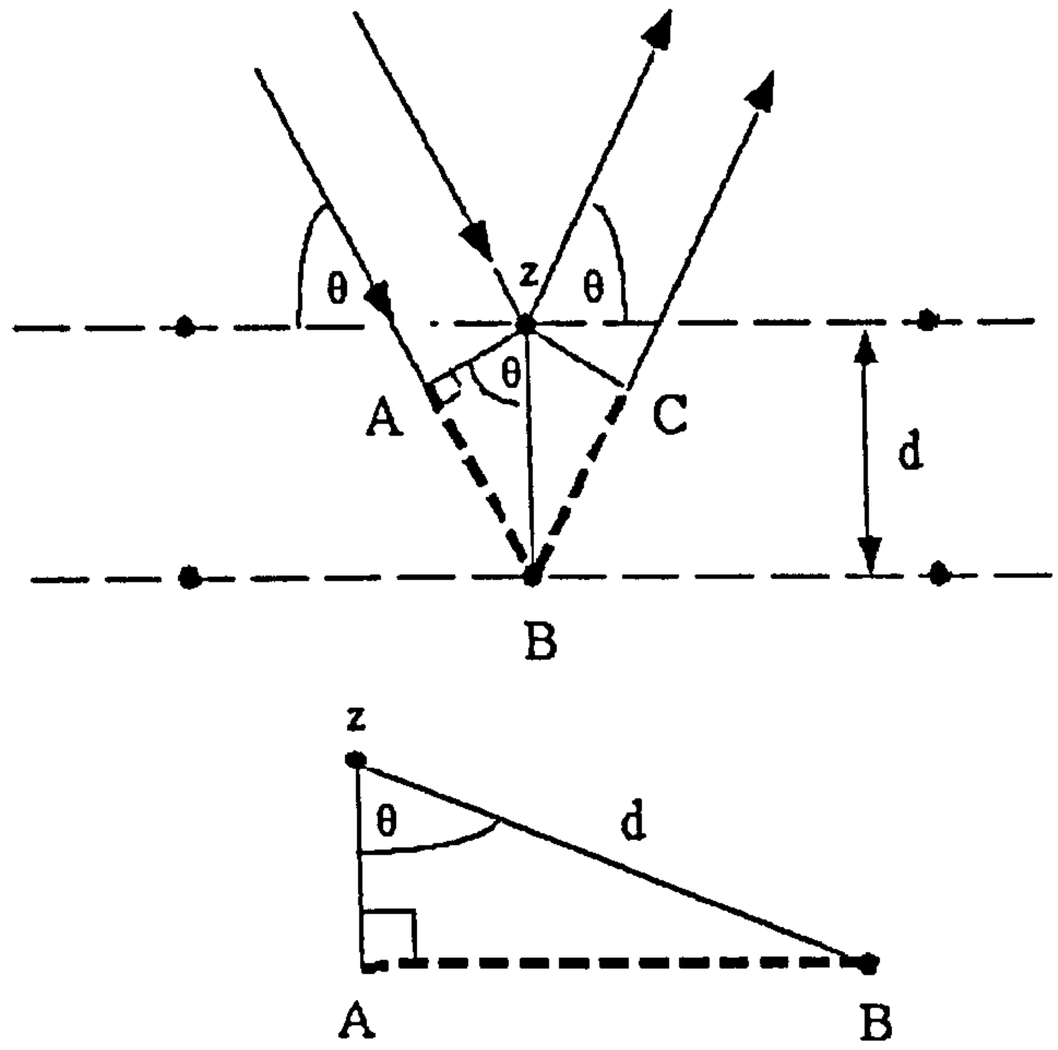

Figure 3.18. Deriving Bragg's Law using the reflection geometry and applying trigonometry. The lower beam must travel the extra distance (AB + BC) to continue travelling parallel and adjacent to the top beam (Schields 2002).

Therefore,

$$n\lambda = AB + BC \qquad \textit{Equation 3.16}$$

And

$$AB = d \sin\theta \qquad \textit{Equation 3.17}$$

Because AB = BC then,

$$n\lambda = 2AB \qquad \textit{Equation 3.18}$$

Then we have,

$$n\lambda = 2d\sin\theta \qquad \textit{Equation 3.19}$$

As amorphous samples have neither 'short-' nor 'long-range' order, unlike crystalline materials, a diffuse x-ray pattern is obtained. This is believed to be the result of the most probable distances between neighbouring atoms and would be expected to have

a Gaussian distribution. However, for purely crystalline samples, this is not seen as the atoms lie in well-defined positions, and hence there will only be distinct sharp peaks observed in the x-ray pattern related to those specific distances that the atoms lie apart (Ottenhof 2003).

This technique has been widely used on starchy materials to relate the structural stage of this biopolymer to changes in texture (Jagannath, Jayaraman et al. 1998, Rindlav-Westling, Stading et al. 1998, Forssell, Hulleman et al. 1999), permeability (Arvanitoyannis, Kalichevsky et al. 1994, García, Martino et al. 2000) and molecular transitions (Mizuno, Mitsuiki et al. 1998).

Next figure shows an example of diffractograms for different native and amorphous wheat, potato and waxy maize starches.

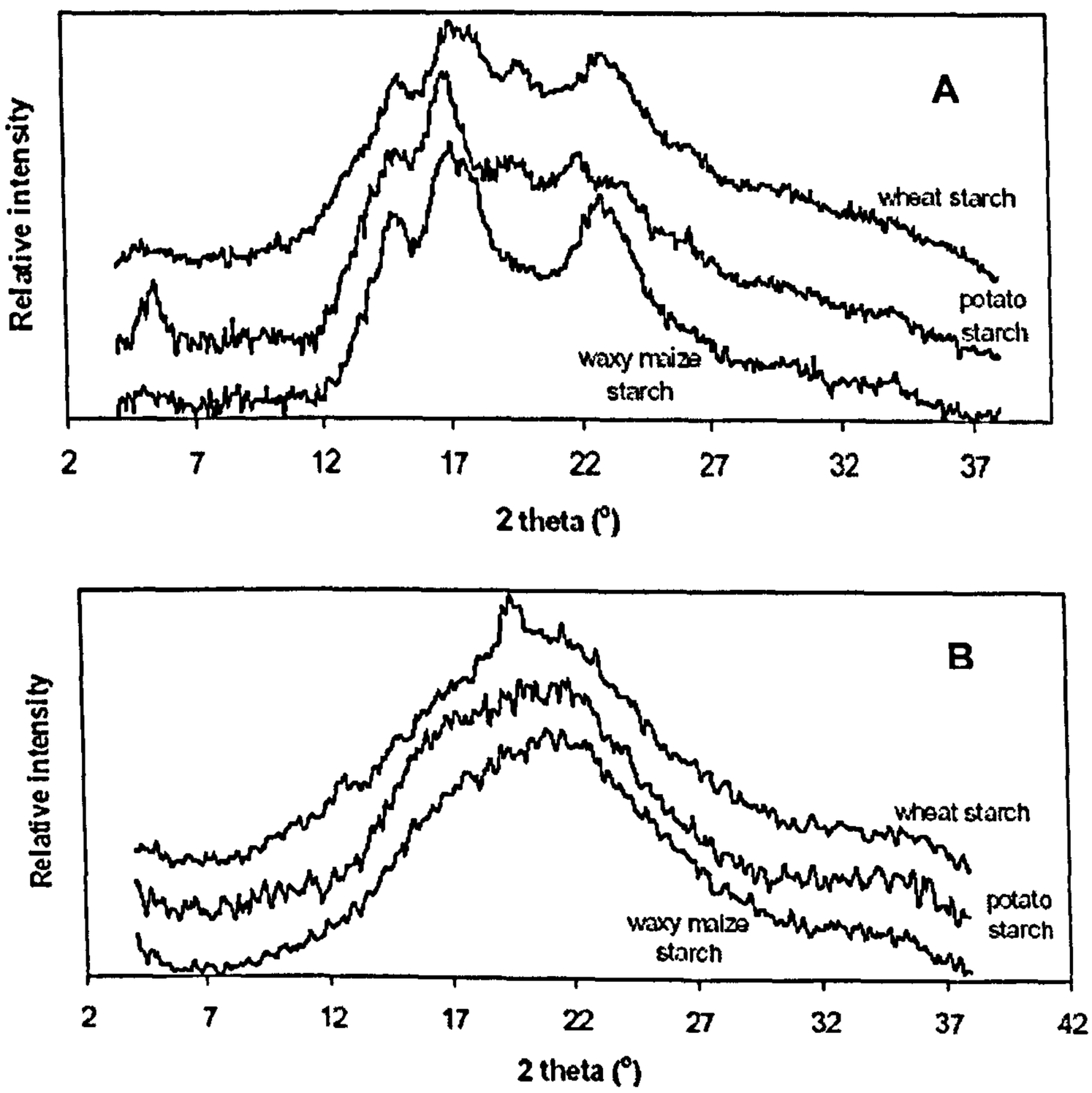

Figure 3.19. X-Ray diffractogram for Native (A) and Amorphous (B) wheat, potato and waxy maize starches (Ottenhof 2003).

3.3.5.1 Methodology

The instrument used was a Brukker D5005 X-Ray diffractometer ($CuK_{\alpha} \rightarrow 0.154$ nm). The experimental settings were typically; step scanning for an angle range from $2\theta = 4^{\circ}$ to 38°, an angular step of 0.05 per 3s and rotational speed of 60 rpm.

TAfter each run, the diffractogram for the empty holder used was subtracted. All the samples (model systems and commercial products) were run in duplicates

3.3.5.2 Sample Preparation

As mentioned before, this technique can evaluate the amount of starch conversion during processing. The diffractograms for the data shown in this section are also discussed in more detail in the results chapters of this thesis.

The freeze dried extruded starch-glycerol samples were ground and sieved to three different particle size fractions; diameter (d) <180 μm, 180< d <212μm and d > 212μm. The latter was used to determined starch conversion during extrusion. Next figure showed the X-ray diffractograms for the three starches with their respective glycerol content.

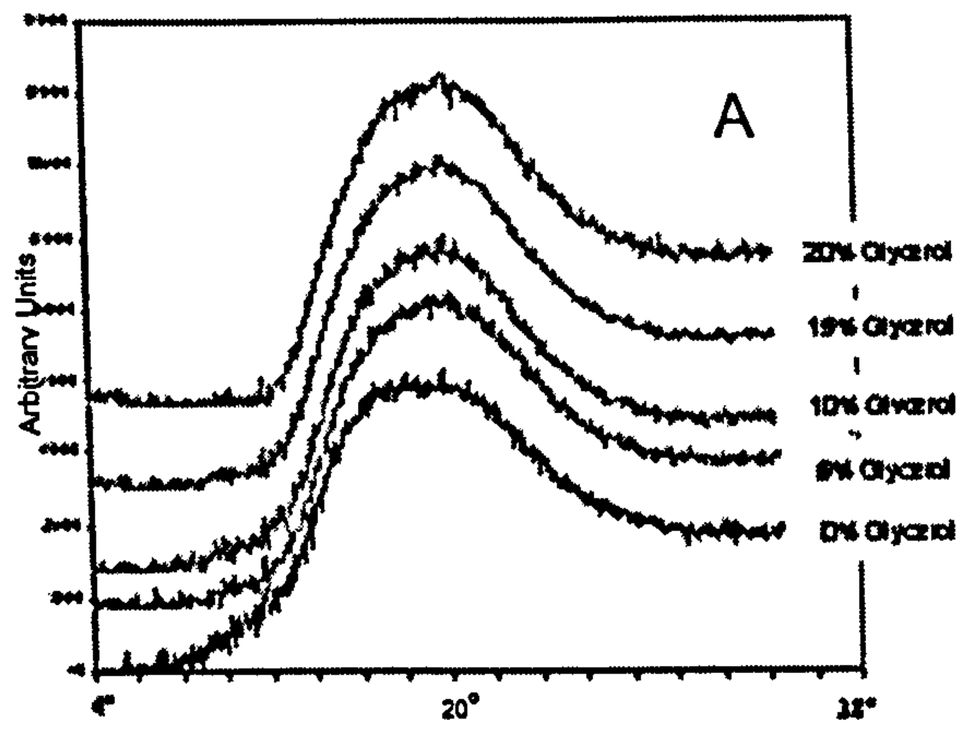

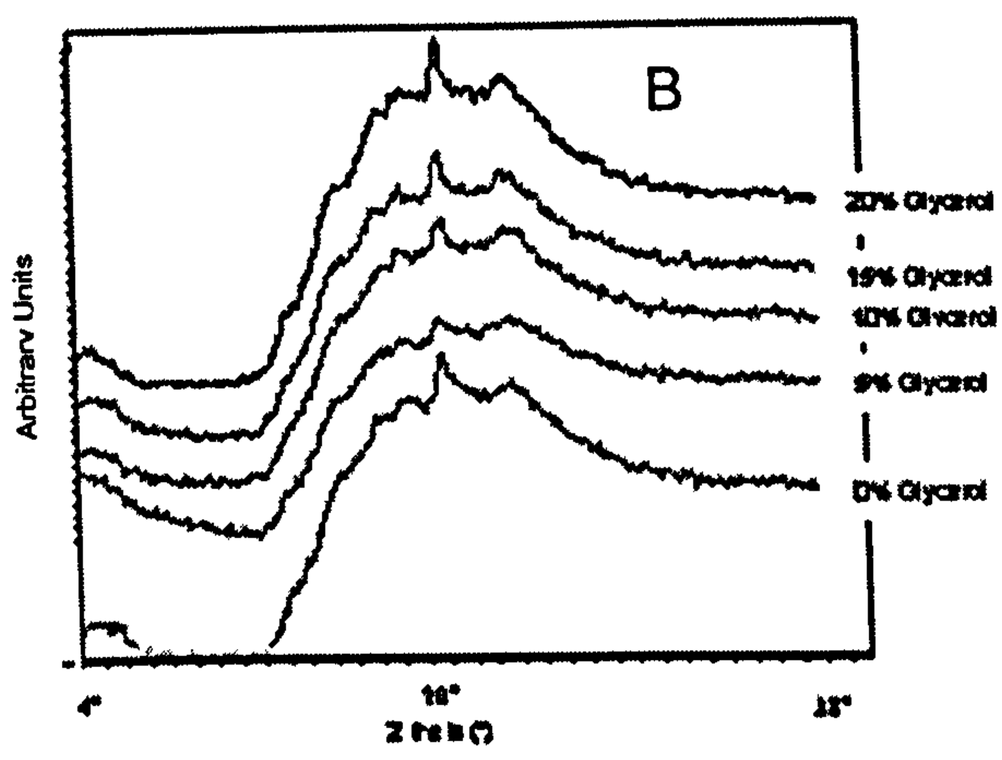

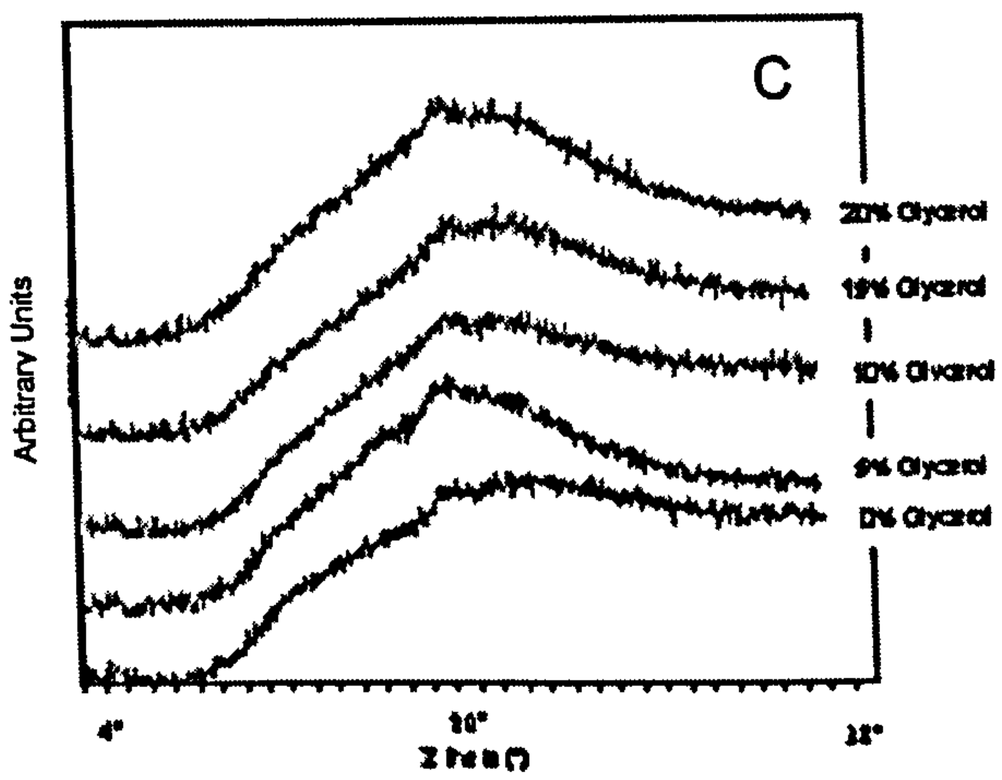

Figure 3.20. X-ray diffractograms for the "Fresh"freeze dried waxy maize starch (A), rice starch (B) and wheat starch (C) extrudates with different glycerol contents.

Although this section is limited to the description of the analytical techniques used, a brief discussion of the diffractograms obtained during sample preparation is also presented.

Figure 3.20-A shows the complete conversion of the waxy maize starch during extrusion. This conversion seems to be complete for all the glycerol contents. For rice starch and glycerol (Figure 3.20-B), the diffractogram shows the presence of a shoulder at ~ 13° and a peak at ~ 20°. The diffraction as these angles represents a more ordered structure formed by the presence of amylose-lipid complex. It is well known the affinity between the non-polar nature of the aliphatic chain of the amylose molecule and the lipids naturally embedded in the native granule (Kugimiya,

Donovan et al. 1980, Kugimiya and Donovan 1981, Buléon, Colonna et al. 1998, Becker, Hill et al. 2001, Gelders, Vanderstukken et al. 2004).

The peak at ~ 18° and ~ 23° in figure3.21-B (dotted lines) seems to be related to native starch not being fully converted during extrusion. This doesn't seem to be related to a lower SME, the values for this parameter seems slightly higher compared to the other two studied starches (table 3.3). This is especially noticeable for the 20%glycerol mixture. It is possible that for this specific starch high moisture and glycerol concentration could have a lubricating effect protecting its native structure from shear effect during extrusion. X-ray diffractograms for wheat starch mixtures (Figure 3.20-C) showed a fairly amorphous structure. Just some small peaks at 20° are present suggesting some formation of amylose-lipid complexes during sample preparation.

In order to assess possible retrogradation on the samples dried for different times at 70°C, starch containing 0 and 20% and dried for short and long drying time were x-ray scanned. Figure 3.22 presents the diffractograms for waxy maize, rice and wheat starch for lowest and higher moisture contents obtained after drying as discussed in section 3.3.2.2.

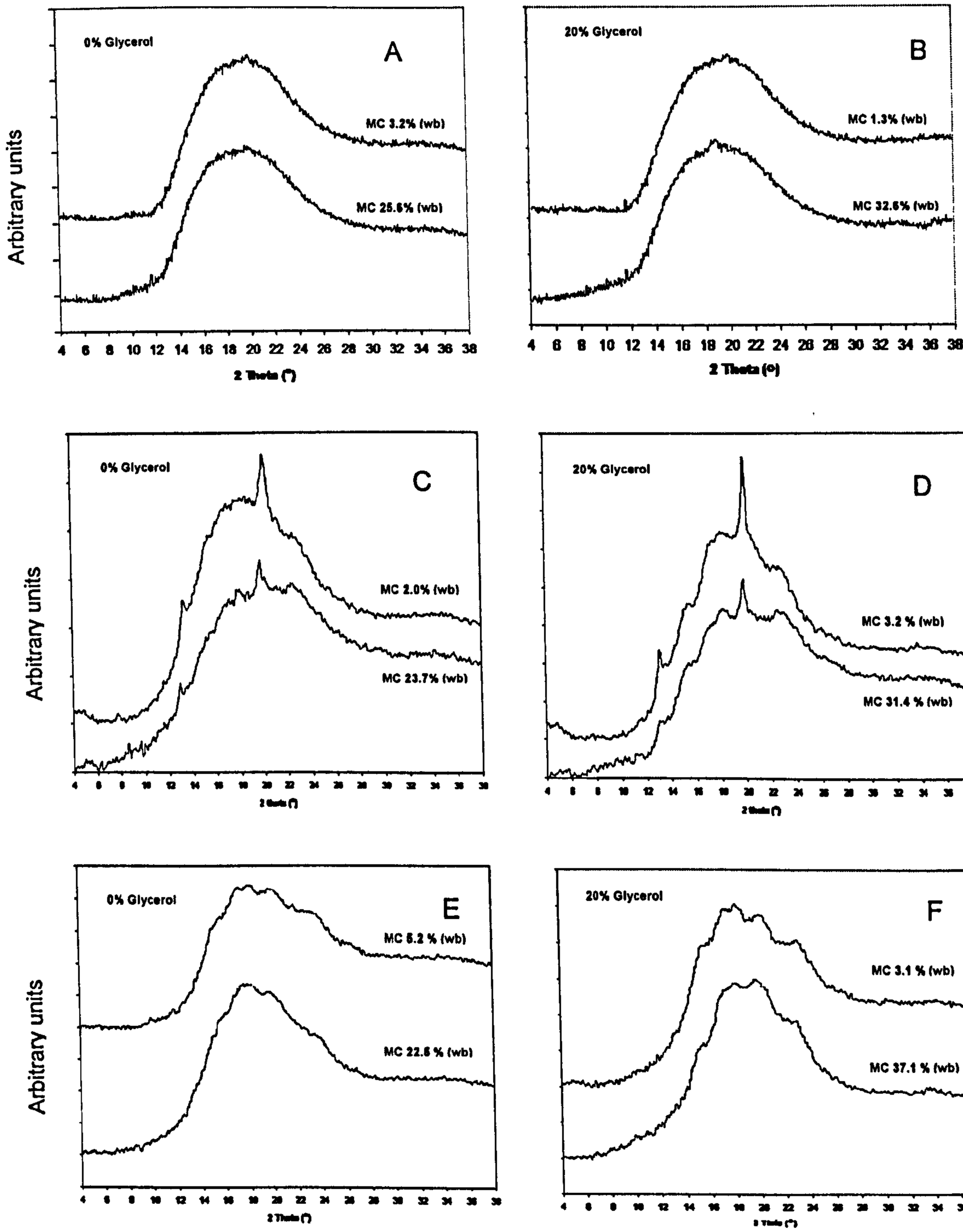

Figure 3.21. X-Ray diffraction patterns for waxy maize (graphs A and B), rice (graphs C and D) and wheat starch (graphs E and F) extrudates with 0% and 20% glycerol.

It is expected an intermediate behaviour for intermediate glycerol (5%, 10%, 15%) and moisture contents (~3%<MC<~30%).

The diffractograms show clearly that the structure of the waxy maize starch extrudates with 0% and 20% glycerol remained completely amorphous after drying (graphs A and B).

In the case of rice starch, amylose-lipid complexes were detected on the wet samples for the control and 20% glycerol extrudates. This was represented by marked peaks at ~ 13° and ~19°. Also some degree of ordered structure was also detected in both samples with small peaks at ~ 17° and ~ 23°. The intensity of these peaks slightly increased after the drying process, which can be observed of the extrudates dried to ~3% (wb).

The diffractograms for wheat starch-glycerol extrudates (graphs E and F) show an amorphous pattern for the control sample and an indication of some crystalline structures on the 20% glycerol sample. In both samples a slight increase in crystallinity was detected after drying, as showed in the curves for a moisture contents ~ 5% (wb).

The data obtained from x-ray diffraction indicates no marked differences in crystallinity between the wet and dried samples in the case of the control and the 20% glycerol starch extrudates. This would suggest that drying process would remove moisture quickly enough to minimise the retrogradation of starch.

In the case of commercial products some of the analysis were done on the whole sample (sliced ~3 mm thick). To avoid sample movement during rotation, the sample was fixed to the holder using Blue-Tack (Bostik, Australia). A detailed discussion related to these diffractograms is presented in chapter 8, section 8.3.1 of this thesis.

4 Sorption Studies of Starch-Glycerol Mixtures

It is well known that small changes in moisture can cause major change in the textural properties of food materials (Lloyd and Kirst 1963, Kirby, Clark et al. 1993, Harris and Peleg 1996, Fontanet, Davidou et al. 1997, Suwonsichon and Peleg 1998).

Water is a small and ubiquitous molecule and its effect on texture can be related to the increase in the free volume of the polymer forming the food matrix. The presence of other small molecule components such as polyols (e.g. glycerol, glycol and sorbitol) can also plasticize the polymer matrix. Polyols are commonly used in the food industry, e.g. pet-care products, as humectants in order to reduce the overall "water activity" of the mixture (The-UK-Glycerin-Producer's-Association 1975) by reducing the water availability due to its tri-hydric nature (three OH groups). This would help to control the microbial stability of the product whist keeping desirable texture attributes.

The objective of the experiment work described in this chapter is to elucidate the effect of polyols, specifically glycerol, on the sorption behaviour of starchy materials when stored under different relative humidities.

A set of model systems; waxy maize, rice and wheat starch mixed with different glycerol concentrations, were prepared by extrusion. The samples were ground to a defined particle size and analysed using the Dynamic Vapour Sorption or DVS (details of this technique are presented chapter 3 section 3.3.1).

Also the kinetics of sorption (diffusivity) was evaluated for the different starch and glycerol mixture, giving information on the mobility of the system, which is an important factor in the prediction of the stability of hydrophilic materials when exposed to different relative humidities.

4.1 Hypotheses

The main hypotheses tested in this chapter were divided and investigated as follows:

- Due to its hygroscopic nature, the presence of glycerol will increase the sorption capacity of starch when equilibrated at different relative humidities (RHs).
- Glycerol will reduce the water activity of a starchy material at constant moisture content.
- Starchy materials and glycerol do not interact and the sorption isotherms for these mixtures can be predicted using the weight fractions of their individual sorption isotherms.
- The presence of glycerol would increase the diffusion coefficient (*D*) of starch based systems due to an increase in molecular mobility.

The following section of this chapter discusses some of the fundamentals related to the development of sorption isotherms and their technological application in food materials

4.1.1 Sorption Isotherm

4.1.1.1 Theoretical Background

Water plays an important role with respect to the properties of food systems. It influences the physical or textural characteristics of food products as well as its chemical stability (Labuza 1994). Moisture loss or gain from one region to another would continue in order to reach thermodynamic equilibrium.

The term water activity (*Aw*) is used to indicate an intrinsic parameter of a food and equilibrium relative humidity, a property of the surrounding atmosphere in equilibrium with the food system under consideration (Van den Berg and Bruin 1981). Today Aw is considered to be a major variable to control and ensure the shelf life stability of many foods

The concept of Aw is presented and discusses in the following sections.

4.1.1.1.1 Free Energy and Definition of Activity

The thermodynamic concept of activity of a component *i* can be explained in terms of its fugacity *(f)* and the fugacity of the component in a standard state, (Lewis 1901, 1907). The term fugacity is related to the concept of Gibbs free energy (*G*), which defines the amount of available energy in a system to perform work (e.g. chemical reaction) at constant pressure and temperature.

When the Gibbs free energy is expressed on a molar basis, it becomes the chemical or thermodynamic potential, denoted by *u*.

For a mixture, each component *i* has its own partial molar chemical potential (equation 4.1) affecting the overall Gibbs value of the system (Van den Berg and Bruin 1981).

$$u_i = \left(\frac{\partial G}{\partial n_i}\right) P,T,n_j \qquad \textit{Equation 4.1}$$

Where u_i, is the chemical potential of the component *i*, *G* is the free energy of the system, n_i and n_j number of moles of component *i* and *j* respectively, *P* is pressure and *T* temperature.

Using the Gibbs-Duhem equation for a system of one single component *i*, at constant temperature ($dt = 0$) and using the ideal gas relationship ($PV = nRT$), the following relation is obtained (at constant temperature) (Van den Berg and Bruin 1981):

$$du_i = \frac{RT}{p} dp_i = RTd\ln p_i \qquad \textit{Equation 4.2}$$

Where *R* is the universal gas constant, *T* the temperature, p_i the pressure of the pure component.

If the component *i* is a liquid, p_i would be the vapour pressure at a given temperature.

This relation contributes to take the more abstract concept of thermodynamic potential to a more simple function with a physical quantity such as pressure.

A generalisation of equation 4.2 by Lewis (1901), made this relation more applicable to real systems by defining a corrected pressure function called *fugacity (f)*.

Fugacity is considered as a measure of the tendency of a component to escape.

An infinitesimal isothermal change in the thermodynamic potential for any component in a mixture whether solid, liquid or gas, pure or mixed, ideal or not, at constant temperature is defined as (Lewis 1901):

$$du_i = RTd\ln f_i \qquad \textit{Equation 4.3}$$

Since the absolute value of chemical potential can not be determined after integration, a reference state at the same temperature is used.

When subtracting the reference relation from equation 4.3 the following is obtained:

$$u_i - u_i^{\theta} = RT\left(\frac{f_i}{f_i^{\theta}}\right) \qquad \textit{Equation 4.4}$$

The ratio (f_i/f_i^{θ}) for a component is called activity (relative activity) a_i of the component *i*:

$$a_i = \left(\frac{f_i}{f_i^{\theta}}\right) \qquad \textit{Equation 4.5}$$

The limitations are that the temperature of the reference state equals the temperature of the mixture and the total pressure is defined.

At equilibrium between different phases, the fugacity of each component is the same throughout the heterogeneous system. In this case, the activity is the same throughout the system when the reference fugacities are defined equally for each phase (Van den Berg and Bruin 1981).

4.1.1.1.2 Water Activity

The activity of water in a mixture (gas phase, in solution, "bound" to a solid) can be expressed in terms of relative fugacity. In other words the fugacity of water in the mixture divided by the fugacity of pure water at the same temperature and pressure. Gal (1972) showed that in experimental terms there is small difference between *water activity* and the concept equilibrium relative humidity (p_w/p_w^θ). Therefore Aw can be express in the following relation;

$$Aw = (p_w/p_w^\theta) \qquad \textit{Equation 4.6}$$

Where p_w is the equilibrium water vapour pressure over the system and p_w^θ the vapour pressure of pure water at the same temperature and pressure.

Van den Berg and Bruin (1981) mentioned the following considerations regarding the definition of water activity.

a) The water activity refers only to the true equilibrium state (real food systems do not always fulfil this requirement)

b) The water activity is defined at a specific temperature and total pressure.

c) The reference state must be well specified.

4.1.1.1.3 Sorption Isotherms

The relationship between the total moisture content and the water activity, over a range of values, at constant temperature, yields the sorption isotherm when expressed graphically. It can be obtained by absorption or desorption.

a) Absorption isotherm: obtained by having a completely dry material which is stored at different relatives humidities measuring the weight gain from the water uptake.

b) Desorption isotherm: obtained by placing an initially wet material in different relative humidities and measuring the loss in weight.

In both cases, "equilibrium" is achieved when there is no water migration from/to the sample during storage (no changes in material mass is detected).

Brunauer, Deming et al. (1940) classified the adsorption isotherms into five general types (figure 4.1)

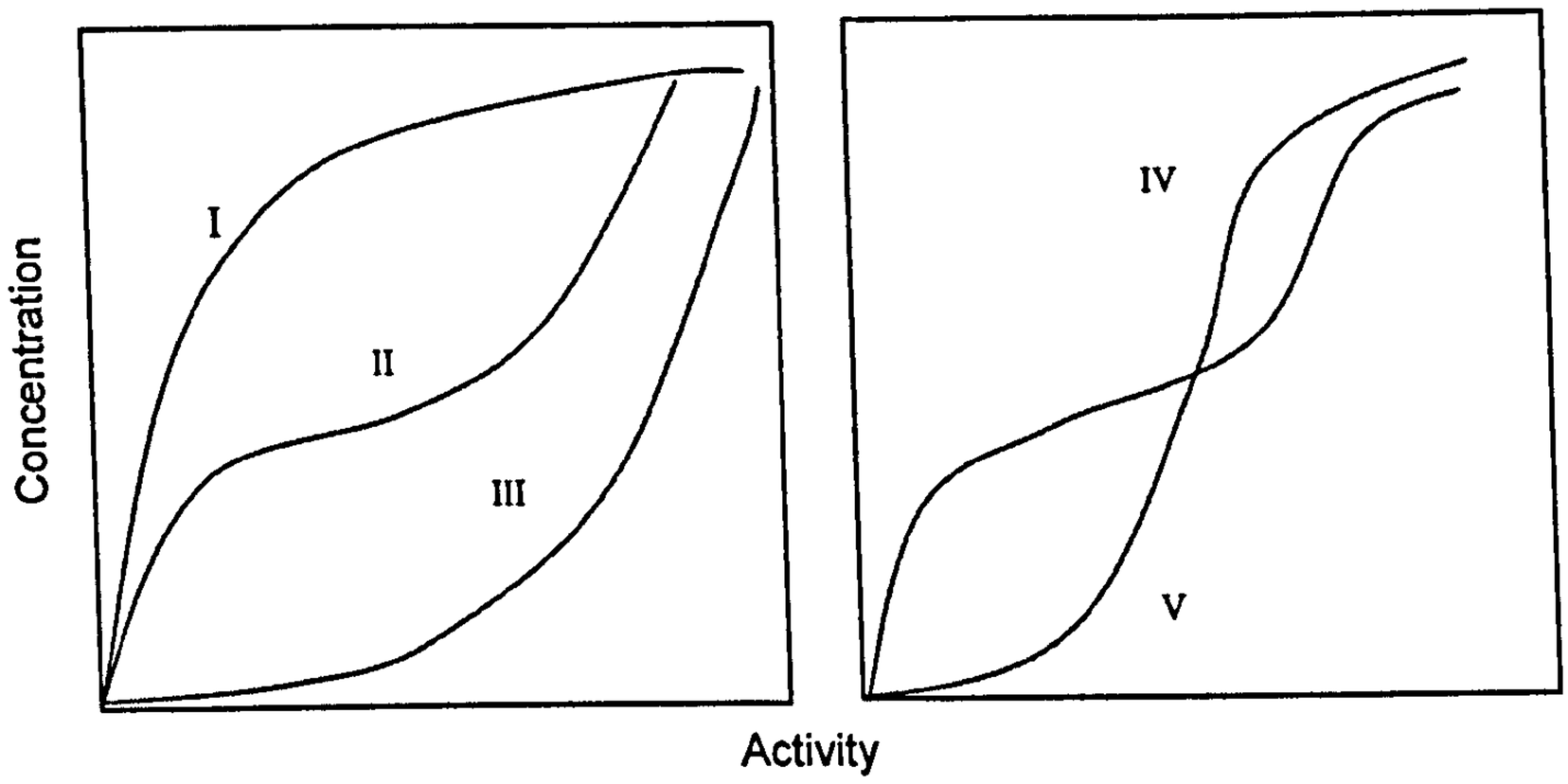

Figure 4.1. General types of sorption isotherms. Modified from (Brunauer, Deming et al. 1940).

Type I is related to the Langmuir sorption behaviour, Type II (combination of Type I and III), Type III, IV and V.

Moisture sorption isotherms of most foods are generally sigmoidal is shape and they have been classified as Type II (Iglesias and Chirife 1982; Peleg 1993), (Bader and Goritz 1994; Labuza 1994; Coupland, Shaw et al. 2000; Al-Muhtaseb; McMinn et al. 2002; Al-Muhtaseb, McMinn et al. 2004).

For interpretation purposes the sorption isotherm for food systems may be divided in three regions (figure 4.2). The distinction between the three areas can not be expressed in terms of precise ranges of water contents, because the boundaries are vague. Rather one can get an indication of the differences in the overall nature of the interaction between water and the solids in the three stages (Van den Berg 1991). Region I represents strongly bound water with an enthalpy of vaporisation considerably higher that of pure water (Van den Berg and Bruin 1981; Van den Berg 1991). The moisture content is often considered to represent the adsorption of the first molecules of water (monolayer). Van den Berg (1981) suggested that stoichiometrically the sorption sites in the starch can be identified as the anhydroglucose monomer units. One molecule of

water per anhydroglucose monomer unit gives a moisture content of 11% (db). Similar figure compared with the monolayer values (m_o) obtained from semi-empirical models.

Usually water molecules in this region are unfreezable and are not available for chemical reaction. Most dried products are empirically observed to display their greatest stability at moisture contents comparable to the monolayer (Van den Berg 1991).

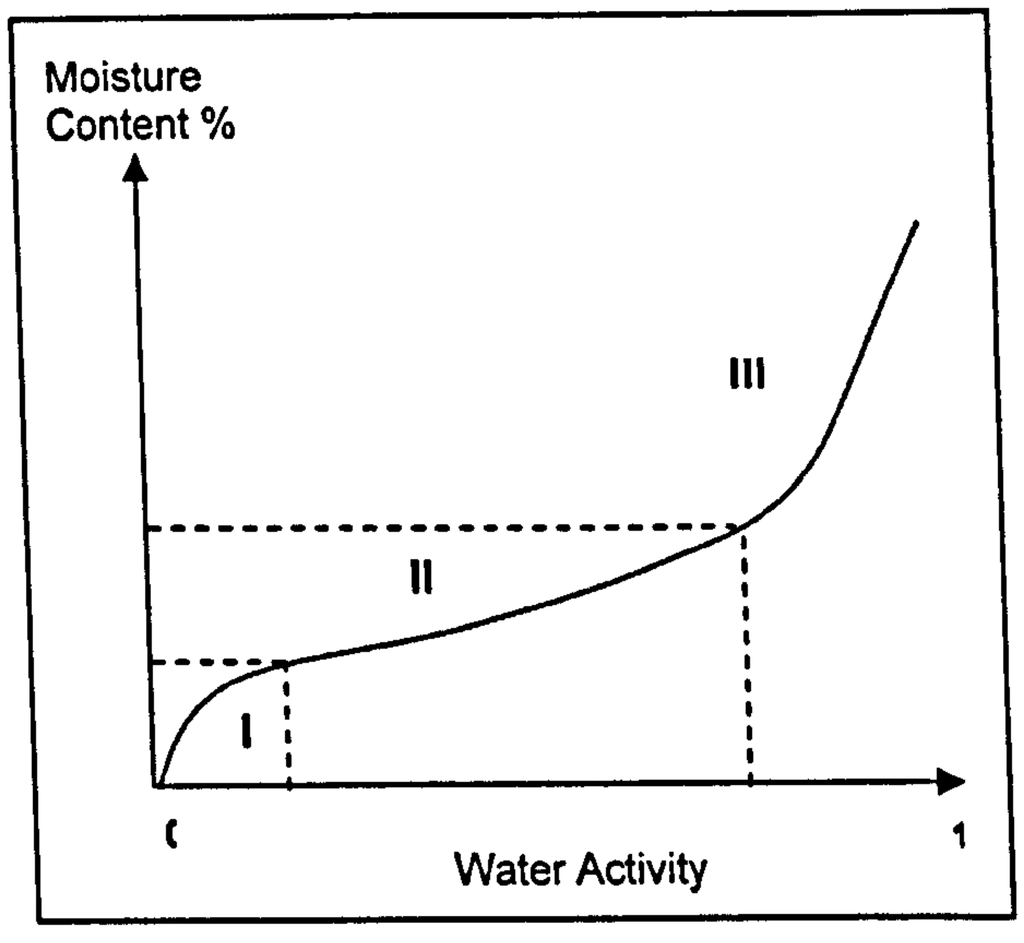

Figure 4.2. Generalised sorption isotherm for food systems

In region II, the water fraction in less strongly bound than in the region I. The enthalpy of vaporisation is little greater than the enthalpy of vaporisation of pure water. These water molecules sorbed near or on the top of the first molecules or penetrate into the newly created spaces of the swollen structure (Van den Berg and Bruin 1981). The water is available as a solvent for low-molecular weight solutes and for some biochemical reactions (Al-Muhtaseb, McMinn et al. 2002). In region II the initially hard and brittle material undergoes a glass transition, by the plasticising effect of water, becoming weak, plastic, or rubbery depending of the polymer.

Compared to the region I, water molecules show a sharp increase in molecular mobility. There is also an increase in the diffusion coefficient of the matrix (Karel and Saguy 1991); taking longer to reach "equilibrium", as the rate of polymer swelling becomes the limiting factor (Van den Berg 1991). Water

present in the material freezes at a lower temperature compared to the bulk water (Al-Muhtaseb, McMinn et al. 2002).

In region III, excess water is present in macro-capillaries or as a part of the fluid phase in high moisture materials. Swelling is exactly in proportion to the volume of water sorbed (Van den Berg 1991).This moisture exhibits nearly all properties of bulk water and thus is capable of acting as a solvent. Microbial growth becomes the major deteriorative reaction in this region (Al-Muhtaseb, McMinn et al. 2002).

Fenema O. R (1996) summarised reaction kinetics as a fuction of water wapour pressure or water activity (AW) .

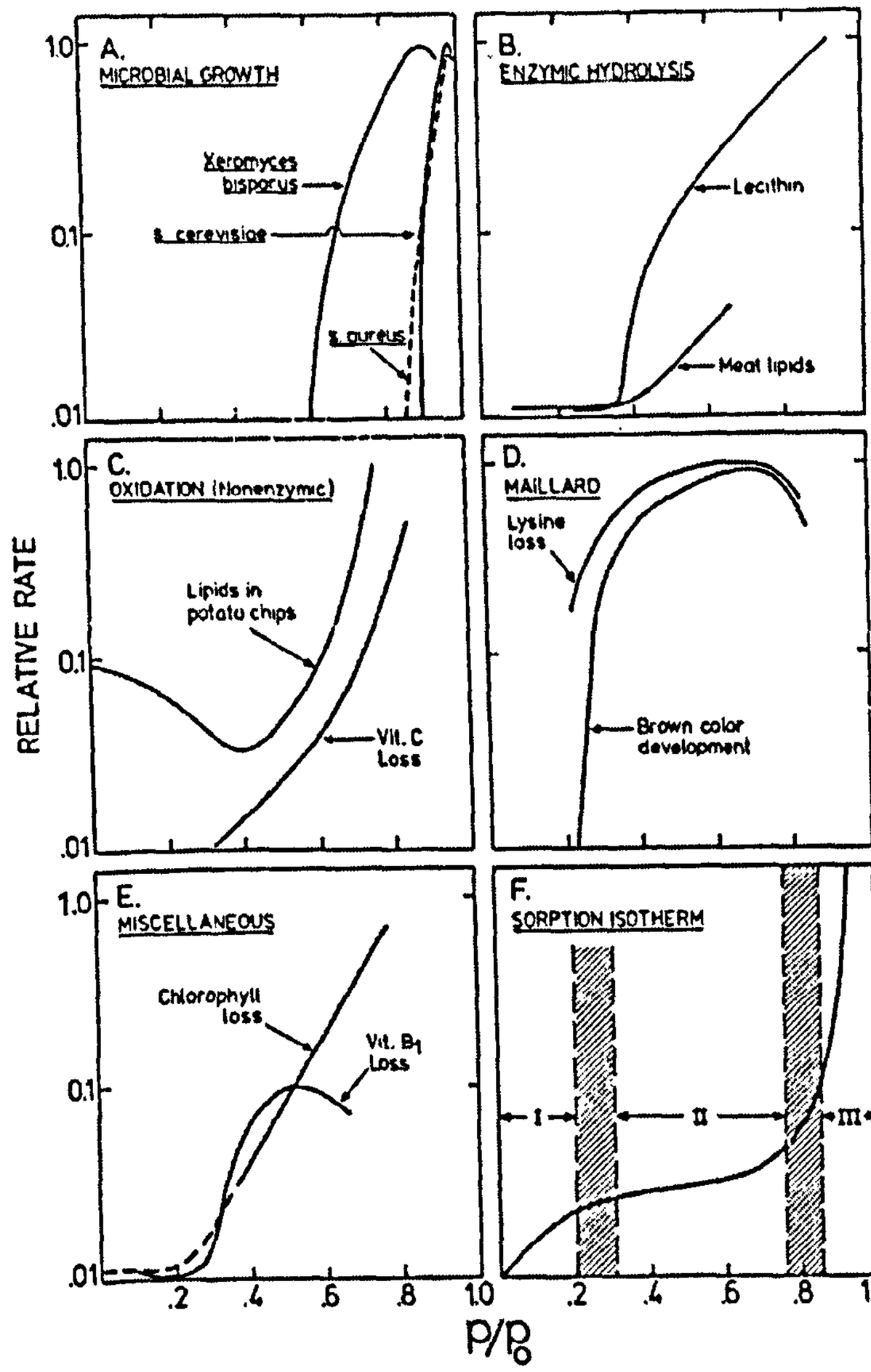

Figure 4.3. Relationships among food stability, sorption isotherm and water activity. (A) microbial growth vs p/p_o). (B) Enzymatic hydrolysis vs p/p_o. (C) Oxidation (non-enzimatic) vs p/p_o. (D) Maillard browning vs p/p_o. Miscellaneous reaction rates vs p/p_o (Fennema 1996)..

The above diagram has been useful in relating the rates of reaction for different food stability parameters to the water activity. Nevertheless, it must be considered that the term "activity" is based on thermodynamic equilibrium, and most real foods do not reach this state between their various components nor with their environment.

Some critics (Franks 1991) have suggested that since the reaction rates (kinetics) shown in the map do not represent a relationship with partial vapour pressure in true equilibrium the stability map is useful, at best, as a quality control tool applicable only for the same products at the same temperature.

The experimental work presented next focuses on the study of the effect of glycerol on the sorption properties of extruded starch-glycerol systems. These properties were also compared between starches from different botanical sources.

4.1.1.2 Results and Discussions

Extruded waxy maize (WMSE), rice (RSE) and wheat starchl (WSE) - glycerol mixtures were freeze dried and ground, using the particle size fraction ~ 180 μm following the protocol described in section 3.3.1.2 from chapter 3 of this thesis. The sorption properties of these samples (~ 4 mg of the ground sample) were evaluated using Dynamic Vapour Sorption (DVS) at 25°C. Details of the experimental protocol are presets in chapter 3 section 3.3.1.1.

Prior the DVS analysis, Wide X-ray Diffraction was performed on all the powder in order to evaluate their crystallinity. The patterns showed an amorphous structure for all the mixtures suggesting a complete starch granule conversion during extrusion (X-ray patterns of the samples are presented in chapter 3 section 3.3.5.2).

4.1.1.2.1 Starch-Glycerol Sorption Comparison

The following figures show the sorption data for waxy maize, rice and wheat starch extrudates each with a glycerol concentration of 0, 5, 10, 15 and 20% (db).

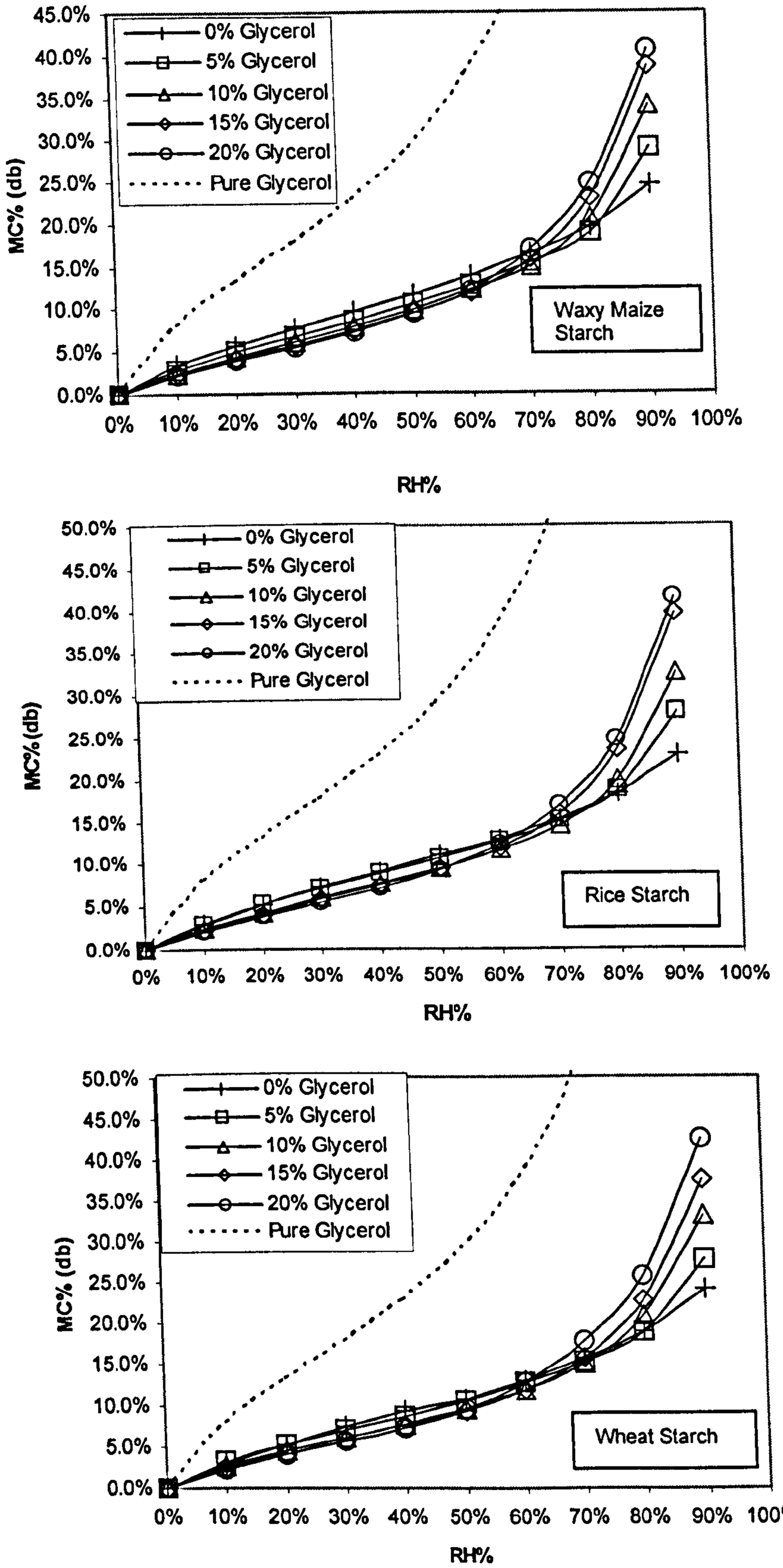

Figure 4.4. Sorption isotherm for waxy maize, rice starch and wheat starch-glycerol extrudate at 25°C.

Due to experimental difficulties, the sorption isotherm for pure glycerol was obtained from the literature (Labuza 1994).

For the three starches, glycerol has a similar effect on sorption behaviour. It seems clear that this polyol contributes to an increase in moisture uptake for RHs >70%. On the other hand for RHs <60%, glycerol does not contribute to an increase in moisture compared to the control (no glycerol). Moreover it seems that higher concentrations of glycerol reduce the water uptake during equilibration in this RH range.

Similar behaviour has been reported for barley starch (Forssell, Mikkila et al. 1996), potato starch (Sala and Tomka 1993; Lourdin, Coignard et al. 1997) and pure amylose and amylopectin (waxy maize starch) (Myllärinen; Partanen et al. 2002). Myllärinen, Partanen et al. (2002) suggested that at low RHs water is displaced from the starch active polar groups by the glycerol. The tri-hydric alcohol structure of glycerol (3 –OH) and the solid acting as an adsorbent at these low RHs may explain these results(Van den Berg and Bruin 1981). At these low vapour pressures hydrogen bonding is the main force involved in the adsorption mechanism, suggesting a predominance of glycerol over water.

A complete opposite behaviour was detected for RH>70% where glycerol seems to facilitate water sorption. At these high water vapour pressures there is an increase in the molecular mobility (long range mobility of the polymer backbone), by the plasticising effect of glycerol and water. It is possible that at these high RHs glycerol molecules move freely absorbing more moisture from the surroundings.

The effect of this polyol on sorption can be more clearly observed by plotting the final moisture content as function of the weight fraction of starch and glycerol (plotted up to 70%RH for clarity).

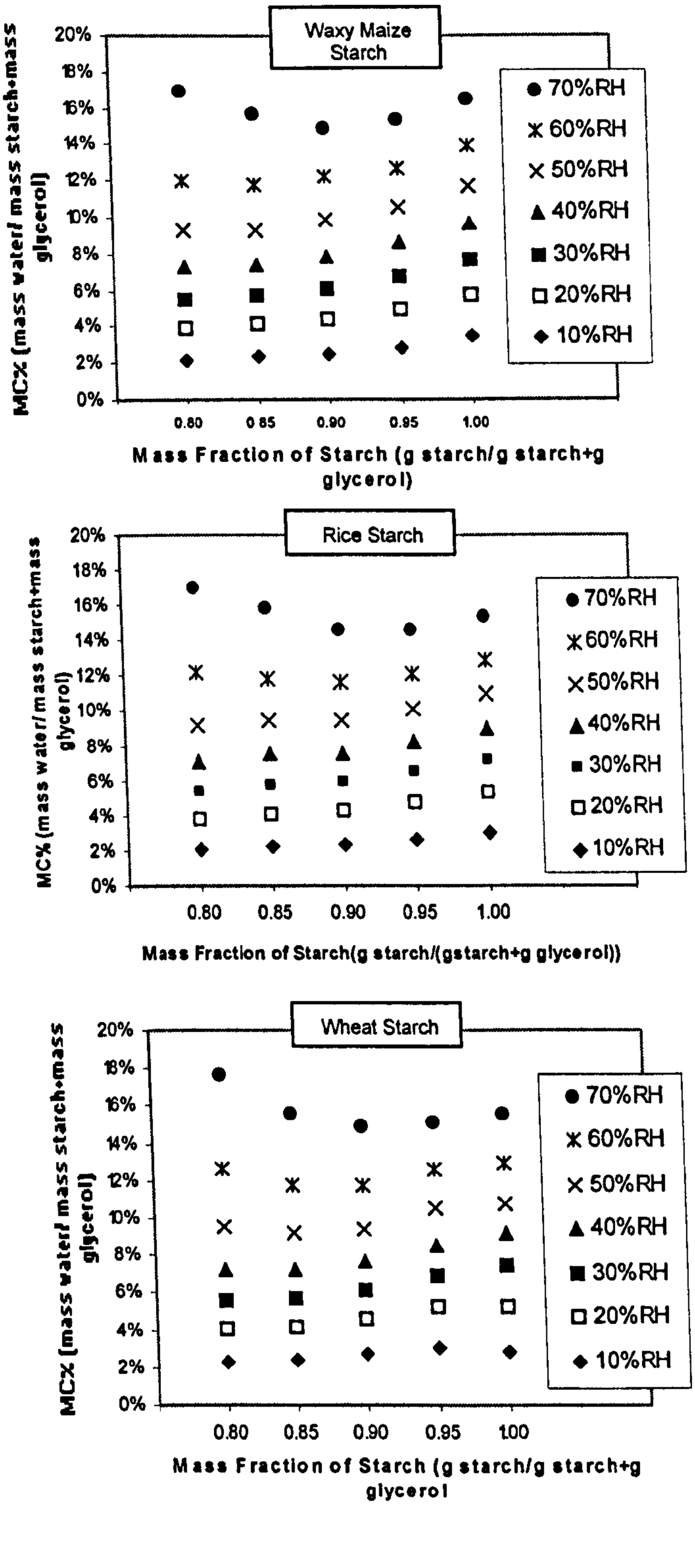

Figure 4.5. Moisture content as a function of weight fraction of starch and glycerol. Based in sorption isotherm data for waxy maize, rice and wheat starch-glycerol extrudate at 25°C.

From figures 4.5, it is clear that glycerol will not contribute to increase the moisture content in the samples for RHs<70%. Moreover a "drying effect" seems evident for RHs <50%.

This behaviour may have an impact of water redistribution of starch containing materials in presence of glycerol. When exposed to RHs <70% (common environmental storage condition), moisture would be pushed out from the starchy matrix going to other components affecting changes in mechanical and stability properties.

When comparing *Aw* for the starch-glycerol mixtures at constant moisture content, different behaviours were obtained. From figure 4.4, at high moisture contents (MC > 15%), adding glycerol would contribute to decrease the *Aw* following the rationale of being a known humectant. For lower moisture contents (MC <10%), adding glycerol contributed to an increase in the *Aw*, in other words the fugacity or chemical potential of water is increased. This situation may be explained by glycerol molecules interacting with starch, increasing the availability of water ultimately leading to physical and/or chemical instability.

4.1.1.2.2 Starch-Starch Comparison

There were not apparent differences in the sorption behaviour between the three different starches in the absence or presence of glycerol. Figures 4.6 and 4.7, show sorption isotherms for waxy, rice and wheat starches grouped by glycerol content.

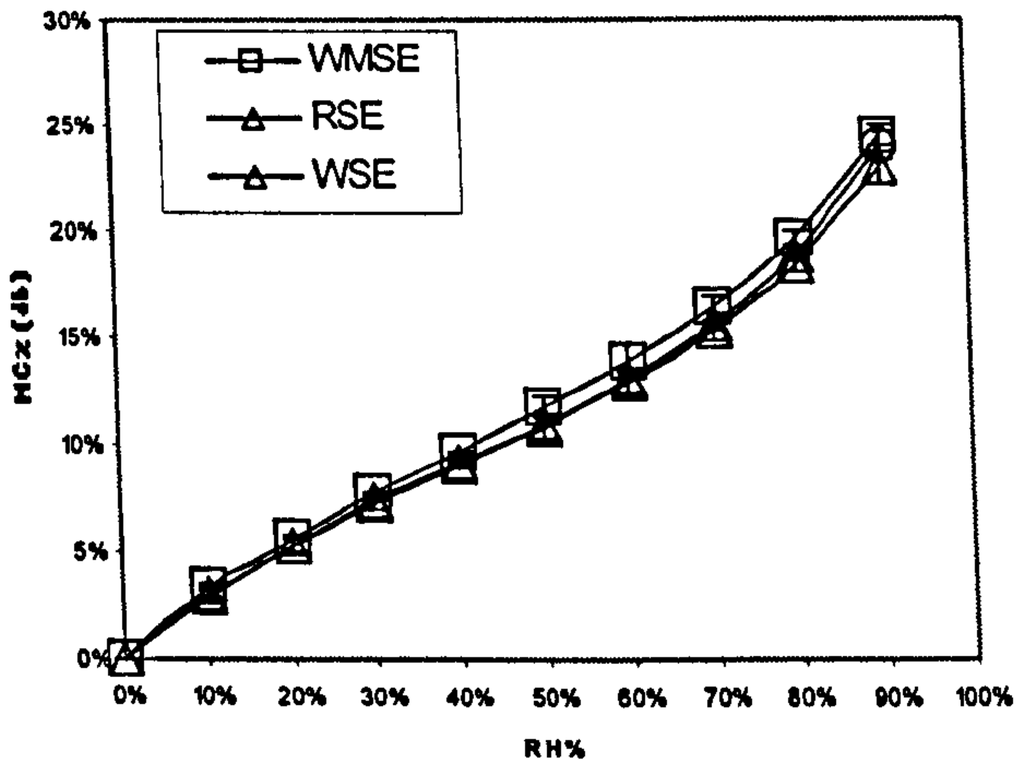

Figure 4.6. Sorption isotherm for waxy (WMSE), rice (RSE) and wheat starch (WSE) with 0% glycerol extrudates at 25°C. Error bars represents the standard deviation of 3 replicates.

Similar behaviour have been reported in the literature for other starchy materials (Iglesias and Chirife 1982).

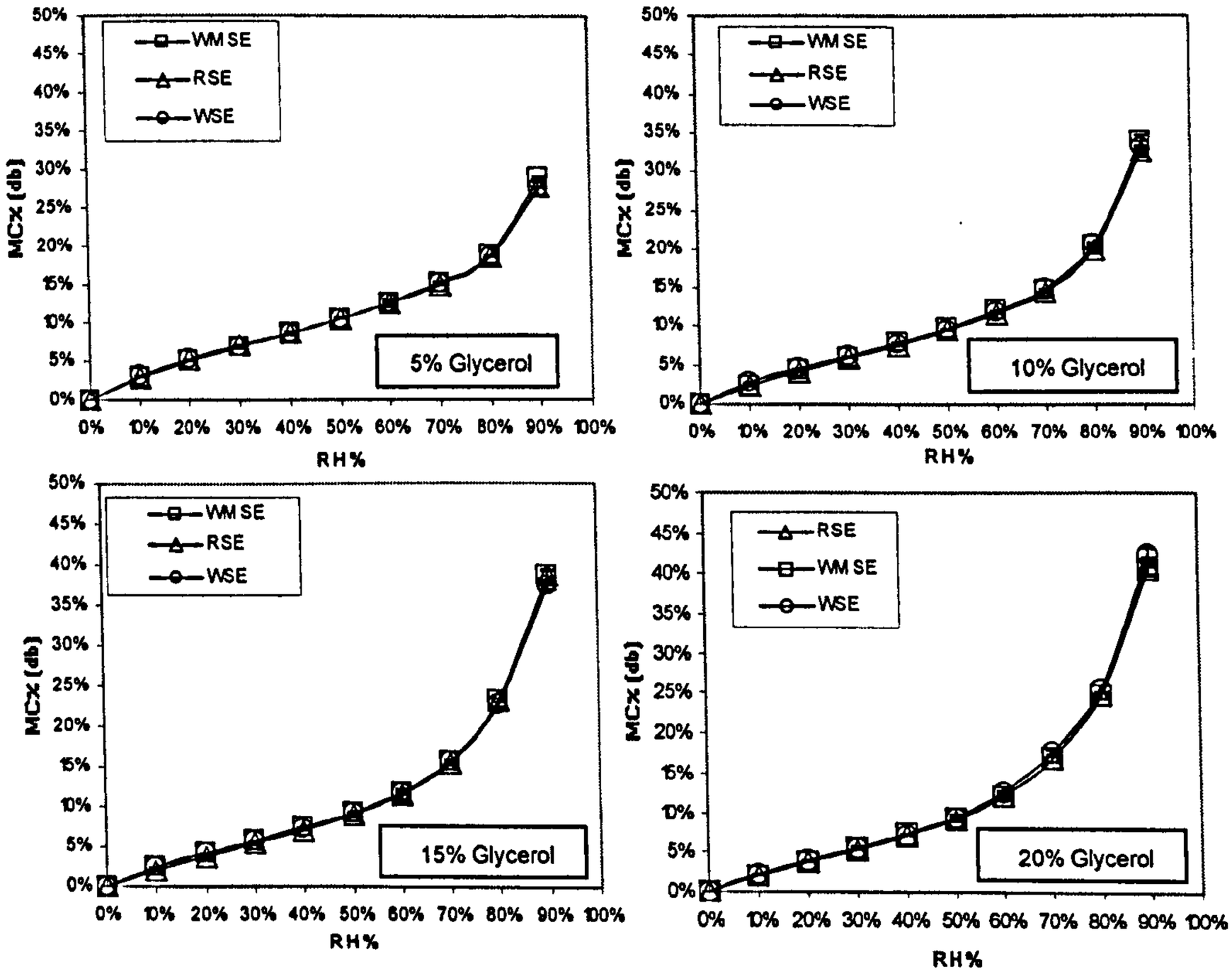

Figure 4.7. Sorption isotherm for waxy (WMSE), rice (RSE) and wheat starch (WSE) with 5%, 10%, 15% and 20% glycerol extrudates at 25°C. Error bars represents the standard deviation of 3 replicates.

Sorption isotherms at 25°C obtained from starch containing ~ 70% amylose starch (Hylon VII, Sigma) also resulted in the same sorption profile (data not shown).

These results suggest that in terms of the overall moisture sorption profile, the presence of a higher concentration of highly branched structures (amylopectin) does not contribute to an increase in moisture content at equilibrium. Therefore the water sorption would be dependent on the glucose unit rather than how this would be arranged at a higher level of organization.

Another interesting finding is the change in shape from a clear Type II isotherm for the control samples (figure 4.6) to Type III like curve when the glycerol content was increased (figure 4.7).

4.1.2 Sorption Isotherm Modelling

As discussed on the previous section, sorption isotherms are useful to establish the expected changes in moisture content when environmental conditions change (relative humidity and temperature). Another important aspect in obtaining these curves is that physical-chemical information from the studied material can be obtained by the application of fundamental models. This approach is discussed on the next section, where a series of models are tested on the obtained sorption data. The accuracy of the predictive values given by the models was also evaluated.

4.1.2.1 Theoretical Background

Van den Berg (1985) described the sorption process at low partial vapour pressures as "a localised physical adsorption on an initially rigid adsorbent". However, the hydrophilic nature of most food materials and the plasticising effect of water at higher relative humidity promote a gradual increase in the system's mobility that can lead to the solubilisation of the polymer.

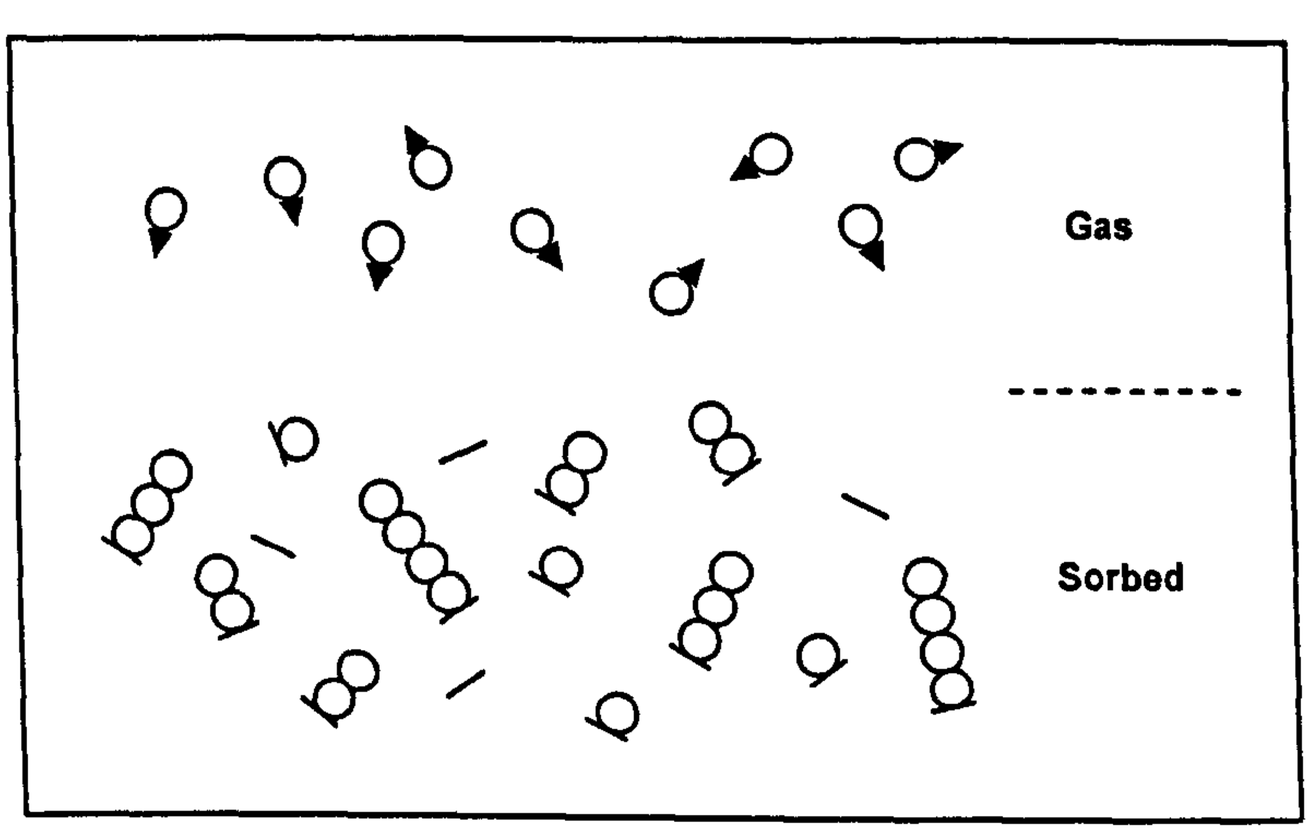

Figure 4.8. Diagram showing the sorption system underlying BET-like models of sorption (Van den Berg 1985). Circles with small arrows represent highly mobile molecules in a gas phase. The circles attached to the surface and to each other represent molecules adsorbed to the polymer chains as monolayer (single circle) and multilayer (circle attached to each other) respectively.

Three models have been used to represent the experimental sorption data: Brunauer-Emmett-Teller model (BET), Guggenheim-Anderson-de Boer (GAB) model and Peleg model.

The BET is commonly used to model up to 50%RHs and the GAB and Peleg models are used for RH up 95%. The parameters used in BET and GAB models can give information related to sorption at low RHs and the energies (heats of sorption) involved during the sorption process. Although the parameters used in the Peleg model do not have any fundamental meaning, it is often quoted as one of the most accurate models to predict sorption isotherms due to the four parameters present in the equation.

4.1.2.1.1 Brunauer-Emmet-Teller model (BET) Model

The BET equation is a generalisation of the Langmuir model for the sorption of a gas onto a solid surface (Brunauer, Emmet et al. 1938). The Langmuir model pictures a chemi-sorption process which leads ultimately to a monolayer film over the surface of the adsorbent. The derived adsorption isotherm results from the assumption of equilibrium between the gas phase and the partially formed monolayer.

Atkins (1998) summarised this as the following relationship:

$$\frac{d\theta}{dt} = k_a P(1-\theta) = -k_d \theta \qquad \textit{Equation 4.7}$$

Where:

k_a, k_d = rate constant for adsorption and desorption respectively

P = partial pressure of the gas

θ = fraction of the surface covered

$(1-\theta)$ = fraction of the surface not covered

Rearranging equation 4.7:

$$\theta = \frac{KP}{1+KP} \quad \text{with} \quad K = \frac{k_a}{k_d} \qquad \textit{Equation 4.8}$$

For adsorption, up to a monolayer, the amount of gas M adsorbed at some pressure P and the amount of gas M_o needed to form a monolayer are related to θ by:

$$\theta = \frac{M}{M_o} \qquad \textit{Equation 4.9}$$

Combining and rearranging equation 4.8 and 4.9:

$$\frac{M}{M_0} = \frac{KP}{1+KP} \qquad \textit{Equation 4.10}$$

Brunauer, Emmet et al. (1938) made the assumption that the evaporation-condensation properties of the molecules of the second and higher adsorbed layers were the same as of bulk water.

Since at equilibrium s_0 (bare surface area that is covered) must remain constant, the rate of condensation ($a_1 p s_0$) on the bare surface is equal to the rate of evaporation for the first ($b_1 s_1 e^{\frac{-E_1}{RT}}$), second and consecutives layers then:

$$a_1 p s_0 = b_1 s_1 e^{\frac{-E_1}{RT}} \qquad \textit{Equation 4.11}$$

$$\downarrow \quad \downarrow$$

$$a_i p s_{i-1} = b_i s_i e^{\frac{-E_i}{RT}} \qquad \textit{Equation 4.12}$$

Where:

a_1 and b_1 = constant

p = pressure of gas

s_1 = first layer surface area covered

E_1 = activation energy related to the heat of sorption

R = gas universal constant

T = temperature

These authors assumed the activation energy (E) and b_i/a_i (g) equal for the second and higher layers on the surface of the solid surface. When expressing these multi-layers surfaces covered in terms of s_0:

$$s_1 = ys_0, \text{where } y = \left(\frac{a_1}{b_1}\right) pe^{\frac{-E_1}{RT}} \qquad \textit{Equation 4.13}$$

$$s_2 = xs_1, \text{where } x = \left(\frac{p}{g}\right) e^{\frac{-E_L}{RT}} \qquad \textit{Equation 4.14}$$

From this generalisation the constant C was obtained from:

$$C = \frac{y}{x} = \frac{a_1 g}{b_1} e^{\frac{(E_1 - E_L)}{RT}} \qquad \textit{Equation 4.15}$$

Where:

E_1 = heat of adsorption monolayer

E_L = heat of condensation second and higher layers

$\frac{a_1 g}{b_1}$ = constant ~ 1 for the gases and surfaces studied by Brunauer, Emmet et al. (1938)

R = gas universal constant

T = temperature

Soekarto and Steinberg (1981) mentioned some definitions for the value C (binding energy). They argued that different authors have referred to this term as "the energy involved in the most tightly bound water or monolayer" while others as "the energy involved in all the bound water, including that beyond the monolayer".

In order to derive the final equation, Brunauer, Emmet et al. (1938) related the total volume of the gas adsorbed to the volume adsorbed to form a monolayer. After a generalisation of summations they obtained:

$$V = \frac{V_m C x}{(1-x)(1-x+Cx)} \qquad \textit{Equation 4.16}$$

At the saturation pressure p_0, an infinite number of layers can build up on the adsorbent. The authors suggested that to make $V = \infty$, when $p = p_0$, x must equal to unity therefore;

$$M = \frac{m_0 C \frac{p}{p_0}}{\left(1-\frac{p}{p_0}\right)\left(1-\frac{p}{p_0}+C\frac{p}{p_0}\right)} \qquad \textit{Equation 4.17}$$

Where :

M = moisture content (%db)

m_o = monolayer value (%db)

C = constant (related to the net heat of sorption)

p/p_0 = gas partial pressure, relative humidity in the case of water (water activity at thermodynamic equilibrium)

Published work on sorption isotherm modelling, has shown that the BET can describe accurately sorption isotherms up to a partial pressure (p/p_0) of ~ 40% (Brunauer, Emmet et al. 1938; Chirife and Iglesias 1978; Iglesias and Chirife 1982; Van den Berg 1985; Peleg 1993; Al-Muhtaseb, McMinn et al. 2002; Raj, Raj et al. 2003). Nevertheless it has proved to be a useful approach to obtained information about the monolayer value and the heat of sorption or binding energy.

Although this approach has been useful to represent sorption isotherms of food materials, it has to be considered that in practice some of the conditions for it application such as *all sorption sites are identical, no interaction between the sorbed molecules, equals rate of sorption and desorption, etc.* are not

encounter in real foods (Franks 1991). Therefore its interpretation should be cautious.

4.1.2.1.2 Guggenheim-Anderson-de Boer (GAB) Model

The three parameter GAB equation was derived independently by Guggenheim, Anderson and de Boer (Van den Berg 1985). It is well known that this can be applied to a wider RHs range than the BET. Published work have reported successful modelling for a range of 10% to 90% RH on starchy materials (Peleg 1993; Bader and Goritz 1994; Al-Muhtaseb, McMinn et al. 2002; Raj, Raj et al. 2003; Timmermann 2003; Al-Muhtaseb; McMinn et al. 2004). In contrast to assuming bulk liquid properties of the multilayer molecules of the BET, the GAB model of sorption distinguishes between these two, which results in the additional parameter K (Anderson 1946; Van den Berg 1985; Bader and Goritz 1994; Al-Muhtaseb, McMinn et al. 2002).

$$M = \frac{m_o C K a_w}{(1 - K a_w)(1 - K a_w + C K a_w)} \qquad \textit{Equation 4.18}$$

Where:

m_o = monolayer value (all sorption sites occupied by one molecule)

C = constant (related to the net heat of sorption)

K = constant (related to the heat of sorption of the multilayer)

Similar to the constant C in the BET model, K is related to energy of interaction between the sorbant molecules and the matrix, but more specifically on the interaction between the multilayer and the bulk liquid.

Therefore K has been defined as (modified from Al-Muhtaseb, McMinn et al. 2002):

$$K = k_o e^{\left(\frac{E_b - E_L}{RT}\right)} \qquad \textit{Equation 4.19}$$

Where:

k_o = entropic factor

E_L = heat of condensation second and higher layers

E_b = heat of condensation of the bulk liquid

R = gas universal constant

T = temperature

The assumption that the state of the sorbant molecules in the second and higher layers is equal but different from the liquid-like state, introduces an additional degree of freedom (parameter *K)* and thus the GAB model gains its greater versatility (Al-Muhtaseb, McMinn et al. 2002).

This extra parameter *K* would assume that the interaction energy levels of the multilayer is somewhere between the interaction between the monolayer molecules and the bulk liquid.

If $K<1$, GAB will give a sorption lower than BET for high RHs. If $K=1$, GAB becomes BET and if $K>1$, the sorption becomes infinity for RHs less than 100%.

When evaluating the effect of temperature on the sorption isotherms it has been concluded that *K* contains an important entropic component part besides some enthalpy, whereas the *C* contains mainly enthalpy (Van den Berg 1985).

4.1.2.1.3 Peleg model

Peleg (1993) suggested that it was not easy to predict on the basis of the fit of the BET or GAB models alone the molecular events that take place at the solid surface. As values such as the monolayer depends not only on the selected model but also on the experimental RH range, the noise in the sorption data and the number of points taken for the regression.

As a consequence of this analysis Peleg defined a new sorption isotherm model based on four parameters:

$$M = k_1 a_w^{n_1} + k_2 a_w^{n_2} \qquad \textit{Equation 4.20}$$

Where:

k_1, k_2, n_1, n_2 are constants with ($n_1<1$ and $n_2>1$)

When the *k* values are of comparable magnitude the first term ($n_1<1$) is always the dominant at lower RHs. At higher RHs either term or both can be dominant or comparable in magnitude.

The mathematical structure and number of constants was not increased just to improve the curve fit (Peleg 1993). It was chosen to show that the sorption sigmoid shape at low RHs is mainly determined by a process of a decreasing rate with respect to RH, similar to the Langmuir sorption kinetics.

The Peleg model has been successfully applied over a wide of different foods for RHs up to 95% (Peleg 1993; Coupland, Shaw et al. 2000; Teoh, Schmidt et al. 2001; Al-Muhtaseb, McMinn et al. 2002; Al-Muhtaseb, McMinn et al. 2004).

The modelling on the different starches glycerol mixtures shows a slightly lower RMSE (error fuction defined in 4.1.2.2) section suggesting a better fit compared to GAB. This can be explained by the extra parameter used during the model optimisation.

It is difficult to interpret the obtained values for the different constants of this model, as they do not have any physical meaning or theoretical background. Nevertheless, they can be used to broadly characterise the different curve shapes. Each of the constants has an effect on the shape of the sorption curves. By plotting modelled data and varying one of the constants keeping the same values for the other three (data not shown) the following has been concluded:

1. Varying K_1 would have an additive (increasing sorption) or subtracting (decreasing sorption) effect through out the whole RH range. With a more significant effect at higher RHs.
2. Varying K_2 would have an exponential effect on the sorption curve at RHs > 60%.
3. Varying n_1 would affect the sigmoid shape of the curve (smaller n_1 increases the S-shape on the sorption curve).
4. Varying n_2 would have a similar effect of varying K_2.

The following section focuses on the application of these models on the sorption data obtained from the DVS. A detailed comparison of the estimated model parameters between starch types and starch containing glycerol is also presented.

4.1.2.2 Results and Discussion

The models presented in the previous section were applied on the extruded starch-glycerol systems. As mentioned before, the obtained parameters for the control and glycerol samples and for the three starches studied were compared after model optimisation.

The fitting procedure was done by minimising the sum of the squared root of the difference between the experimental and modelled data (SRD). The software used was Solver add-in in Excel (Office Suite 2003, Microsoft Corp.). The Relative Mean Standard Error (RMSE) was calculated by dividing SRD by the number of experimental points (n).

Table 4.1 shows the values for the fitted BET model for the three different starches and glycerol concentrations. The data were modelled up to a relative humidity of 50% (as literature suggests). The RMSE values from the modelling for all the mixtures were small (< 1%) proving a good fit.

Although there is not a marked difference in the monolayer value (mo) between starch types it seems that waxy maize shows a greater value (mo ~ 6.6%) compared to wheat and rice starches for the control, 5% and 10% glycerol samples (mo ~ 6.3). This may be explained by the higher amylopectin concentration compared to rice and wheat starch. Amylopectin being a highly branched molecule compared to amylose, it is likely to have more active site available for water molecules binding.

Also amylose-lipids complexes present in wheat and rice starches that may have formed during/after sample preparation (extrusion) may hinder water sorption by either making the amylose less available for sorption or reducing the flexibility of the matrix.

This trend in the differences in the monolayer value between waxy maize, wheat and rice was not clear for glycerol concentration of 15 and 20%. It is possible this polyol filling some of the active sites of the branched amylopectin

in waxy maize decreasing the difference in the monolayer value from this starch type from rice and wheat starches.

This numerical approach helped to obtained more valuable information from the sorption curves as compared to subjective observation of the experimental data were no clear differences where detected for the three studied starches (section 4.1.1.2.2).

When comparing the monolayer value of the same starch type with different glycerol contents, a clear trend was obtained. This correlation was similar for all three starch types. When glycerol concentration increased, the monolayer value decreased, e.g. ~ 6% for the starches containing 20% glycerol. It seems that at low relative humidities glycerol decreases the availability of active sorption sites reducing the surface area exposed for water molecules.

For the constant *C*, there was not a clear correlation between the three starches and not significant differences were obtained. For example, looking at control samples (no glycerol), the greater value was obtained for waxy maize starch. But for the starches containing glycerol the higher value for *C* was for wheat starch.

Comparing the same starch type with different glycerol concentrations, there was a marked decrease in *C* when the glycerol content increased.

Following the definition by Brunauer, Emmet et al. (1938) the constant *C* is related to the difference in heat of sorption between the monolayer (E_1) and the multilayer or bulk water (E_L). In other word a decrease in the *C* would suggest a decrease in the value of E_1 (for monolayer) as E_2 (for multilayer) should remain constant. A lower E_1 would mean water molecules less strongly bound to the matrix sorption sites when glycerol is present.

Table 4.1. BET and GAB parameters for waxy maize, rice and wheat starch-glycerol mixtures. The presented values were obtained from applying the models to the mean value obtained from three replicates.

BET				
Starch Type	**Glycerol% (db)**	**Monolayer (m_o)**	***C***	***RMSE***
Waxy Maize	0%	6.70%	8.85	0.14%
Rice	0%	6.32%	7.98	0.16%
Wheat	0%	6.35%	7.86	0.32%
Waxy Maize	5%	6.18%	7.23	0.13%
Rice	5%	5.89%	7.08	0.15%
Wheat	5%	5.97%	8.92	0.12%
Waxy Maize	10%	5.89%	5.81	0.08%
Rice	10%	5.60%	6.14	0.10%
Wheat	10%	5.39%	8.43	0.10%
Waxy Maize	15%	5.49%	6.11	0.06%
Rice	15%	5.65%	5.60	0.08%
Wheat	15%	5.34%	6.70	0.04%
Waxy Maize	20%	5.57%	4.89	0.07%
Rice	20%	5.60%	4.76	0.04%
Wheat	20%	5.63%	5.29	0.03%

GAB					
Starch Type	**Glycerol% (db)**	**Monolayer (m_o)**	***C***	***K***	***RMSE***
Waxy Maize	0%	9.4%	6.8	0.72	0.14%
Rice	0%	8.9%	6.4	0.72	0.13%
Wheat	0%	8.7%	6.4	0.73	0.20%
Waxy Maize	5%	6.6%	9.1	0.86	0.60%
Rice	5%	6.0%	9.7	0.88	0.61%
Wheat	5%	6.6%	9.9	0.85	0.44%
Waxy Maize	10%	5.8%	8.0	0.92	0.42%
Rice	10%	5.6%	8.1	0.93	0.34%
Wheat	10%	5.6%	9.2	0.93	0.17%
Waxy Maize	15%	5.8%	5.8	0.95	0.14%
Rice	15%	5.9%	5.6	0.95	0.20%
Wheat	15%	5.8%	6.0	0.94	0.08%
Waxy Maize	20%	6.3%	3.8	0.95	0.23%
Rice	20%	6.6%	3.5	0.94	0.17%
Wheat	20%	6.9%	3.5	0.94	0.25%

Table 4.1 also shows the GAB parameters obtained after fitting the model on the experimental data of the different starch-glycerol mixtures.
The RMSE for all the samples was less than 1% indicating a good fit.

The monolayer value m_o was similar for the three different starches with the higher values for the 0%glycerol samples (~9% db). Similar values have been reported in the literature for starchy materials. Bader and Goritz (1994) obtained a value of $m_o \sim 9.1\%$ (db) for high amylose corn starch, Peleg (1993) $m_o \sim 9.9\%$ (db) for potato starch and Steebdam, Henderic et al. (2001) calculated a value ~ 8.0 % (db) for wheat starch.

Similarly to BET, monolayer values decreased for the three different starches when the glycerol concentration increased in the samples.

There were differences in the obtained modelling parameters m_o obtained from BET and GAB models. The m_o values from BET were lower than from GAB equation. This difference was also detected when the GAB equation was applied up to 50% RH. There is no a clear explanation of this difference, it is possible that the extra parameter K in GAB may affect the value of m_o during model fitting. Nevertheless, literature suggests that the values from the GAB model are closer to the theoretically expected values for the monolayer (11% db) (Van den Berg 1985).

When comparing the values for C, there was not a clear trend between the different starches. On the other hand, a clear difference was detected for the same starch type with different glycerol contents. The higher values were obtained ($C \sim 9.5$) for the 5% glycerol samples and the lower ones ($C \sim 3.5$) for the 20% glycerol.

Similarly to the rationale followed on the BET values, the constant C is also related to the adsorption energies of the monolayer. Therefore the decrease in this value would suggest water molecules less strongly bounds to the active sites of the matrix at low RHs.

When glycerol is present, its hydroxyl groups would occupy these sites reducing the sorbant-matrix interaction enthalpy giving a smaller value for C.

The differences in C from GAB and BET come mainly from the fitting procedure that in the case of GAB it includes the extra parameter K which contributes similarly to C. Therefore a smaller C will be obtained when K increases due the higher water absorption at higher RHs.

When analysing the K, similar values were detected between the three different starches. On the other hand there was clear trend for this value at different

glycerol concentrations for the same starch type. It is a clear that when glycerol content increased the K value increased.

Following the definition in equation 4.19, the increase in the value of K would suggest an increase in the interaction energy between the molecules in the multilayer and the bulk liquid.

It is likely that some free hydroxyl groups from the glycerol molecules bound to the matrix contribute to increases the overall interaction energy of the sorbant in the multilayer domain at higher RHs. Anderson (1946) has suggested that the entropy of adsorption at the second and subsequent layers is more negative that the entropy of condensation, which may indicate that the absorbent in the layers is more ordered than the liquid phase.

Following this rationale, the increase in K when glycerol is present can be explained by the hygroscopic effect of this polyol attracting water molecules and contributing to an increase in the heat of absorption for the multilayer.

Table 4.2 show the values for the four adjusted parameters from the Peleg equation after fitting optimisation. The obtained RMSE were < 1% suggesting a good fit.

Table 4.2. Peleg model parameters after optimisation (constraints: $n_1 < 1$ and $n_2 > 1$). The presented values were obtained from applying the model to the mean value obtained from three replicates.

Starch Type	Glycerol% (db)	K_1	K_2	n_1	n_2	RMSE
Waxy Maize	0%	19.7%	12.4%	0.76	6.07	0.10%
Rice	0%	18.6%	11.6%	0.78	6.35	0.06%
Wheat	0%	18.8%	13.1%	0.79	6.32	0.15%
Waxy Maize	5%	19.8%	37.1%	0.87	11.72	0.19%
Rice	5%	18.7%	38.5%	0.87	11.66	0.15%
Wheat	5%	18.5%	28.7%	0.80	9.41	0.18%
Waxy Maize	10%	18.7%	45.5%	0.91	9.61	0.13%
Rice	10%	17.6%	43.4%	0.89	9.15	0.11%
Wheat	10%	16.2%	41.6%	0.79	7.77	0.13%
Waxy Maize	15%	16.6%	52.4%	0.87	7.60	0.09%
Rice	15%	16.9%	55.0%	0.88	7.73	0.04%
Wheat	15%	16.2%	49.7%	0.85	7.45	0.15%
Waxy Maize	20%	16.7%	55.0%	0.92	7.16	0.15%
Rice	20%	17.5%	54.4%	0.96	7.15	0.20%
Wheat	20%	17.1%	54.5%	0.91	6.75	0.26%

The values on table 4.2 for the control samples were similar to the values reported in the literature for starchy materials. For example Peleg (1003) obtained $K_1 \sim 21\%$, $K_2 \sim 16\%$, $n_1 \sim 0.7$ and $n_2 \sim 6$ for potato starch. Al-Muhtaseb, McMinn et al. (2004) obtained $K_1 \sim 19\%$, $K_2 \sim 9\%$, $n_1 \sim 0.6$ and $n_2 \sim 8$ for amylopectin starch.

The analysis comparing the model parameters between pure extruded waxy maize, rice and wheat starches did not show clear differences. In the case of the samples containing glycerol, marked differences in these parameters were detected compared with the pure starch extrudates.

The decrease in K_1 and increase in n_1 represent a flatter curve at low RHs, equivalent to the smaller monolayer values from BET and GAB. On the other hand, the increase in K_2 and n_2 are related to the increase in the sorption behaviour at high RHs (RH>60%).

This model represents an alternative to the classic BET and GAB models. It can be used to accurately represent sorption isotherms due to the presence of an extra parameter in the equation.

The drawback of using this model is the lack a theoretical background in its development or any physical meaning in the values obtained.

4.1.3 Prediction of Sorption Isotherms for Multi-Component Starch-Glycerol Mixtures

The practicability in determining the sorption isotherms for individual components is the possible prediction, based on their concentration, of sorption profiles for complex formulations. In practical terms this approach has shown to be not accurate, as it is believed that interaction between components may influence the moisture uptake during equilibration. The next section focuses on different approaches commonly used to predict sorption isotherms based on sorption curves of individual components.

4.1.3.1 Theoretical Background

The prediction of sorption isotherms for food mixtures becomes important when new recipes are produced. Usually this is done on trial and error basis, thus leading to long times for new products to be developed. The use of sorption isotherms for each component and its associated weight fraction has

been frequently used, with different degrees of success, to estimate sorption curves of complex food mixtures (Salwin and Slawson 1959; Berlin, Anderson et al. 1968; Labuza 1968; Lang and Steinberg 1980; Leiras and Iglesias 1991, Kaminski and Al-Bezweni 1994; Labuza 1994, Rahman 1995). In practice, it is assumed that individual components or ingredients do not interact with each other and the water activity for each moisture content is the same for all the components (Labuza 1968; Lang and Steinberg 1980; Leiras and Iglesias 1991).

A simple formula commonly used to predict the equilibrium moisture content (EMC) for a mixture is proposed by Lang and Steinberg (1980):

$$M_{cal} = \frac{\sum W_i M_i}{\sum W_i} \qquad \textit{Equation 4.21}$$

Where M_{cal} is the calculated total moisture content at specific water activity (Aw), W_i is the individual component weight expressed on a dry basis and M_i is the equilibrium moisture content, dry basis, of each component a the specific Aw.

Although this approach has been successfully applied to some binary and tertiary mixtures (Lang and Steinberg 1980), inaccurate predictions have been obtained for the low end of water activity. Iglesias, Chirife et al. (1980) and Leiras and Iglesias (1991) showed that this kind of approach was usually inaccurate for low moisture content (±16% error). Moreover they observed that the obtained values were always greater that the experimental data suggesting some interaction between the mixture constituents. Based on a derivation by Salwin and Slawson (1959), Kaminski and Al-Bezweni (1994) introduced the interaction coefficient ξ_i, representing the physico-chemical interaction between particular components.

If an interaction occurs, the moisture content of a component i^{th} (X_{ei}) becomes $\xi_i X_{ei}$.

For an n-component mixture the mean moisture content in the mixture X_{em} is defined as:

$$X_{ei} = \sum_{i=1}^{n} W_{Si}\xi_i X_{ei} \qquad \textit{Equation 4.22}$$

Where W_{Si}, is the mass fraction of the i^{th} component in the mixture. The water activity (Aw) in the air in contact with the mixture is the same for all components. The relationship between moisture content in the single i^{th} component and the water activity can be determined from the equation describing the sorption/desorption isotherm for a given component (BET and GAB models) (Kaminski and Al-Bezweni 1994).

Following the description of these two approaches, both models are used to predict the sorption isotherm for starch and different concentrations of glycerol and to quantify possible interaction between this polyol and starchy matrix

4.1.3.2 Results and Discussion

The prediction of sorption isotherms for starch-glycerol mixture was calculated using the weight fraction contribution approach. Knowing the mixture composition and the complete sorption data for pure glycerol and for the studied starches, the prediction using equations 4.21 and 4.22 for the mixture was attempted and the obtained curve was compared against the experimental data.

Figure 4.9 shows the sorption isotherm for wheat starch extrudates-glycerol mixtures and the predicted values given by the component weight fraction model (equation 4.21). Very similar behaviours were obtained for the extruded waxy maize and rice starch glycerol model systems (data not shown).

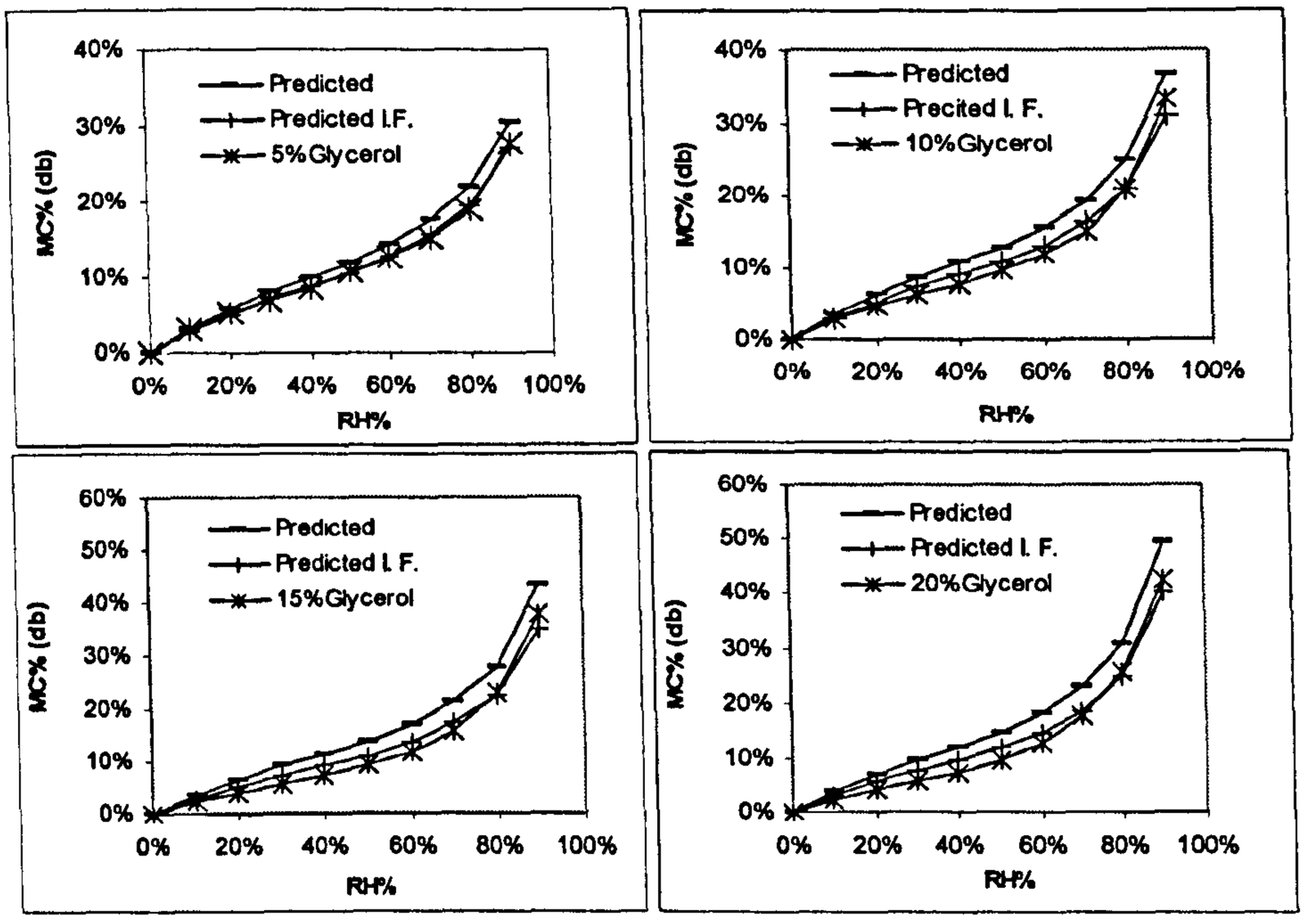

Figure 4.9. Sorption isotherms comparison for wheat starch-glycerol between predicted moisture content, the predicted values including the interaction factor (I. F) and experimental values (-✳-).

From the curve labelled *Predicted* it is clear that the values given by the weight fraction model, are an overestimate of the moisture content compared to the experimental data.

Leiras and Iglesias (1991) and Iglesias, Chirife et al. (1980) have attributed this overestimation on the probable interaction between components which may decrease that availability of sorption sites.

In order to account for this interaction, the factor ξ was estimated by fitting the equation 4.22 to the same experimental data. The curve labelled *Predicted I. F.* shows an improvement in the fitting when the interaction factor was included.

Tables 4.3 summarise the values obtained for the interaction factor and the relative mean standards error (RMSE) for each fit.

Table 4.3. Interaction factor ξ and relative standard error RMSE for waxy maize, rice and wheat starch-glycerol

Waxy Maize Starch			
	I. F.	*RMSE*	*(RMSE)*
5% Glycerol	0.88	0.8%	2.0%
10% Glycerol	0.83	1.4%	3.3%
15% Glycerol	0.81	1.5%	4.0%
20% Glycerol	0.76	1.7%	5.5%

Rice Starch			
	I. F.	*RMSE*	*(RMSE)*
5% Glycerol	0.91	0.5%	1.4%
10% Glycerol	0.84	1.2%	3.0%
15% Glycerol	0.88	1.8%	3.0%
20% Glycerol	0.80	1.8%	4.7%

Wheat Starch			
	I. F.	*RMSE*	*(RMSE)*
5% Glycerol	0.89	0.4%	1.7%
10% Glycerol	0.84	1.1%	2.9%
15% Glycerol	0.81	1.5%	4.0%
20% Glycerol	0.81	1.7%	4.5%

(RMSE): relative standard error for prediction not including ξ; I.F.: interaction factor;RMSE: relative standard error.

The improvement in the fit using the interaction factor ξ can be quantified by the decrease in RMSE.

As expected, the similar sorption isotherms obtained for the three starches (figures 4.6 and 4.7), gave similar interaction factors ξ.

The factor ξ was < 1 and it decreased when the concentration of glycerol increased suggesting some interaction between the matrix and the polyol. This correlates well with a greater fit improvement for the mixture with higher glycerol content (20%) from a RMSE of ~6% to ~2%.

Another important aspect in sorption studies is the kinetic of solvent exchange between materials and their environment. This can help to understand and to predict the structural behaviour and stability of these materials over time. In the case of food materials the study of water diffusivity into a hydrophilic polymer such as starch can help to control water dependent processes (e.g. chemical reactions, structural relaxations, etc.) that occur during storage extending product shelf life.

Next section presents a brief review about the fundamentals of diffusion and the diffusivity models commonly used in polymeric systems.

4.1.4 Diffusivity

The understanding of diffusion (water transport) into a particular food system can give information relating the kinetics of sorption and the structural mobility of the sorbant. This would have a big influence on processes such as cooking, drying, microbial spoilage (relating water sorption to changes in Aw) for the quality of a range on food products during storage (Hopkinson, Jones et al. 2001).

The aim of this section is to evaluate the effect of glycerol on the diffusion kinetics of water on the extruded waxy maize, rice and wheat starches when equilibrated at different RHs. As stated in section 3.3.1.1. of this thesis, in the case sorption at low RHs, an exponential model was used to obtained sorption valued at time equal infinity.

4.1.4.1 Theoretical Background

4.1.4.1.1 Fick's Law(Case I Diffusion)

In 1855, Fick proposed his law of mass diffusion by analogy with Fourier's law of heat conduction (Crank 1993). The flux of penetrant through a membrane is proportional to the local concentration gradient.

$$F = -D\frac{\partial C_d}{\partial x} \qquad \textit{Equation 4.23}$$

Where F is the rate of transfer per unit area section, C_d the concentration of diffusing substance, x the space coordinate measured normal to the section, D is the diffusion coefficient. The negative sign shows that diffusion occurs from high to low concentration.

The fundamental differential equation derived for diffusion comes from equation 4.24.

$$\frac{\partial C_d}{\partial t} + \frac{\partial F_x}{\partial x} + \frac{\partial F_y}{\partial y} + \frac{\partial F_z}{\partial z} = 0 \qquad \textit{Equation 4.24}$$

This derivation considers a rectangular parallelepiped element of volume with defined faced area for x, y and z coordinates (Crank 1993).
If the diffusion coefficient is constant and is one dimensional (gradient of concentration is only along the x-axis), then:

$$\frac{\partial C}{\partial t} = D\frac{\partial^2 C_d}{\partial x^2} \qquad \textit{Equation 4.25}$$

Equations 4.23 and 4.25 are commonly referred to as Fick's first and second laws of diffusion.

4.1.4.1.2 Non Fickian Diffusion

The diffusion behaviour of many glassy polymers cannot be accurately described only by a concentration-dependant form of Fick's law with constant boundaries conditions, especially when the penetrant causes extensive swelling of the polymer (Crank 1993).
In rubbery polymers, well above the glass transition, which respond rapidly to changes in their conditions (e.g. sorbant concentration, temperature), the polymer chains adjust so quickly to the presence of the penetrant that they do not cause diffusion anomalies and the diffusional mechanism can be regarded as Fickian (Crank 1993). In case of polymers deep in the glassy state the diffusion rate is much higher than the structural molecular relaxation making the difference in solvent concentration the main variable driving diffusion. In this particular case the diffusional mechanism is also Fickian.
The properties of a glassy polymer approaching its Tg tend to be time-dependant (relaxation component). Deviations from Fickian behaviour are considered to be associated with finite rates at which the polymer structure may change in response to the sorption and desorption of penetrant molecules (Crank 1993, Peppas and Peppas 1994).
Hopfenberg and Frisch (1969) summarised the transport phenomena in a plot of temperature v/s penetrant activity.

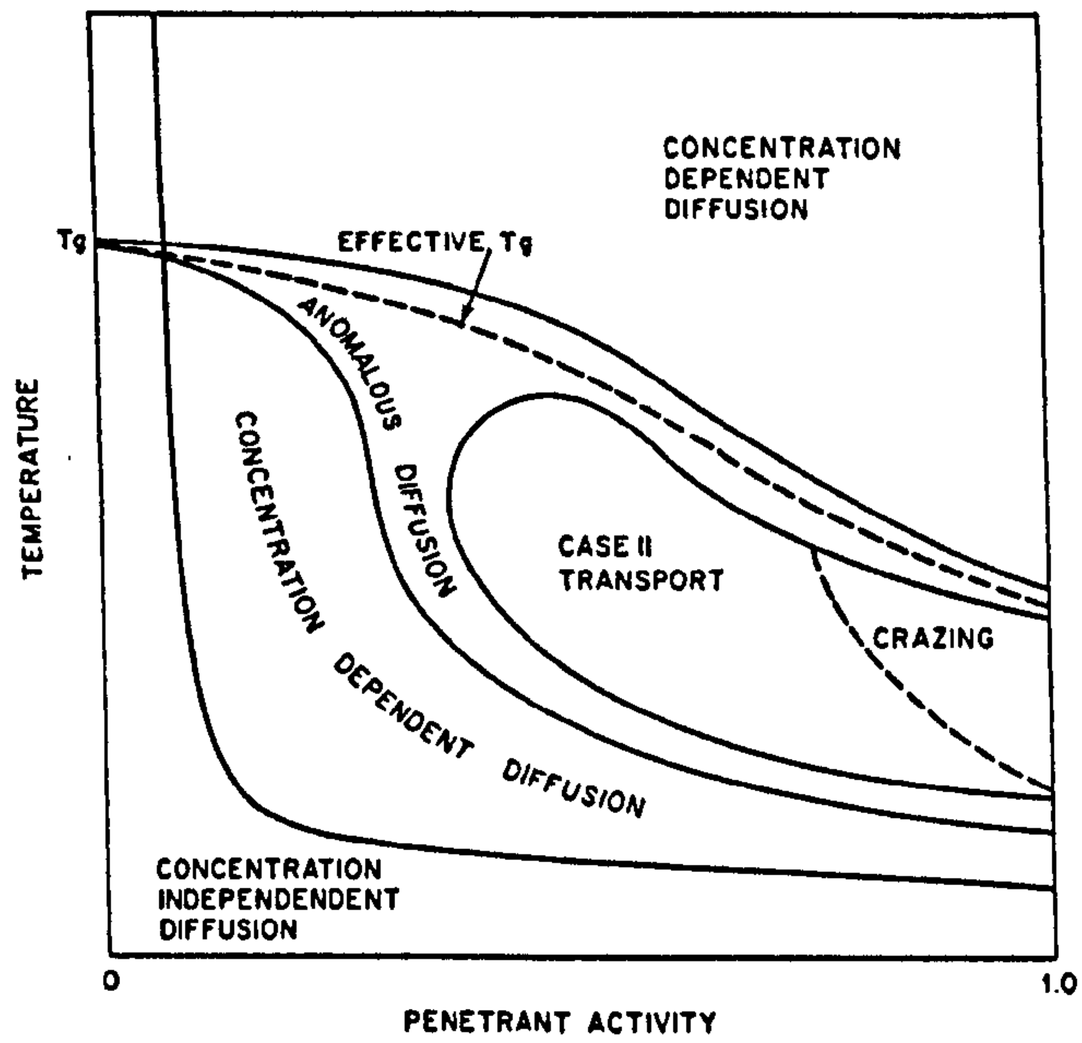

Figure 4.10. Hopfenberg-Frisch chart of transport phenomena (Hopfenberg and Frisch 1969).

These authors describe this diagram as follow:

"For activities from 0 (infinitely dilute vapour) to 1 (pure liquid or saturated vapour) at temperatures well bellow Tg, and for all temperatures at activities close to 0, concentration independent Fickian diffusion is generally observed. At higher temperatures and activities, D shows a dependence on concentration. If the temperature is closer to Tg, D begins to depend on time as well as on concentration.

At moderate penetrant activities where swelling is appreciable and the temperature is less than 10°C from Tg, the diffusion mechanism may change from Fickian (Case I) to stress relaxation-controlled process (Case II) in which the penetrant advances in sharply defined front at a nearly uniform velocity. The term "anomalous diffusion" occurs under conditions where a combination of Case I and Case II take place".

Alfrey, Gurnee et al. (1966) classified the diffusional mechanisms based in the relative rates of diffusion and polymer relaxation:

i. Case I or Fickian diffusion in which the rate of diffusion << or >> rate of molecule relaxation.

ii. Case II diffusion in which the rate of diffusion > rate of molecule relaxation.

iii. Non-Fickian or anomalous diffusion which occurs when the diffusion and relaxation time are comparable.

4.1.4.1.3 Analysis of Diffusional Mechanism

A quantitative basis from the Hopfenberg-Frisch chart was derived by Vrentas and Duda (1977). They define the *Diffusional Deborah Number* (*De*). Like the diffusional exponent *n*, *De* is a simple way of elucidate the water uptake mechanism.

The nature of the sorption process can be distinguished by the ratio of two characteristic times: (i) a characteristic *relaxation time*, λ, for the macromolecular/penetrant system and (ii) a characteristic *diffusion time*, θ, for the same system.

The *De* number is written as:

$$D_e \equiv \frac{\lambda}{\theta} \qquad \textit{Equation 4.26}$$

Peppas and Sinclair (1983) proposed a semi-empirical equation to define water transport in glassy polymers.

$$\frac{M_t}{M_\infty} = kt^n \qquad \textit{Equation 4.27}$$

Where *k* is a constant incorporating characteristics of the molecular network system and *n* is the diffusional exponent that is indicative of the transport mechanism.

Fickian diffusion and Case II transport are defined by *n* equal to ½ and *n* equal to 1, respectively. Anomalous transport behaviour is intermediate between Fickian and Case II, where it is reflected by values on f *n* between ½ and 1.

The above mechanism of discerning the diffusional mechanism is commonly used for planar geometries. For spherical and cylindrical systems the time dependency can predict just 15% of the total penetrant uptake (Peppas and Peppas 1994). Therefore in order to improve the prediction up to 60% of the total water uptake a new set of values for the exponent n were defined; $n = 0.43$ for Fickian diffusion, $0.43 < n < 0.85$ Anomalous diffusion and $n = 0.85$ for Case II diffusion (Peppas and Peppas 1994).

4.1.4.1.4 Diffusion in Spherical Geometries

For one-dimensional radial diffusion in a sphere of radius a, under boundary conditions, with a constant penetrant diffusion coefficient D, Fick's second law may be written as (Peppas and Peppas 1994):

$$\frac{\partial C}{\partial t} = D\left(\frac{\partial^2 C}{\partial r^2} + \frac{2}{r}\frac{\partial C}{\partial r}\right) \qquad \textit{Equation 4.28}$$

Where:

$$T = 0 \quad 0 < r < a \qquad C = C_I$$

$$T > 0 \quad r = a \quad C = C_o$$

The solution to Fick's law under the above specified conditions for short time behaviour is (Peppas and Peppas 1994):

$$\frac{M_t}{M_\infty} = 6\left(\frac{Dt}{a^2}\right)^{1/2}\left[\frac{1}{\pi^{1/2}} + 2\sum_{n=1}^{\infty} ierfc\frac{na}{\sqrt{Dt}}\right] - 3\frac{Dt}{a^2} = 6\left(\frac{Dt}{\pi a^2}\right) - 3\frac{Dt}{a^2} \qquad \textit{Equation 4.29}$$

Where:

M_t = mass at time t

M_∞ = mass at time infinity

D = diffusion coefficient

a = sphere radius

ierfc = integrated complementary error function

4.1.4.1.5 Estimation of diffusion coefficient

Water vapour diffusivity into hydrophilic polymers is a complex phenomenon due to its high cohesive energy and hydrogen-bonding capacity.

The diffusion coefficient (*D*) of water in hydrophilic polymers usually increases with increasing water concentration (*C*), while in hydrophobic polymers *D* may vary inversely with *C*, generally attributed to the clustering of dissolved water molecules in the polymer (Felder and Huvard 1980).

In this work, *D* was obtained from each 10% RH step increase from 0 to 90%RH (see figure 4.12). Although *D* can be considered constant for each step, especially at low RH (small changes in moisture content), the obtained *D* should not be considered as an absolute value but as an average.

4.1.4.1.5.1 Initial Slope Method

For Fickian diffusion it is possible to deduce an average diffusion coefficient from the initial gradient of the sorption curve when plotted against the square root of the time (Crank 1993).

For a spherical geometry, Peppas and Peppas (1994) suggested that diffusivities (Fickian) can be obtained, for short times (60% of the total sorption), from the empirical equation 4.27 when $n = 0.5$ and $k = 6(D/\pi a^2)^{1/2}$. Thus, becoming:

$$\frac{M_t}{M_\infty} = \frac{6}{a}\left(\frac{D}{\pi}\right)^{1/2} t^{1/2} \qquad \textit{Equation 4.30}$$

Figure 4.11 shows an example of sorption data where the red dotted line represents the area of the curved considered to obtain *D*. The blue line defined the ranged at which the slope was considered. The selected range for Mt/M_{inf} was from 10% to 60%. The lower range (10%) was selected after considering the time for the headspace around the sample to equilibrate after a change in relative humidity. The top range (60%) was selected based on the considerations given by Peppas and Peppas (1994).

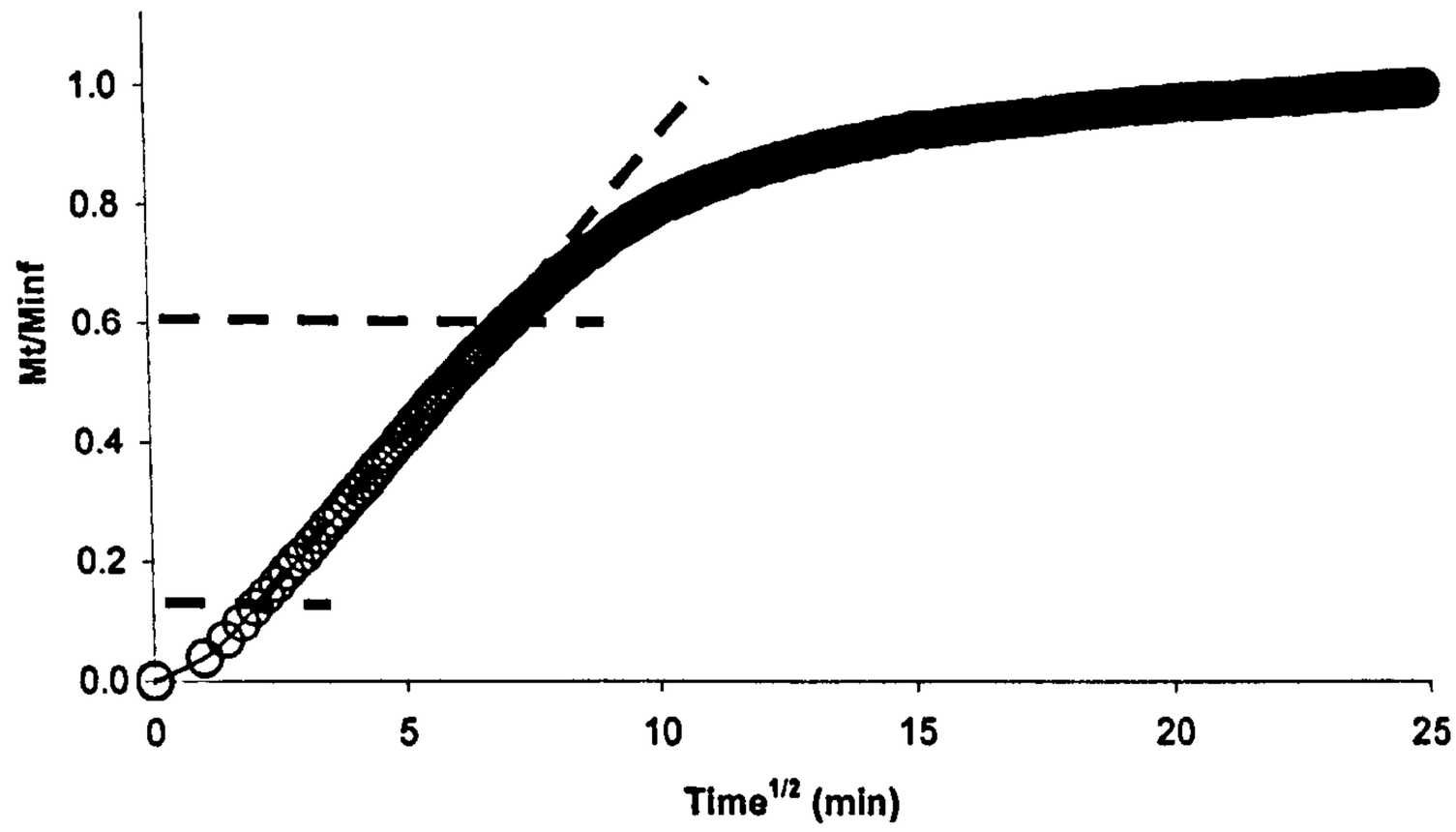

Figure 4.11. Example of a sorption curve (rice starch extrudates from 20% to 30%RH at 25°C).

In the case of non-Fickian diffusion (Case II) for a thin polymer of cross-sectional area A and thickness l, the swollen region is defined by $X \leq x \leq l/2$, where X is the position of the advancing front. There is a uniform concentration of water equal to the equilibrium water concentration C_o. In the glassy region defined by $0 \leq x \leq X$, only the initial water is present.

The sorption kinetics is assumed to be controlled by a rate-limiting relaxation phenomenon, the simple first-order kinetic expression describing sorption can be written as follow (Peppas and Peppas 1994):

$$\frac{dM_t}{dt} = k_0 A \qquad \textit{Equation 4.31}$$

When considering the amount of water M_t imbedded is the swollen region of volume $A(l/2 - X)$, equation 4.31 can be written as:

$$\frac{M_t}{M_\infty} = \frac{2k_0}{C_0 a} t \qquad \textit{Equation 4.32}$$

For alternative geometries, the above model has generalised in the following form:

$$\frac{M_t}{M_\infty} = 1 - \left(1 - \frac{k_0}{C_0 a'} t\right)^N \qquad \textit{Equation 4.33}$$

Where a' is the sample radius for cylindrical and spherical samples and the film half-thickness, l/2, for planar samples. The exponent N is determined by the sample geometry and has a value of 1 for films, 2 for cylinders and 3 for spheres.

4.1.4.2 Results and Discussion

The diffusion coefficients were estimated for all the extruded starch-glycerol samples from each sorption steps on the obtained sorption isotherms curves (figure 4.12).

4.1.4.2.1 Diffusion Coefficient Calculation

As mentioned in chapter 3 section 3.3.1.2, the freeze-dried starch-glycerol extrudates were ground and sieved to a particle size of ~ 180μm. Prior the analysis all the samples showed an amorphous like structure under X-Ray diffraction (chapter 3 section 3.3.5.2).

The diffusion coefficient (D) for each of these extruded starch-glycerol systems was calculated using equation 4.30 and assuming Fickian diffusional mechanism. This model was applied to each of the sorption equilibration steps from the sorption isotherms obtained at 25°C using the Dynamic Vapour Sorption (DVS) technique. An example describing the sorption step for rice starch and 5% glycerol is depicted in figure 4.12. The reported D values are the statistical mean of 3 replicates.

It has to be mentioned that the assumption that the particles are spherical is probably not entirely correct. Other geometries could be present within the powder influencing the modelling of the experimental data. Nevertheless, these limitations are common for all the samples analysed, validating this approach as a comparison method to evaluate the sorption kinetics between starches with different glycerol concentrations.

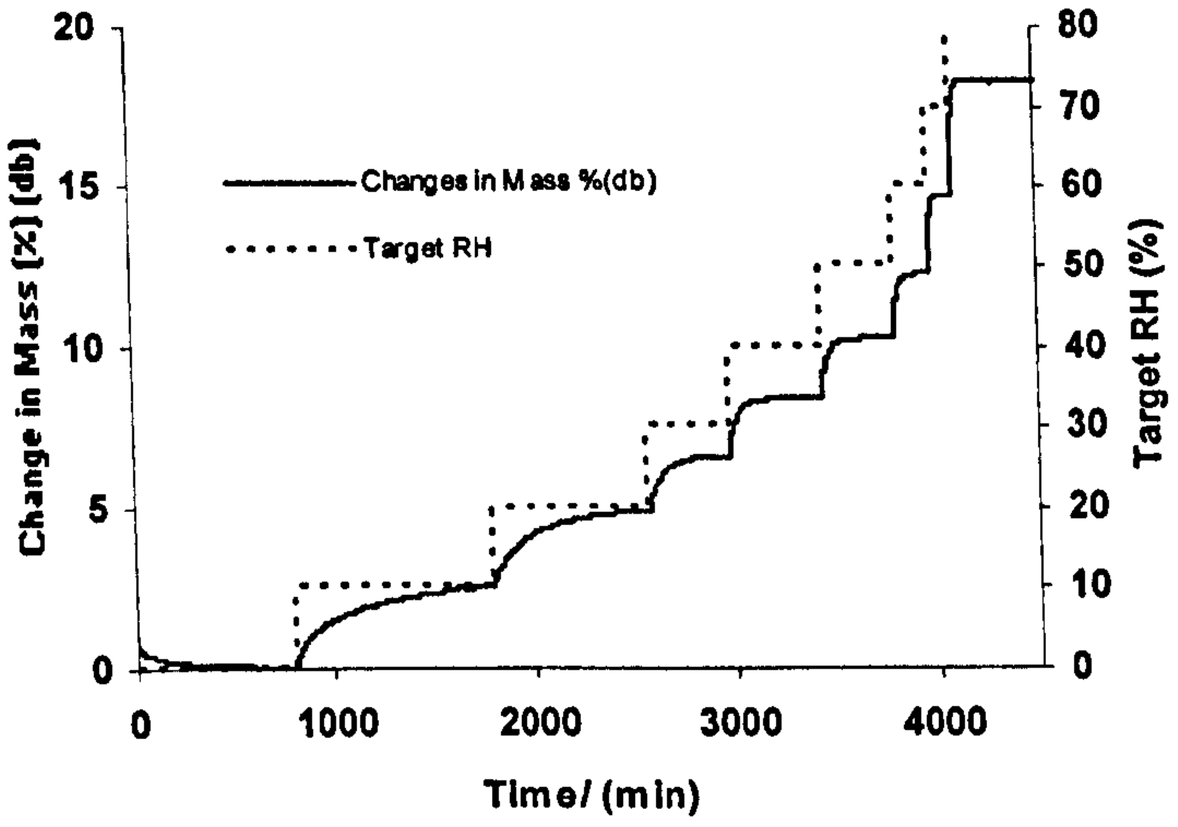

Figure 4.12. Example of sorption isotherm for rice starch and 5%glycerol extrudate (25°C). The continuous line represents changes in weight whereas the dotted line in the equilibration relative humidity step.

4.1.4.2.2 Effect of Glycerol on Diffusion Coefficient of Starch

Figure 4.13 and 4.14 show the obtained *D* for waxy maize, rice and wheat starch glycerol mixtures as a function of the equilibrating relative humidity. A very similar behaviour was obtained for all three starches.

With a minimum *D* value of ~3.0E-14 m^2/s at the lower end of the RHs and a maximum of ~7.5E-14 m^2/s found at higher RHs. Similar values have been found in the literature for starchy based materials (Hopkinson, Jones et al. 1997, Sudharsan, Ziegler et al. 2004). Ottenhof (2003) measured the diffusion coefficient *D* for waxy maize starch obtaining a value of ~ 5.0E-14 m^2/s for an equilibration RH ~ 15% and 1.0E-14 m^2/s for a RH ~ 90%.

The moisture content of the three starch types for RHs <50% is ~ 10% (db) (figures 4.6 and 4.7) which would suggest that they are in the glassy state (Farhat, Blanshard et al. 2000).

The increase in *D* in the glassy state, may be explained by the "jump distance λ" idea applied by Tromp, Parker et al. (1997) on glucose syrup and maltose-water mixtures. They suggested that the estimation of jump distance λ can give information related to how the molecules in a matrix are packed together and how this can affect *D*. Low values of λ were calculated for a low Mw mixture

(maltose-water), whereas high λ were estimated for the higher Mw mixture (glucose syrup DE47). The authors explained this by suggesting that in the case of low Mw, the molecular structure is more densely packed compare to the higher Mw samples were a random packing order of the oligomeric chains creating voids where water rich regions may exist.

Applying this rationale on a glassy starch matrix, the increase in the diffusion with RH may explained by the formation of voids by the random order polymer chains (high Mw) where water molecules can penetrate creating water rich zones where moisture would diffuse quicker increasing the overall D value.

Another idea that might explain the increase of D in the glass is the presence of secondary transition. β-relaxations, associated to side groups or segments of the main chain (Rudin 1999), would suggest that fractions of water in the glassy carbohydrate may retain some orientational mobility (Parker and Ring 1995).

For the range studied, glycerol didn't seem to significantly increase the diffusion coefficient. The maximum values for the control samples were ~5.0E-13 m^2/s and 7.5E-13 m^2/s for ~ 20% glycerol mixtures (red dotted line in figures 4.13 and 4.14).

Where glycerol did have an effect was at the RH at which the maximum D was obtained. In the case of the control sample the RH was ~ 80% whereas for the 20%glycerol extrudates the RH was ~55% (blue dotted line in figures 4.13 and 4.14). This behaviour can be explained by the plasticiser effect of the glycerol reducing the amount of water present in the matrix to reach similar diffusivities.

An interesting situation (for the three starches) occurs at the higher end of RHs where D clearly decreased. This decrease also seems to be related to the amount of glycerol present in the samples regardless of the starch type. Figures 4.13 and 4.14 show that when glycerol concentrations increase, the RH at which D values reached a maximum started to fall decreased.

It is unlikely that this change in the diffusion values comes from just the swelling of the particles at high relative humidities as it was not detected for the control samples (no glycerol)

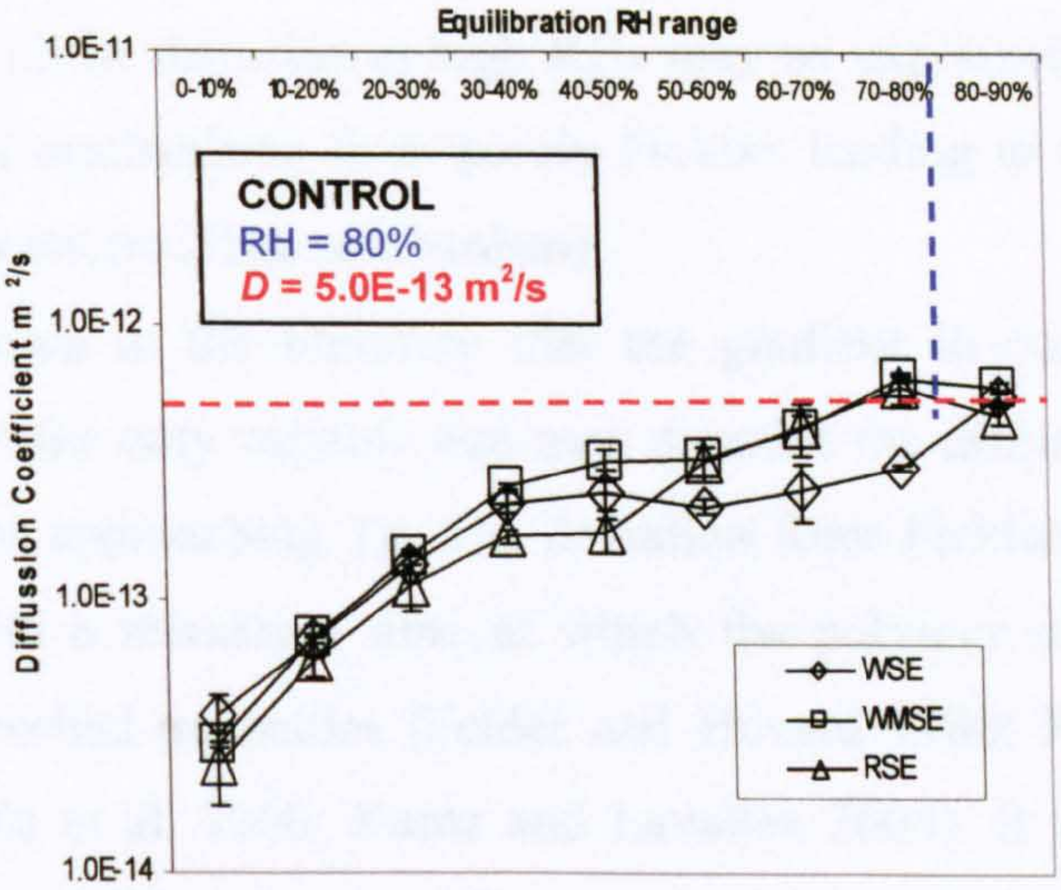

Figure 4.13. Diffusion Coefficient (D) for waxy maize (WMSE), rice (RSE) and wheat starch (WSE) at 25°C (control samples).

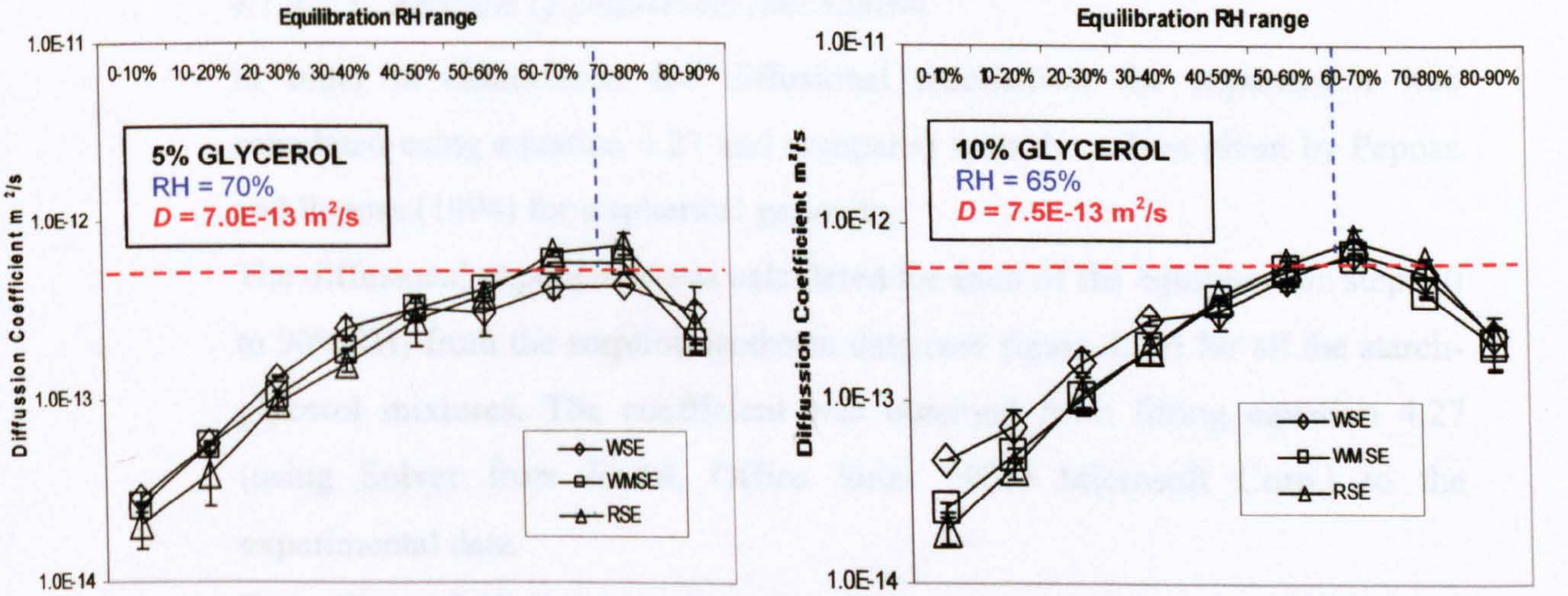

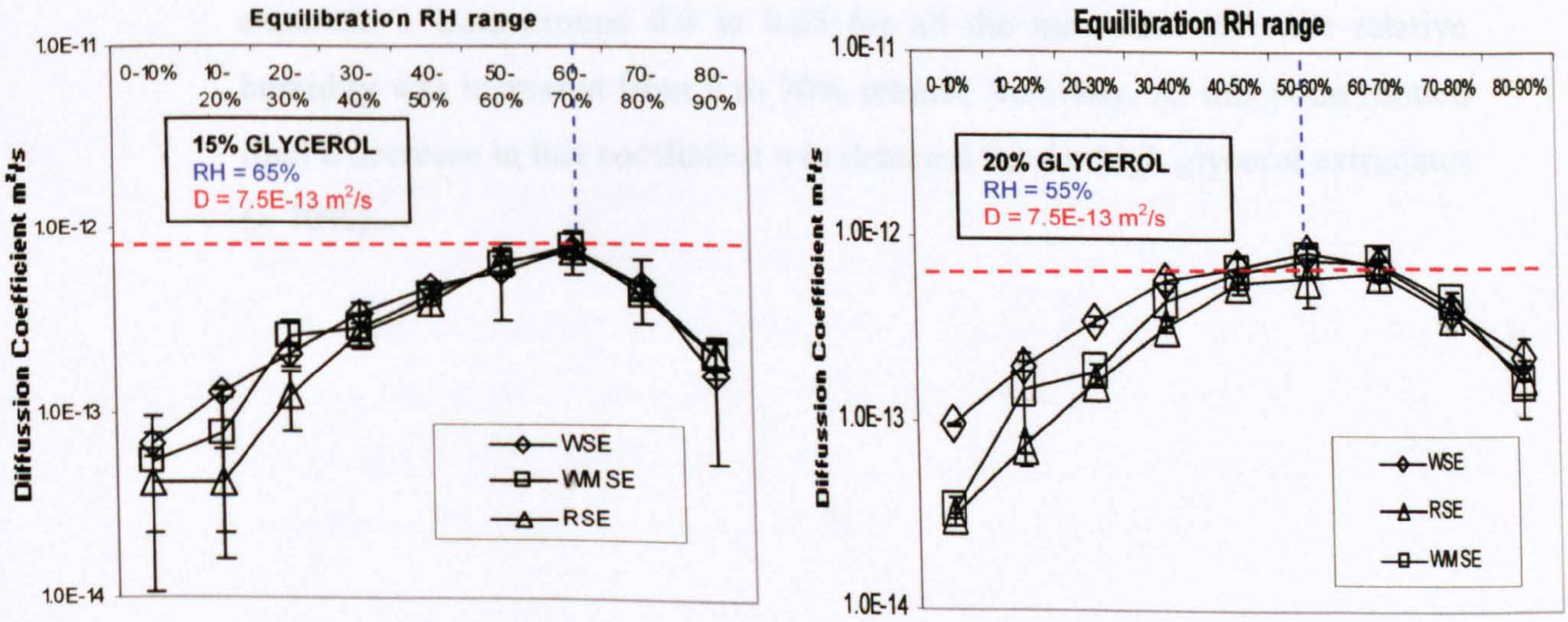

Figure 4.14. Diffusion Coefficient (D) for waxy maize (WMSE), rice (RSE) and wheat starch (WSE) with 5%, 10%, 15% and 20% glycerol at 25°C.

This decrease in the diffusion at high RHs may be explained by the change in the diffusional mechanisms from purely Fickian leading to Case II (including the anomalous intermediate mechanism).

It is well known in the literature that the gradient in concentration in the polymer is not the only variable that may describe the diffusivity in the glassy state and when approaching Tg. The deviation from Fickian behaviour can be associated with a relaxation time at which the polymer structure rearranges itself to the sorbed molecules (Felder and Huvard 1980; Peppas and Peppas 1994; Roy, Xu et al. 2000; Kuntz and Lavallee 2004). It is possible that for high RHs sorption steps a different diffusional mechanism is present suggesting that the Fickian model used to obtain *D* was not entirely appropriate.

4.1.4.2.3 Analysis of Diffusional Mechanism

In order to characterise the diffusional mechanism the exponent *n* was calculated using equation 4.27 and compared with the values given by Peppas and Peppas (1994) for a spherical geometry.

The diffusional exponent *n* was calculated for each of the equilibration steps (0 to 90%RH) from the sorption isotherm data (see figure 4.12) for all the starch-glycerol mixtures. The coefficient was obtained from fitting equation 4.27 (using Solver from Excel, Office Suite 2003, Microsoft Corp.) to the experimental data.

From figure 4.15 it seems clear that there was an increase in the diffusional exponent *n* from around 0.4 to 0.65 for all the mixtures when the relative humidity was increased from 0 to 70% relative humidity. At this point (dotted line) a decrease in this coefficient was detected for the high glycerol extrudates (> 10%).

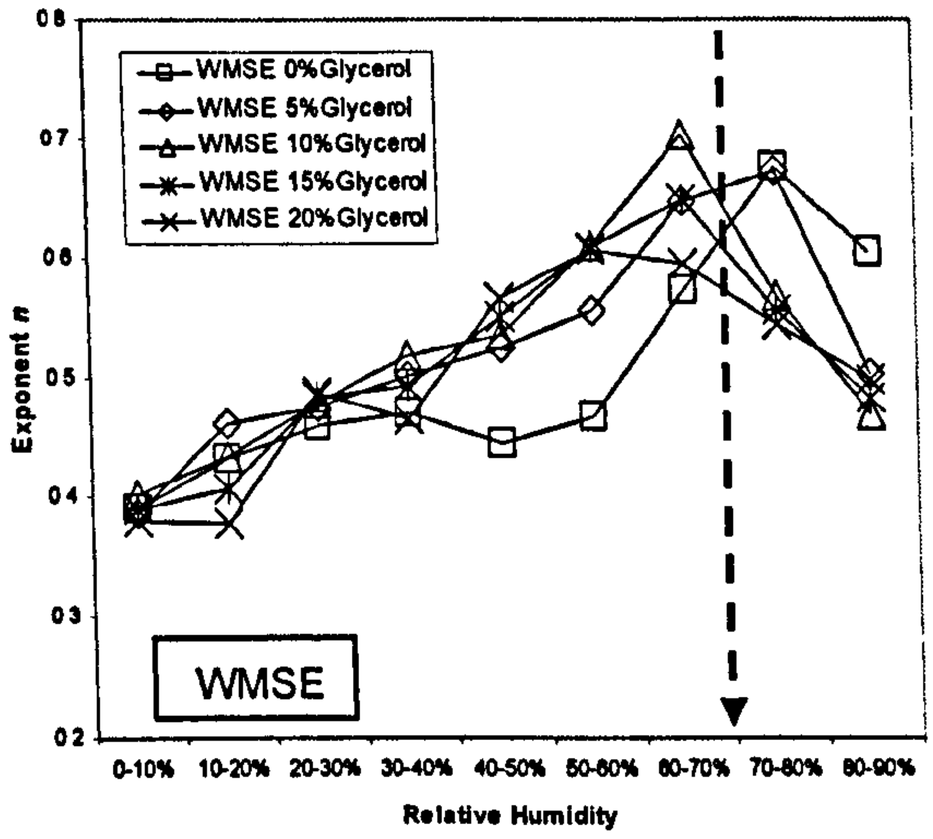

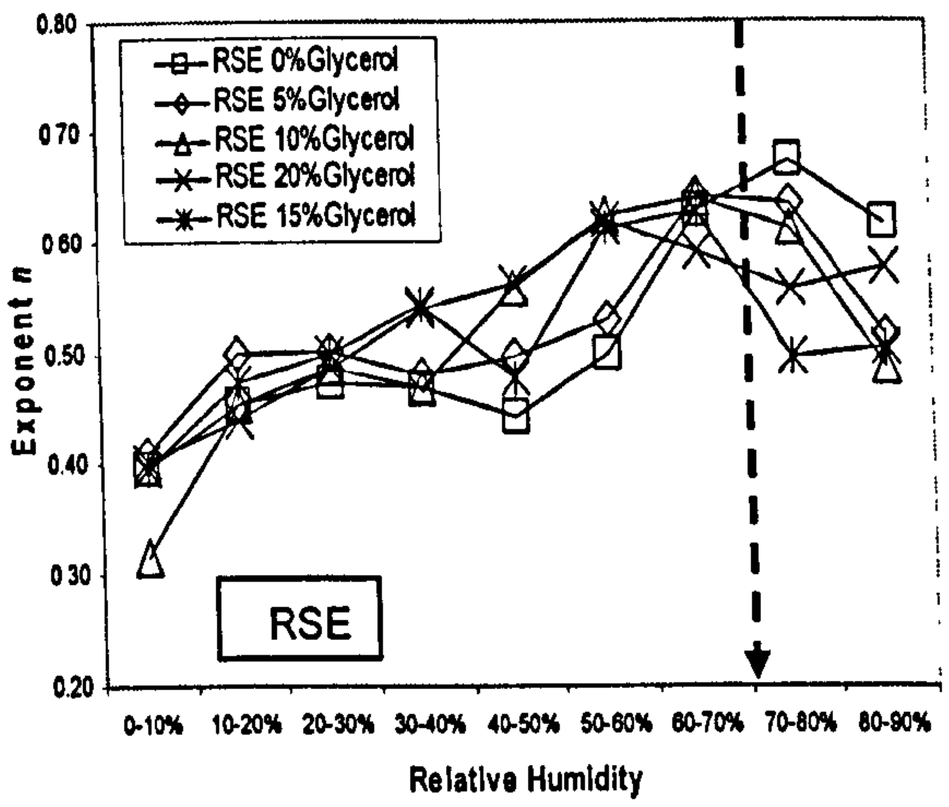

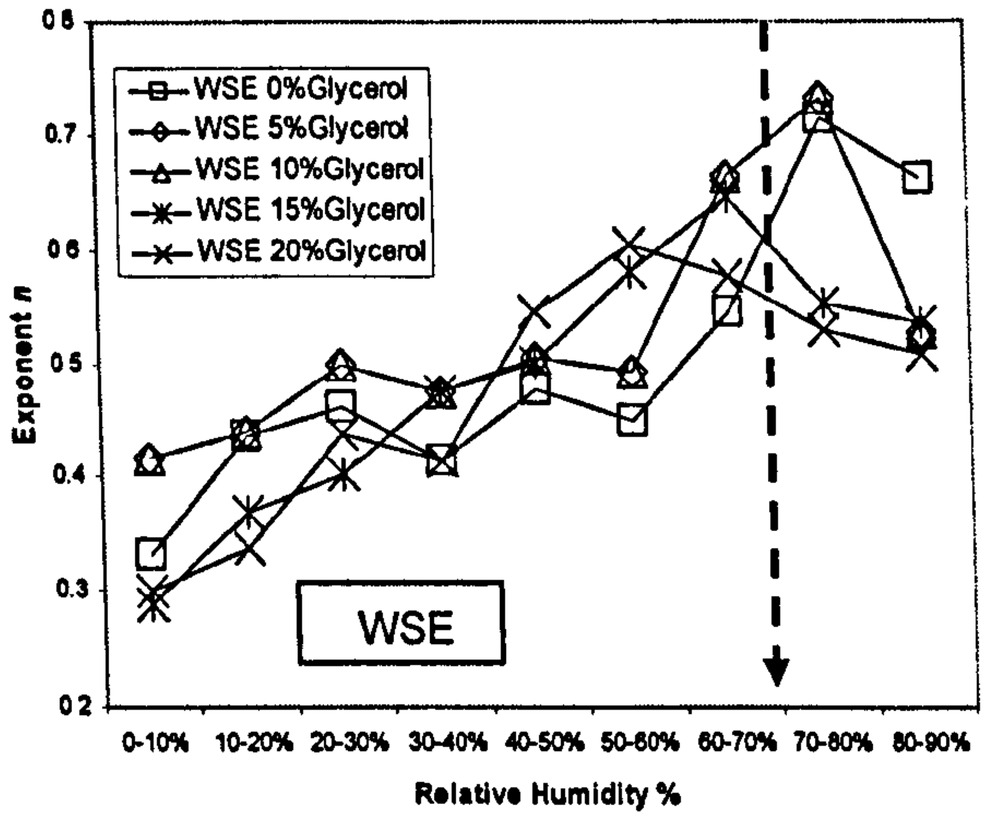

Figure 4.15. Values of the diffusional exponent *n* calculated from each sorption relative humidity for waxy maize (WMSE), rice (RSE) and wheat starch-glycerol extrudates (WSE).

This change in the exponent can be related to a change in the diffusional mechanism. The diffusion data with *n* values < 0.4 can be related to a Fickian diffusional mechanism. In the case of the values > 0.4 and <0.8, the diffusion can be described by the coupling of Fickian and Case II mechanism (Peppas and Peppas 1994). Finally, the decrease in the coefficient at higher RH could be related to a change to Fickian diffusion once the samples are in the rubbery state.

As it was mentioned in section 4.1.4.1.2, it is known from the literature that the change in diffusional mechanisms is dependant on the molecular mobility in the system (Felder and Huvard 1980, Crank 1993, Peppas and Peppas 1994, Parker and Ring 1995, Hartley 1996, Kuipers, Vervelde et al. 2003).

Figure 4.16 shows the diffusional exponent *n* as a function of the difference between the experimental temperature (25°C) and the glass transition temperature (Tg) measured by Differential Scanning Calorimetry (DSC). More information related to DSC experimental protocol and Tg data are available in chapter 3 section 3.3.4 and chapter 5 respectively.

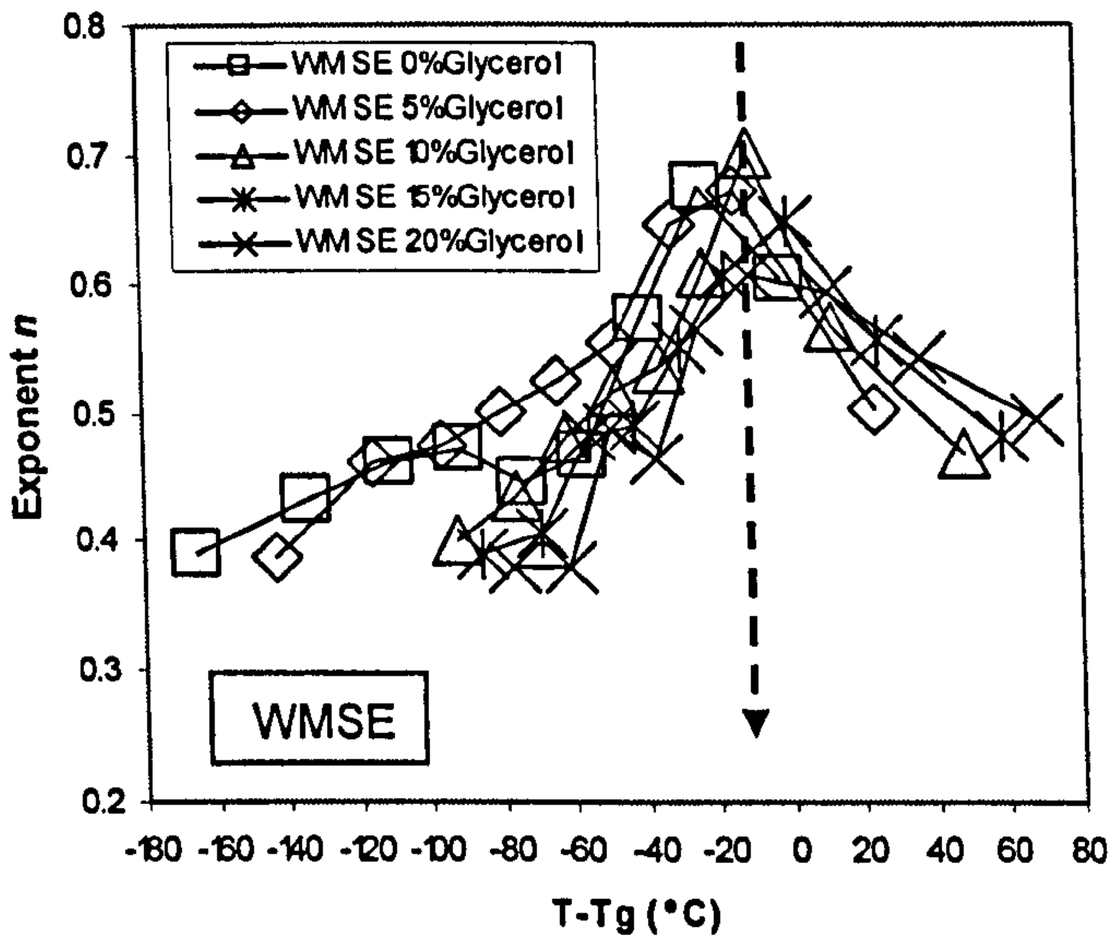

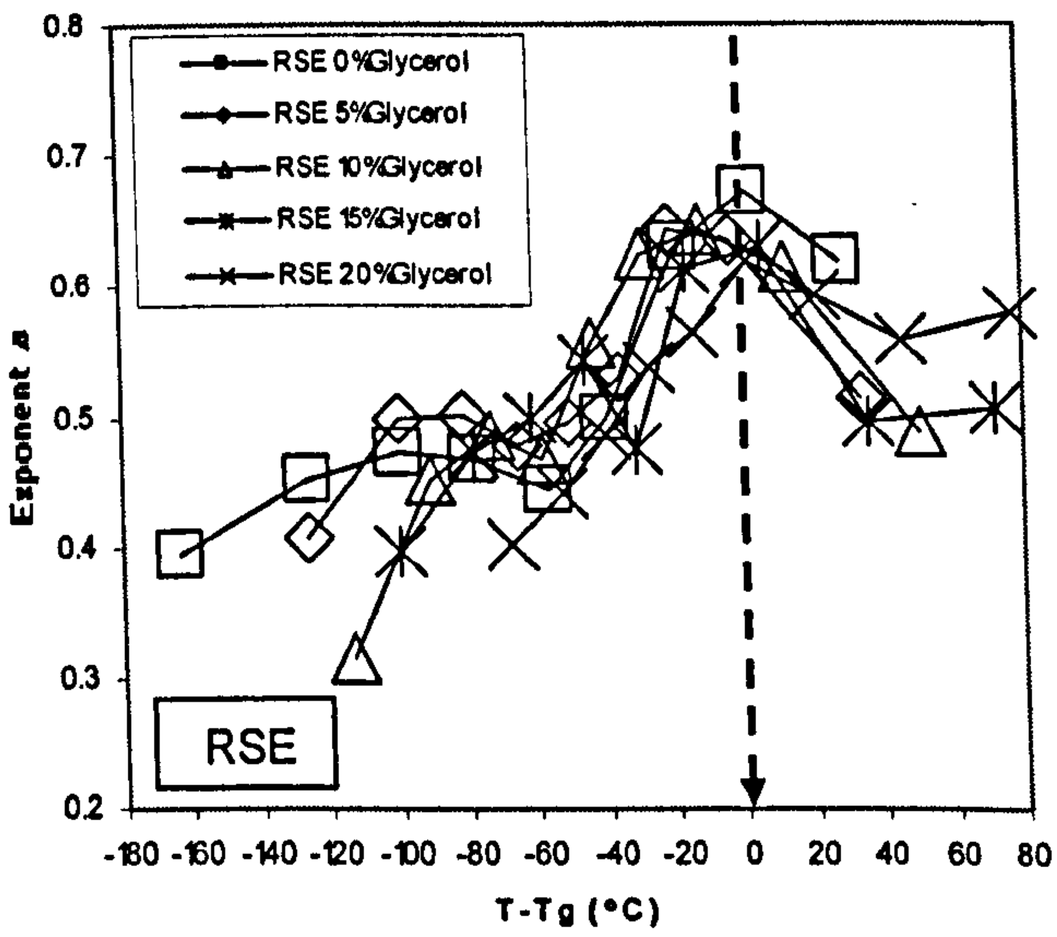

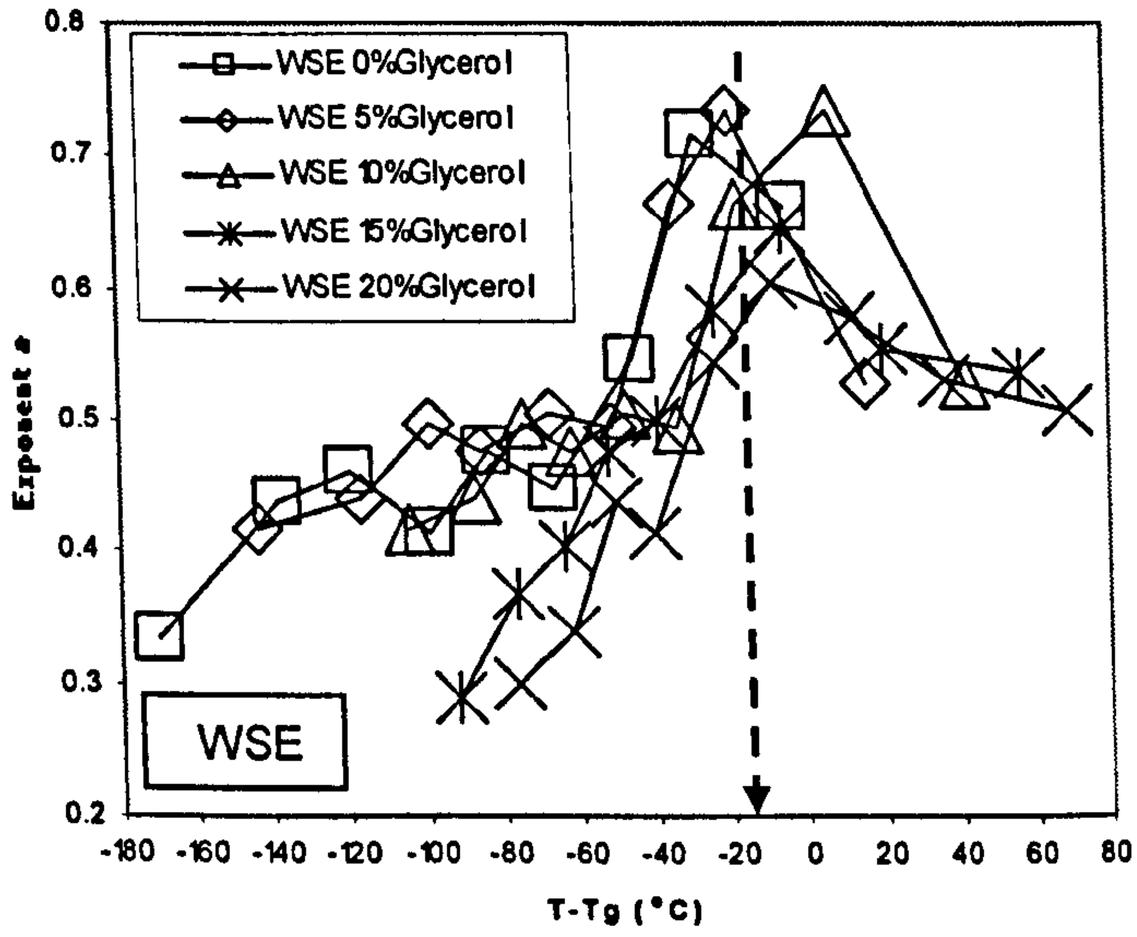

Figure 4.16. Values of the diffusional exponent *n* as a function of T(25°C)-Tg for waxy maize (WMSE), rice (RSE) and whet starch-glycerol (WSE) extrudates.

The above figures showed the reduction in the exponent *n* occurs when the starch glycerol systems approached their glass transition temperature. This behaviour was observed for all the three starches.

It seems when their physical state is in the glassy state, an elastic diffusional mechanism is present, represented by an exponent n < 0.4. In this case there is effectively no time variation of the polymeric structure during the diffusion process and can be described by Ficks's law (Vrentas and Duda 1977).

The decrease in the exponent *n* in the rubbery state (T-Tg > 0°C) can be explained by an increase in the molecular relaxation process, that now occurs faster compared to the diffusive transport and both the polymer and the solvent behave like pure viscous fluids (Vrentas and Duda 1977). This mechanism can also be described by Fick's law. Based on the chart summarised by Hopfenberg and Frisch (1969) (figure 4.10), a coupling of Case I and Case II diffusion may occur simultaneously, resulting in the so called Anomalous diffusion.

Although this approach may help to associate the reduction in *D* to different diffusional mechanism, it does not give information behind the decrease in the slope of the sorption curves at high RHs leading to a reduction in the diffusion coefficient.

Looking under the optical microscope at the starch-glycerol particles after each DVS run, clear differences in the particle shape were observed between the control sample and the 20% glycerol. Figure 4.17 shows a set of microscope pictures of the particles from waxy maize, rice and wheat starch 0% glycerol (on the left) and 20% glycerol (on the right).

It is clear that on the 0% glycerol samples the particles shapes did not change during the sorption experiments; keeping a well define structure. However micrographs of the 20% glycerol showed particles loosing their integrity, collapsing or sticking together and hence affecting the overall sample geometry. This behaviour was similar for the 10% and 15% glycerol and to less extent for 5% glycerol samples (which was similar to the control). During this process the particles size would effectively become bigger.

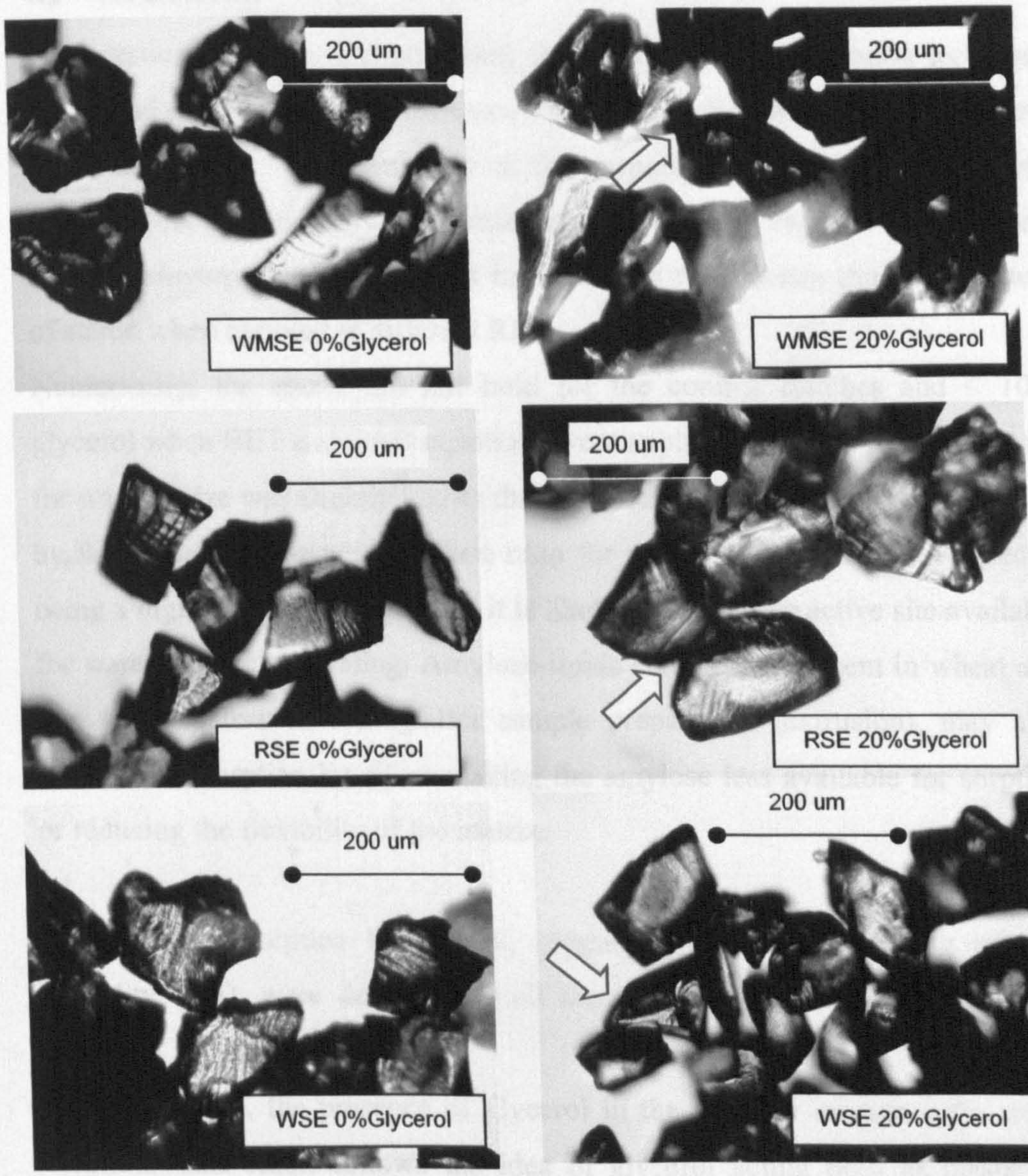

Figure 4.17. Picture of particles after DVS experiment for waxy maize, rice and wheat starch extrudate with 0%glycerol and 25% moisture db (left) and 20%glycerol and 45% moisture (right). Red arrow indicates points at which particles are joined together.

This increase in the particle size can be also related to Tg. At this point the structure of the starch matrix becomes more mobile (rubbery) decreasing its viscosity facilitating particles interaction. An increase in the powder particle size would lead to a reduction in the surface area exposed to sorption decreasing the rate (reduction in the sorption slope) at which the material would absorb moisture.

Glycerol, being a plasticiser, would contribute and hence reduce the moisture content needed to reach Tg. This would lead to a change in the particle integrity at lower RHs compared to the control sample..

4.2 Conclusions

The sorption isotherm obtained from the dynamic vapour sorption technique (DVS) did not show a clear difference between the waxy maize, rice and wheat starch extrudates. The similarity in the sorption curves between the three starches (control and glycerol containing extrudates), suggest that different amylose/amylopectin ratios do not influence the equilibrium moisture content of starch when exposed at different RHs.

Numerically, the above did not hold for the control starches and < 10% glycerol when BET and GAB equations were applied. The monolayer value m_o for waxy maize was slightly higher than for rice and wheat. This was explained by the higher amylopectin/amylose ratio for waxy maize starch. Amylopectin being a highly branched molecule, it is likely to have more active site available for water molecules binding. Amylose-lipids complexes, present in wheat and rice starches formed during/after sample preparation (extrusion), may also affect water sorption by either making the amylose less available for sorption or reducing the flexibility of the matrix.

Two different sorption behaviours, depending of the equilibrating relative humidity (RH), were detected for all the three starches when glycerol was present.

For RHs >70%, the presence of glycerol in the polymer increased the water sorption. This result follows the idea of glycerol acting both as plasticiser increasing the molecular mobility of the system and as a hygroscopic compound contributing to the hydration of the system. This behaviour was accurately represented by the GAB model where the K constant increased in the presence of glycerol suggesting an increase in the heat of sorption (binding energy in the multilayer domain) at high RHs.

For RHs < 60%, the presence of glycerol seemed to decrease the equilibrium moisture content. This behaviour was clearly observed on the moisture content v/s weight fraction graphs where an increase in the moisture content was detected when the glycerol mass fraction decreased (RHs <60%). These results correlated well with the obtained monolayer value m_o from BET and GAB models. This value decreased when the glycerol concentration in the mixture increased. Theoretically the decrease in this parameter suggests less sorption

sites available for water molecules. The reduction in these sorption sites could be related to glycerol-polymer interactions which are clearly favoured over that of glycerol-water.

The reduction in the m_o correlates well with the decrease in the constant C from the BET and GAB models for the glycerol samples, which would suggest a reduction in the heat of sorption at the monolayer due to fewer water molecules interacting with the polymer.

The predictions of sorption isotherms based on the components' weight fractions showed that glycerol not only may interact with starch at the low end of relative humidities but it seems to indicate that it may occur at higher end as well.

The above was clearly observed with an improvement in the model fit for the starch-glycerol mixtures when an interaction factor (ξ <1) was used. This improvement was detected through out the whole RHs range. The value of the interaction parameter increased with glycerol concentration supporting the hypothesis of a reduction in sorption sites by the presence of this polyol.

Diffusivities were similar for the three starch species. An increase in the diffusion coefficient was detected when the RH increased. This increase could be related to voids, water rich zones, created from the random chain packing and/or secondary transitions know to occur in the glass (β-relaxation.). The latter by an increase in the movement of local groups associated to the main chains of the polymer. It is interesting that no difference could be detected between the different starches despite the change in total branched chains structure from ~ 100% (waxy maize starch) down to only 70% for rice and wheat starches.

The presence of glycerol increased the diffusion coefficient at similar moisture concentrations. This was confirmed at a RH ~ 60%, where there were no differences in moisture content between the control and the glycerol samples, relating this increase in D to this polyol. An unexpected reduction in the diffusion coefficient occurred at the high end of RHs was detected for the all starch-glycerol extrudates.

This sorption behaviour can be related to the glass transition temperature by two scenarios.

1. First, by a change in diffusional mechanisms. Deep in the glassy state, where the relaxation of the polymer is extremely slow (due to its high viscosity) Fickian diffusion occurs (n<0.4). When approaching Tg a coupling of Fickian and Case II diffusion is present (0.4<*n*<0.8). Above Tg, where the matrix becomes rubbery, the relaxation rate of the chains in the polymer is much higher than the diffusion time being represented again by Fickian law.
2. Second, by a change in the particle geometry. This was detected for the all the starch-glycerol mixtures after DVS experiments. After reaching their glass transition temperature the samples become rubbery, decreasing its viscosity, facilitating the interaction between the particles. This behaviour would lead to less surfaces area exposed to the surroundings decreasing the sorption rate.

The findings discussed above do not entirely agree with the hypotheses presented at the beginning of this chapter. It was clearly showed that the capacity of glycerol to influence water sorption in starches was highly dependant on the relative humidity (RH). Similarly, the effect of this polyol on the water activity (Aw) of these systems also increased or decreased depending on the surroundings RH. Weight fraction models did not accurately represent the obtained sorption profiles for which an interaction factor was used.
Diffusivities in the studied starches increased by the presence of glycerol only up to certain RH, after which a decrease was detected. This point was identified as the mixture Tg where particle geometrical integrity was altered.

5 Glass Transition on Starch-Glycerol Systems

As it has been mentioned in section 2.1.7, the glass transition temperature or Tg is one of the most important factors used in the prediction of the mechanical performance and stability of amorphous and semi-crystalline polymers. The Tg can also influence the mechanism and kinetics of the system towards thermodynamic equilibrium.

The work described in this chapter aimed to evaluate the effect of polyols, specifically glycerol, on the glass transition temperature of starch-water based systems. It also aims to evaluate possible differences in Tg between common starches when mixed with polyols and water.

Finally, Tg values obtained from calorimetry (DSC) and mechanical spectroscopy (DMTA) are compared using a wheat-water-glycerol mixture as a reference system.

5.1 Hypotheses

The hypotheses that will be investigated in this chapter are:

- Tg will be affected by water and glycerol and their plasticization effect is only predictable if the systems remain homogenous.
- All amorphous or processed starches will behave the same way in regard to their Tg in the presence of plasticisers, no matter their botanical origin or amount of amylose they contain.
- DSC and DMTA can be used to give comparable values for the Tg of starchy systems. The Tg values can be predicted by existing models based on thermodynamic properties and individual weight fractions.

Next paragraphs present a brief overview on the glass transitions temperature, its application to food systems and its prediction by different models.

5.2 Theoretical Background

Extensive work on synthetic polymers has given a substantial increase in the fundamental understanding of the glass transition and its effect on the mechanical and stability performance on these materials.

Perez (1994) generalised some of the findings in the literature behind the definition of glass transition temperature for amorphous polymeric systems as follows.

1. There is a sufficiently well defined phenomenon as the "glass transition" manifested by many glass-forming materials that it is reasonable to expect a major component in its explanation to be independent of chemical differences between the glass formers.
2. This change is characterised by a simultaneous decrease in entropy, heat capacity and an increase in viscosity. It is generally not considered to be a phase transition in the strict sense, despite the sharpness in changes of some properties such as the second derivative of free enthalpy (heat capacity, expansion coefficient, compressibility) and the dynamic behaviour (viscosity) during decreasing temperature.
3. The glass to rubber transition is mainly a kinetic and relaxational phenomenon, suggesting that configuration models are immobilised abruptly when T<Tg.

In the decade of the eighties, the value of a polymer science approach to the study of the glassy state phenomenon, glass transition and their importance to the materials structure and water relationships in foods and processes was increasingly recognised (Slade and Levine 1995). This innovative approach was developed to unify structural aspects of foods, viewed as kinetically metastable, completely amorphous or partially crystalline, dependant on mobility and conceptualised in terms of "water dynamics" and "glass dynamics" (Slade and Levine 1991a).

Intensive research has been carried out on the dependence of amorphous starch properties at the glass-rubber transition (Zeleznak and Hoseney 1987; Slade and Levine 1988; Orford, Parker et al. 1989; Scandola, Ceccorulli et al. 1991;

Hallberg and Chinachoti 1992; Kalichevsky 1992; Kalichevsky, Jaroszkiewicz et al. 1993; Nicholls, Appelqvist et al. 1995; Parker and Ring 1995; Baik, Kim et al. 1997; Forssell, Mikkiläa et al. 1997; Van Soest and Knooren 1997; Jiugao, Songzhe et al. 1998; Biliaderis, Lazaridou et al. 1999; Farhat, Blanshard et al. 2000; Mousia, Farhat et al. 2000; Moates, Noel et al. 2001; Parker and Ring 2001; Bindzus, Livings et al. 2002; Moraru, Lee et al. 2002; Ribeiro, Zimeri et al. 2003; Sombatsompop and Chaochanchaikul 2004).

5.2.1 Factors Influencing Tg

Zeleznak and Hoseney (1987) discussed differences in Tg between native and amorphous starches. This difference was attributed to the degree of crystallinity in native starches (30%), which could restrain the molecular dynamics of the amorphous component, given rise to a higher Tg value.

Orford et al. (1989) discussed the effect of the malto-oligosaccharides degree of polymerisation (DP) on Tg. They found that at constant moisture content, Tg increased when DP increased but remained constant (167°C) at greater DP values. Similar behaviour was found for polymers (13%MC) with DP from 2 to 13 and amylose and amylopectin, where a constant Tg value was measured for DP of 13 and the starch components. The Tg of pure amylose and amylopectin, is experimentally inaccessible due to thermal degradation before reaching the transition temperature (Forssell, Mikkiläa et al. 1997; Parker and Ring 2001). Prediction of Tg for dried amylopectin has been estimated to be 230 ± 10 °C (Orford, Parker et al. 1989).

The plasticizing effect of water and other low molecular weight compounds on Tg of carbohydrates has been reported extensively (Zeleznak and Hoseney 1987; Orford, Parker et al. 1989; Orford et al. 1990; Slade and Levine 1991; Kalichevsky 1992; Lourdin, Coignard et al. 1997; Mousia 2000; Moates, Noel et al. 2001). Orford (1989) detected a significant decrease on Tg when moisture content increased on malto-oligomers. This effect was more significant at lower moisture concentrations with a decrease in Tg of 100°C for an increase in 6% moisture on maltose, maltotriose and maltohexaose. Zeleznak and Hoseney (1987) obtained similar results for wheat starch.

Other small molecules have been used to depress the glass transition of carbohydrates. Orford et al (1990) studied the effect D-glucose forming

maltotriose and maltohexaose. The found an inverse linear relationship between the Tg and the mole fraction of D-glucose, demonstrating the plasticizing effect of the monomer. Farhat et al (2000 and 2000b) showed a reduction in Tg when sucrose was added to waxy maize starch-water extrudates. The plasticizing effect was more significant when the moisture content was < 20% (wb).

As mentioned on Chapter 3, other small molecular weight compounds that are commonly used as plasticisers are liquid polyols (e. g. glycerol and glycol). These compounds have some advantages over small molecular weight carbohydrates. They have a higher plasticizing effect due to its smaller molecular weight and its liquid nature at ambient temperature makes the production of the so-called thermoplastic starches possible. Polyols also show a low volatibility, which helps to increase the stability of materials when exposed to different environmental conditions.

In terms of its plasticizing properties, calorimetry (DSC) has shown that 29% (wb) of glycerol decreased the Tg of amorphous barley starch (MC 1% wb) to 70°C (Forssell, Mikkiläa et al. 1997).

Mechanical spectroscopy (DMTA) has also shown the plasticizing effect of glycerol starch components. Forssell et al. (1997) and Moates et al. (2001) studied the effect of this polyol on the Tg of barley starch and pure amylose films respectively. They detected a decrease on tan δ peak when the glycerol concentration increased, indicating that the main mechanical relaxation of the polymer occurred at lower temperature. This transition is related to a decrease in the elastic modulus (E') and a relative increase in energy release as heat during measurements represented by the loss modulus (E'').

One of the drawbacks that limit the use of thermoplastic starches on industrial applications is their sensitivity to small variations in moisture. When exposed to environmental conditions, which influences the materials mechanical performance. If other plasticizers, such as glycerol are added to the mixture, the sensitivity to moisture will increase even further due to the hygroscopic nature of this polyol. Therefore, creating a model to predict the effect of variations in composition on Tg can prove to be very useful. This can help to formulate products accordingly in order to minimise the impact of environmental conditions such as temperature and relative humidity.

5.2.2 Prediction of Tg for Multi-Components Mixtures

There are several models available for the prediction of Tg for multi-components mixtures. Some of the approaches commonly used for polymer-diluent systems are described in the following paragraphs.

5.2.2.1 Gordon-Taylor Model (1952)

Following the free volume theory, the prediction of the glass transition temperature of a miscible polymer-diluent can be described by the equation 5.1. It has been successfully used to predict the plasticization of water-carbohydrate and water-proteins (Roos 1995). One of the main limitations of this model is that it can only be used for binary mixtures.

$$Tg = \frac{w_d Tg_d + k w_p Tg_p}{w_d + k w_p} \qquad \textit{Equation 5.1}$$

where:

p = polymer

d = diluent

w = weight fraction

k = empirical factor

5.2.2.2 Couchman-Karasz Model (1978)

The development of the Couchman-Karasz models is based on the assumption that Tg is in nature a second order transition. It also considers a continuity in entropy and volume when the glass transition is reached.

This model provides a relation that expresses a single Tg value for a mixture in terms of the Tg of each of the individual components. To apply this model, the compounds present in the mixture must be fully compatible (miscible).

The final derived equation was based on the analysis of the total entropy of the mixture, the weight fraction and entropies of each on the components. The mixing excess entropy was neglected by assuming similar values in the glass and liquid.

$$\ln Tg = \frac{w_d \Delta Cp_d \ln Tg_d + w_p \Delta Cp_p \ln Tg_p}{w_d \Delta Cp_d + w_p \Delta Cp_p} \qquad \textit{Equation 5.2}$$

where:

ΔCp_p = specific heat capacity of the polymer

ΔCp_d = specific heat capacity of the diluent

Tg_p = Tg of polymer

Tg_d = Tg of diluent

w_p and w_d = weight fractions of the polymer and diluent respectively

5.2.2.3 ten Brinke-Karasz-Ellis Model (1983)

ten Brinke et al. (1983) discussed the applicability of Couchman-Karasz on polymer-diluent systems. They concluded that the assumption of this model of full compatibility between components and invariability of ΔCp with temperature was not totally accurate. They also explained the over reduction on Tg by plasticizers by not taking possible cross-linking between the polymeric chain.

They proposed a derived version of Couchman-Karasz model described by the following equation:

$$Tg = \frac{w_d \Delta Cp_d Tg_d + w_p \Delta Cp_p Tg_p}{w_d \Delta Cp_d + w_p \Delta Cp_p} \qquad \textit{Equation 5.3}$$

If the relation $\frac{\Delta Cp_p}{\Delta Cp_d} = k$ is considered, this equation becomes similar to the Gordon-Taylor model.

Next paragraphs present the experimental work carried out on starch-glycerol extrudates. In the first part, the glass transition (Tg) of these samples was

analysed and fitted using the equations presented in the previous section. Then, the experimental work focuses on the comparison of this parameter obtained by DSC and DMTA.

5.3 Results and Discussion

To test the hypotheses presented in section 5.1, different cereal starches were extruded. During the thermo-mechanical extrusion process different amounts of glycerol were added (more details of sample preparation are presented in chapter 3, section 3.2.3.1).

A new set extruded waxy maize, rice and wheat starches-glycerol samples were dried as described chapter 3, section 3.3.2.2. Prior to the analysis, the moisture content of each of starch glycerol samples was measure gravimetrically. The obtained values are presented in the following table.

Table 5.1. Moisture content (*) of waxy maize, rice and wheat starches-glycerol samples after drying at 70°C for different times.

Waxy Maize Starch								
Drying Time (h)	0% Glycerol	Drying Time (h)	5% Glycerol	Drying Time (h)	10% Glycerol	Drying Time (h)	15% Glycerol	Drying Time (h)	20% Glycerol
10.0	5.1% (0.11%)	10	5.3% (0.22%)	10.5	3.6% (0.23%)	10.0	5.0% (0.19%)	10.5	3.8% (0.21%)
3.5	10.0% (0.23%)	3.5	10.7% (0.33%)	3.5	10.7% (0.21%)	3.5	8.5% (0.27%)	4.0	6.8% (0.31%)
2.5	12.8% (0.32%)	1.0	20.3% (0.24%)	1.2	15.3% (0.25%)	2.5	12.0% (0.21%)	2.5	11.0% (0.30%)
1.0	17.8% (0.23%)	0.5	27.9% (0.45%)	0.5	24.0% (0.39%)	0.5	24.0% (0.35%)	0.5	22.2% (0.41%)
0.5	29.2% (0.19%)	--	--	--	--	--	--	--	--
Rice Starch									
	0% Glycerol		5% Glycerol		10% Glycerol		15% Glycerol		20% Glycerol
10.0	4.9% (0.17%)	10	4.9% (0.19%)	10	4.6% (0.17%)	10	6.0% (0.14%)	10	6.8% (0.15%)
3.5	10.0% (0.23%)	3.5	11.9% (0.20%)	3.5	12.1% (0.20%)	3.5	9.9% (0.17%)	3.5	8.6% (0.17%)
2.5	14.0% (0.35%)	1.0	17.4% (0.29%)	2.0	14.8% (0.25%)	2.5	11.3% (0.24%)	2.5	11.4% (0.21%)
1.0	19.3% (0.42%)	0.5	23.6% (0.39%)	1.0	21.7% (0.35%)	2.0	13.6% (0.31%)	1.0	19.8% (0.45%)
0.5	24.7% (0.41%)	--	--	--	--	1.0	21.4% (0.42%)		--
Wheat Starch									
	0% Glycerol		5% Glycerol		10% Glycerol		15% Glycerol		20% Glycerol
10.0	7.9% (0.17%)	10	6.8% (0.22%)	10.0	6.0% (0.21%)	10	5.0% (0.26%)	10	6.9% (0.21%)
3.5	12.0% (0.21%)	3.5	10.3% (0.20%)	3.5	9.8% (0.25%)	3.5	9.2% (0.19%)	3.5	10.4% (0.33%)
1.0	17.1% 0.37%)	1.0	15.2% (0.31%)	1.0	16.2% (0.30%)	2.5	11.5% (0.23%)	2.5	13.3% (0.29%)
0.5	25.0% (0.31%)	0.5	20.6% (0.29%)	1.0	16.2% (0.27%)	0.5	19.6% (0.31%)	1.5	16.1% (0.31%)
	--		--	0.5	22.4% (0.40%		--	1.0	17.1% (0.36%)
	--		--		--		--	0.5	21.5% (0.44%)

(*) Moisture content was measured in duplicates using a vacuum oven at 70°C overnight. Values in bracket are the arithmetic difference between duplicates

Low (< 7% wb) and high moisture (> 25% wb) content starches were X-rayed showing a small increase in crystallinity (data not shown). The diffractograms were very similar to the patterns shown in chapter 3, section 3.3.5.2.

The Tg values obtained for the different starch-water-glycerol mixtures were calculated from the mid-point of the step change in heat capacity from the DSC trace. Details of this methodology are given on chapter 3, section 3.3.4.

Typical thermograms are shown in figure 5.1, where the Tg values are obtained from the half point of the change in heat flow. The change in heat capacity can be obtained from the first derivative of the heat flow data.

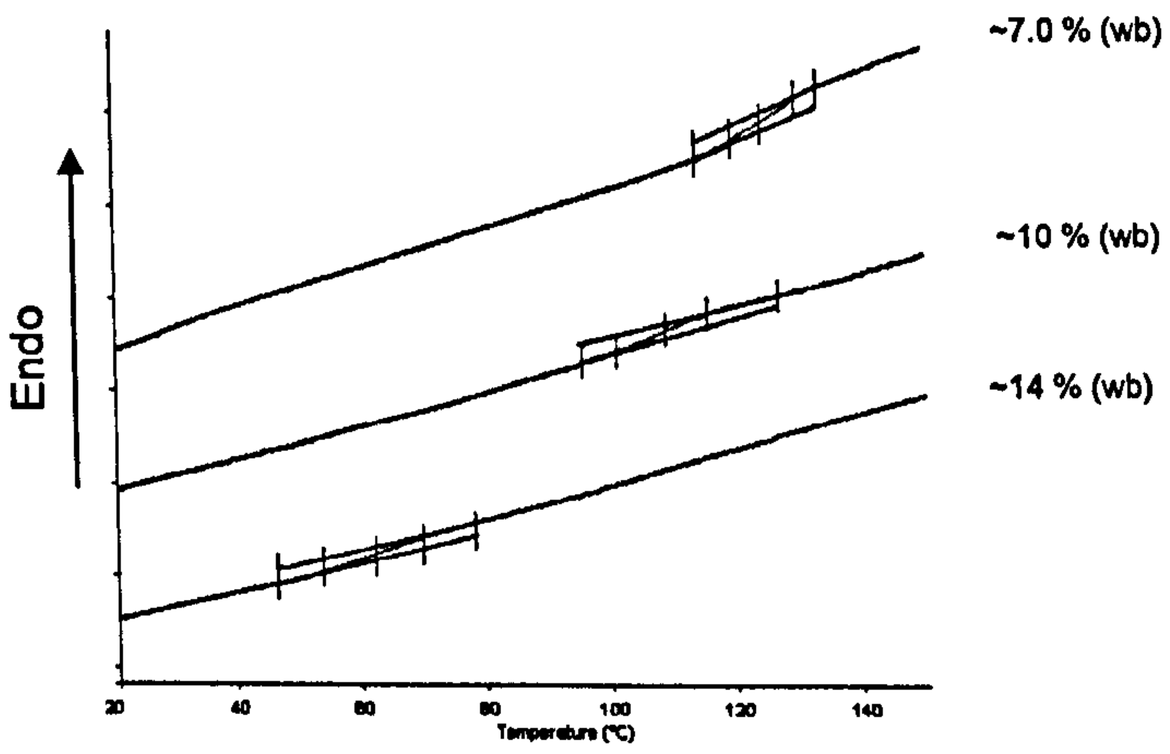

Figure 5.1. DSC thermograms (2nd run) showing the change in heat flow related with the glass transition temperature (normalised by starch weight). Waxy maize starch and 7.0, 10 and 14% (wb) moisture content.

In the case of DMTA, details of the methodology used on this technique and examples of measurements are presented in chapter 3, section 3.3.3.1. The extruded ribbons were reshaped as specified, section 3.3.3.2

5.3.1 Effect of Glycerol on Tg of Starch-Water Systems

Figure 5.2 shows the dependence of Tg on moisture and glycerol concentrations for waxy maize, rice and wheat starches respectively. Figure 5.2 (A) shows a significant decrease in Tg of the waxy maize starch (no glycerol) when moisture content increased from 5% to 25% (db). For this range of moisture change, Tg decreased from ~170°C to ~25°C. Similar reduction for this starch type have been reported in the literature. (Kalichevsky, Jaroszkiewicz et al. (1992) measured a decrease of 110°C when the moisture was increase from 10% to 20% (db). Farhat, Blanshard et al. (2000) detected a

reduction of Tg from ~ 80°C to 0°C when the moisture content was changed from 15% (db) to 40% (db).

For moisture contents greater than 25% (wb), the reduction in Tg by the plasticizing effect of water was less effective. This is shown by a levelling off of the Tg curve at high moisture contents. Zeleznak and Hoseney (1987) found similar results for wheat starch, with no substantial decrease in Tg (15°C) for moisture contents greater than 25 % wb suggesting the formation of separated water rich phase which does not contribute to a further decrease in the polymer Tg.

When glycerol was added to the mixture, a decrease in Tg was detected compared to the control sample at the same moisture contents. The decrease in Tg was proportional to the amount of glycerol added to the starch. This in agreement with the dependence of Tg on molecular weight and the decrease of the average molecular weight of the mixture as the concentration of the polymer decreased when the polyol was added. Also the notion that the free volume is increased by the addition of glycerol can also contribute to the decrease of the temperature of this transition (Slade and Levine 1993).

The behaviour of the reduction in Tg with moisture content for the 5% glycerol-waxy maize starch mixture was similar to the control sample (0% glycerol). A steep decrease in Tg at low moisture content and a levelling off behaviour at moisture contents > 20% (wb) were detected.

Similarly, in the case of the glycerol concentrations greater than 10% a decrease of Tg was more significant at moisture contents < 15% (wb), levelling off for concentrations > 20% (wb).

An interesting finding was that the curvature of the plasticization effect by water became less pronounced as the glycerol content increased. This effect can be clearly seen on figure 5.2 (A), where the shape of the plasticization curve is almost linear for the 15 and 20% (db) glycerol-starch extrudate. This suggests that the plasticizing effect of glycerol is effective just for the lower end of moisture content, pushing the curve to lower Tg values. When water molecules are present at significant levels, they would displace glycerol from the plasticising sites due to it greater ubiquity and affinity with amorphous starch. This mechanism would help to explain the similarity in Tg between the

different glycerol concentration samples for moisture contents greater than 20% (wb).

In the case of rice (figure 5.2 B) and wheat starches (figure 5.2 C), the behaviour of Tg as function of moisture and glycerol was very similar to waxy maize starch This would suggest that although there are some structural differences between starches, this would not have a significant effect on the overall Tg of the mixture. A more detailed comparison between the obtained Tg values for these starches is described on section 5.3.2.

At the high end of moisture levels, little differences are observed for Tg, irrespective of the glycerol levels when they are present in excess of 10%. The lower Tg value detected was ~ 5°C for all the starch-glycerol for the high-end moisture contents. The Tg values at these high level of moisture were difficult to obtaine mainly due to the endotherm generated in these samples from the ice melting during the heating step. This endoderm probably overlapped the changes in heat flow at Tg, making it accurate determination difficult.

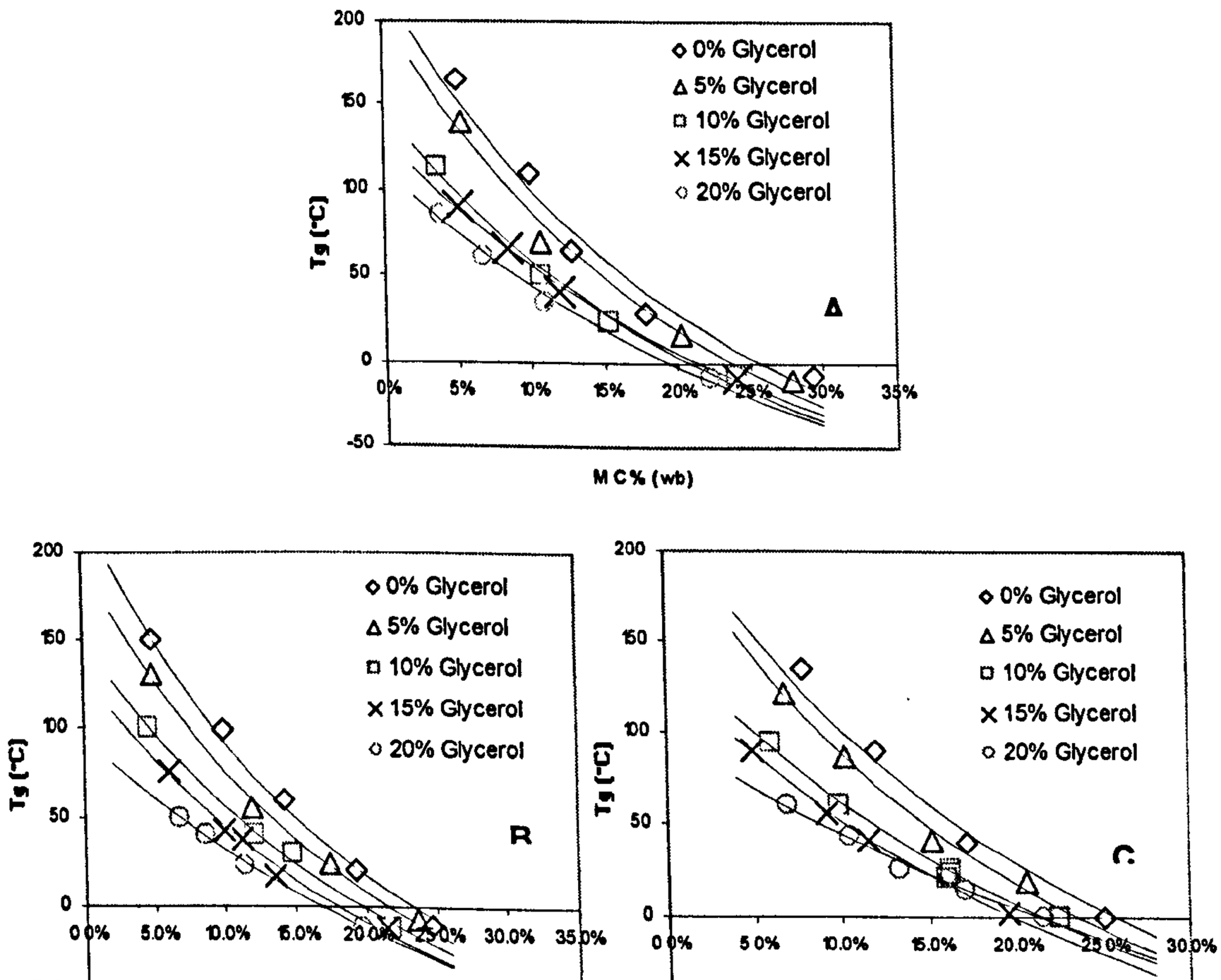

Figure 5.2. Tg values obtained from DSC for Waxy (A), rice (B) and wheat starch (C) extrudate-glycerol Tg vs MC (wb)

A more detailed analysis on the effect of glycerol was done using statistical experimental design (Design Expert version 6, Stat-Ease) using extruded wheat starch as reference. Figure 5.3 shows the effect of glycerol on Tg for dry and wet wheat starch extrudates. The dark line representing the 7% (db) moisture extrudates shows a significant decrease in Tg when glycerol concentration increased to 0 to 20% (db). In the case of the red line representing a moisture of 30% (db), glycerol does not have any additional plasticizing effect. This dependence of the plasticising effect of glycerol on moisture content would suggests the idea of this polyol forming a separate phase in the presence of high concentrations of water.

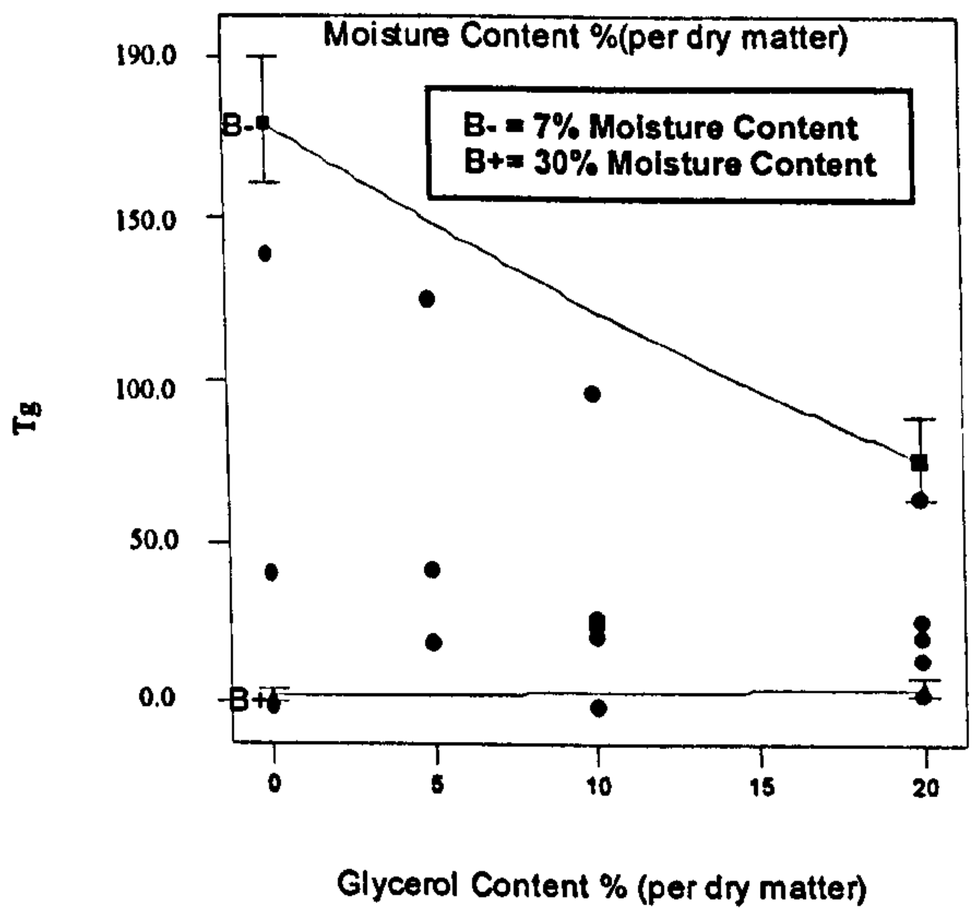

Figure 5.3. Effect of glycerol concentration on Tg of wheat starch-glycerol extrudates with 7% (B-) and 30 (B+) moisture content and a glycerol concentration from 0% to 20%. Green dots are experimental data obtained from DSC.

5.3.2 Tg comparison between Waxy Maize, Rice and Wheat Starches

Although the glass transition of different starches has been reported in the literature (Biliaderis, Page et al. 1986; Levine and Slade 1986; Forssell, Mikkiläa et al. 1997; Lourdin, Coignard et al. 1997; Mousia, Farhat et al. 2000; Bindzus, Livings et al. 2002), a direct comparison between starches from different botanical source using the same analytical method and experimental conditions have been difficult to find.

The present section aims to compare the variations in Tg of extruded waxy maize, rice and wheat starches at similar concentrations of water and glycerol. To do this comparison, the experimental data presented in the previous section (section 5.3.1) were grouped by glycerol concentration.

The next set of figures (5.4 to 5.5) shows the glass transition temperature for the three starch types as a function of water content grouped by glycerol concentration.

The overlapping of the Tg curves did not show a significant difference between the three different starches (standard deviation within 5°C). This behaviour was similar for most of the glycerol concentrations, just the Tg values for rice starch seemed to be lower for the 20% (db) glycerol group.

The Tg's for the different starch types seems to be related to the dependence of this parameter of molecular weight rather than the botanical source (amylose/amylopectin ratio and/or the presence of amylose-lipid complexation).

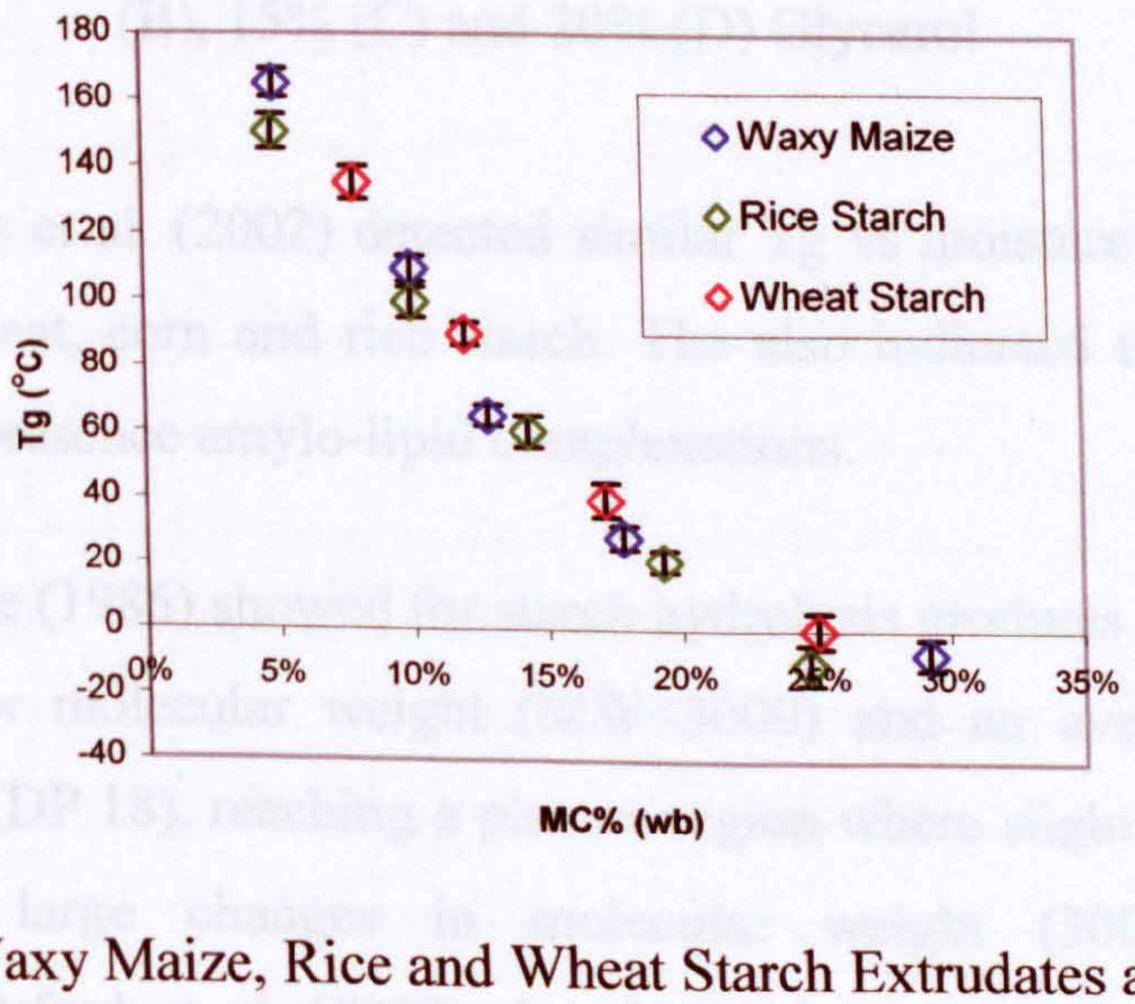

Figure 5.4. Waxy Maize, Rice and Wheat Starch Extrudates and No Glycerol

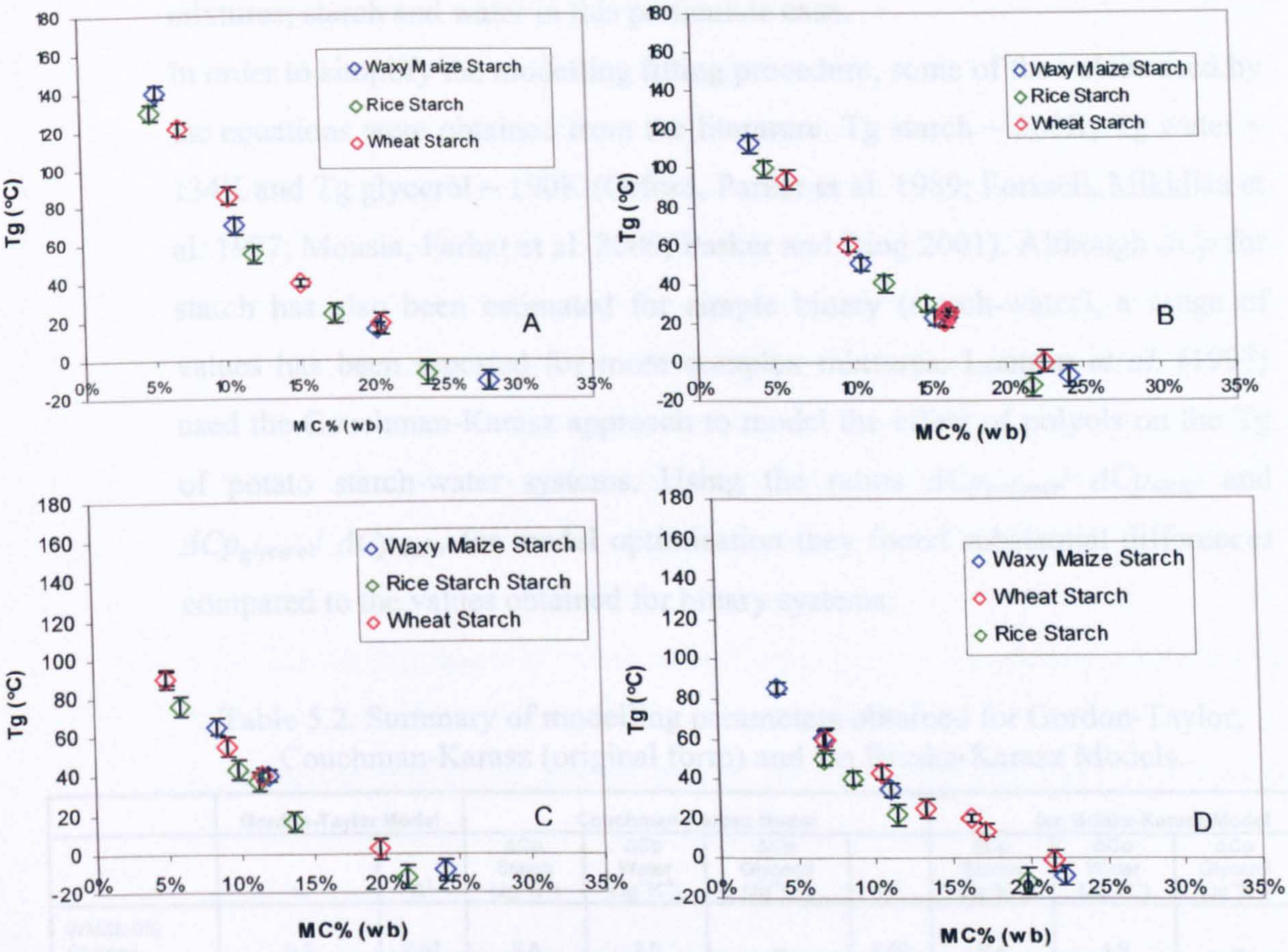

Figure 5.5. Waxy Maize, Rice and Wheat Starch Extrudates and 5% (A), 10% (B), 15% (C) and 20% (D) Glycerol

Bindzus, Livings et al. (2002) detected similar Tg vs moisture content profile for extruded wheat, corn and rice starch. The also indicated that Tg was not affected by the presence amylo-lipid complexations.

Slade and Levine (1986) showed for starch hydrolysis products a rapid increase in Tg from low molecular weight (MW<3000) and an average degree of polymerisation (DP 18), reaching a plateau region where slight increases in Tg are seen for large changes in molecular weight (3000<MW<60000; 18<DP<370). Orford *et al.* (1989) also detected a plateau for the Tg values when DP > 18 for malto-oligomers, amylose and amylopectin.

5.3.3 Modelling Tg from Starch-Glycerol Systems

Table 5.2 shows a summary of the modelling parameters after optimisation for Gordon-Taylor, Couchman-Karasz and ten Brinke-Karasz equations applied on the experimental DSC Tg data. The Gordon-Taylor equation was only applied

to the control samples (no glycerol) as it was originally derived for binary mixtures; starch and water in this particulate case.

In order to simplify the modelling fitting procedure, some of the values used by the equations were obtained from the literature. Tg starch ~ 500K; Tg water ~ 134K and Tg glycerol ~ 190K (Orford, Parker et al. 1989; Forssell, Mikkiläa et al. 1997; Mousia, Farhat et al. 2000; Parker and Ring 2001). Although ΔCp for starch has also been estimated for simple binary (starch-water), a range of values has been reported for more complex mixtures. Lourdin *et al.* (1997) used the Couchman-Karasz approach to model the effect of polyols on the Tg of potato starch-water systems. Using the ratios $\Delta Cp_{polymer}/\ \Delta Cp_{water}$ and $\Delta Cp_{glycerol}/\ \Delta Cp_{water}$ for model optimisation they found substantial differences compared to the values obtained for binary systems.

Table 5.2. Summary of modelling parameters obtained for Gordon-Taylor, Couchman-Karasz (original form) and ten Brinke-Karasz Models.

	Gordon-Taylor Model		Couchman-Karasz Model				ten Brinke-Karasz Model			
	k	R^2	ΔCp Starch ($Jg^{-1}K^{-1}$)	ΔCp Water ($Jg^{-1}K^{-1}$)	ΔCp Glycerol ($Jg^{-1}K^{-1}$)	R^2	ΔCp Starch ($Jg^{-1}K^{-1}$)	ΔCp Water ($Jg^{-1}K^{-1}$)	ΔCp Glycerol ($Jg^{-1}K^{-1}$)	R^2
WMSE 0% Glycerol	0 2	0.97	0 8	2 0	–	0.97	0 4	1.9	–	0 97
WMSE 5% Glycerol	–	–	0 8	2.0	0.9	0.98	0.6	2.5	0.9	0.98
WMSE 10% Glycerol	–	–	0.8	2.0	1.8	0.99	0.5	2.5	1.8	0.99
WMSE 15% Glycerol	–	–	1.0	2 3	2.0	1.00	0.6	2 6	1.8	1.00
WMSE 20% Glycerol	–	–	1.1	2.5	2.1	0.99	0.7	2.9	2.0	0.99
RSE 0% Glycerol	0.2	1.00	0.7	2.0	–	1.00	0.4	1.9	–	1.00
RSE 5% Glycerol	–	–	0 9	2.2	1.2	1.00	0.6	2.6	1.2	1.00
RSE 10% Glycerol	–	–	0.9	2.3	1.8	1.00	0.5	2.7	1.6	1.00
RSE 15% Glycerol	–	–	0.8	2.3	1.5	0.99	0.5	2 9	1.5	0 99
RSE 20% Glycerol	–	–	1.0	2.4	2.2	1 00	0.6	2.8	2 0	1.00
WSE 0% Glycerol	0.2	0.99	0.8	2.0	–	0 99	0.4	1.9	–	0.99
WSE 5% Glycerol	–	–	0 9	2.6	0.7	0.99	0 6	2.9	0.8	0 99
WSE 10% Glycerol	–	–	0 8	2 0	1.8	0.99	0.5	2 4	1.7	0 99
WSE 15% Glycerol	–	–	1.0	2 5	1.9	1 00	0.6	2.8	1.7	1.00
WSE 20% Glycerol	–	–	1.1	2.0	2.5	0 99	0.6	2.6	2.3	0.99

The Tg values for starch, water and glycerol used for the three equations were: Tg starch ~ 500K; Tg water ~ 134K and Tg glycerol ~ 190K (Orford, Parker et al. 1989; Forssell, Mikkiläa et al. 1997; Mousia, Farhat et al. 2000; Parker and Ring 2001).

Before going into the discussion of the results, it has to be considered that the modelling of the experimental data was done on the mean of three measurements on 4 to 5 data points, therefore it is difficult to discuss any statistical significance between the obtained modelled parameters for individual samples, but clear changes are observed for glycerol addition in all three series of starches. ANOVA reported no significant differences ($P>0.05$) between ΔCp values for starch and glycerol obtained from Couchman-Karasz and ten Brinke-Karsz equations for the three starches with similar glycerol contents. The same analysis was performed for each starch type containing different glycerol concentrations. Significant differences were detected ($P<0.05$) in these two values, supporting the hypothesis that glycerol has a plasticizing effect when it is added to extruded starches.

Similarly, in the case of the obtained ΔCp for water, no significant differences were detected ($P>0.05$) between the three starches. In the case of the assessing the effect of glycerol on this parameter, significant differences ($P<0.05$) were detected between the values reported only by the ten Brinke-Karasz model.

ANOVA was not used on the values obtained from the Gordon-Taylor model which showed clearly no differences between waxy maize, rice and wheat starches.

As it was mentioned before, Gordon-Taylor model was applied only to the control samples. Table 5.2 shows the k values obtained after fitting the equation to the experimental data. The obtained values for waxy maize starch were k ~0.2. Similar values have also been reported in the literature Mousia, Farhat et al. (2000) obtained a k values from 0.25 for waxy maize starch. . The same value was obtained for the rice and wheat starches. The squared regression coefficient (R^2) ranged from 0.9 to 1.0, demonstrating a good correlation between the experimental and the theoretical values.

The ΔCp values from the Couchman-Karasz modelling for the control samples was ~ 0.8 $Jg^{-1}K^{-1}$ for waxy maize, rice and wheat starch $Jg^{-1}K^{-1}$. This value seems high compared to the value usually taken as a reference for this material (~0.5 $Jg^{-1}K^{-1}$). In the case of water, the ΔCp value was ~2.0 $Jg^{-1}K^{-1}$ for the three starches, which is in accordance with value 1.94 $Jg^{-1}K^{-1}$ used elsewhere, (Kalichevsky, Jaroszkiewicz et al. 1992)

When glycerol was included in the mixtures, ΔCp for the starch increased slightly from 0.8 $Jg^{-1}K^{-}$ for 5% to 1.1 $Jg^{-1}K^{-1}$ when the polyol content increased to 20% (db). In the case of water, ΔCp increased from 2.0 to 2.5 $Jg^{-1}K^{-1}$ when the glycerol concentration increased. A different behaviour was detected for wheat starch and 20% glycerol, where the ΔCp of water decreased back to 2.0 $Jg^{-1}K^{-1}$. This was attributed by the clear overlapping in the Tg values between the 15% and 20% glycerol extrudates as depicted on figure 4.3.

The ΔCp of glycerol showed it to be more dependent on its concentration, increasing more than 50% for the three starches when glycerol concentration reached 20%.

The increase in ΔCp of the starch demonstrated the model overestimating the plasticizing effect of water and glycerol on the starch Tg. Orford *et al.* (1990) reported a good fit for a maltohexaose-water system using Couchman-Karasz but an over-reduction in Tg for a maltohexaose-glucose-water system. They attributed this modelling inaccuracy to two main considerations. The first one is related to the assumption of invariability of ΔCp with temperature and the second perhaps more importantly, the components are assumed to form a regular mixture both in the rubbery and glassy states. It is known that specific interactions of species can lead to deviations from the idealised behaviour. ten Brinke *et al.* (1983) suggested that any indication of solvent phase separation would give a flatter decrease on Tg for increasing in solvent concentration. For this particulate, case a glycerol rich separated phase would have the potential to attract water from the matrix affecting the overall Tg of the mixture even further.

When the ten Brinke-Karasz model was applied to the Tg values for the control samples, the obtained ΔCp were ~ 0.4 $Jg^{-1}K^{-1}$ for the three starches types and ~1.9 $Jg^{-1}K^{-1}$ for water ($R^2 = 0.97$). These values are comparable to those used in the literature for the prediction of Tg for starch based systems (Orford, Parker et al. 1989; Kalichevsky 1992; Kalichevsky, Jaroszkiewicz et al. 1993).

When glycerol was included in the mixture, the ΔCp for the three starches increased from ~ 0.4 $Jg^{-1}K^{-1}$ to ~ 0.6 $Jg^{-1}K^{-1}$. The ΔCp of water for waxy and rice starches increased from ~ 1.9 $Jg^{-1}K^{-1}$ to ~ 2.8 $Jg^{-1}K^{-1}$ when glycerol increase to 20% but it the case of wheat starch the ΔCp of water decreased

slightly to 2.6 $Jg^{-1}K^{-1}$ for 20% glycerol. This numerical decrease can also be related to the overlapping in the Tg values for this mixture (figure 4.3).
Similarly to the Couchman-Karasz modelling, the changes in ΔCp of glycerol also increased near 50% from ~ 1.0 $Jg^{-1}K^{-1}$ to ~ 2.0 $Jg^{-1}K^{-1}$ when the concentration of this polyol reached to 20%.

5.3.4 Tg Comparison from DSC and DMTA

Studies of the glass transition temperature (Tg) have largely concentrated on the use of differential scanning calorimetry (DSC). This technique, which detects the heat flow changes associated with both first-order (melting) and second-order (glass transition) transitions of polymeric materials, has provided valuable insights into the order-disorder phenomena of granular starches (Donovan 1979; Biliaderis, Page et al. 1986; Zeleznak and Hoseney 1987; Slade and Levine 1988; Orford, Parker et al. 1989; Orford et al. 1990; Kalichevsky 1992).
Dynamic mechanical thermal analysis (DMTA) is used to characterise the molecular motions and relaxation behaviour of viscoelastic materials and it is particularly suited to study the molecular motions that give rise to the glass transition (Kalichevsky, Blanshard et al. 1993). One of the advantages of this analytical technique over DSC is its higher sensitivity to detect small molecular relaxations such as secondary and tertiary transitions which usually occur at lower temperatures than the main transition or Tg.
Another important feature of this technique is related to information given by its extension or bending mode, from which the dynamic Young's modulus (E*) can be obtained. This parameter can be related to the perceived hardness of materials in terms of the measured stiffness of the material
In order to make meaningful comparisons of glass transitions temperatures measured by DSC and DMTA it is important to understand that the techniques measure different parameters associated with Tg. In the case of DSC the measurement heating rate and sample history should be reported. For DMTA, as well as heating rate and sample history, the frequency and the parameters tan δ, E' and E'' associated to transition temperature should also be stated.
Kalichevsky *et al.* (1993) suggested that to sensibly compare the transition temperature given by these two analytical techniques, measurements at

different heating rates on the DSC would allow a linear extrapolation to zero heating rate.

In the case of DMTA, the shift in tan δ with frequency can be modelled using the Arrhenius rate equation. The zero heating rate Tg from DSC may be used in this equation to calculate the effective measurement to obtained a loss modulus (E'') peak at the same temperature. They stated that for synthetic polymers, DSC zero heating rate Tg normally corresponds to a tan δ peak at a dynamic frequency of approximately 0.001 Hz.

Kalichesvky *et al.* (1992) used an empirical approach comparing directly Tg values for amylopectin from DSC (heating rate 10°C/min) and DMTA (heating rate 2°C/min and bending frequency at 1 Hz). They found that the DMTA measurements parameter that gave the closest values to the DSC data was not tan δ or the onset of the decrease in the elastic modulus (E') but the an intermediate value which was closely related to the second peak of the loss modulus or E''.

Figures 5.6, shows a Tg comparison between the values obtained from DSC and tan δ, E' and E'' from DMTA. The data points shown represent the Tg values obtained for wheat starch as function of different glycerol and water levels.

The accuracy of DMTA Tg values (E', tan δ and E'') as a function of the DSC data was evaluated by a linear regression (Design Expert version 6, Stat-Easy).

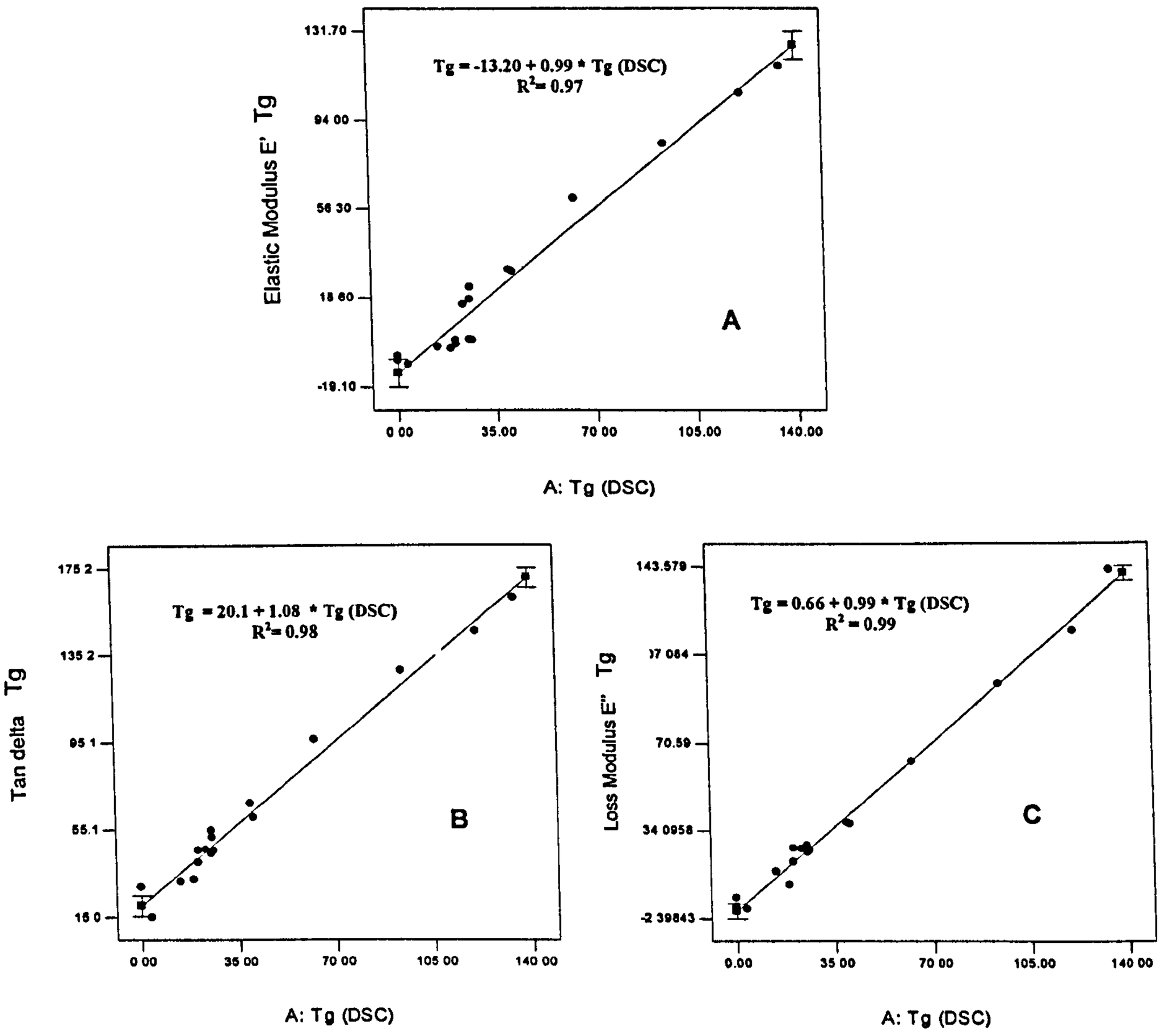

Figure 5.6. Comparison between the Tg for wheat starch-glycerol extrudates reported from DMTA (y axis) and DSC (x axis). DMTA E' vs DSC (A); DMTA tan δ vs DSC (B); DMTA E'' vs DSC (C). Lines in each graph represent the linear regression. DMTA heating rate: 3°C/minute; DMTA frequency 10Hz. DSC heating rate: 10°C/minute.

Figure 5.6 (A), shows the linear equation for the regression between the Tg obtained from the elastic modulus E' and DSC. In this case, the regression model gave a Tg value of -13.2 °C when the obtained the DSC Tg was 0°C. In the case of Tg given from the peak of tan δ, the regression model gave a difference of 20.1 °C when the obtained DSC Tg was 0°C.

Similar to Kalichevsky's (1992) findings, the Tg values calculated from the loss modulus (E'') showed to be the most comparable to the Tg measured by DSC with a difference of just 0.7°C at the origin.

Although there are some theoretical limitations in the direct comparison between theses two analytical techniques, in practical terms it can prove to be useful in predicting mechanical properties from a simple calorimetric measurement under defined experimental conditions.

5.4 Conclusions

It was showed that the Tg of the starch extrudates was reduced by the presence of water and glycerol.

The water plasticisation of the pure starches was successful modelled by Gordon-Taylor and ten-Brinke equations. In the case of the Couchman-Karasz model, an overestimation of the reduction in Tg was detected at high water fractions, represented by an increase in the ΔCp given for starch.

In the case of tertiary mixtures (starch-water-glycerol), Couchman-Karasz and ten-Brinke equations overestimated the plasticising effect of this polyol. Nevertheless the latter model gave more comparable ΔCp values to those in the literature. The difference in the two models may be related to ten-Brinke model accounting for different ΔCp in glassy and rubbery states and possible interactions between the polyol and the starchy matrix.

The significant increase in ΔCp of starch, water and glycerol in the presence of high concentrations of glycerol was attributed inconsistency of the predictive models due to the occurrence of glycerol rich zones in the samples. This would agree with one of the hypothesis presented at the beginning of the chapter.

As suggested by the second hypothesis stated, there was not a significant difference in the glass transition temperature between extruded waxy maize, rice and wheat starch at the same moisture content. This was also true when glycerol was included in the mixture. This may be explained by the well-known Tg dependence on molecular weight, which would remain relatively constant before a certain degree of polymerisation is reached. Amylose and

amylopectin are well above this limit, supporting the possible Tg independence from compositional factors such as amylose/amylopectin ratio.

Finally, a good correlation was obtained between the glass transition temperature given by DSC and DMTA. From the elastic modulus E', loss modulus E'' and tan δ from DMTA, the second peak of the E'' gave the most comparable values to calorimetry, with a difference of just 0.7 °C when the Tg at 0°C reported from DSC was taken as a reference.

Although the experimental conditions should be clearly stated, this type of correlation would allow some degree of prediction of the modulus profile of starch based materials based on their calorimetric Tg values.

6 Mechanical Properties of Starch Glycerol Systems

The mechanical property of foods materials is one of the most important variables considered to assess the quality of manufactured foods. It is known that it is a dynamic phenomenon changing along the supply chain (e.g. processing, distribution and storage) having a direct impact at the point of consumption.

Small changes in temperature or water content (or other plasticizers) can have a significant affect on the physical state due to phase transitions (Roos 1995). Examples include the plasticization of breakfast cereals or instant coffee agglomerates when exposed to a moist atmosphere and the hardening of these materials upon drying (Peleg 1994 a).

The experimental work presented here aims to evaluate the effect of moisture and glycerol on a particular mechanical property, called stiffness, of three extruded starches (waxy maize, rice and wheat starch). The discussion also focuses on the application of empirical models and statistical design to predict the effcet of glycerol and/or water on the mechanical properties of these materials.

6.1 Hypotheses

The main hypothesis tested by the experimental work presented in this chapter has been divided into the following:

- Starches from different botanical sources have significant differences in their mechanical properties (stiffness) and this difference would depend on amylose concentration.
- Glycerol has a significant effect on the mechanical properties of starch and the extent of this effect would be independent of its botanical source.
- The main parameter affecting the mechanical transition from a glassy-stiff to a ductile-rubbery like material is the glass transition temperature or Tg.

The following section briefly discusses and clarifies some of the concepts associated with the mechanical analysis of polymers, the effect of plasticisers on mechanical properties (e.g. modulus) and the application of predictive models.

6.2 Theoretical Background

Polymers are materials that consist of long chain molecules whose atoms are held together by primary covalent bonds. The molecules may be linear, branched or of network formation (figure 6.1).

Generally, the method to classify polymer is related to their physical (molecular interconnection) rather than chemical structure. Thus they can be classified as:

1. Thermoplastics polymers, which are linear or branched with no physical linking between molecules and are held together by relative weak secondary forces (e.g. Van de Waal). They can melt on heating and solidify upon cooling.
2. Rubbers, which have light cross-linking and are capable of large elastic deformations.
3. Thermosets, which are heavily cross-linked conferring a rigid structure being degradable on heating.

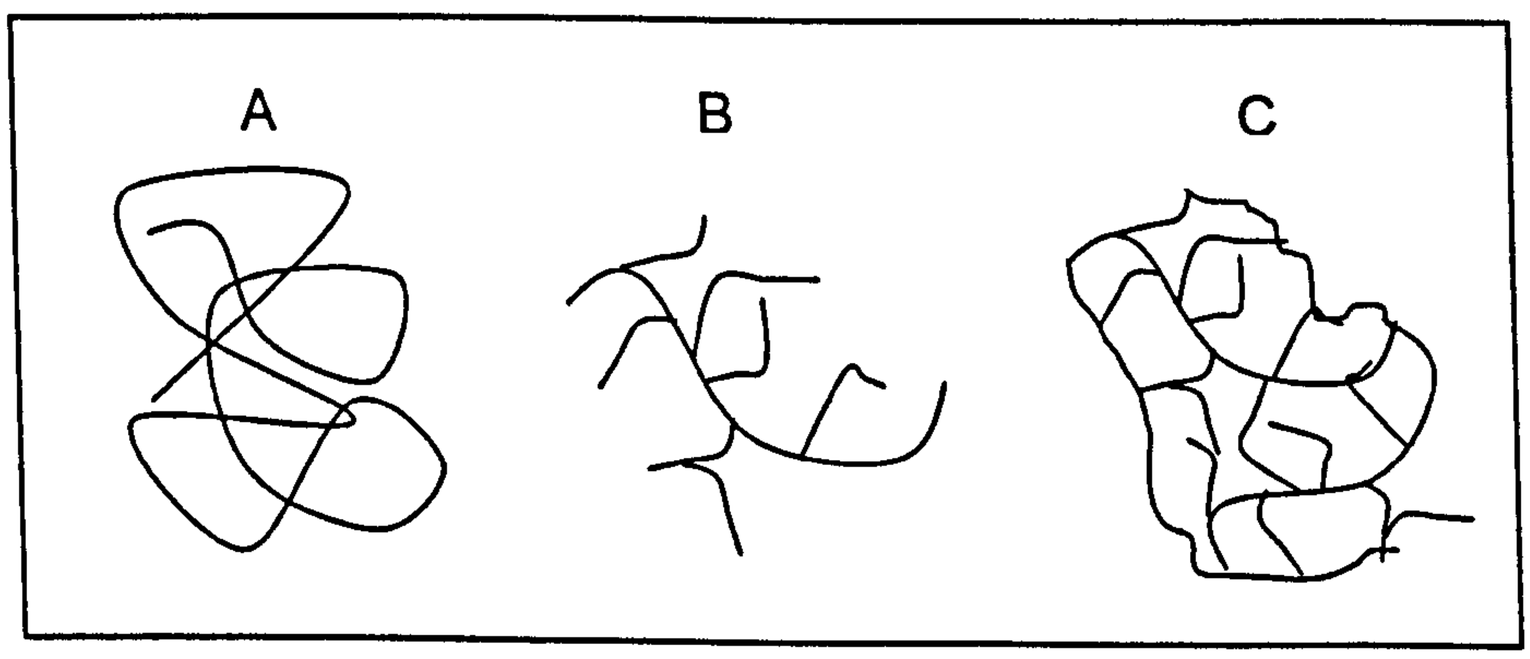

Figure 6.1. Different types of polymer molecule: (A) linear; (B) branched; (C) network.

As it has been mentioned in the introduction of this chapter, the mechanical properties of plastic materials are often the most important properties because the majority of end–user applications involve some degree of mechanical work on these materials. A common situation occurs when design engineers select the use of materials based on properties such as modulus, tensile strength and elongation measured at standard condition in the laboratory and do not consider the effect of environmental conditions, such as relative humidity and temperature. A thorough understanding of the mechanical properties, test employed to determine such properties and the effect of adverse conditions on mechanical properties over a long period is extremely important (Shah 1998).

Stiffness of materials is represented by the measurement of the modulus of elasticity, which relates the effect of a certain strain on the applied stress.

6.2.1 Modulus of Elasticity

One the properties commonly used to assess the stiffness of materials is the modulus of elasticity. This parameter is derived from the stress (force applied to produce a deformation in a unit area) versus strain (change in length per unit of the original length) curve (figure 6.2).

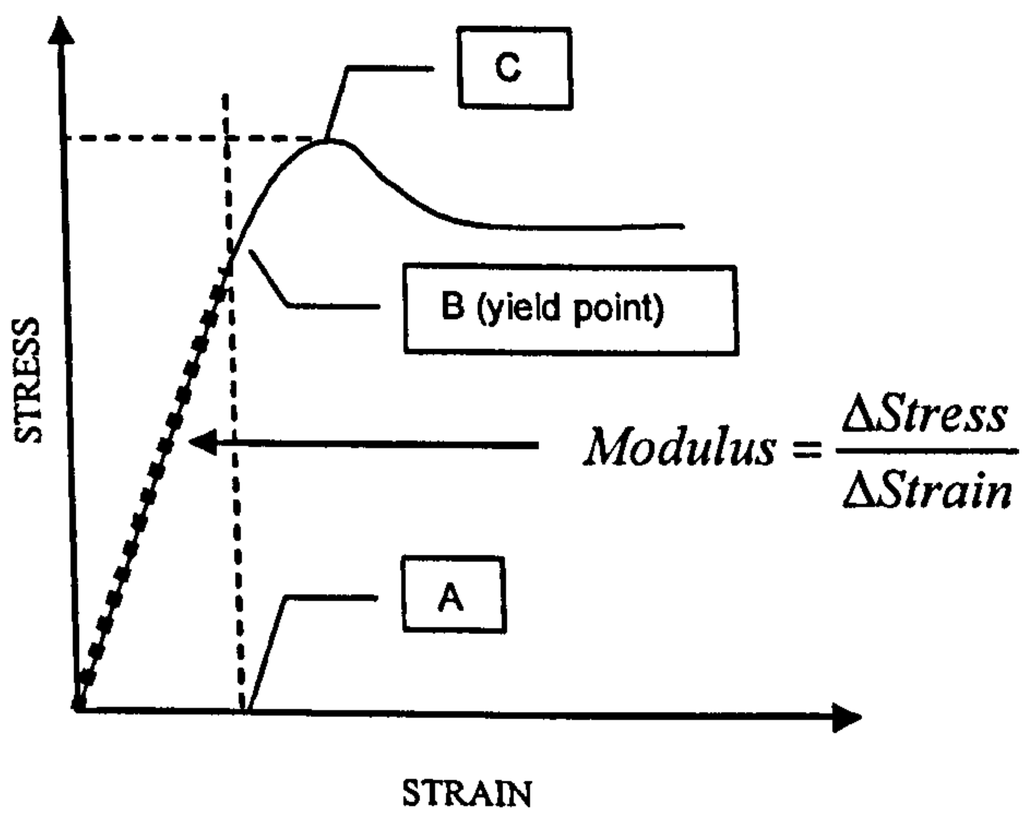

Figure 6.2. Typical stress-strain curve (modified from Dobraszczyk and Vincent 1999).

The initial portion of the stress-strain curve between points A and B is linear and it follows Hooke's law, which states that for an elastic material the stress is proportional to the strain. The slope of the linear portion of the curve, where the material behaves as perfect elastic, represents the material modulus or stiffness. The extension that occurs beyond point *C* is not recoverable, which would have corresponded to a material with a plastic behaviour. In this case, the molecules are displaced with respect to each other and can not slip back to their original position and therefore a permanent deformation or set occurs (Shah 1998).

Based on the ISO 178: 1993 standard (*Plastics-Determination of Flexural Properties*), the modulus of elasticity in flexure or flexural modulus is defined as the ratio between the stress difference (δ_2 - δ_1) and the correspondent strain difference ($\varepsilon_2 - \varepsilon_1$) from the portion of the stress-strain curve which follows Hooke's law.

The modulus can take the following forms (Rutherford and Brown 1980).

1. initial modulus, the slope of the stress-strain curve at zero strain,
2. tangent modulus, the slope of the stress-strain curve at an arbitrary strain and
3. secant modulus, the slope of a straight line drawn from the origin to a specific strain level of the stress-strain curve.

In the particulate case of the work presented here, the modulus was calculated using approach 2 (more details of the calculation of the modulus from flexural test can be found in chapter 3, section 3.3.2.

The various effects of phase transitions (e.g. melting, Tg) times on mechanical properties suggest that changes in the modulus can occur over a broad range of such transitions temperatures. The modulus is also highly dependant of the experimental time scale (e.g. frequency), composition (e.g. presence of plasticizers) and environmental conditions (e.g. temperature).

In the case of food polymers (e. g. starch, gelatine), water has a significant plasticizing effect, affecting the overall mechanical performance of these materials. This effect has been extensively studied, particularly in the case of cereal starches (Lloyd and Kirst 1963; Healey, Rubistein et al. 1974; Attenburrow, Goodband et al. 1989; Kirby, Clark et al. 1993; Peleg 1993; Peleg 1994 a; Harris and Peleg 1996; Laohakunjit and Noomhorm 2004).

6.2.2 Effect of Moisture Content on the Modulus

Changes in the mechanical properties as function of water content can be described with the modulus curves, which reflect the change in viscoelastic properties. Foods with a glassy structure have a high modulus and viscosity giving a high stiffness. A dramatic decrease in the modulus occurs when plasticizing effect is sufficient to cause the transformation to a supercooled liquid or rubbery state (Roos 1995).

A schematic representation of the effect of water activity-moisture content on the modulus of a polymer is given in figure 6.3. Water plasticization decreases the modulus as the glass transition is depressed to below ambient temperature.

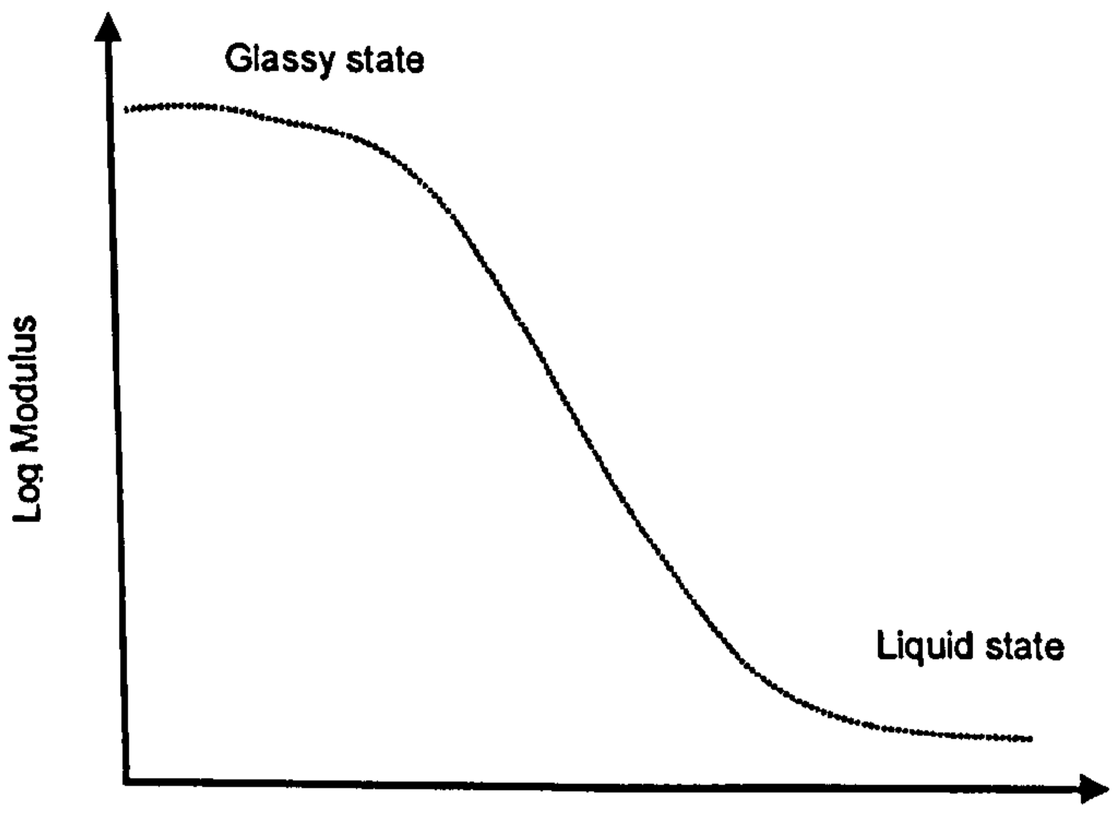

Figure 6.3. Schematic representation of the effect of water plasticization on the modulus of amorphous biopolymers and food materials (modified from Roos 1995).

Experimental data on cereal starches (Peleg 1994a) have shown that at low moisture contents the polymer behaves as hard and brittle material; characteristics of a glassy state. Increasing concentration of plasticizers (e.g. water) would have a reducing effect on the modulus after which a plateau is reached, characteristic of a rubbery state. Kalichecsky *et at.* (1992, 1993) showed that the decrease in the modulus of extruded starches was related to a decrease in the glass transition temperature (Tg) from the plasticizing effect of water.

6.2.2.1 Modelling of the Effect of Moisture Content on the Modulus of Elasticity

It is well known that the dependency of the rheological properties of polymers at temperatures above Tg can be accurately described by the William-Landen-Ferry (WLF) model (William, Lande et al. 1955).

$$\log a_T = -C_1(T - T_s)/(C_2 + T - T_s) \qquad \textit{Equation 6.1}$$

where a_T is the shift factor expressed as the ratio between the viscosity of the polymer at a given temperature T and its viscosity at a reference temperature T_s, and C_1 and C_2 are constants (William, Lande et al. 1955).

The shift factor a_T from WLF model can be used to represent other mechanical properties such as physical changes in food materials (Roos and Karel 1990; Slade and Levine 1993) .

An Arrhenius model has also been used, although to a lesser extent, to predict the effect of temperature on these properties well above the polymer melting temperature (Tm) (Peleg 1994 a). It has also been successful used predict changes in the viscoelastic properties of polymeric materials at temperatures below Tg.

It is between Tm and Tg where the WLF model has proved to accurately model the very high viscosity dependency on temperature.

Although it has been proved that both models can be used in food systems, the temperature range at which they are applied has to be

carefully considered (Slade and Levine 1991a).

Peleg (1994) stated that in both polymers and biomaterials, the transition from a glassy to a low viscosity and rubbery material has a change of concavity (sigmoidal shape). Because the WLF and Arrhenius models imply a modulus transition that have only an upward concavity, it has been suggested that a consistent description of the mechanical behaviour of biomaterials at and around Tg requires an alternative model (Peleg 1993).

Peleg (1994 a and b) proposed a mathematical expression, based on Fermi's distribution model, to describe the sigmoidal relationship between a pertinent mechanical parameter (e.g. stickiness, caking, modulus) and temperature (at constant moisture content or water activity) or that between the mechanical parameter and moisture content or water activity (at a constant temperature) by the form of;

$$Y(T) = \frac{Y_S}{\left\{1 + \exp\left[\frac{T - T_C}{a'}\right]\right\}} \qquad \textit{Equation 6.2}$$

$$Y(M) = \frac{Y_S}{\left\{1 + \exp\left[\frac{M - M_C}{a'}\right]\right\}} \qquad \textit{Equation 6.3}$$

$$Y(Aw) = \frac{Y_S}{\left\{1 + \exp\left[\frac{Aw - Aw_C}{a'}\right]\right\}} \qquad \textit{Equation 6.4}$$

Where *Y(T)*, *Y(M)* and *Y(Aw)* are the magnitudes of any mechanical integrity parameter a the corresponding temperature *T*, moisture content *M* and water activity *Aw* respectively. Y_s is the magnitude of this mechanical parameter in the glassy state, and *Tc*, M_c and Aw_c are characteristic temperature, moisture content and water activity at which the curve inflection point occurs. The *a*'s in the three equations are empirical constants with units of those of the independent variables. The magnitude of this parameter describes the steepness of the region depicting the decrease in modulus. Thus, when the *a*'s → 0, the shape of the curve approaches that of a step function, and when they have a relatively large value the relationship becomes flatter.

Although Peleg (1994 a) proved the validity of the proposed models on a range of published experimental data (different materials and testing methods), he stressed the empirical nature of these equations. They cannot be used as predictive models and it is also doubtful that the magnitude of their constants can be derived directly from the composition or fundamental physical properties of the materials.

Despite the above, this model can prove to be useful when comparing materials with different compositions (e.g. plasticizer concentrations) under the same experimental conditions.

The next section in this dissertation, presents a discussion on the effect of glycerol on the flexural modulus of waxy maize, rice and wheat starches prepared by hot extrusion and equilibrated at different moisture contents.

6.3 Results and Discussion

This section is divided into four parts. The first one concentrates on the effect of plasticizers, water and glycerol, on the flexural modulus of amorphous extruded starches. The second and third parts focus on a direct and an indirect (using an empirical model) comparison of this mechanical parameter between these starches grouped by plasticizer concentration.

Finally, the effect of the glass transition temperature (Tg) on the flexural modulus is presented and analyzed using statistical experimental design.

6.3.1 Effect of moisture and glycerol contents on the flexural modulus starch extrudates

The sample preparation method and analytical technique used to evaluate the flexural modulus of the different starch-water-glycerol mixtures has been specified in chapter 3, section 3.3.2.

Figure 6.4 depicts the relationship between the flexural modulus and moisture content for waxy maize (A), rice (B) and wheat(C) starches-glycerol extrudates.

The control samples (0%glycerol) showed an abrupt reduction in the modulus when the moisture content reached around ~ 12% (wb).

Kalichevsky, Jaroszkiewicz et al. (1992), detected a decrease in the elastic modulus (E') of waxy maize starch at a moisture content ~ 15% (db). Nicholls, Appelqvist et al. (1995) also measured a reduction in the bending modulus and maximum stress of waxy maize at ~ 12% moisture. Stading, Rindlav-Westling et al. (2001), using DMTA, measured a change in the elastic modulus (E') at similar range of moisture content for amylose and amylopectin (~12% (db)). Attenborough et al. (1993) using wheat starch wafers as a model system followed an analogy from the effect of plasticizers on synthetic polymers. They attributed this decrease in the modulus mainly to two mechanisms; (a) the plasticizer molecules screen off the attractive forces between the polymer chains and/or (b) the plasticizer molecules enlarge the spaces between polymer chains allowing chain segments greater freedom of movement. This is manifested by a

decrease in Tg. Similar interpretations have been suggested for other biopolymers (Slade and Levine 1993; Peleg 1994 a).

The presence of glycerol clearly influenced the magnitude of the modulus over the whole range of moisture contents for rice and wheat starches. The modulus for the 0% glycerol of both starches reached a maximum of ~ 500 N/cm^2 for moisture content < 10%wb. When glycerol was added to the mixture the modulus decreased to near ~ 300 N/cm^2 for the 20% glycerol mixture. The reduction of the modulus at low moisture content, although in the glassy state, can be explained by a change in the solid/plasticizer (starch/glycerol) ratio.

In the case of waxy maize starch, no differences in the flexural modulus were detected at low moisture contents between the control, 5% and 10% glycerol samples. Only 20% glycerol showed a significant reduction in the modulus at moisture contents < 5%.

A detailed analysis of the obtained data for waxy maize starch shows that the magnitude of the modulus for the control and 5% glycerol was significantly smaller than the values obtained for rice and wheat starches. Indeed, the mechanical measurements of pure waxy maize were extremely difficult due to the brittleness of the material making the analysis difficult. Similar difficulties were observed for waxy maize starch and 5% glycerol. van Soest *et al.* (1996), commented experimental difficulties in measuring the elastic modulus of waxy maize extrudates as the material became too brittle at moisture contents < 8% .

It is possible that the branched nature of amylopectin does not actually comply at the same time scale as applied stress rate compared to the amylose containing starches (rice and wheat). Although in the glassy state, amylose would have less structural constraints due to its more linear structure absorbing some of the energy being transferred from the mechanical bending.

Figure 6.4 also show that in the presence of glycerol the abrupt reduction in stiffness shifted to lower moisture content. The extent of the reduction and the steepness of this transition seem to be correlated with the glycerol concentration in the sample.

Acting in a similar manner to water, glycerol acts as a plasticizer contributing to the reduction of the glass transition temperature affecting the overall stiffness of the starch structure (Attenburrow and Davis 1993; Kirby, Clark et al. 1993; Forssell, Mikkila et al. 1996; Lourdin, Bizot et al. 1997; Lourdin, Bizot et al. 1997; Myllärinen, Partanen et al. 2002; Graaf, Karman et al. 2003; Laohakunjit and Noomhorm 2004)

A more detailed discussion is presented in section 5.3.3.

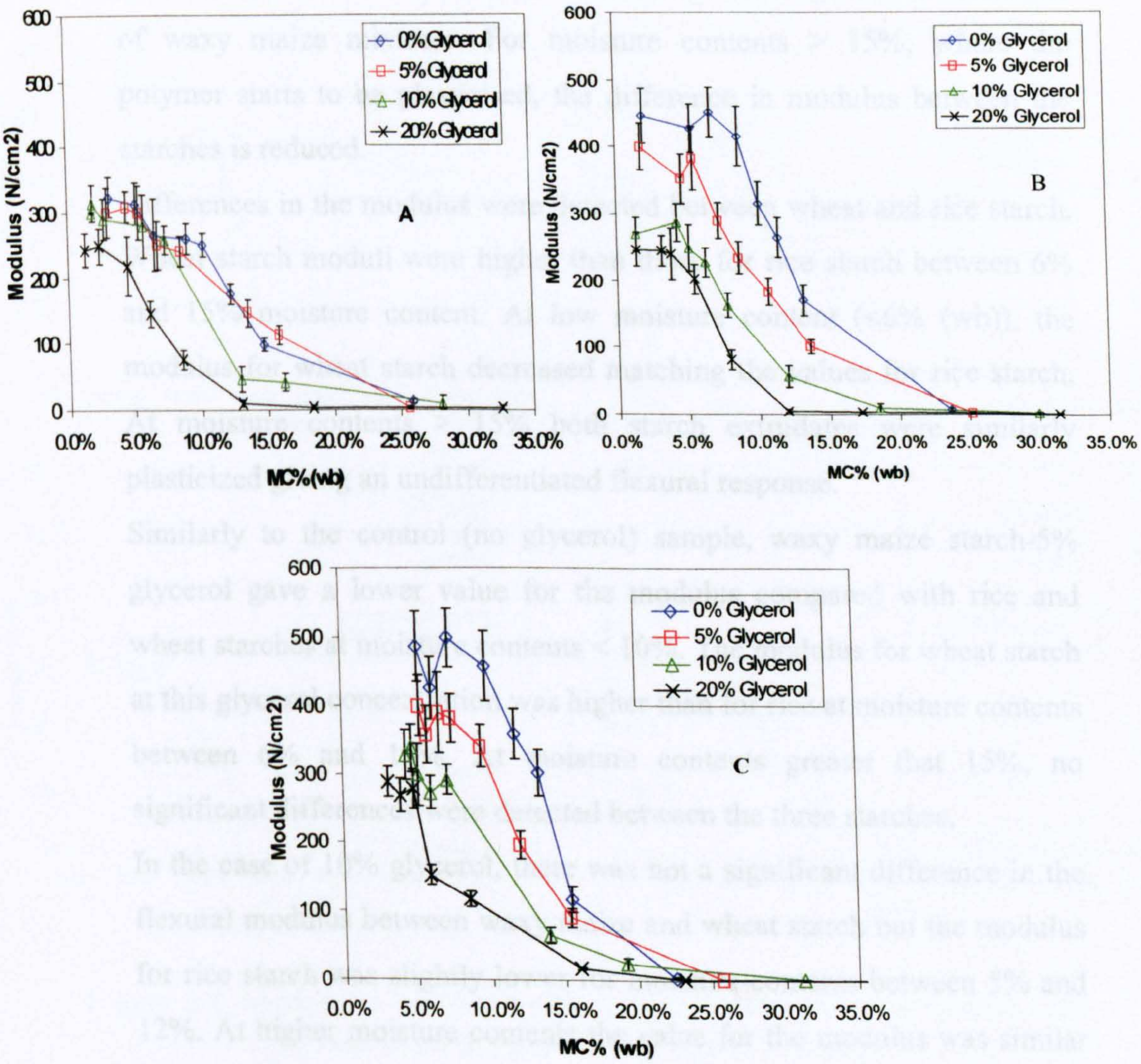

Figure 6.4. Modulus v/s Moisture Content (wb) for waxy maize starch-glycerol (A), rice starch-glycerol (B) and wheat starch-glycerol (C) extrudates at ambient temperature (25°C). Error bars represents ± 1 standard deviation of 5 measurements.

6.3.2 Effect of starch variety on extruded starch-glycerol mixtures

Although experimental data on the effect of plasticizers on mechanical properties on different starches is available in the literature, a direct comparison using the same sample preparation protocol and analytical technique has not been found.

Figure 6.5 displays a comparison of the effect of moisture content on the flexural modulus of elasticity grouped by glycerol content.

When looking at the values obtained from 0% glycerol extrudates, a marked difference in the modulus is observed for waxy maize relatively to rice and wheat starches at moisture contents < 15% (wb). As already mentioned, the low values for the modulus are attributed to the brittleness of waxy maize mixtures. For moisture contents > 15%, where the polymer starts to be plasticised, the difference in modulus between the starches is reduced.

Differences in the modulus were detected between wheat and rice starch. Wheat starch moduli were higher than those for rice starch between 6% and 15% moisture content. At low moisture content (<6% (wb)), the modulus for wheat starch decreased matching the values for rice starch. At moisture contents > 15% both starch extrudates were similarly plasticized giving an undifferentiated flexural response.

Similarly to the control (no glycerol) sample, waxy maize starch-5% glycerol gave a lower value for the modulus compared with rice and wheat starches at moisture contents < 10%. The modulus for wheat starch at this glycerol concentration was higher than for rice at moisture contents between 6% and 15%. At moisture contents greater that 15%, no significant differences were detected between the three starches.

In the case of 10% glycerol, there was not a significant difference in the flexural modulus between waxy maize and wheat starch but the modulus for rice starch was slightly lower for moisture contents between 5% and 12%. At higher moisture contents the value for the modulus was similar for the three starches.

It is possible that the formation of amylose-lipid complexes present in the rice starch extrudates (X-ray diffraction patterns shown in chapter 3,

section 3.3.5.2) contributed to reduce the availability of amylose for plasticization at low moisture contents, driving the plasticizing molecules (water and glycerol) to the branched amylopectin reducing the overall modulus of these samples.

Finally for the starch extrudates containing 20% glycerol, no marked differences in the flexural modulus were observed between the studied starches at the lower end of moisture contents (< 7%).

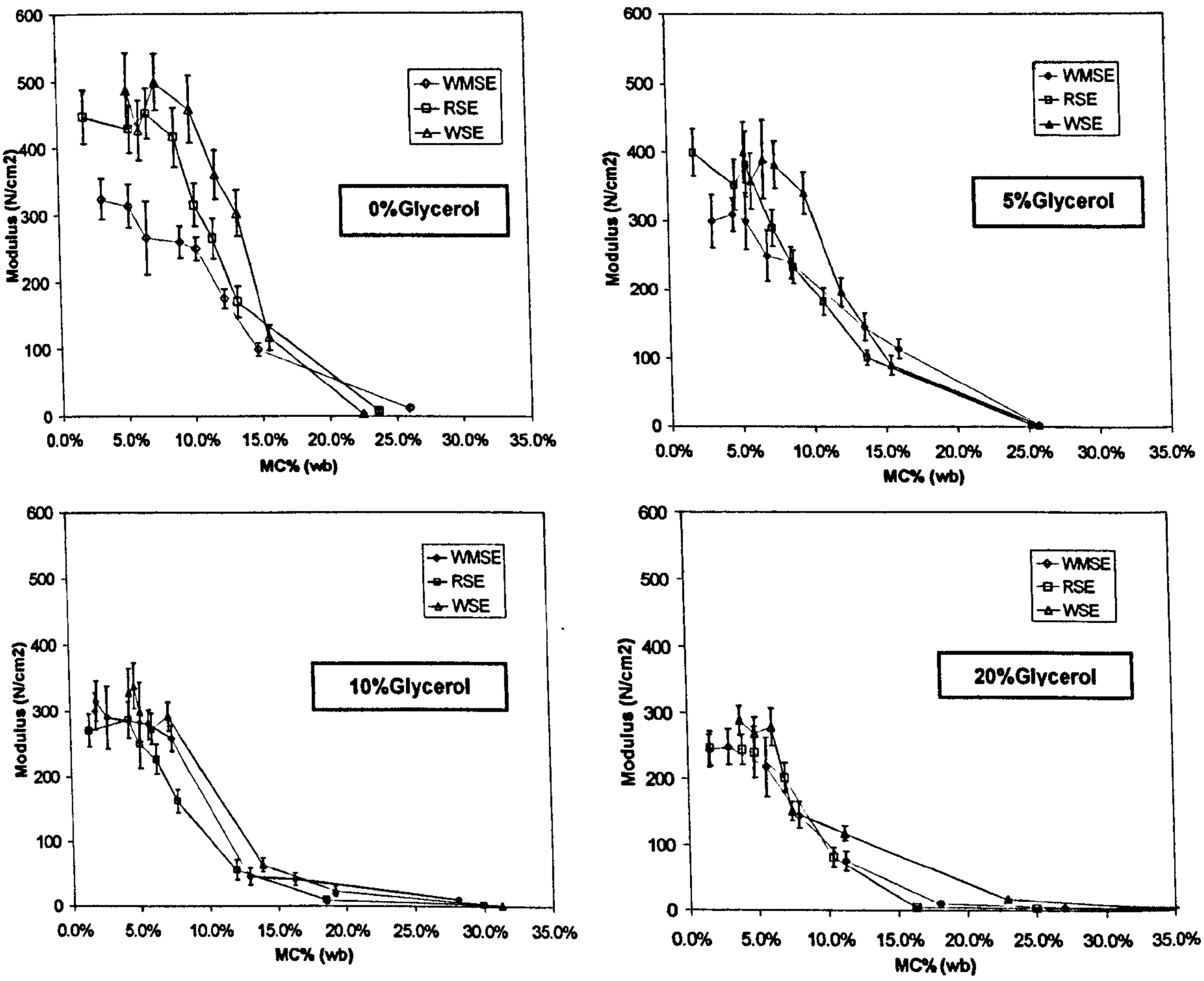

Figure 6.5. Modulus v/s Moisture Content for extruded waxy maize, rice and wheat starch grouped by glycerol content.

The next section focuses on the application of an empirical model on the obtained experimental data, adding to the comparative analysis of the

effect of different starches and glycerol concentrations on the flexural modulus of these mixtures.

6.3.3 Modelling the Effect of Moisture on The Flexural Modulus

One of the difficulties in using the three point bending test technique to evaluate the mechanical properties of materials is the significant standard error associate with this method. Although using a high number of replicates would minimise this deviation, objective comparison between sets of data becomes extremely difficult.

In order to numerically compare the effect of moisture and glycerol on the modulus between three starches, a derivation of Fermi's model as used by Peleg (1993, 1994 a, 1994 b) was applied to the experimental data.

The obtained modulus versus moisture content profiles for each of the starches and glycerol concentrations where modelled using equation 6.5. The modelling optimisation was done using software Solver add-in in Excel (Office 2003, Microsoft Corp.)

$$Y(M) = \frac{Y_S}{\left\{1 + \exp\left[\frac{M - M_C}{a'}\right]\right\}} \qquad \textit{Equation 6.5}$$

Where $Y(M)$ is the magnitude of any mechanical parameter at the corresponding moisture content M. Y_s is the magnitude of this mechanical parameter in the glassy state and M_c is the characteristic moisture content at which the curve inflection point occurs. a' is an empirical constant describing the steepness of the region depicting the decrease in modulus.

Before modelling, the value for the variable Y_s was calculated from the mean of the first three values (from the lower moisture content) on the high modulus plateau. M_c and a' where obtained from the modelling iteration.

Table 6.1 shows the values for the modelling parameters and regression coefficients after optimisation for each of starch-glycerol extrudates.

Table 6.1. Modelling paremeters Y_s, M_c *and* a' after optimisation

	Y_s (N/cm^2)	M_c	a'	R^2
WMSE0%Glycerol	301	13.2%	2.1%	0.98
WMSE5%Glycerol	303	13.7%	3.3%	0.98
WMSE10%Glycerol	302	10.3%	1.8%	0.99
WMSE20%Glycerol	237	7.3%	1.4%	0.99
RSE0%Glycerol	442	12.3%	1.7%	0.99
RSE5%Glycerol	378	10.1%	1.9%	0.98
RSE10%Glycerol	269	9.1%	1.7%	0.98
RSE20%Glycerol	244	7.2%	1.0%	1.00
WSE0%Glycerol	471	14.0%	1.5%	0.98
WSE5%Glycerol	383	12.6%	1.8%	0.98
WSE10%Glycerol	322	11.2%	2.0%	0.99
WSE20%Glycerol	278	7.6%	1.4%	0.95

Table 6.1 shows R^2 coefficients after modelling for all the samples were near ~ 1.0 demonstrating a good fit for the different mixtures.

In order to optimise the analysis of the data after the modelling, the data displayed on table 6.1 have been reorganised and plotted against glycerol concentration and grouped by starch type (figure 5.6).

Figure 6.6 shows the variations of the parameter Y_s (modulus in the glassy state) with glycerol concentration for each of the three starches. Although all the samples were in the glassy state (based on the Tg values shown in chaper 4), there is a decrease in the flexural modulus when glycerol concentration increases. As mentioned before, this decrease can be related to an increase in the starch/polyol ratio, in other words, the proportion of solid material in the mixture is reduced, affecting the flexural stress required for a predefined deformation or strain.

A very similar mechanical behaviour was observed for wheat and rice starches. In the case of waxy maize starch, lower values of modulus were obtained for the control and 5% glycerol. This difference is explained by the highly brittle nature of the extrudates at this polyol concetrations. A different bahaviour was detected for this starch type at 10% and 20% glycerol, which followed a similar trend as rice and wheat starches.

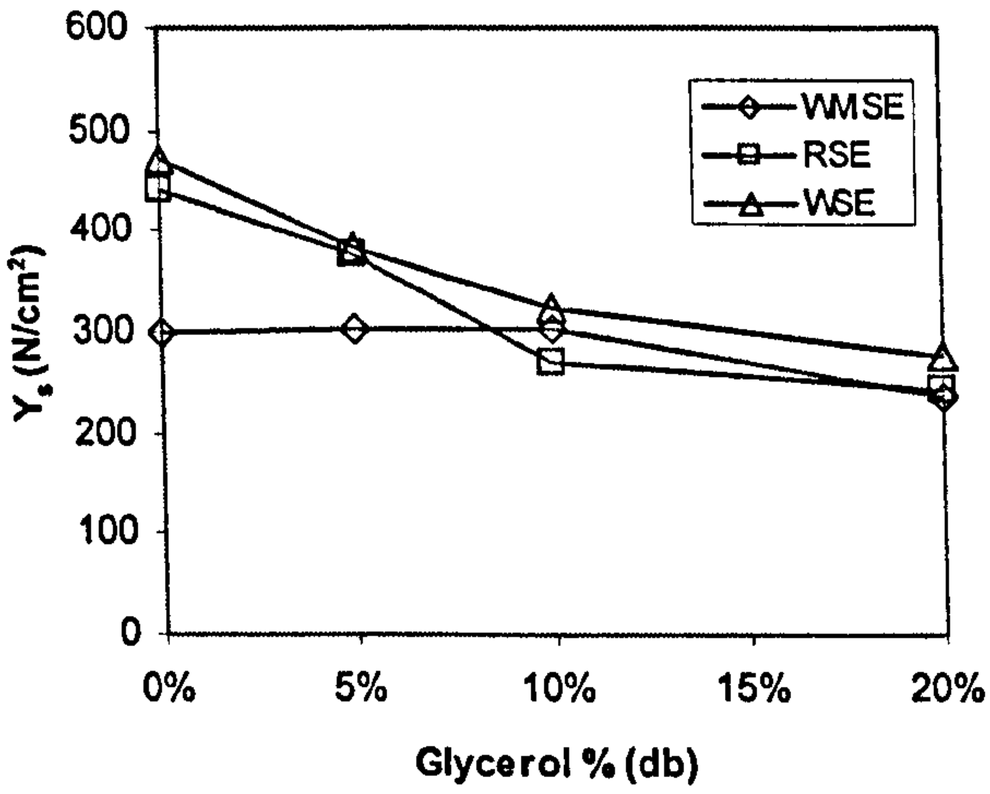

Figure 6.6. Modelling Paremeter Y_s (modulus in the glassy state) v/s glycerol content for waxy maize, rice and wheat starch extrudates

The application of the model also showed the plasticisication effect of glycerol. Figure 6.7 depicts the effect of glycerol on the moisture content at which the modulus begins to decrese, following the transition from a very hard-glassy material to a ductile-rubbery one.

It is clear that when glycerol concentration was increased in the mixture, the moisture content required to reach the modulus inflection point was reduced. This can be clearly observed in figure 6.7 where the moisture content decreased from ~13% (wb) for the control sample (0%glycerol) to ~7% for the 20% glycerol. This have been explained in terms of a reduction in the glass transition temperature of the polymer by the plasticiser effect of this polyol (Slade and Levin 1993, Kirby et al. 1993, Arvanitoyannis and Biliaderis 1999, Biliaderis, Lazaridou et al. 1999, Liu 2001, Mathew and Dufresne 2002, Myllärinen, Partanen et al. 2002).

Despite this consideration, care has to be taken in not confusing glass to rubber transion with brittle to ductile transition. Ward (1971 and 1983) states that whilst in certain cases the ductile-brittle tansition coincides with Tg this is not generally true. It is assumed that the brittle fracture and plastic flow are independent processes and both at lower temperatures than the glass transition temperature.

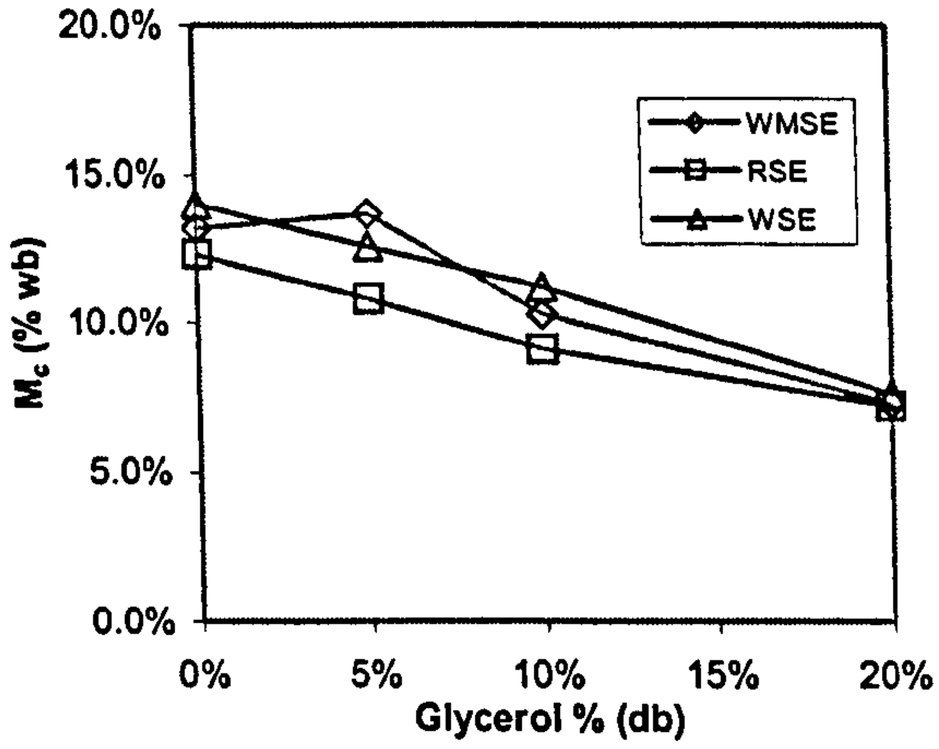

Figure 6.7. Modelling Paremeter M_c (moisture content at modulus transition) v/s glycerol content for waxy maize, rice and wheat starch extrudates

Figure 6.8 shows the modelling parameter *a'* as a function of glycerol content for each of three starches. As mentioned previously, when this value gets close to 0, the transition from a stiff to a ductile material would take the shape of a step function. When *a'* reaches large values, this relationship would be a flatter in shape (Peleg 1994).

There were not marked differences between the starches in the steepness of the modulus inflection point. The high values for waxy maize starch at 0% and 5% glycerol are explained by the brittle nature of these mixtures at low moisture resulting in lower values for the modulus. This would have a flattening effect on the function as the difference in the value of the stiffness in the glassy and rubbery would be reduced. This rationale is supported by similar *a'* values for waxy maise, rice and wheat starches starch at higher glycerol content (> 10%).

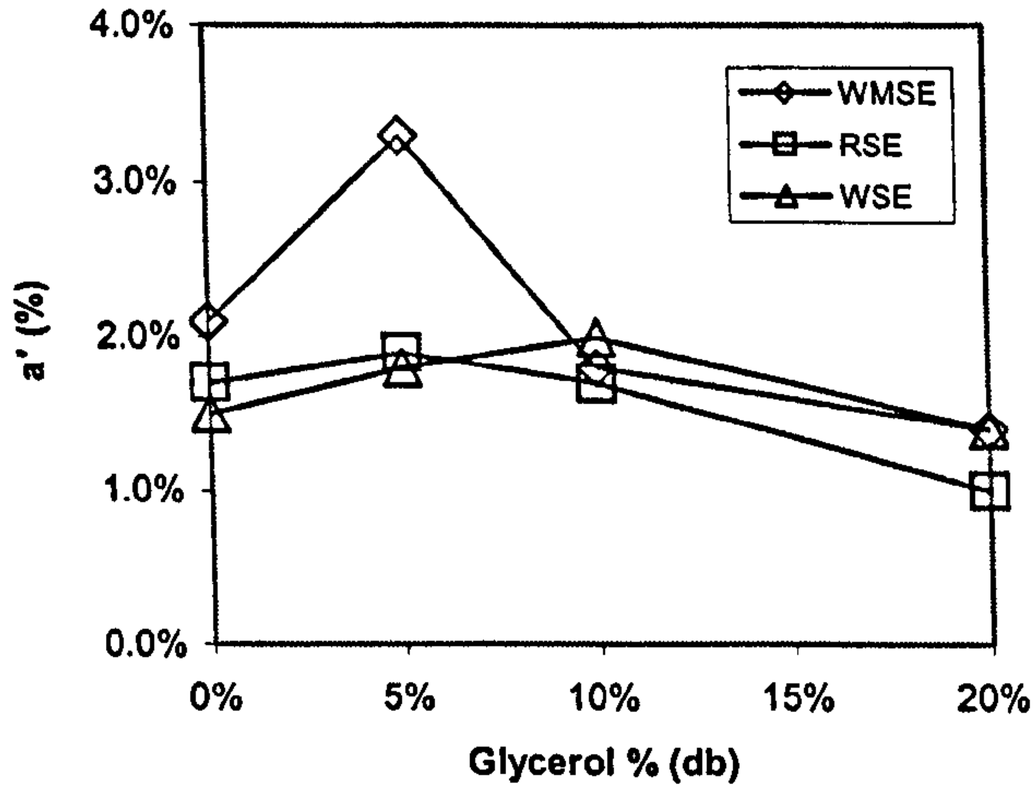

Figure 6.8. Modelling Paremeter *a'* (steepness of modulus transition) v/s glycerol content for waxy maize, rice and wheat starch extrudates

6.3.4 Effects of the Glass Transition Temperature (Tg) on the Flexural Modulus

It has already been mentioned that the glass transition temperature or Tg has a significant effect on the mechanical properties of polymers. Research on synthetic and bio-polymers have shown that below this temperature the material behaves as an elastic-solid and when the experimental temperature is higher than Tg, the polymer behaves as a rubber-ductile like material.

Figure 6.9 shows the flexural modulus for waxy maize, rice and wheat starches grouped by glycerol content and plotted as a function of the difference between the analysis temperature (25°C), and glass transition temperature (T-Tg) (Tg values presented in chapter 4).

For the graphs contaning 0% and 5% glycerol extruded samples, rice and wheat starched showed a very similar profile reaching a maximum plateau for modulus at T-Tg of -100°C.

The modulus for waxy maize starch was significant lower for T-Tg < -50°C, behaviour which has been already explained before in this chapter. These curves also show the modulus inflextion point related to the transition from solid-stiff material to a ductile-rubbery one not occurring at Tg (measured by DSC) but at a temperature around 80°C below it.

For the starch group contaning 10%glycerol, there were not marked differences in the modulus for the three starches, reaching the plateau value at a T-Tg of -70°C. The inflection point in the modulus for these extruded mixtures also occur below Tg, with a differences with the experimental temperature of -65°C.

Similarly, the 20%glycerol starch extrudates did not show differences between the three studied starches, with a maximum modulus value at a T-Tg of -50°C. The difference between Tg and the temperature of analysis at the drop of the modulus for three starches was near -40°C.

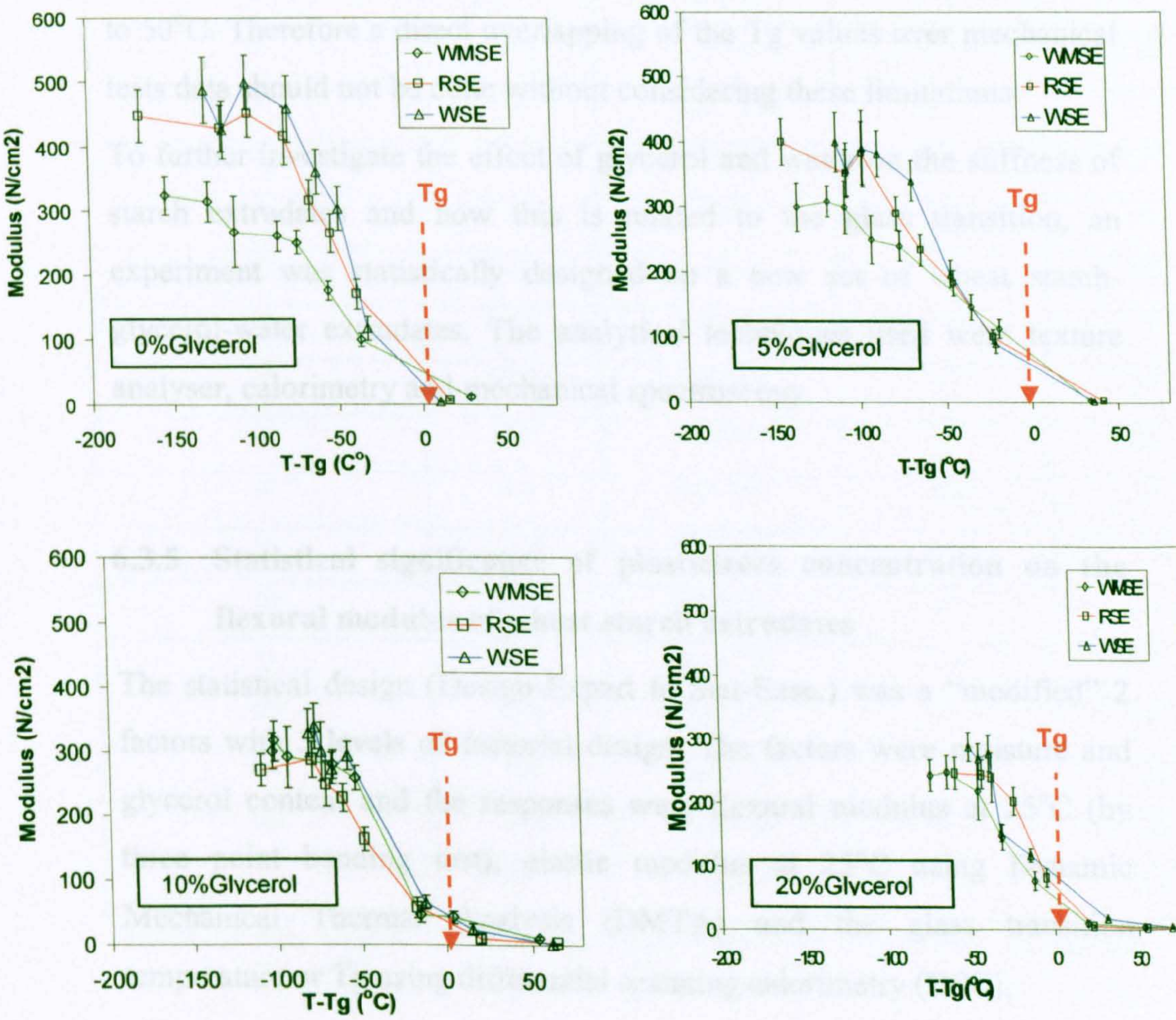

Figure 6.9. Modulus of elasticity for waxy maize, rice and wheat starch – glycerol mixture plotted against T-Tg (°C), with T = 25°C. Error bars represent ± 1 standard deviation of 5 measurements.

This experimental data shows clearly that marked changes in the stiffness of these particular model systems were not at the glass transition temperature (measured by DSC). Dobraszczyk and Vincent (1999) pointed out that the commonly reported Tg is based on calorimetry (e.g. DSC). Calorimetry relates Tg to the changes in heat capacity of the material but not the change in the mechanical characteristics during this transition. The authors suggest that mechanical tests are more sensitive to evaluate mechanical transitions because they are able to measure the actual modulus.

Kalichevsky *et al.* (1992) also suggested that the Tg value would vary depending on the analytical method (e.g. DSC, DMTA) and the experimental settings (e.g. heating rate, frequency) giving differences up to 50°C. Therefore a direct overlapping of the Tg values over mechanical tests data should not be done without considering these limitations.

To further investigate the effect of glycerol and water on the stiffness of starch extrudates and how this is related to the glass transition, an experiment was statistically designed on a new set of wheat starch-glycerol-water extrudates. The analytical techniques used were texture analyser, calorimetry and mechanical spectroscopy.

6.3.5 Statistical significance of plasticizers concentration on the flexural modulus of wheat starch extrudates

The statistical design (Design-Expert 6, Stat-Ease.) was a "modified" 2 factors with 3 levels of factorial design. The factors were moisture and glycerol content and the responses were flexural modulus at 25°C (by three point bending test), elastic modulus at 25°C using Dynamic Mechanical Thermal Analysis (DMTA) and the glass transition temperature or Tg using differential scanning calorimetry (DSC).

The starch used was wheat starch mixed with different glycerol contents, which had been thoroughly converted by thermomechanical extrusion into ribbon like geometries. The final glycerol concentrations in the samples were 0, 5, 10 and 20% and a moisture content of 40% wb. In

order to obtained extrudates with different moisture contents, the strips were dried for different times at 70°C. Details of sample preparation protocol and methods of analysis are the specified in chapter 3.

The values for moisture and glycerol concentrations after sample preparation and the obtained experimental data for the flexural modulus, elastic modulus (E') and Tg are presented in next table.

Table 6.2. Factors and Responses considered in the experimental design

Factor 1	Factor 2	Response 1	Response 2	Response 3
Glycerol % (MC/starch)	MC % (db)	Modulus (N/m2)	Log (E') N/m2	Tg C° (DSC)
0	20.7	3.0E+06	8.6	40
0	33.4	9.8E+04	7.5	0
0	8.6	8.0E+06	8.8	135
5	18.8	1.5E+06	8.7	41
5	7.7	8.1E+06	9.1	121
5	27.3	1.8E+05	7.7	19
10	21.3	4.7E+05	8.5	26
10	31.8	1.7E+04	7.6	0
10	21.1	4.6E+05	8.1	26
10	21.3	3.1E+05	8.4	23
10	7.0	8.1E+06	9.0	94
10	21.4	3.6E+05	8.0	25
10	20.9	4.6E+05	8.0	21
20	23.1	2.1E+05	8.0	21
20	32.9	3.6E+04	7.2	4
20	8.9	2.9E+06	8.9	63
20	18.4	6.4E+05	8.5	26
20	24.7	8.8E+04	7.8	14

Each of the values are the calculated mean of duplicates (moisture content, E' and Tg) and 5 replicates (flexural modulus).

6.3.5.1 Response 1: Flexural Modulus from Texture Analyser

A statistical model was obtained to represent the effect of glycerol and water on the flexural modulus at 25 °C. The model selected by the software was linear after a transformation from exponential to natural log. ANOVA showed the model to be statistically significant (Prob.>F = 0.0001). As expected, moisture content (Prob.>F = 0.0001) and glycerol concentration (Prob.>F = 0.0009) were significant factors affecting on the flexural modulus of the extrudates.

ANOVA

Source	F value	Prob > F	
Model	109.9	< 0.0001	significant
Glycerol %	16.9	< 0.0009	significant
Moisture Content %	192.1	< 0.0001	significant

MODEL: *Natural Log*

Ln(Flexural Modulus)) = +18.02 - 0.07 Glycerol Concentration - 0.20 Moisture Content

Equation 6.6

$R^2 = 0.94$

Numerically, the model shows the factor "Moisture Content %" having a greater significant effect compared to the factor "glycerol" on the softening of the extrudates, which agrees with the idea of being a more efficient plasticizer. This effect can be easily observed on figure 6.10, where a 3D (A) and a contour (B) plots represent the effects of moisture and glycerol on the flexural modulus. It is clear that water has a greater effect on the modulus compared to glycerol. The contour plot shows the combination of water and glycerol concentrations needed to obtain a specific value for the modulus; e.g. small variation in moisture content would be equivalent to larger variations in glycerol for a specific modulus value.

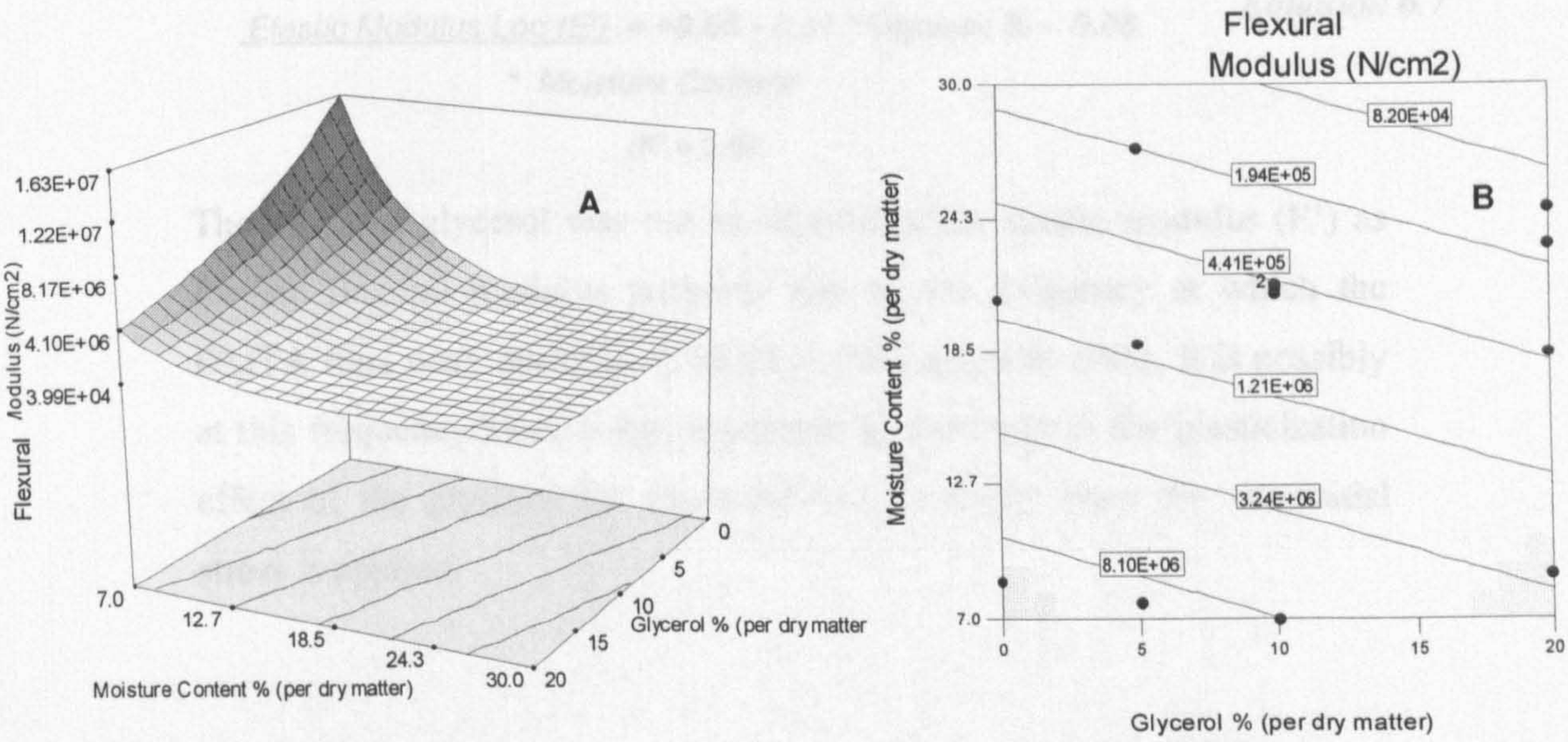

Figure 6.10. Elastic Modulus 3D (A) and Contour plot (B), (red dots are experimental data) showing the effect of moisture and glycerol content on stiffness of wheat starch extrudate.

6.3.5.2 Response 2: Elastic Modulus E' from DMTA (taken at 25°C)

The model selected by the software was linear but in this particulate case no transformation was needed as the data from DMTA is given already in Log scale. The obtained model was significant (Prob.>F = 0.0001).

Anova analysis showed that the elastic modulus was affected by the moisture content (Prob.>F = 0.0001) and to a lesser extent by glycerol (Prob.>F = 0.0988).

ANOVA

Source	F value	Prob > F	
Model	62.52	< 0.0001	significant
Glycerol %	3.10	0.0988	*significant*
Moisture Content %	118.13	< 0.0001	significant

MODEL: *Linear*

Elastic Modulus Log (E') = +9.66 - 0.01 * Glycerol % - 0.06 * Moisture Content *Equation 6.7*

(R^2 = 0.89)

The effect of glycerol was not as significant for elastic modulus (E') as for the flexural modulus probably due to the frequency at which the DMTA runs were performed, which is this case was 10Hz. It is possibly at this frequency there is not enough time relatively to the plasticization effect of the glycerol for the material to comply when the sinusoidal stress is applied.

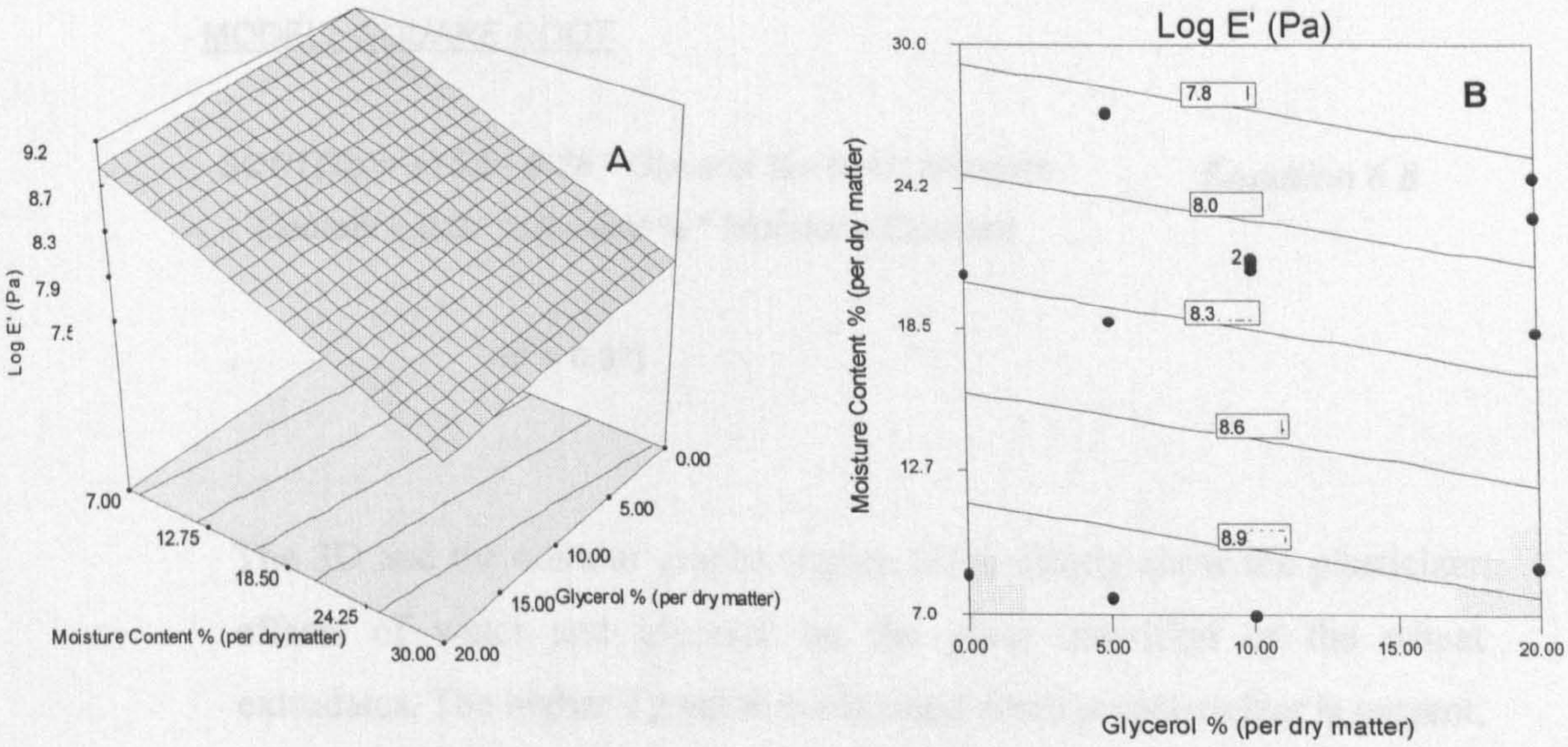

Figure 6.11. DMTA Elastic Modulus (E') represented on a 3D (A) and contour plot (B), (red dots are experimental data) showing the effect of moisture and glycerol content on stiffness of wheat starch extrudate..

6.3.5.3 Response 3: Glass Transition Temperature from DSC

The plasticising effects of water and glycerol on the glass transition temperature were also modelled using Design Expert. The selected model by the software was quadratic.

The model showed to be statistically significant (Prob.>F= 0.0001) with both factors, moisture content (Prob.>F= 0.0001) and glycerol contents (Prob.>F= 0.0006), being significant to the model.

ANOVA also showed that the term (glycerol*water) was significant to the model (Prob.>F = 0.0001).

ANOVA

Source	F Value	Prob > F	
Model	170.2	< 0.0001	significant
Glycerol%	82.5	< 0.0006	significant
Moisture Content%	615.1	< 0.0001	significant
Glycerol*MC	6.1	< 0.0006	significant

MODEL: *SQUARE ROOT*

*SQRT(Tg)= +15.5 - 0.28 * Glycerol % - 0.46* Moisture Content + 0.01 * Glycerol % * Moisture Content* *Equation 6.8*

(R^2 = 0.97)

The 3D and the contour graphs (figure 6.12) clearly show the plasticizer effects of water and glycerol on the glass transition of the wheat extrudates. The higher Tg value is obtained when no plasticizer is present, then Tg is decreased when the concentration of water and glycerol increased.

One of the advantages in using this statistical approach compared with the traditional two-dimensional data plotting is that the plasticizing effect of water and glycerol can be numerically assessed independently. Indeed, from the 3D and contour graphs is clear that water is a more efficient plasticizer than glycerol.

Another finding that was observed, especially in the contour graph, is the plasticising effect of glycerol only occurs for a specific moisture content range. Indeed, for moisture content higher that 25%, glycerol does not

contribute to the reduction of Tg, keeping this value near 11°C. If the moisture content is reduced, glycerol begins to have a significant effect on Tg, with its maximum effect at the lower end of moisture present. This result supports the finding and discussion in chapter 4 of this thesis where it has been suggested that a sufficient amount of water molecules would displace the glycerol from the starchy matrix leading to the formation of a glycerol rich phase in the mixture especially at higher end of glycerol contents.

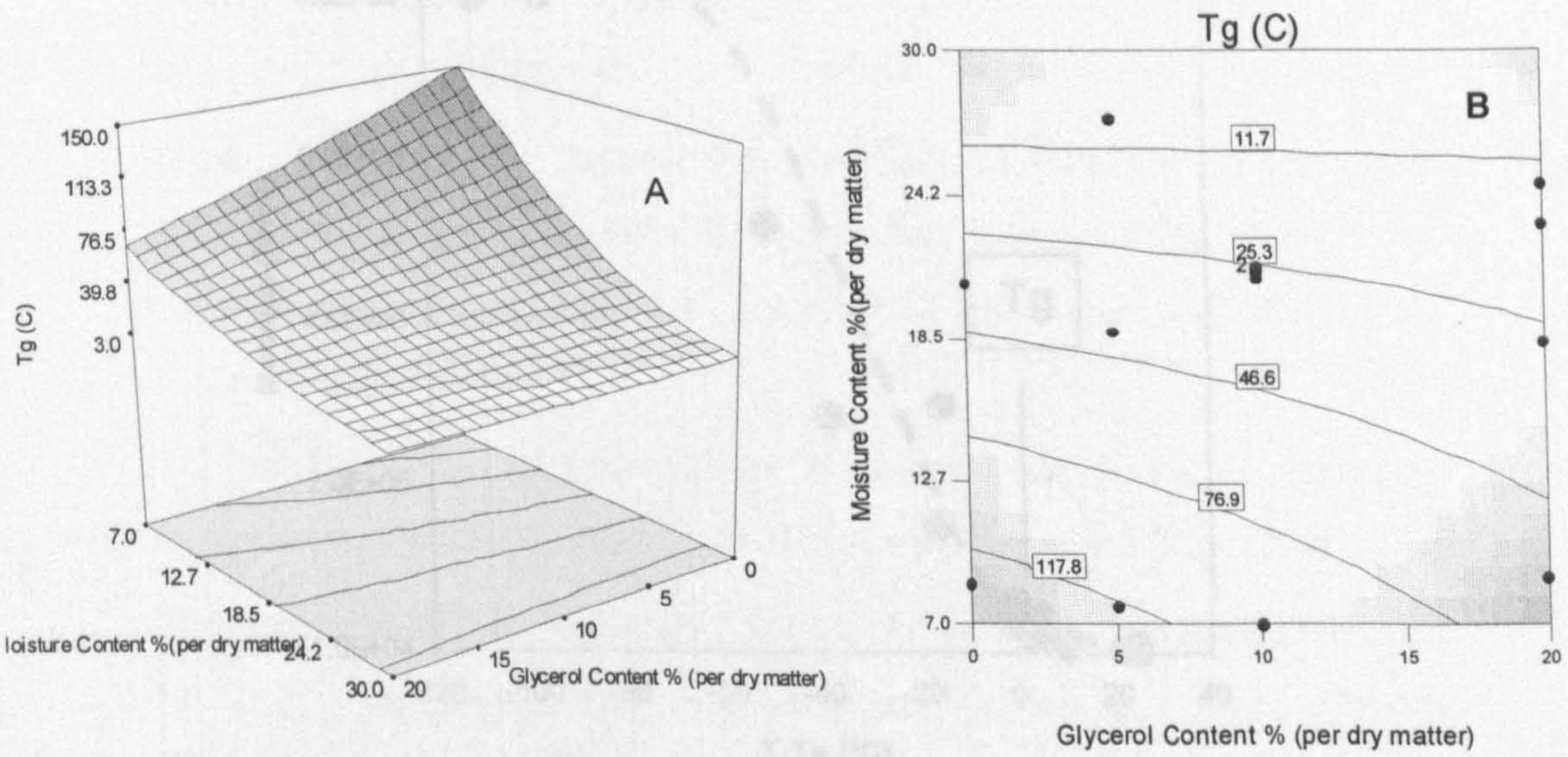

Figure 6.12. 3D and contour plot showing the effect of moisture and glycerol content on Tg of wheat starch extrudate (red dots are experimental data).

6.3.5.4 Effect of Tg on the Stiff to Ductile transition of wheat starch extrudates

In order to evaluate the effect of Tg on the stiffness, the Tg's of the prepared wheat starch-glycerol-water mixtures (measured by DSC) were plotted against the obtained flexural modulus (data from table 6.2).

Figure 6.13, shows the values obtained for flexural modulus and the difference between the experimental temperature (25°C) and Tg.

Similarly to findings in section 6.3.4., the transition from a stiff to ductile occurs at T-Tg of around -80°C, supporting the argument that Tg obtained from DSC does not directly predict the changes in flexural mechanics of these model systems.

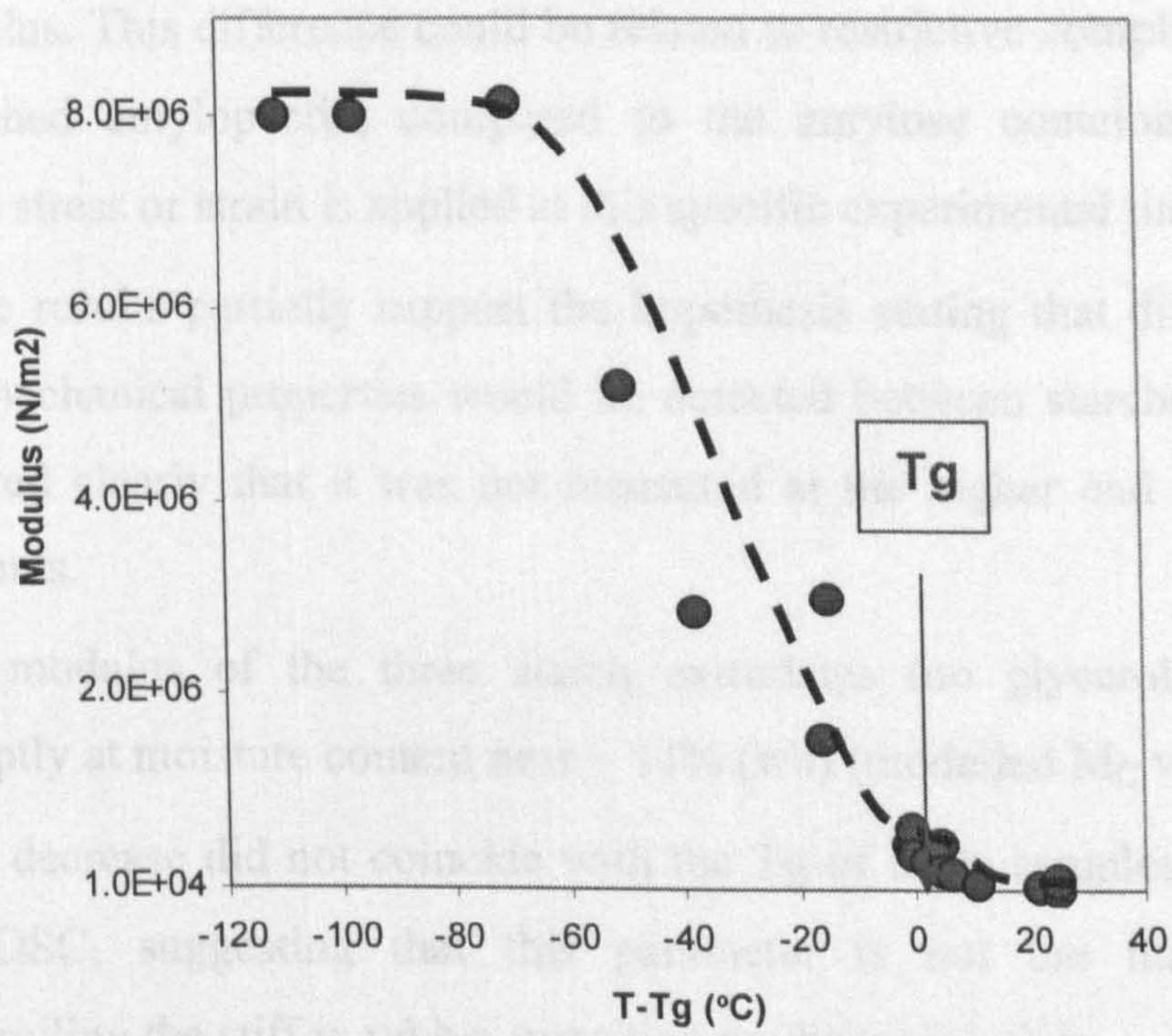

Figure 6.13. Flexural modulus v/s T-Tg (°C) for different wheat starch-glycerol-water mixtures

6.4 Conclusions

The analysis of the flexural response of waxy maize, rice, and wheat starch water extrudates indicated two different behaviours depending on the moisture content. For moisture contents > 10%, there were not marked differences between the three starches but for moisture content < 10%, the flexural modulus was lower for waxy maize starch but similar for rice and wheat starches. This would suggest that amylose content does affect the flexural properties of starch over the specified moisture content range. Waxy maize showed to be highly brittle, resulting in much lower modulus. This difference could be related to restrictive compliance of the branched amylopectin, compared to the amylose containing starches when stress or strain is applied at this specific experimental time scale.

These results partially support the hypothesis stating that differences in the mechanical properties would be detected between starches as it was showed clearly that it was not measured at the higher end of moisture contents.

The modulus of the three starch extrudates (no glycerol) decreased abruptly at moisture content near ~ 13% (wb) (modelled M_C value).

This decrease did not coincide with the Tg of these samples as describe by DSC, suggesting that this parameter is not the main variable controlling the stiff to rubber transition on these materials.

Although glycerol showed to be a less efficient plasticizer than water, it had a significant effect on the reduction of the flexural modulus of the three starches for moisture contents < ~ 15% (wb). For higher moisture contents, glycerol did not contribute to the softening of the extrudates which was mainly controlled by water present in the matrix.

The reduction in moisture content to reach the inflection point in the flexural modulus (modelled M_C value) by the presence of this polyol was also very similar for the three starches, decreasing it from ~13% for the control to ~7% for the 20% glycerol samples, indicating a behaviour that is independent on starch botanical source. Although, it seemed that this effect is related to plasticization by this polyol, it did not coincide with

the Tg of the samples reaching the experimental temperature (T-Tg = 0°C).

Despite the empirical nature of a statistical design, it proved to be a useful tool for the analysis of the independent or combined effect of the plasticizers (water and glycerol) on the Tg and flexural properties of these particular model systems.

7. Mechanical Stability of Wheat Starch Glycerol Systems

When starch based materials are stored, changes in the textural attributes are generally expected. Depending on their physical state and environmental conditions during storage, the increase in hardness may be related to two different ageing processes. If they are stored in the glassy state (Tg < storage temperature), the increase in stiffness is generally associated to a structural relaxation phenomenon or "physical ageing" occurring in the material. If they are stored in a rubbery state (Tg > storage temperature), the increase in hardness is usually related to a molecular reordering process commonly known as retrogradation.

Back in 1968, Collison defined retrogradation as a crystallisation process, which arises because of the strong tendency for hydrogen bond formation between the hydroxyl groups on adjacent starch molecules. Due to the economical implications associated to this ageing process, it has claimed an important proportion of the research carried out in cereal science.

Polyols have been commonly used in starch based products to reduce the availability of water to microorganisms, extending the shelf-life without affecting their textural attributes. Although, the main known functionality of these compounds is their plasticising effect, work have been published suggesting that polyols may interact with the starch polymeric chains reducing the rate at which theses materials retrograde.

The experimental work presented in this chapter aims to clarify the effect of polyols on low to intermediate moisture content on starch based materials. A model system based on wheat starch and different concentrations of glycerol was prepared by hot extrusion. The fresh samples were aged until no more increase in ageing parameters was detected. The kinetic associated with retrogradation was modelled using the Avrami equation.

7.1 Hypotheses

The main ideas testes in this chapter are summarised in the following paragraphs.

- The main factor affecting the retrogradation kinetics of this system is the difference between the glass transition temperature of the system (Tg) and the storage temperature (T-Tg). There is a positive correlation between rate of retrogradation and the difference between these two temperatures.
- When the Tg value of these mixtures becomes equal or lower that the storage temperature, there will be a reduction in the retrogradation kinetic. This reduction is associated to a phase transition of the material from rubbery to a glassy state.
- The presence of glycerol will affect the rate of retrogradation by its plasticising nature, shifting the Tg of these systems and hence influencing the difference T-Tg.

7.2 Theoretical Background

The cooking or processing of starch, in excess water conditions and temperature, causes the so called "gelatinisation" which incorporates swelling or even disruption of starch granules, depending upon the severity of the treatment applied and the composition of the material (Karim, Norziah et al. 2000). This will transform the crystalline order present in native starch to a completely amorphous structure. This crystalline to amorphous transition can also be achieved under lower water conditions the by application of mechanical energy and temperature (eg. extrusion).

The behaviour of gelatinised starches on cooling and storage, generally termed "retrogradation" (Atwell, Hood et al. 1988), is of great interest to food scientist and technologists since it has a great impact on quality, acceptability and shelf-life of commercial foods (Miura, Nishimura et al. 1992; Baik, Kim et al. 1997; Van Soest and N. Knooren 1997; Jagannath, Jayaraman et al. 1998; Jouppila, Kansikas et al. 1998; Klucinec and Thompson 1999; Farhat, Blanshard et al. 2000; Takaya, Sano et al. 2000; Del Nobile, Martoriello et al. 2003; Ottenhof 2003; Varavinit, Shobsngob et al. 2003; Kohyama, Matsuki et al. 2004; Bello-Pérez, Ottenhof et al. 2005; Lionetto, Maffezzoli et al. 2005; Ottenhof, Hill et al. 2005).

Molecular re-association or retrogradation may be originated by two or more starch chains forming a simple junction zone point. This may then develop into more extensively ordered regions, which under favourable conditions, would result in crystalline order (Atwell, Hood et al. 1988; Van Soest and Knooren 1997).

More details about the fundamentals related to the re-crystallisation of amorphous rubbery starches is discussed in chapter 2, section 2.1.6.

The mixing compatibility of glycerol with starch and the presence of hydroxyl groups in its structure suggest that possible interaction with amorphous amylose and amylopectin may occur. If this interaction exits, differences in the retrogradation kinetics are expected.

The next sections investigate these possible interactions by assessing the effect of these polyol on the retrogradation kinetics of these systems.

7.2.1 Effect of Polyols on the Retrogradation Kinetics

Generally the addition of polyols to starch based products aims to improve the texture attributes of these materials without increasing the availability of water. Being small molecular weight molecules, these compounds have a plasticizing effect on the polymeric fraction, reducing its glass transition to temperatures below the storage temperature. This reduction in Tg would change the polymer from hard-glassy to a ductile- rubbery material.

Although the understanding of the effect of polyols on the structural and mechanical stability of starchy products has been improved over the years, its effects on the retrogradation of these materials over time has not been completely clarified.

Work done on plasticised synthetic polymers Guo *et al.* (1988) showed a decrease in "permeability" when 10% of the plasticizer was added suggesting that strong interactions between the plasticizer and the polymer (probably by means of hydrogen bonds) induced a loss of macromolecular mobility. A similar idea is proposed by Scandola *et al.* (1991). They presented two types of polymer-water interactions; (a) for quantities less than 10%, the polymer-water system formed by hydrogen bonds is more compact than the polymer-polymer system.

(b) Above 10%, a looser network is formed due to the occurrence of water-water interactions.

Van Soest *et. al.* (1994) detected a decrease in the Avrami reaction rate constant *k* when the amount of glycerol increased in a waxy maize starch 10% (db) gel. They hypothesized possible hydrogen bond interactions between glycerol and the amylopectin chains of the starch. Van Soest *et. al.* (1997) suggested that it was difficult to evaluate the effect of glycerol fraction on the retrogradation kinetics, as the overall composition of the mixture varied during conditioning due to the high hygroscopicity of this polyol, increasing the moisture content during storage.

It has been suggested that this increase in the plasticizer content would have a lowering effect on the glass transition increasing the retrogradation rate (Van Soest and Vliegenthart 1997). Work on the retrogradation of waxy maize starch described this dependency of starch reordering rate on temperature as a bell shape function, with the higher rate value for a temperature at midpoint between the glass transition temperature (Tg) and the melting temperature (Tm) (Farhat, Blanshard et al. 2000). Hence, changes in the plasticiser concentration would shift the Tg and Tm to different values affecting the overall kinetic of retrogradation process.

The formation of glycerol-starch interaction has also been investigated by Smits *el al.* (1999) using differential scanning calorimetry (DSC) and solid-state nuclear magnetic resonance spectroscopy (NMR). They showed an irreversible exothermal transition (between 50-150 °C) for dried starch mixed with glycerol, enthalpy of which was proportional of the glycerol concentration, suggesting the formation of a polyol-starch polysaccharide interaction. NMR data for glycerol in the matrix showed a decrease in flexibility and conformational limitations after the thermal transition.

Similar work was carried out by Kruiskamp *et al.* (2001) on dried amylopectin from potato starch mixed with ethylene glycol and glycerol. They also measured exothermal transitions (by DSC) when these mixtures were heated over 150°C, which was attributed to polyol-starch interaction. An interesting finding was that the interaction exotherm decreased over time, which was

explained by the reduction in the amorphous fraction of the starch mixtures over time.

Smit *et al.* (2003) investigated the influence of small plasticizers on the retrogradation of gelatinised potato and wheat starch in presence of water (30% db). They showed that adding to potato starch polyols such as glycol and glycerol (< 4 OH groups) there were an increase on the final starch crystallinity index. An opposite behaviour was detected for polyols with bigger molecule sizes such as threitol (4 OH groups) and xylitol (5 OH groups). When these compounds were added to potato starch, a decreased in the retrogradation kinetic was detected after storage. On the same study, similar experiments were performed on wheat starch but for this type of starch there was not a clear trend between number of hydroxyl groups and the reduction or increase in the retrogradation kinetics. This was attributed to the differences in amylopectin chain length and crystal polymorph for the wheat compared with potato starch.

It seems that two behaviours can be expected when glycerol is added to amorphous starch based materials depending on the moisture content present. For low moisture contents (< ~10%), available hydroxyl groups present in the amylopectin/amylose chains would be occupied by glycerol molecules, which could lead to interaction between this polyol and these polymers. If the water conentration increases, it is likely that these molecules, which are smaller than glycerol, could reduce the interaction effect of this polyol. Under these conditions the effect of glycerol on the starch would be limited to plasticization, increasing the molecular mobility of the system.

As already mentioned, the implications of this phenomenon in food products are of great interest in academic research and industry. Significant research has focused on understanding by the application of predictive modelling. The next section presents the use of one of the equations commonly used to obtained quantitative information about the retrogradation kinetics of starch based materials.

7.2.2 Modelling Retrogradation Kinetics

Retrogradation of starch has been considered to be a crystallization process, which can be detected from a change in the appearance of a starch gel or paste, changes in X-ray diffraction patterns, or as an increase in the gelatinisation exotherms in DSC measurements (Roos 1995).

Many different models exist for following the retrogradation kinetics, however the Avrami model (equation 7.1) appears to be the most widely used for retrogradation studies (Ottenhof 2003). The derivation of this equation can be found on Sperling, L. H. (1986).

$$U(t) = \left[\frac{Y_\infty - Y_t}{Y_\infty - Y_0}\right] = e^{-k_r t^n} \qquad \textit{Equation 7.1}$$

Where:

$U(t)$ = is the uncrystallised starch fraction at time t

k_r = crystal growth rate

n = Avrami coefficient that is thought to depend on the type of crystal nucleation and the dimensions in which growth take place.

Y_t = physical parameter describing the retrogradation dependency on time t

Y_o = value of physical parameter at time = 0

Y_∞ = value of physical parameter at time equal infinity (end plateau.

In order to model experimental data on retrogradation, equation 7.1 can be algebraically rearranged as (Farhat, Blanshard et al. 2000):

$$Y_t = Y_\infty (Y_\infty - Y_o) e^{-k_r t^n} \qquad \textit{Equation 7.2}$$

After obtaining the Avrami coefficient and the crystal growth rate (Solver from Excel, Office 2003, Microsoft Corp.), the rate of retrogradation G (s^{-1}) can be estimated from:

$$G = k_r^{\frac{1}{n}} \qquad \textit{Equation 7.3}$$

The fitting optimization can be done by independently adjustable adjusting Y_o, k and n.

Although the application of this model has undoubtedly helped to improve the understanding of the retrogradation of starches, the interpretation of the Avrami coefficients should be treated with caution. Del Nobile *et al.* (2003) commented that for example the parameter n should be considered as a fitting variable rather than of the original interpretation of an integer number representing the mechanism of crystal growth.

In order to test the hypotheses presented in section 7.1, a model system was formulated based on wheat starch and glycerol.

The first part of the experimental work aims to evaluate the effect of different concentrations of glycerol on the storage of amorphous wheat starch extrudates. The second part attempts to clarify the influence of glycerol on the starch retrogradation kinetics. Finally, samples containing different plasticiser concentrations were used to evaluate the retrogradation kinetic as a function of the temperature difference between the samples Tg and storage temperature.

7.3 Results and Discussion

The analytical techniques used were calorimetry (DSC), large deformation testing (Texture Analyser) and mechanical spectroscopy (DMTA).

The model system used for this study was wheat starch with 0%, 10% and 20% glycerol. The samples were prepared by thermomechanical extrusion and shaped to ribbons, which were then dried to different moisture contents as described in chapter 3. seccion.3.3.2.2.

The experimental work presented in the next section, focuses on the study of the mechanical stability of starch systems (wheat starch) with similar moisture contents but different concentrations of glycerol.

7.3.1.1 Mechanical Stability of Wheat Starch-Glycerol Extruded Systems During Storage

Fresh extruded wheat-glycerol samples were dried to moisture contents < ~ 7% and then stored at 75%RH using a saturated salt solution. The weight changes were recorded in order to achieve a moisture content of around ~ 17% (db) (common moisture content found in intermediate moisture commercial formulations). After the desired moisture content was obtained, the samples were stored for 15 days at 40°C. Moisture content was measures before and after the storage period using the same analytical method (24 hours at 105°C). The flexural modulus was calculated according to the method presented in chapter 3, section 3.3.2.

Figure 7.1 shows a comparison of the flexural modulus obtained using three point bending test method (TPBT) for the control (no glycerol) and wheat starch-glycerol mixtures. The moisture content for all the samples remained constant suggesting that the change in modulus was originated by changes in the molecular structure of starch-glycerol extrudates.

Although there was an increase in the flexural modulus for the control samples, it was not significant (ANOVA $P>0.05$), but this increase was significant for the starch containing 10% and 20% glycerol ($P<0.05$). For the latter, the modulus increased near three times at the end of the storage period. This difference in the increase of the stiffness between the control and the glycerol containing samples may be related to their glass transition (Tg). Indeed, as it has been described in several references cited in this thesis (Kalichevsky 1992; Van Soest and Vliegenthart 1997; Farhat, Blanshard et al. 2000), Tg will significantly affect retrogradation rate of starchy materials.

In the case of the control sample (no glycerol) the difference between the ageing temperature (T = 25°C) and its glass transition temperature (Tg ~ 55 °C (data presented on chapter 5), was -30°C, suggesting that this sample was in glassy state during storage where no retrogradation occurs.

The slight increase in the modulus may be explained by another ageing phenomenon that may occur in the glassy state. It is well documented that amorphous starches undergo molecular relaxation to a lower energy state (Hutchinson 1995; Borde, Bizot et al. 2002; Lourdin et al. 2002) when stored at temperatures below their Tg. This so-called "enthalpy relaxation" can a have a significant effect on the mechanical and structural properties of amorphous materials such as an increase in stiffness and brittleness and a decrease in the specific volume due to structural densification (Lourdin et al. 2002, Chung and Lim (2003); Lourdin, Colonna et al. 2002).

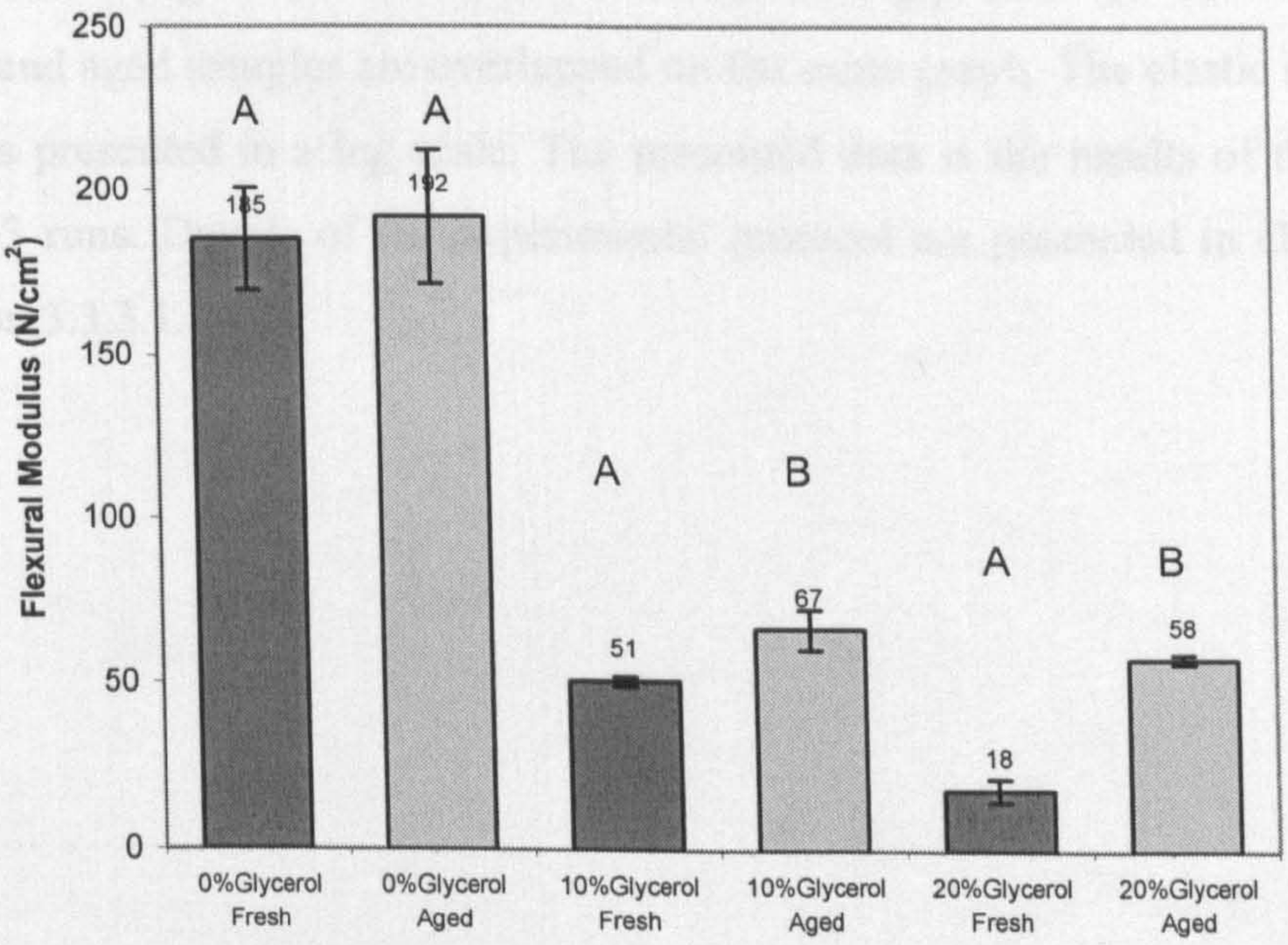

Figure 7.1. Flexural modulus comparison for fresh and aged (15 days at 40°C) for wheat starch-glycerol and ~ 17% (db) moisture content extrudates. Error bars represent ± 1 standard deviation from 5 measurements. Letters on top of each bar represents statistical difference.

In the case of wheat starch and 20% glycerol a significant increase (difference >2 standard deviations) in the modulus was detected between the fresh and aged samples. For this sample the difference (T-Tg) was ~ 24°C. This value shows that this material was stored in the rubbery state, where retrogradation is expected to occur. Similar mechanism can explain the increase in the flexural

modulus for the extrudate containing 10%glycerol during storage where T-Tg was ~ 20°C.

Mechanical Spectroscopy (DMTA) was also used on the same wheat starch-glycerol mixtures to evaluate the changes in their mechanical properties during storage. This technique not only gives information on the changes in modulus, but also about the structural relaxation of amorphous fraction that might occur at different temperatures. These transitions are commonly associated to the so-called secondary relaxation (β-relaxations) and primary or main transitions (α-relaxation) normally associated with Tg (Haines 2002).

Figure 7.2, shows the elastic modulus (E') v/s temperature (left) and tan δ v/s temperature (right) for the control, 10% and 20% glycerol. The curves for the fresh and aged samples are overlapped on the same graph. The elastic modulus data is presented in a log scale. The presented data is the results of the mean from 3 runs. Details of the experimental protocol are presented in chapter 3, section 3.3.3.1.

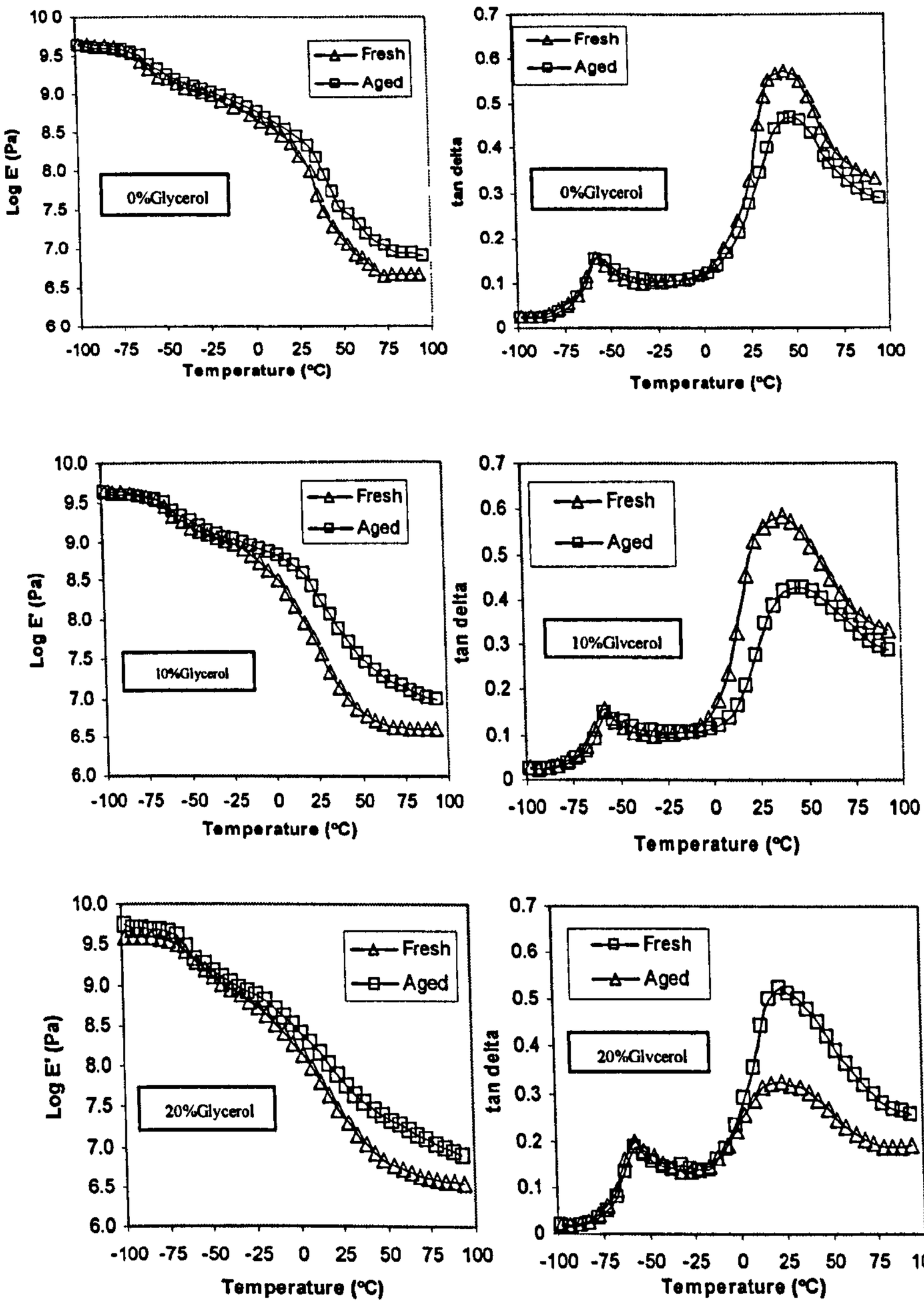

Figure 7.2. Wheat starch-glycerol and ~ 17% (db) moisture content DMTA (10Hz) comparison for "fresh" and "aged" extrudates (15 days at 40°C). The heating rate was 3°C/minutes and the set strain was x 4 (62 μm amplitude).

The graphs at the top of figure 7.2 show the results for the control sample (no glycerol). The elastic modulus-temperature graph shows the typical profile for this type of materials, with two mechanical relaxations; a small transition at ~ –60°C and a significant reduction in *E'* at ~ 23°C. The first transition has been attributed to secondary transitions due to the motion of short lengths or local groups of the polymer backbone (Lourdin, Bizot et al. 1997; Haines 2002). The main transition identified at higher temperatures has been explained by long range translation movements between the polymer chains, which is associated to the glass transition temperature (Tg) of the polymer. Below this temperature the material is in glassy state represented by a high values for the modulus (10^9 Pa). When the Tg is reached, an abrupt decrease in the modulus can be observed (3 to 4 orders of magnitude) due to the transition from a stiff/glassy to ductile-rubbery materials with values for the elastic modulus $<10^6$ Pa.

This secondary and main transition can also be observed for tan δ v/s temperature. As it has been described on chapter 3 of this dissertation, tan δ represents the ratio between the loss (*E''*) and the elastic modulus (*E'*). Therefore, any mechanical relaxations occurring during the analysis are represented by an increase in the value of tan δ. This transition was observed on the control sample, where a small peak appeared at ~ –55°C and much bigger one at ~ 50°C, both of which can be respectively related to the transition detected at ~ –60°C and ~ 23°C on the elastic modulus (*E'*) v/s temperature curve. Taking the peak of tan δ as Tg (~40°C) would suggest that during ageing at 40°C, the extrudate physical state was more glassy like than a rubber.

In the case of wheat starch and 10% and 20% glycerol extrudates, similar profiles were obtained on the elastic modulus (*E'*) v/s temperature and tan δ v/s temperature curves. Two mechanical relaxation were detected, a small decrease on *E'* occurring at ~ -60°C for both glycerol contents, which is similar to the temperature at which the same transition was detected for the control sample. The main transition occurring at higher temperature was dependent on the glycerol concentration. Indeed, wheat starch-10%glycerol showed the main reduction in *E'* occurring at ~ 21°C and for wheat starch-20%glycerol occurred at ~ 0°C.

The tan δ v/s temperature curve obtained from these samples showed a small peak at ~ -55°C for both mixtures. In the case of the main peak for 10% glycerol sample, the estimated Tg was approximately 15°C and for 20% glycerol sample was around 5°C. These reductions in the temperature of the reduction in *E'* and main peak of tan δ are in line with the findings in chapter 5 where the plasticising effect of glycerol was clearly demonstrated on three different starches.

Looking at the overlapped curve for the aged samples on the elastic modulus *E'* v/s temperature, it seems that below Tg there were not differences between any of the fresh and aged samples. This can be explained by the unrelaxed molecular state of the amorphous fraction at this temperature range during the analysis. When the temperature during the analysis reached the Tg of each of the samples, a higher value for *E'* was detected for the aged extrudate.

If 25°C is used as a reference temperature, the elastic modulus increased around ~ 2% for the control sample after ageing. In the case of wheat starch 10% glycerol, the increase in the modulus was approximately 9% at the same temperature. For the mixture containing 20% glycerol the increase was approximately 8% after storage. As expected, the greater increase in the modulus was for the glycerol containing samples that were aged in the rubbery state (Tg < storage temperature).

It is known that the structural relaxation of the polymer can be associated only to its amorphous fraction (Lionetto, Maffezzoli et al. 2005), therefore the increase in the modulus can be related to an increase in the polymer crystallinity or molecular order from retrogradation during storage. Indeed, the tan δ v/s temperature curved show a decrease in the tan δ peak for the aged samples, suggesting a decrease in molecular mobility of the amorphous fraction of the polymer associated with the already mentioned increase in the crystalline phase. Moreover, the extent of the decrease in this value seems to be related to the amount of glycerol present in the mixture, where a ~ 21% decrease was detected for the control sample, a ~ 35% was detected for the 10% glycerol and ~ 66% reduction for the 20% extrudate. This would imply that the increase in the proportion of crystallinity of the high glycerol extrudate was higher that on the pure wheat starch sample. These findings also correlate

well with the texture measurement using the TPBT (figure 7.1) method were the greater increase in stiffness occurred on the 20% glycerol wheat extrudates.

The increase in crystallinity of the starch-glycerol extrudates after storage was also evaluated using differential scanning calorimetry (DSC). Figure 7.3 depicts the DSC traces (in excess water) for all the starch-glycerol mixtures grouped as "Fresh" and "Aged".

After the first DSC run, all the samples showed a major peak detected at ~ 66°C (red dotted line) and a smaller one appearing at ~102°C (blue dotted line). Both endotherms were irreversible at the experimental time scale (as shown on 2nd run scan on both graphs).

The endotherm detected at the lower temperature can be associated with the gelatinisation of ordered or crystalline starch (Donovan 1979; Biliaderis 1990; Cooke and Gidley 1992). The endotherm at higher temperature is usually associated to the disruption of amylo-lipid complex starting to form soon after the complete conversion of the starch (Buléon, Colonna et al. 1998).

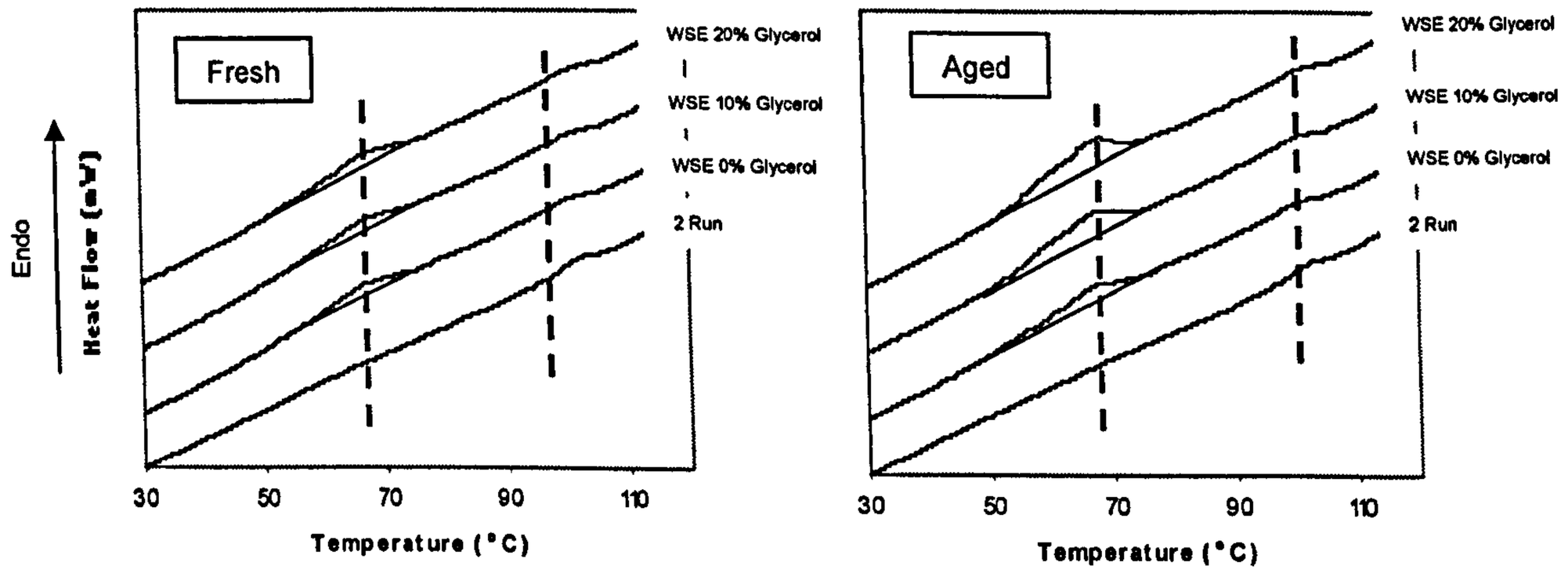

Figure 7.3. DSC thermograms for the "fresh" and "aged" wheat starch-glycerol extrudates. The samples were measured in excess water and a heating rate of 10°C/ minutes.

Table 7.1 shows the endotherm onset and peak temperature and the area (enthalpy) associated to the thermal energy absorbed by the extruded starch samples. Looking at the fresh samples (table 7.1. A), small endotherms were detected at ~ 66°C for the control (no glycerol) and the starch-glycerol

mixtures. It is difficult to identify these endotherms as being unconverted native starch or from retrogradation during the conditioning of the samples. In the literature it is suggested that retrograded starches show smaller endotherm enthalpies, lower peak temperature and a greater difference between the peak onset and end point temperature than native starch structures. This has been explained by the formation of less perfect crystals during retrogradation (Waigh, Gidley et al. 2000; Tester and Qi 2004).

Table 7.1. DSC gelatinisation temperatures and enthalpies for the "fresh" and "aged" (15 days at 40°C) wheat starch-glycerol extrudates after the 1st run. The measurement was performed in excess water (3:1 = water:starch); values shown are the average of three measurements.

(A). Fresh Extrudates	Onset 1st Peak (°C)	Temperature 1st Peak (°C)	Final 1st Peak (°C)	ΔH 1st Peak (J/g starch)	Temperature 2nd Peak (°C)	ΔH 2nd Peak (J/g starch)
WSE 0%Glycerol	51.2 (0.22)	65.7 (0.34)	75.6 (0.23)	1.21 (0.09)	102.1 (0.9)	0.99 (0.05)
WSE 10%Glycerol	51.6 (0.31)	65.0 (0.46)	75.8 (0.33)	1.45 (0.10)	103.3 (0.7)	0.87 (0.04)
WSE 20%Glycerol	51.3 (0.34)	66.0 (0.43)	76.8 (0.36)	1.49 (0.07)	100.5 (0.8)	0.63 (0.07)

(B.) Aged Extrudates	Onset 1st Peak (°C)	Temperature 1st Peak (°C)	Final 1st Peak (°C)	ΔH 1st Peak (J/g starch)	Temperature 2nd Peak (°C)	ΔH2nd Peak (J/gstarch)
WSE 0%Glycerol	50.4 (0.42)	66.3 (0.46)	74.7 (0.53)	1.32 (0.08)	102.3 (0.8)	0.95 (0.07)
WSE 10%Glycerol	50.0 (0.35)	66.8 (0.52)	76.4 (0.47)	3.81 (0.15)	104.1 (0.6)	1.37 (0.08)
WSE 20%Glycerol	49.3 (0.23)	67.0 (0.37)	76.5 (0.33)	5.83 (0.19)	100.3 (0.8)	0.97 (0.06)

Values in brackets represent the standard deviation of three measurements.

Table 7.1 (A and B) does not show a marked difference in the peak temperature of the main exotherm, onset and end point between the fresh and aged samples. This would suggest that its origin was not from native starch but from retrogradation during sample preparation.

Differences in the enthalpy for the main endotherm (at ~ 66°C) were detected between the fresh and aged samples. The greater differences occurred for the starch-glycerol mixture where an increase of ~ 1.6 times (160%) from the initial value was measured for wheat starch 10% glycerol extrudates and an increase of ~ 2.9 times (290%) for the 20% glycerol wheat starch sample. The increase in enthalpy for the control samples after storage was not significant.

The small endotherm detected at higher temperature (~ 102 °C) also increased after storage. The control sample showed an increase of ~ 43% and ~ 53% increase for starch with 10% and 20% glycerol. These findings suggest that the increase in molecular mobility due to the presence of glycerol would promote a

greater interaction during storage between lipids and amylose that becomes available during extrusion.

The differences in the increase in enthalpy for the starch conversion between the pure wheat starch and starch-glycerol extrudates correlated well with the findings using the TA (TPBT method) and DMTA.

Although a direct comparison between these techniques is difficult as the data has not been normalised (fresh → 0% to aged → 100%) due to absence of the ageing values at time equal infinity (complete retrogradation), it has been shown that for the moisture content studied (~ 17% db) glycerol contributed to increase molecular mobility by reducing the samples Tg (as shown in chapter 5), which had an effect on the mechanical and molecular behaviour of these samples represented by an increase in the flexural and elastic moduli, an increase in the conversion enthalpies and a decrease in the peak values of the tan δ curves.

Further discussion on the effect of this polyol on the retrogradation kinetics of this ordering process is presented in the next section.

7.3.1.2 Retrogradation Kinetics of Wheat Starch-Glycerol Extruded Systems

This section aims to evaluate the effect of glycerol of the retrogradation kinetic of wheat starch by assessing this parameter on samples containing similar moisture contents but different concentration of glycerol (0, 10 and 20% glycerol mixture as shown on table 7.2).

The monitoring of the ageing of these samples (changes on the mechanical properties) was done by measuring the changes in flexural modulus over time using the Texture Analyser (TPBT method). This technique presents some advantages over calorimetry as it gives direct information on the changes in texture over time.

The samples were stored at 25°C (± 1°C) until complete retrogradation (no further detectable increase in the modulus). Each of the starch-glycerol samples after extrusion was dried at 70°C for different times in order to obtained three

different moisture contents (sample preparation followed same protocol as described in chapter 3, section 3.3.2.2)

As the evaluation of the modulus at different ageing times was done on the same samples, a small strain (0.3%) was applied during the measurement. In order to avoid moisture change during the analysis, each of the extruded ribbons were covered with a layer of silicone oil (Corning, USA). After the measurement the samples were wrapped and stored in hermetically sealed aluminium bags and put back to incubate at 25°C (± 1°C).

Table 7.2. Moisture content (wb) of wheat starch (WSE) and wheat starch-glycerol extrudates after drying for different times at 70°C.

	Drying Time (h)	*Control Sample*	*WSE 10% Glycerol*	*WSE 20% Glycerol*
Moisture Content % 1	3.0	11.2 (0.14)	8.3 (0.13)	12.1 (0.18)
Moisture Content % 2	1.5	14.4 (0.12)	15.5 (0.16)	15.9 (0.18)
Moisture Content % 3	1.2	19.5 (0.16)	18.3 (0.20)	18.8 (0.17)

Moisture content was estimated gravimetrically by drying the samples in vacuum at 70°C overnight overnight. Values represent the mean of replicates measurements with its associated difference between the first and second measurement (values in brackets).

Figure 7.4 show the changes in the flexural modulus of wheat starch extrudates with moisture contents of 11.2%, 14.4% and 19.5% (db). The modulus for the sample containing 11.2% moisture increased slightly during storage, from ~ 250 N/cm^2 to ~ 290 N/cm^2 over 800h. This increase was simply described by a linear function. Similarly, the wheat starch extrudate containing 14.4% moisture shows a very little increase in modulus over the same storage time, from ~ 140 N/cm^2 to ~ 145 N/cm^2. This curve was also modelled by simple linear function.

The difference in the modulus values between these two mixtures at time equals 0 hours (~ 250 N/cm^2 for the 11.2% moisture and ~ 140 N/cm^2 for the 14.4% moisture) can be attributed to the difference in solids fraction but also by the softening effect of moisture on the stiffness of these samples. Indeed, figure 6.4 C in chapter 6 indicates that both points, although in the glassy state,

are on the transition zone from a stiff to a ductile material, where small variation in moisture can have a significant impact on the mechanical properties of wheat starch extrudates.

A different behaviour was observed for the wheat starch extrudate containing 19.5% moisture. After a slow increase in the modulus for storage time < ~ 300 h, a steep increase in this parameter was detected, from ~ 250 N/cm^2 to ~ 1600 N/cm^2 when ageing time reached 600h. After this time, the value for flexural modulus remained constant. This s-shaped ageing profile has been interpreted as the results of a combined function of crystal growth rate and the density of nucleation (Farhat, Blanshard et al. 2000). The rate of nucleation is high at temperatures close to Tg, due to extensive supercooling. Propagation increases with increasing temperature by facilitation the molecular diffusion until the melting temperature Tm is reached, where a liquid phase is thermodynamically more favourable (Roos 1995).

The small increase at ageing time < ~ 300 h, can be explain by the small difference between the Tg of this sample (~20°C) and the ageing temperature (25°C). It is possible that crystal nucleation was favoured over propagation. The latter being the stage of the re-crystallisation process usually detected by this method.

It has been suggested that large deformation tests such as three point bending test (TPBT) are sensitive to detect the second stage of the retrogradation process, when the actual helices aggregate together (Ottenhof 2003). Following this rationale, it is possible that the formation of the initial double helix of the amylopectin present in the wheat starch extrudates at ageing time < ~ 300 h) was not detected.

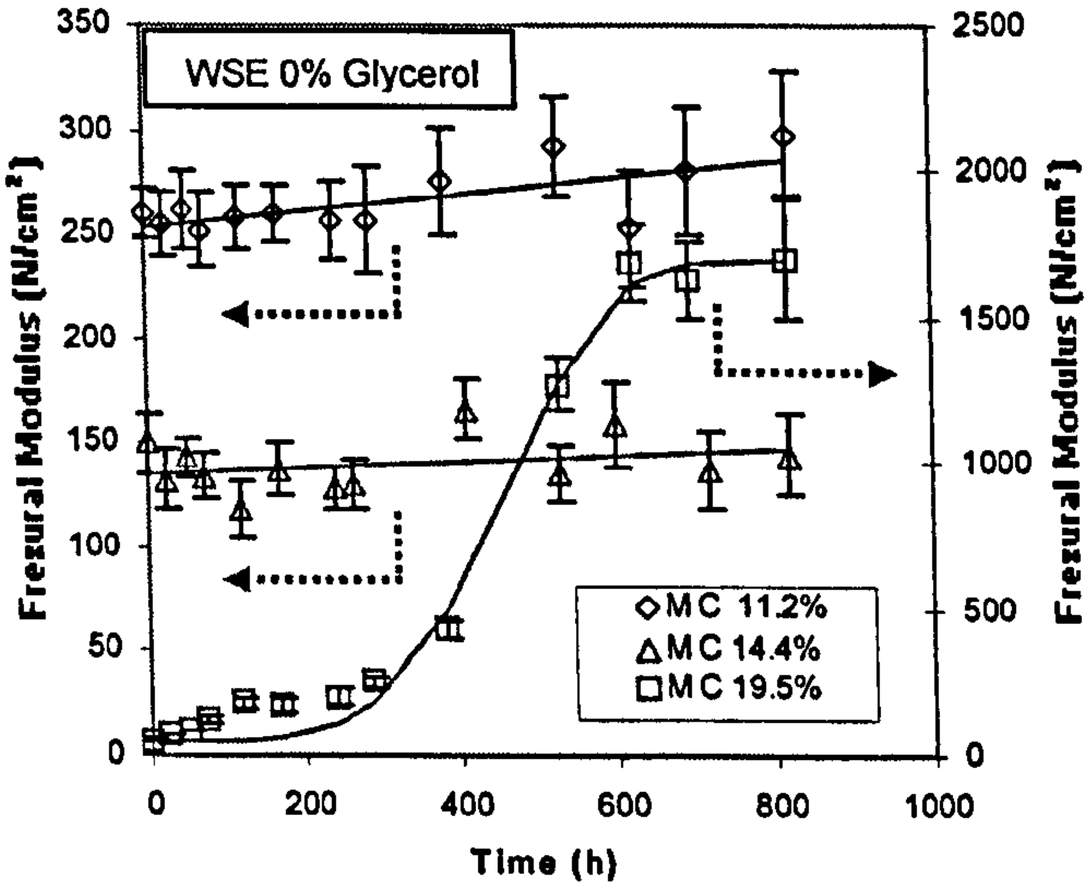

Figure 7.4. Changes in the flexural modulus (TPBT) for wheat starch-water extrudates stored at 25°C. Error bars represent ± 1 standard deviation of 5 measurements.

As discussed previously in this chapter, the difference in ageing profile can be related to the difference in molecular relaxation mechanisms. This would be dependent on the actual physical state of the material at the starting point of the storage. Based on the results presented on figure 5.4 in chapter 5, the glass transition for wheat starch with 11.2% and 14.4 % (db) is ~ 90°C and ~ 60°C respectively suggesting the samples were stored in their glassy state.

The mechanical properties of amorphous polymers below their Tg can also be affected during storage. As already discussed on this chapter, the ageing mechanism below Tg or "physical ageing" is characterised by the reduction of the available free volume leading to structure densification and an increase in the material stiffness and brittleness. This ageing mechanism is kinetically slower than retrogradation suggesting that the small increase in the flexural modulus during the storage occur via this molecular relaxation phenomenon.

In the case of wheat starch and 10% glycerol containing ~ 8.3% moisture, the modulus showed a similar increase as for the control sample (0% glycerol) stored in the glassy state (11.2% moisture). Indeed, the obtained Tg for wheat starch with this moisture and glycerol concentration was ~ 70°C, a temperature

which is well above the storage temperature (25°C), suggesting that these samples were also stored in the glassy state.

As expected, the ageing profiles for the wheat starch 10% glycerol (figure 7.5 left), containing ~ 15.5% and ~ 18.3% moisture, retrograded as they were stored in the rubbery state (the estimated Tg for these mixtures was ~ 20°C and ~ 10°C respectively (figure 5.5 (B) in chapter 5).

In the case of wheat starch and 20% glycerol (figure 7.5 right), the three moisture contents retrograded, with a steep increase in the modulus at very short times until ~ 250h, after which the increase in of the modulus began to level off reaching at plateau at ~350h. Indeed, the Tg of the three starch type glycerol systems was below the storage temperature (< 25°C) (figure 5.5 (D) in chapter 5).

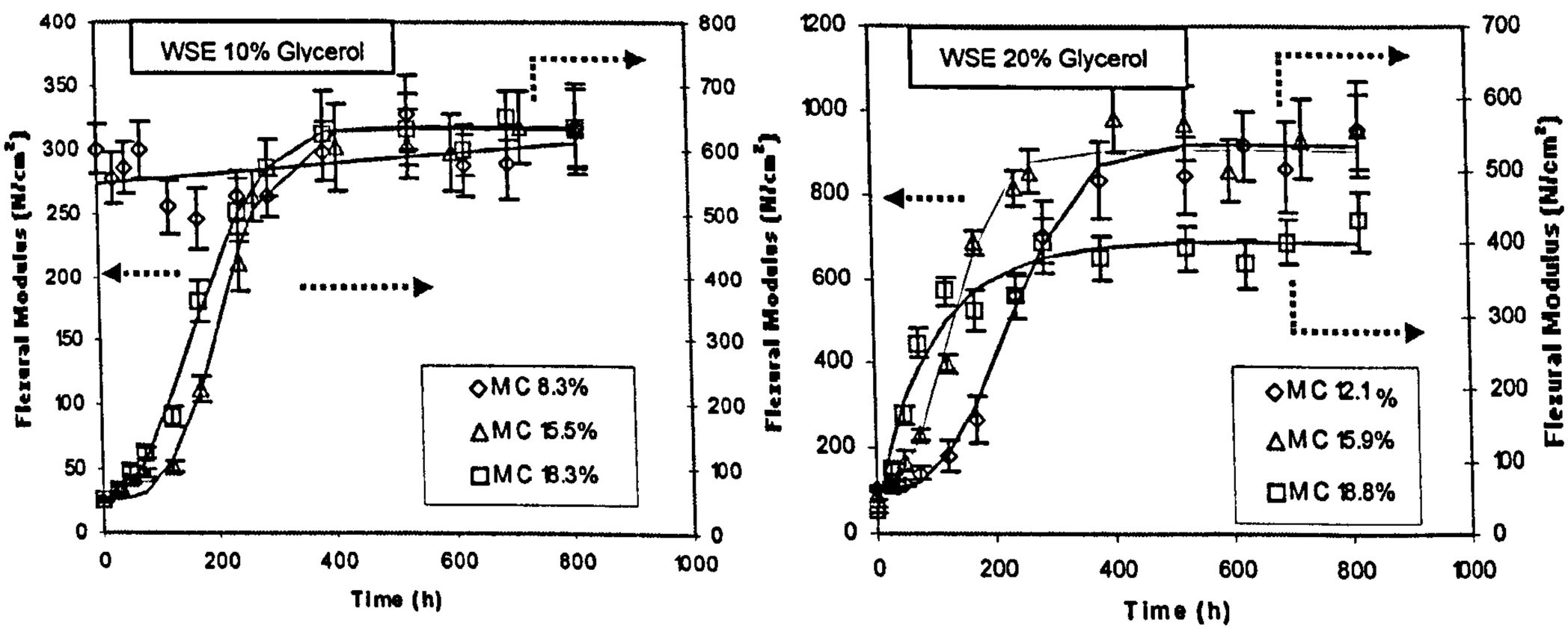

Figure 7.5. Changes in the flexural modulus (measured by TPBT) for wheat starch and 10%, 20% glycerol extrudates stored at 25°C. Error bars represent ± 1SD

Each of the curves showing an increase in the modulus according to a re-crystallisation mechanism was modelled using the Avrami equation (*equation 7.1*). Table 7.3 shows the retrogradation kinetic parameter G (h^{-1}), after fitting this model on the experimental data (Solver in Excel, Office 2003, Microsoft Corp.)

Table 7.3. Retrogradation kinetic for wheat starch-glycerol extrudates at various moisture contents modelled by Avrami equation. Samples aged at 25°C.

	G (h^{-1})	R^2
WSE 0%G 19.5%MC	2.0E-03	0.99
WSE10%G 15.5%MC	4.3E-03	0.99
WSE10%G 18.3%MC	5.0E-03	0.99
WSE 20%G 12.1%MC	2.7E-03	0.98
WSE20%G 15.9%MC	6.5E-03	0.99
WSE20%G 18.8%MC	9.6E-03	0.97

* MC: moisture content dry weight (db)

It seems there is a correlation between the concentration of plasticisers and the increase in the value *G*, varying from 2.0E-03 h^{-1} for the control sample (no glycerol) with ~19.5% moisture to 9.6E-03 h^{-1} for the wheat starch containing 20% glycerol and ~19% moisture content.

Figure 7.6 (A) depicts the change in the retrogradation rate (*G* h^{-1}) with moisture and glycerol content. It seems that increasing the amount of glycerol would increase the retrogradation rate. If ~ 16% moisture content is taken as a reference, the retrogradation rate increased from 4.3E-03 h^{-1} for wheat starch and 10% glycerol to 6.5E-03 h^{-1} for the starch extrudate containing 20% glycerol.

Figure 7.6 (B) shows the same retrogradation rate data but plotted against T-Tg, where T is the storage temperature (25°C) and Tg is the glass transition for each of the samples (data presented in chapter 5). It is interesting to note that the *G* values for most of the wheat starch-glycerol extrudate fall on the same curve describing the increase in the retrogradation rate when the difference T-Tg also increased.

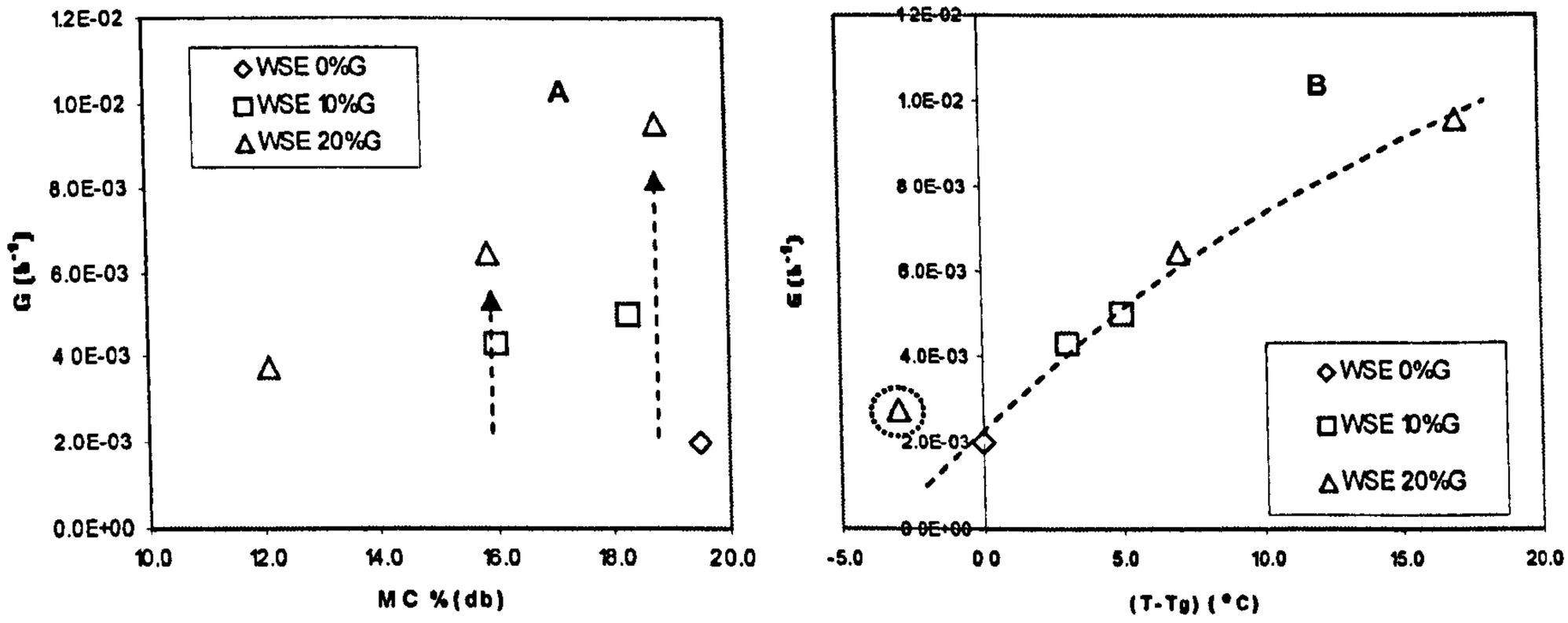

Figure 7.6. Retrogradation parameter G (h^{-1}) v/s Moisture Content % (db) (A) and G (h^{-1}) v/s T-Tg (°C) (B) for wheat starch-glycerol undergoing re-crystallisation. T is the storage temperature (25°C).

Just the G value for wheat starch 20% glycerol and ~ 12.1% moisture (circled data point) seems to be high for its measured Tg. It is unlikely to be an experimental artefact as the moisture content was tightly controlled and the modulus plotted value calculated from the mean of 5 replicates.

Looking figure 5.2 C in chapter 5, the extrudates containing 20% glycerol seems to be slightly overlapped onto the 10% glycerol samples at moisture contents > 12% wb. It was argued that a glycerol rich phase might have formed at this polyol concentration. This polyol rich phase would attract water molecules from the starchy matrix, increasing the overall Tg of the sample. It is possible that this phase could be slowly redistributed through out the polymer reducing its Tg. A lower Tg would result in a higher T-Tg value, shifting the obtained circled G towards the right values plotted in this graph.

The plasticizing nature of glycerol makes the evaluation of its effects on the starch retrogradation very complex. In an attempt to clarify this point, fresh wheat starch-glycerol extruded samples were equilibrated to similar moisture contents by drying the extruded samples for a short time at 70°C. The final moisture content of all the samples after equilibration was ~ 35% db. These

samples were incubated at 40°C until no further increase in the retrogradation was detected.

As shown in figure 5.3 in chapter 5, at ~ 30% db moisture content, glycerol does not seem to reduce Tg of wheat starch. Therefore, equilibrating these samples at constant moisture, would eliminate the plasticising factor from any significant change on the retrogradation rate occurring on these systems.

Differential scanning calorimetry (DSC) was used to monitor the changes in enthalpy related to the disruption of re-crystallised wheat starch after ageing at different times. TPBT was not used; at this moisture content range it is very difficult to control variations in moisture content during the measurement.

The calculation of the kinetics parameters was done by applying the Avrami model (equation 7.1) on the changes of the endotherm enthalpy during extrudate storage. DSC stainless steel pans were filled with pure wheat starch as the control, wheat starch 10% glycerol and wheat starch 20% glycerol extruded samples. The pans were sealed and scanned from 5°C to 140°C. In order to normalise the conversion enthalpies of all the samples to 0 J/g at storage time = 0 h, all the pans were scanned once and then stored at 40°C. After each measurement the same pans were stored back at 40°C until sufficient data points were obtained for a complete ageing profile from fresh to completely retrograded samples.

Figure 7.7 depicts the DSC scans for the wheat starch extrudates (control sample) and wheat starch and 20% glycerol after aged at 40°C. It is clear that there is an increase in the endotherm associated to the conversion of an ordered structure that was formed during storage. The peak temperature at which the melting endotherm started to form during storage was ~ 117°C (4.5 hours). This value correlates well with the finding on a retrogradation study by Lionetto *et al.* (2005) where the retrogradation of wheat starch extrudate with similar moisture content was also monitored by DSC. They detected a similar endotherm developing at 106°C during the samples storage. This slight difference in conversion temperature can be attributed to the higher moisture content of the samples used in this experiment (35% db) compared to 37% db used in Lionetto's work.

An interesting finding on these scans was the development of a shoulder at lower temperature (~75°C), which also increased with storage time. The origin of this endotherm is not clear, but is has been suggested that crystal perfection (annealing) may occur during the heating of the sample leading to a second endotherm at higher temperatures (Biliaderis, Page et al. 1986). Kinetically, it is unlikely to occur at the time scale of this experiment where the heating rate of each sample was 10°C/minute, in other words it would take just 4 minutes from the first endotherm at 75°C to the second peak at 117°C. The presence of two crystalline starch polymorphs mixed together is also unlikely as the moisture content present on the samples (35% db) and the storage temperature (40°C) at which the samples were aged conditions would favour the formation of only Type A crystal polymorph.

A more convincing hypothesis to explain this type of DSC traces is that the lower temperature endotherm is related to the disruption of the packing of double-helices of the amylopectin A and B chains, while the higher temperature endotherm reflects the actual dissociation of double helices (Lionetto, Maffezzoli et al. 2005).

Very similar values, in terms of endotherm peak temperatures, conversion enthalpy and curve shape (shoulder at lower temperatures) were detected for the wheat starch, 10% and 20% glycerol mixtures (DSC scans for 10% glycerol not shown).

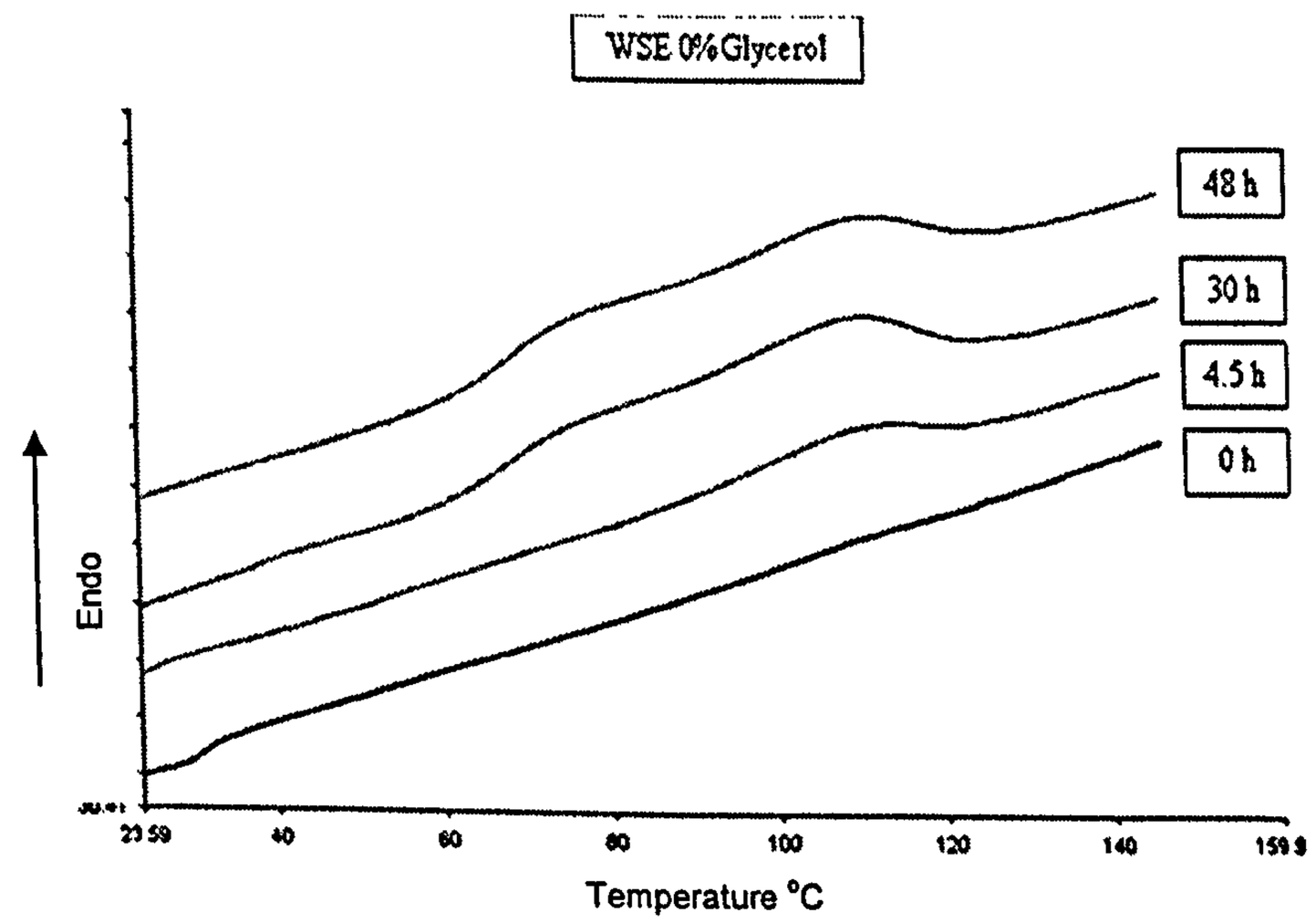

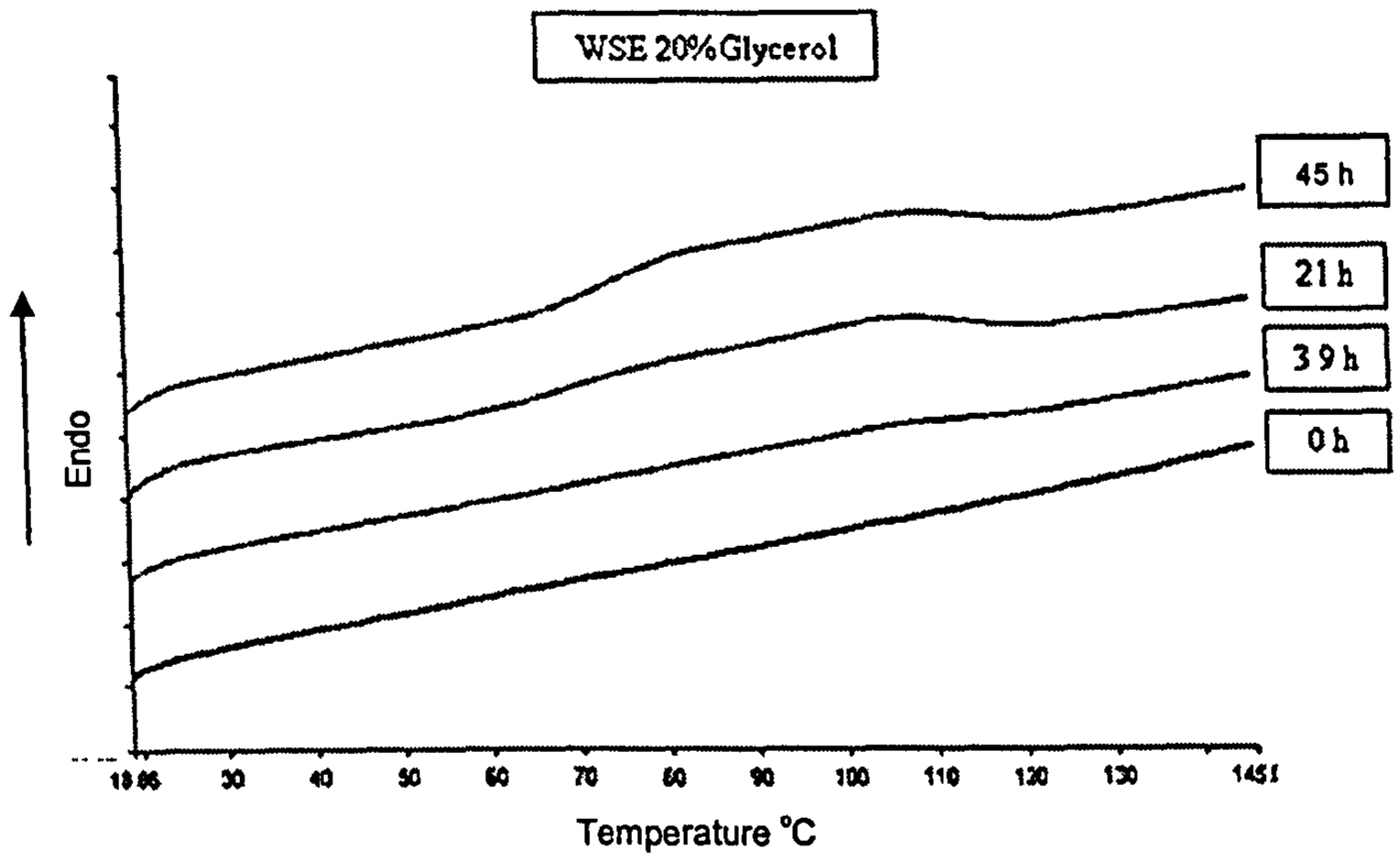

Figure 7.7. DSC scans (1st run) for wheat starch (top) and wheat starch-20% (bottom) glycerol 35% (db) extrudates after ageing at 40°C for different times.

The increase in enthalpy for the extruded samples was plotted against time. Figure 7.8 shows the typical retrogradation profile for a starch based material; a steep increase in enthalpy soon after the sample was stored and then a gradual reduction on the rate of this increase towards a final plateau.

All the samples showed a rapid increase in conversion enthalpy, from 0 to ~ 7 J/g of starch, for storage time < ~ 22 hours. Reaching this point, the retrogradation rate decreased towards a final plateau value of ~ 9 J/g of starch.

Although this value seems be slightly higher when compared with the literature for wheat starch retrograded systems (~ 5 J/g obtained by Joupilla and Roos 1997, Karim 2004, Kohyama 2004, Otthenhof 2005), none of them reported the development of second peak during retrogradation. As it has been discussed previously, Lionetto *et al.* (2005) detected similar endotherms with two overlapped peaks on the aged wheat starch samples with similar moisture contents. The enthalpy measured for the fully retrograded samples were ~ 8 J/g starch, which is very similar to the enthalpy measured on the control and wheat starch-glycerol samples during this experiment.

Overlapped over the experimental data points in figure 7.8, are the modelled curves (dotted lines) from the optimisation of the Avrami equation. The final values for the rate of retrogradation ($G\ h^{-1}$) on figure 6.5 showed there were not

mayor differences between the control sample and the extrudates containing 10% and 20% glycerol ($G \sim 7.5$ E-02 h^{-1}).

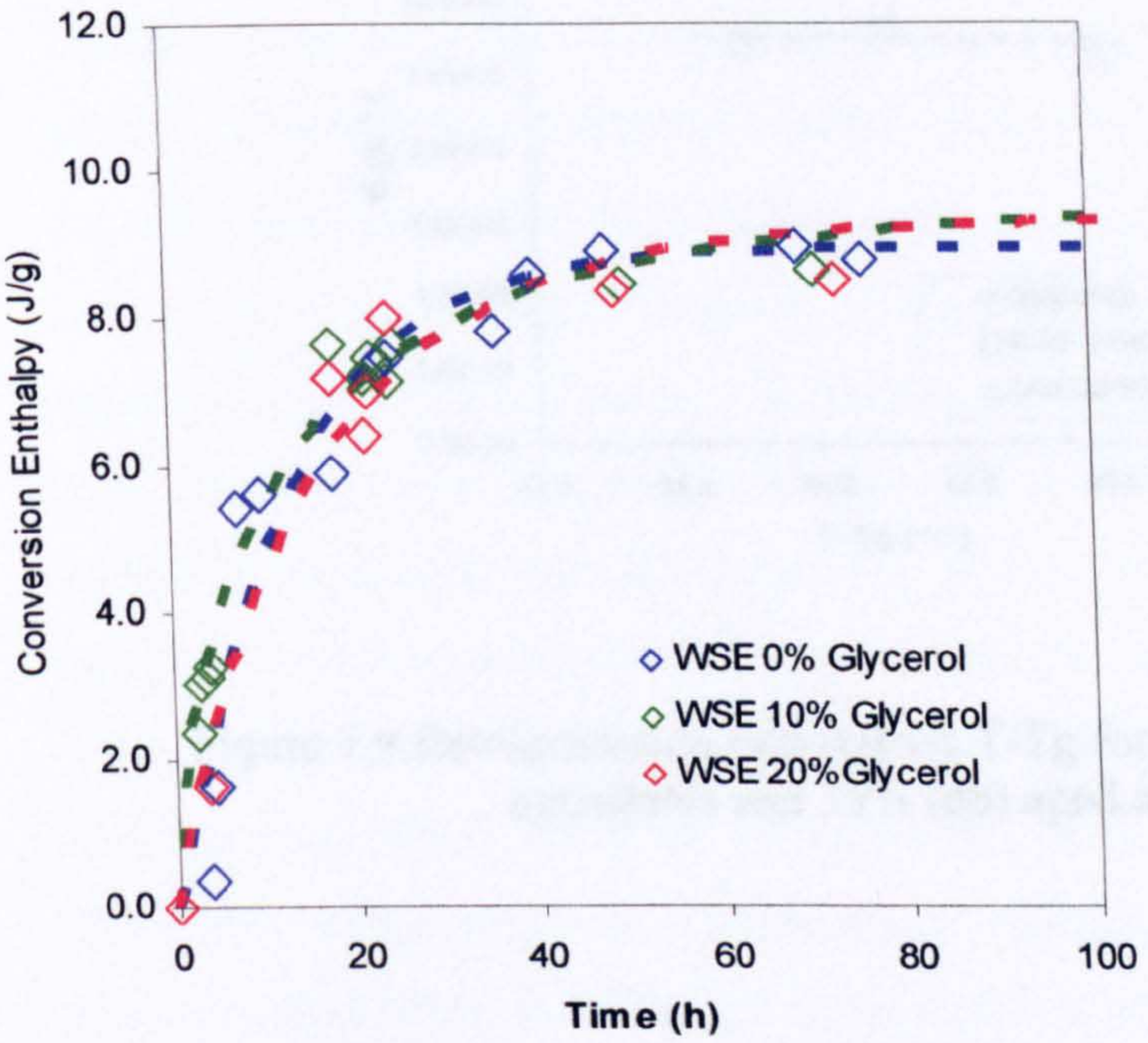

Rate of retrogradation	G (h^{-1})
WSE 0%Glycerol	7.4 E-02
WSE 10%Glycerol	7.6 E-02
WSE 20%Glycerol	7.2 E-02

Figure 7.8. Changes in conversion enthalpy for wheat starch and wheat starch-glycerol and 35% (db) moisture extrudates aged at 40°C. Table indicates the values for the retrogradation rate G (h^{-1}) obtained after applying Avrami equation.

These findings suggest that glycerol does not have an effect on the retrogradation kinetics of wheat starch when the starchy matrix has been highly plasticised by sufficient amounts of water. This can be clearly observed on figure 7.9, where G values are plotted against the difference in the storage temperature and the samples glass transition temperature (T-Tg).

It is possible that at the studied moisture content (35% db), glycerol molecules are partially displaced by the more ubiquitous nature of water, reducing any potential interaction between this polyol and the polymeric chains of amylopectin/amylose.

7.4 Conclusions

It seems clear that adding glycerol to intermediate moisture wheat starch would increase the extent of hardening of these materials over time (as shown by large deformation (TPBT) and small deformation measurement (DMTA)). The kinetics associated to this increase can be explained by the ageing mechanism, which is determined by molecular mobility of the system during the storage.

For the lower moisture content mixtures, the increase in the modulus seems to be related to the so-called "physical ageing" where structural relaxation and subsequent densification occur. Although, it seems unlikely that glycerol may have an effect on the relaxation kinetics by molecular interactions with the starch, it is possible that its plasticising effect could have varied the T-Tg value. It is well accepted in the literature that the closer the Tg value is to the ageing temperature, the faster the molecular relaxation will occur (Lourdin, Colonna et al. 2002). When the Tg of starch-glycerol mixture was higher than the storage temperature, the increase in the modulus was associated to starch retrogradation. This would support the initial hypothesis suggesting that the kinetic of hardening would be a function of the transition temperature from the glassy to rubbery state.

As suggested at the beginning of this chapter, the obtained retrogradation rate value (*G)* from of Avrami equation, showed to be positively correlated with the concentration of glycerol as demonstrated by plotting *G* values as a function of T-Tg.

The ageing experiment on wheat starch-glycerol systems containing high moisture contents (35%db) showed that the retrogradation rate (*G*) did not show any dependency on this polyol concentration. This can be explained by the already water plasticised polymeric chains of the starch. Increasing the amount of glycerol (~10% and 20%) would form a polyol rich phase reducing its plasticising effect on the starch and hence the T-Tg values would not have varied significantly.

8 Mechanical Stability of Starch Based Pet-Care Products

Pet-care products are the fastest growing sectors in the pet food market with a turnover of near £230 millions in 2004 in Europe.

These novel products have several advantages from traditional wet based foods. They are typically very simple to serve and don't need refrigeration during storage. They have been designed to have other functionalities besides nutrition such as having an abrasive effect to remove dog's tooth plaque. The formulation of these materials are commonly based on cereal starches that are believed to have the function of holding together other compounds and to provided desired textural attributes.

One the main characteristic of these materials is their low water activity (Aw), which allow them to be microbiologically stable over long periods of time. In order to achieve this reduction in the water vapour pressure in the product, polyols such as glycerol are usually included during formulation. It is believed that the hygroscopicity of these compounds attracts water molecules in the mixture reducing the overall Aw. Other effect of these low molecular weight compounds is their plasticizing effect, decreasing the glass transition temperature (Tg) of the starchy matrix, contributing to the softness/ductility of these products.

Although the low Aw of these products makes them safe to be consumed after long storage (> 6 months), changes in their texture have been reported. These changes are related to a substantial increase in the hardness, possibly affecting the product digestibility and increasing the risk of injuries to animals teeth and digestive track. The mechanism causing these changes in texture are not well understood, neither the influence of storage variables such as temperature and relative humidity.

The aim of the experimental work presented here is to identify the hardening mechanism driving this process and to test predictive models already applied on simpler systems.

8.1 Hypothesis

The ductile nature of these commercial products is directly related to the glass transition temperature of the starchy component, which suggests they are in a rubbery state at ambient temperature (~ 25°C). Hence the textural changes in the structure of these products during storage are related to a recrystallisation process of the starch component. Therefore difference in magnitude between the storage, the glass transition temperature (Tg) of the polymer is the main variable controlling this process during storage.

The experimental work focused firstly on the characterisation of these complex materials using different analytical techniques. Later, the water sorption and ageing kinetics were assessed and modelled using the equations already tested on extruded starch glycerol systems studied and discussed in previous chapters of this thesis.

8.2 Background Information

Extrusion cooking of pet foods can be regarded as the cooking of raw ingredients, shaping and cutting the product into a specific shape and size in a very short space of time, while simultaneously destroying detrimental micro-organisms. The ingredients are mixed into homogenous dough and cooked in an extruder (steam/pressure) and forced through a specially designed die plate under pressure and heat (figure 8.1). This causes rapid cooking of the starches within the product, resulting in increased digestibility.

After cooking, the semi-finished products are then allowed to cool, before being sprayed with a coating which includes liquid fat and proteins, to enhance digestibility and add protein and fat to the food. Hot air drying then reduces the total moisture content to ~10%.

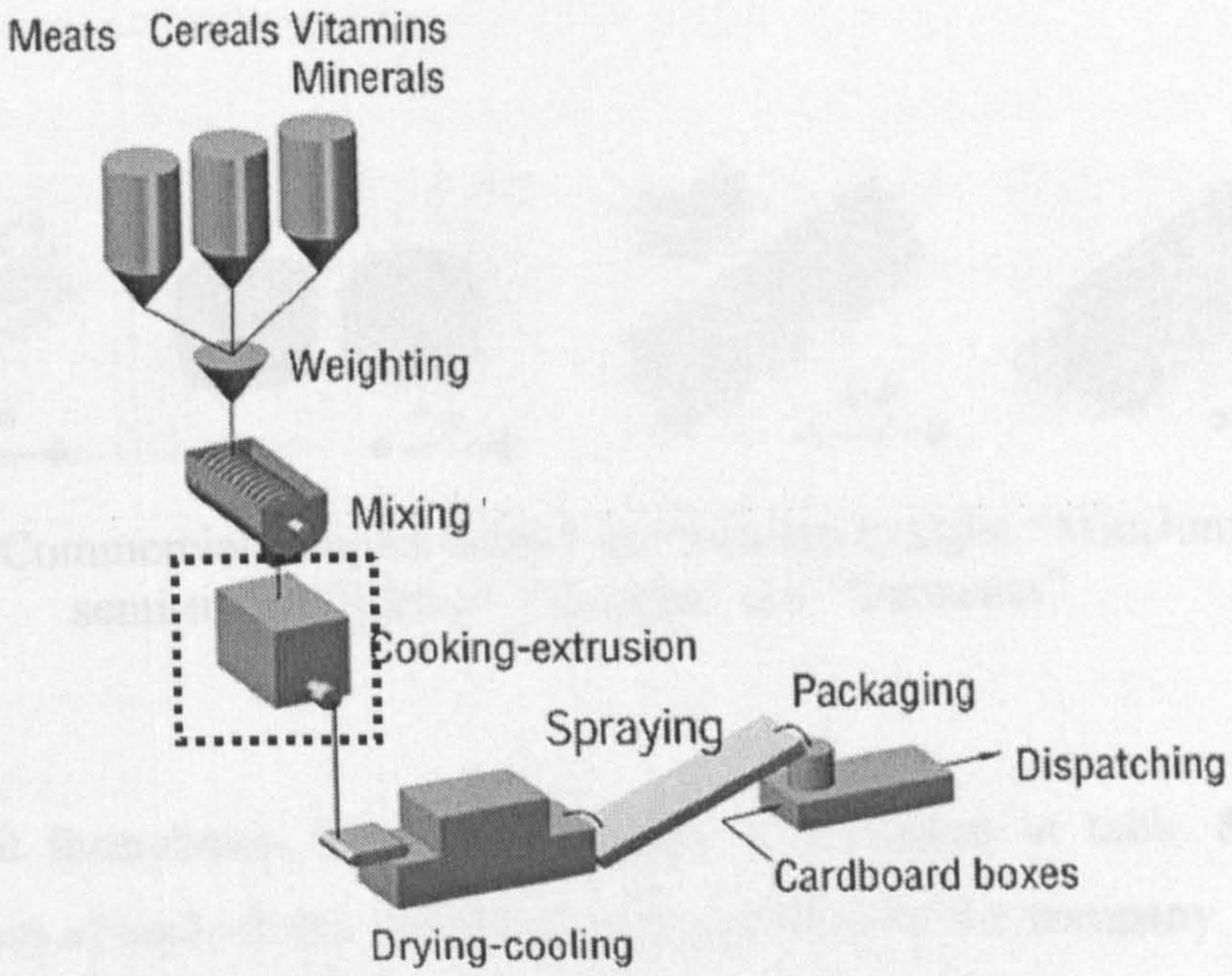

Figure 8.1. General diagram describing the pet-food extrusion process.

For this type of products, extrusion-cooking presents some advantages over other pet food technologies. It is a high productive operation unit compared to other dry food manufacturing processes as it allows for the continual production of different sizes and shapes of product without delay in production

In the next section, the experimental work done on various pet-care products, which have the common problem of texture instability (increasing stiffness during storage) is presented.

8.3 Experimental Work on Pet-Care Products

In the first part of this work, the characterisation of the physical state of a number of different pet-care products is discussed. The second part focuses mainly on the mechanical stability of two products selected based on the manufacturer interest.

The samples analysed were commercial pet-care products sent by Masterfoods, manufactured in UK and France (figure 8.2).

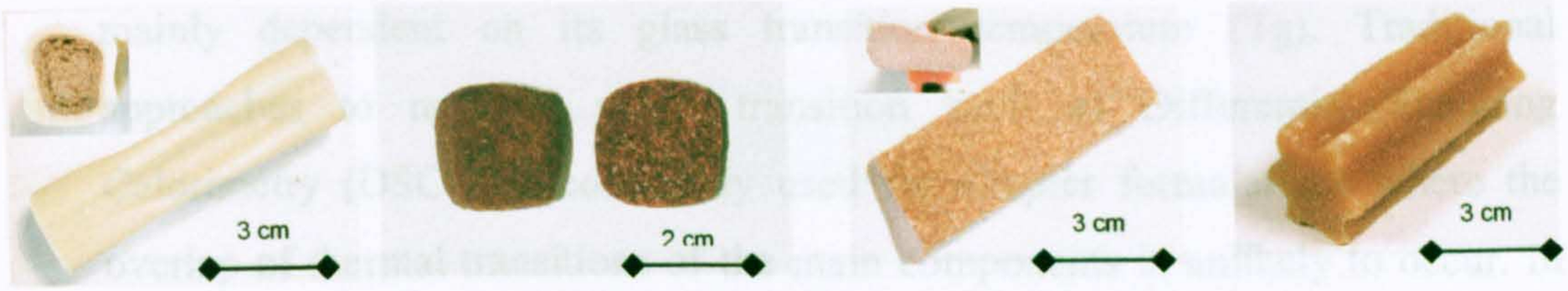

Figure 8.2. Commercial samples named as, from left to right, "MiniJumbone", semi-moist "Kibble", "Rancho" and "Dentastix"

The general formulation for these products is presented in table 8.1. The concentration of each of the ingredient was provided by the company with the exception of the water activity and moisture content, which were measured experimentally. The fresh samples were kept at –80°C prior to the analysis.

Table 8.1. General formulation for Pet-care products as provided by Masterfoods.

Product	Rice Flour	Wheat Flour	Other Compounds	Salts	Glycerol	Glycol	Water Activity (*)	MC % (wb) (**)
MiniJumbone	35%	26%	8% (icing sugar)	6%	7%	3%	0.61 (0.04)	13.7% (0.2%)
Kibble	48% (wheat, maize)		20% (meat derivatives, fat 2%)	5%	7%	3%	0.55 (0.02)	17.0% (0.3%)
Rancho	45%	10%	10% (whey Permeate, poultry liver)	6%	15%		0.50 (0.03)	14.2% (0.3%)
Dentastix	40%	15% (pregelatinised starch)	14% (guar gum + gelatine)	8%	10%		0.60 (0.02)	13.7% (0.2%)

(*) Water activity was measured on the ground sample in triplicates using a Aw meter AquaLab Series 3 Model TE (Decagon Devices inc.).
(**) The moisture content of the samples was determined gravimetrically (vacuum oven 70°C overnight). The final value is the mean from three measurements.

In order to improve our understanding of the mechanical behaviour of these materials, it is important to evaluate the physical state of the main components as it may contribute to the overall stability of these products. Analytical techniques used in the characterisation of the extruded starch-glycerol models

were used on these systems. These include Texture Analyser (TA), Dynamic Mechanical Thermal Analyser (DMTA), Differential Scanning Calorimetry (DSC) and X-ray diffraction.

8.3.1 Characterisation of Pet-Care Products

As discussed before, the ageing mechanism of the polymeric component is mainly dependent on its glass transition temperature (Tg). Traditional approaches to measure phase transition such as Differential Scanning Calorimetry (DSC) are commonly used for simpler formulations where the overlap of thermal transitions of the main components is unlikely to occur. In the case of these commercial products, which contain a significant number of ingredients, calorimetric scans are not simple to interpret. Hence the first part of the experimental work presented is focused on the determination of the viscoelastic properties of the commercial product using Dynamic Mechanical Thermal Analysis (DMTA). This technique can report the changes in the stiffness (modulus) of the material at different temperature and frequencies, giving information on phase transitions such as the glass transition temperature or Tg for the product. Literature has also suggest that the reported tan δ value can shown the level of miscibility between the components (Mousia, Farhat et al. 2000). It has also been suggested that this parameter can indicate changes in molecular mobility of the polymer during storage (Lionetto, Maffezzoli et al. 2005).

Differential Scanning Calorimetry (DSC) and X-ray diffraction are used to assess the degree on crystallinity (molecular order) of the main polymeric components forming these mixtures.

8.3.1.1 Mechanical Spectroscopy of Pet-Care Products

Table 7.1 shows the complexity of these materials which contain cereals, proteins, polyols and water as major components. The advantage of using DMTA over calorimetry on this type of compositions is that the reported results are based on the mechanical spectroscopy profile on the mixture as a whole, rather than responses of each individual component. This has a significant value as a representation of the overall modulus of these products at different temperatures and frequencies.

Each of the samples were shaped as shown in figure 8.3 (no reformulation was needed). The dimensions for each sample were typically 15 mm length, 7 mm width and 2 mm thickness. The samples were covered with silicon oil (Corning, USA) to avoid moisture loss during the analysis. The test was done in triplicate.

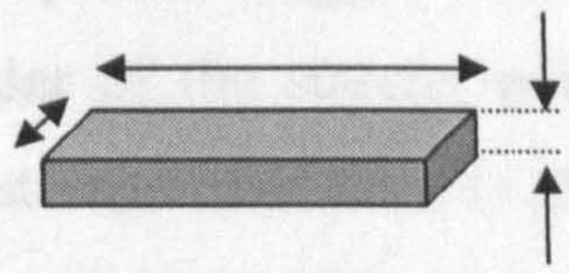

Figure 8.3. Sample shape for DMTA

The instrument used was a Rheometric Scientific Mk III DMTA. The experimental settings were: temperature range from -100°C to 120°C, heating rate of 3°C/min, and the set strain was x 4 (62 μm amplitude). The frequencies tested were 2, 5 and 10 Hz.

Next section shows the DMTA results for the commercial samples listed in table 8.1. For clarity, the data for changes on the elastic modulus (E'), loss modulus (E'') and tan δ versus temperature have been reported for 10Hz only.

Figure 8.4 depicts the DMTA profile for the commercial products named "MiniJumbone". Although complex in its composition, the DMTA data shows a typical profile for a single polymeric structure, suggesting a good integration between components. The decrease in the elastic modulus with temperature was four orders of magnitude and a major peak was detected in the tan δ versus temperature curve.

As can be observed in figure 8.2, the "MiniJumbone" is created by two different sections, a dark coloured core and a light coloured material on the surface.

The elastic and loss modulus data suggests that both sections have different mechanical properties indicating different composition. Indeed, curve A in figure 8.4 shows that the elastic and loss modulus being higher for the surface material at any given temperature, suggesting a stiffer material.

The glass transition (Tg) of the "core" and the "surface" components estimated from the tan δ peak was ~ 40°C and ~ 20°C respectively (vertical lines in figure 8.4 B). If the second peak of the loss modulus is considered, value seemed to be ~ -5°C for the "core" and ~ -15°C for the "surface" material (vertical lines in figure 8.4 A).

The reported Tg values for this product suggest that the physical state of the overall mixture and in particular of the starchy polymeric component is in rubber-like state under normal storage conditions (~25°C). This correlated well with the flexible nature of this product at ambient temperature.

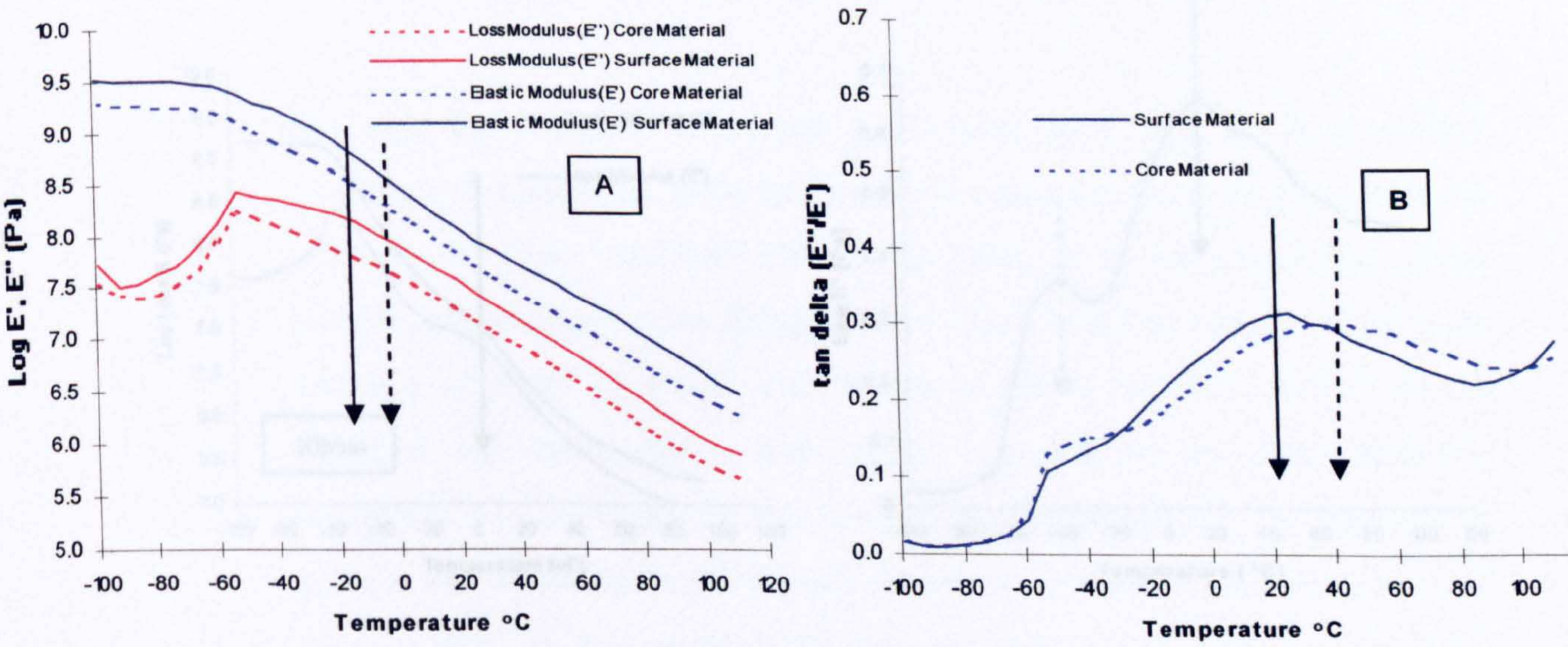

Figure 8.4. DMTA profile for commercial product "MiniJumbone". Curve A depicts the elastic (E') and loss modulus (E'') v/s temperature. Curve B shows the tan δ values v/s temperature. Measurements at 10 Hz.

Similarly, the other commercial products evaluated by DMTA showed a significant reduction in *E'* at the glass to rubber transition, with a decrease in 3-4 orders of magnitude in this value (figure 8.5 left). The estimated Tg values (*E"* second peak) for all the products were below the 25°C supporting the ductile-like mechanical behaviour at ambient temperature (table 8.2).

Table 8.2. DMTA glass transition values based on tan δ, elastic modulus (E') and the loss modulus (E'').

Commercial Product	*Tan δ Tg*	*E' Tg*	*E'' Tg*
MiniJumbone	20/40 °C (2.1)/(2.8)	-30/-40 °C (2.8)/(2.4)	-5/-15 °C (1.1)/(1.0)
Kibble	18 °C (0.9)	0 °C (1.1)	8 °C (1.0)
Rancho	22 °C (1.2)	5 °C (0.8)	10 °C (1.1)
Dentastix	30 °C (0.9)	5 °C (1.5)	20 °C (1.8)

(*) Values in bracket represent the standard deviation of three measurements.

The values for tan δ (figure 7.5 right) show clearly a second peak at lower temperature (~ -40°C) for the commercial products "Kibble" and "Dentastix" (green dotted line). The intensity of this peak was much lower for the products "MiniJumbone" and "Rancho" where it appeared as a small shoulder at the left of the tan δ peak.

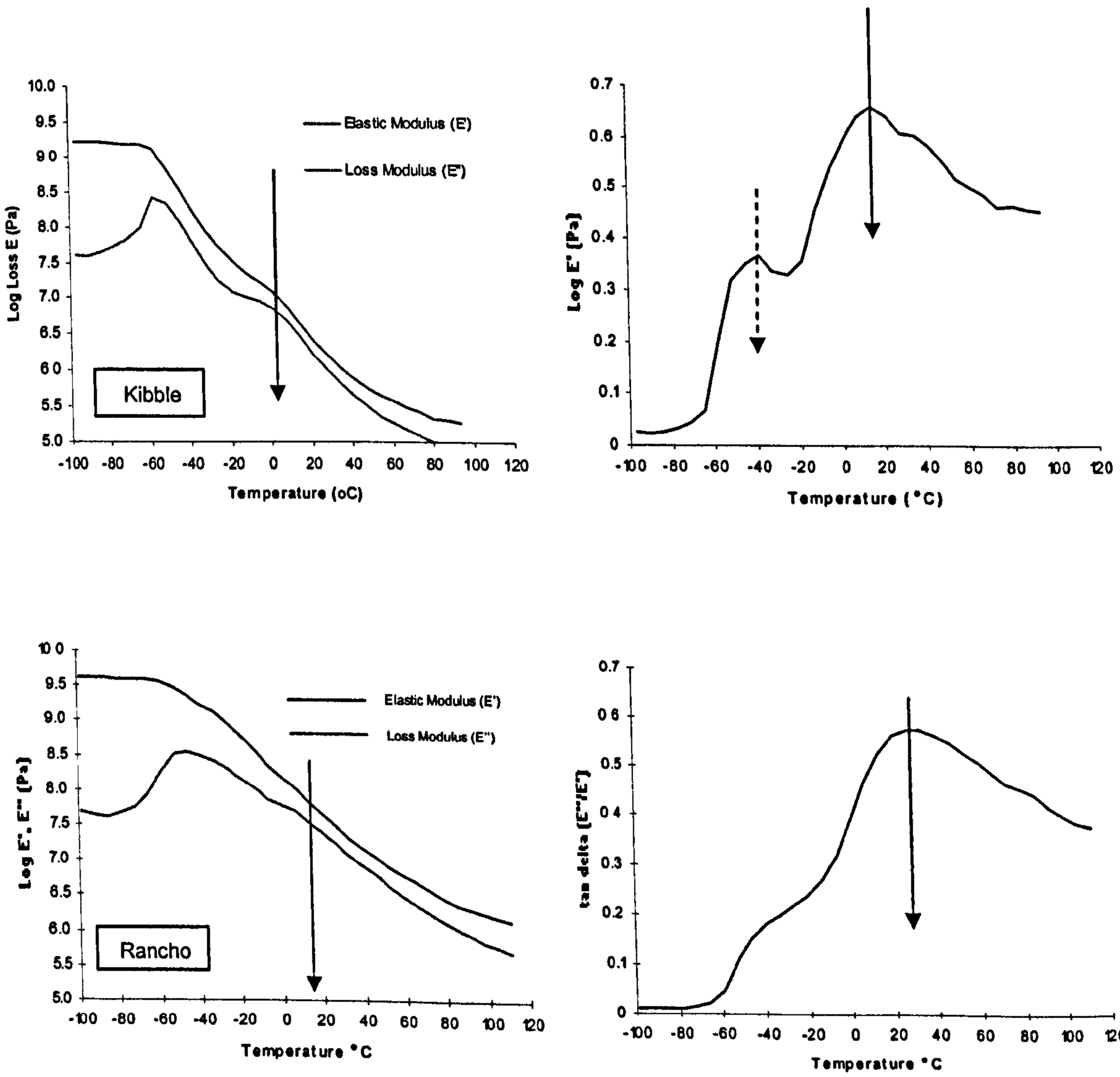

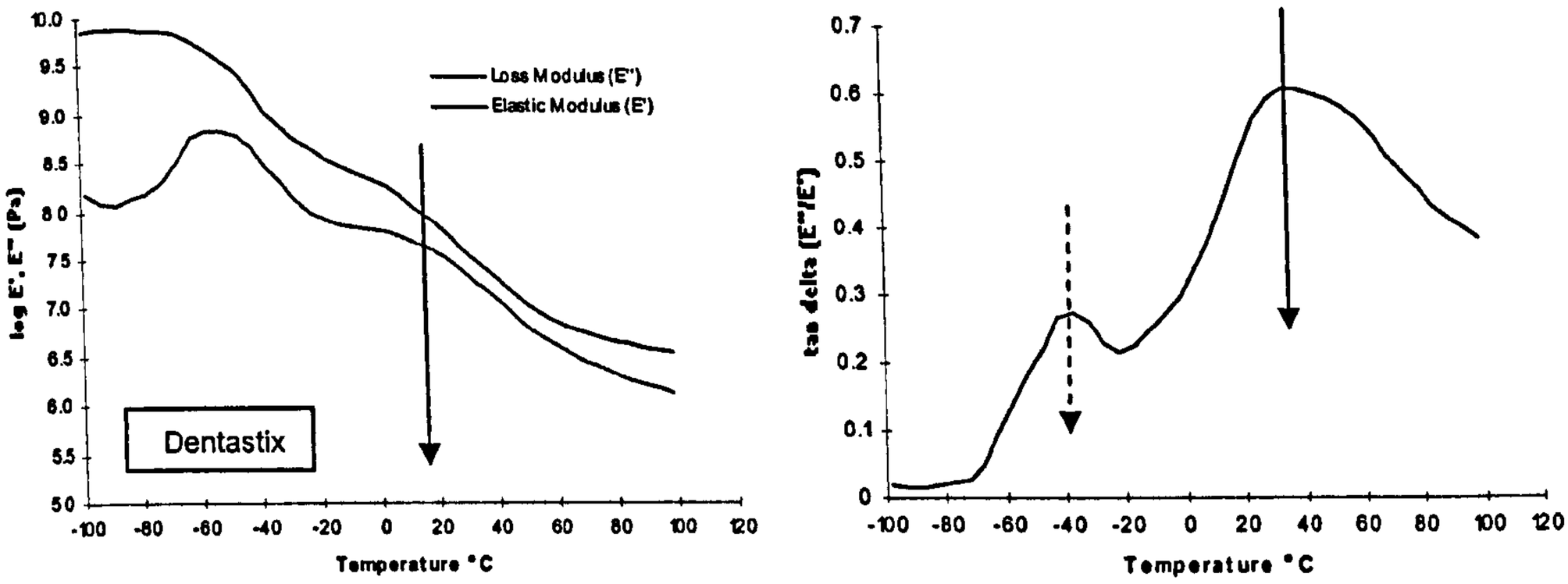

Figure 8.5. DMTA profile for "Kibble", "Rancho" and "Dentastix". Curve on the left depicts the elastic (E') and loss modulus (E'') v/s temperature. Curve on the right shows the tan δ values v/s temperature. Measurements at 10Hz.

Although, the origin of the second peaks have been attributed to secondary transitions (β-transition), related to local/short range mobility of polymer chain (Kalichevsky 1992; Swallowe 1999; Price 2002), it was not detected on all the samples suggesting another interpretation. They could be originated from the presence of phase separated components in the formulation. Indeed, in the literature has been shown that DMTA can detect the glass transition temperature of each of the phase-separated components, for example in gelatine and starch mixtures (Mousia, Farhat et al. 2000). This behaviour will be dependent on the compatibility between components and their molecular weights (Farhat 1996).

In the case of the formulation of "Kibble" with ~ 48% cereal starches it also contains ~ 20% meat derivatives (e.g. proteins). It is well known that proteins may not integrate well with starch, leading to a phase separated-type structure, (Mousia, Farhat et al. 2000).

Similarly, "Dentastix" contains ~ 55% cereal starches but in this case it also includes 14% gelatine and arabic gum in its formulation. It is possible that these two polymeric components did not integrate with starch, forming a separated phase with its own Tg.

Following this rationale, the DMTA profile for the products "MiniJumbone" and "Rancho" did not show a second transition of such magnitude at low temperatures on tan δ curve which could be explained by the lower concentration of other hydrocolloids in their formulations.

Now that the glass transition temperature (Tg) of the products was estimated, the next stage was to evaluate the degree of structural ordering present in these formulations. To do this, each sample was scanned using Differential Scanning Calorimetry (DSC) and by X-Ray diffraction.

8.3.1.2 Differential Scanning Calorimetry on Pet-Care Products

Pet-care products were characterised using calorimetry (DSC 7, Perkin Helmer). Prior the analysis, all the samples were ground under cryogenics conditions and mixed with distilled water at a solid water ratio of 1:3 (table 8.3) and equilibrated overnight by continuous rotation. The typical experimental conditions were: temperature scanning normally from 20°C to 130°C at a heating rate of 10°C/minute, cooling to 10°C at a cooling rate of 30°C/minute, re-heating from 5°C to 140°C at a heating rate of 10°C/minute. The samples were loaded into stainless steal DSC pans. The reported endotherm for all the samples are referred as J/g of samples.

Table 8.3. Example of sample preparation (*) in excess water for DSC measurements.

	Empty pan (g)	Pan + Sample (g)	Pan + Sample +Water (g)	Weight sample + water (g)	Sample (g)
MiniJumbo Core	0.315	0.324	0.349	0.034	0.009
MiniJumbo Surface	0.313	0.322	0.362	0.049	0.009
Kibble	0.313	0.324	0.349	0.036	0.011
Rancho	0.315	0.327	0.355	0.040	0.012
Dentastix	0.321	0.332	0.381	0.059	0.011

(*) DSC measurements were performed in triplicates.

Figure 8.6 shows the first and second scans for "MiniJumbone" core and surface components. The core material showed a small endotherm at ~ 55°C with an enthalpy of ~ 1.2 J/g on the first run but it was not detected on the second run, suggesting an irreversible transition at the time scale of the

analysis. The temperature at which the transition occurred, its enthalpy and irreversible nature would suggest the presence of unconverted or retrograded starch. Indeed, these are typical of the well documented conversion enthalpies at similar temperatures when analysed under excess water conditions for the retrograded starch samples (Karim et al. 2000; Hagenimana, Pu et al. 2005; Ottenhof, Hill et al. 2005) .

A second endotherm was detected at ~ 101°C, but in this case, it was detected on the first and second scan showing its reversibility. The detection temperature and endotherm (~ 0.67 J/g) can be associated with amylose-lipid complexes. These are formed when amylose molecules are leached out from the starch granule during processing, which then interact with the lipids present in the starch (e.g. wheat starch) and/or with the lipids added during the product formulation.

The surface material of the "MiniJumbone" showed a different DSC profile compared to the central core, with three endotherms detected on the first run. The first endotherm (going from low to high temperature) was measured at ~ 60°C with an enthalpy of ~ 0.44 J/g. This peak was not detected on the second run suggesting an irreversible transition associated to unconverted/retrograded starch material.

The second endotherm was also irreversible and was detected at ~ 85°C with an enthalpy of ~ 2.6 J/g. The origin of this peak seems to be related to the unconverted rice flour fraction in the formulation. Indeed, figure 8.7 shows the DSC scan (solid : water = 1:3) for the rice flour used in the formulation of these products.

The enthalpy for the pure rice flour was estimated in ~ 11 J/g, which if divided be the proportion of rice flour present in the product (25%) gives approximately ~ 2.7 J/g, which is similar to the enthalpy measured for the commercial mixture (~ 2.6 J/g). The shoulder detected at the onset of this peak might be related to other varieties rice flour blended together. Indeed, Hagenimana et al. (2005) using DSC to study the gelatinisation of single and mixed rice varieties showed that for certain mixtures two endotherms were detected and that the area of these peaks was proportional to the starch relative concentration.

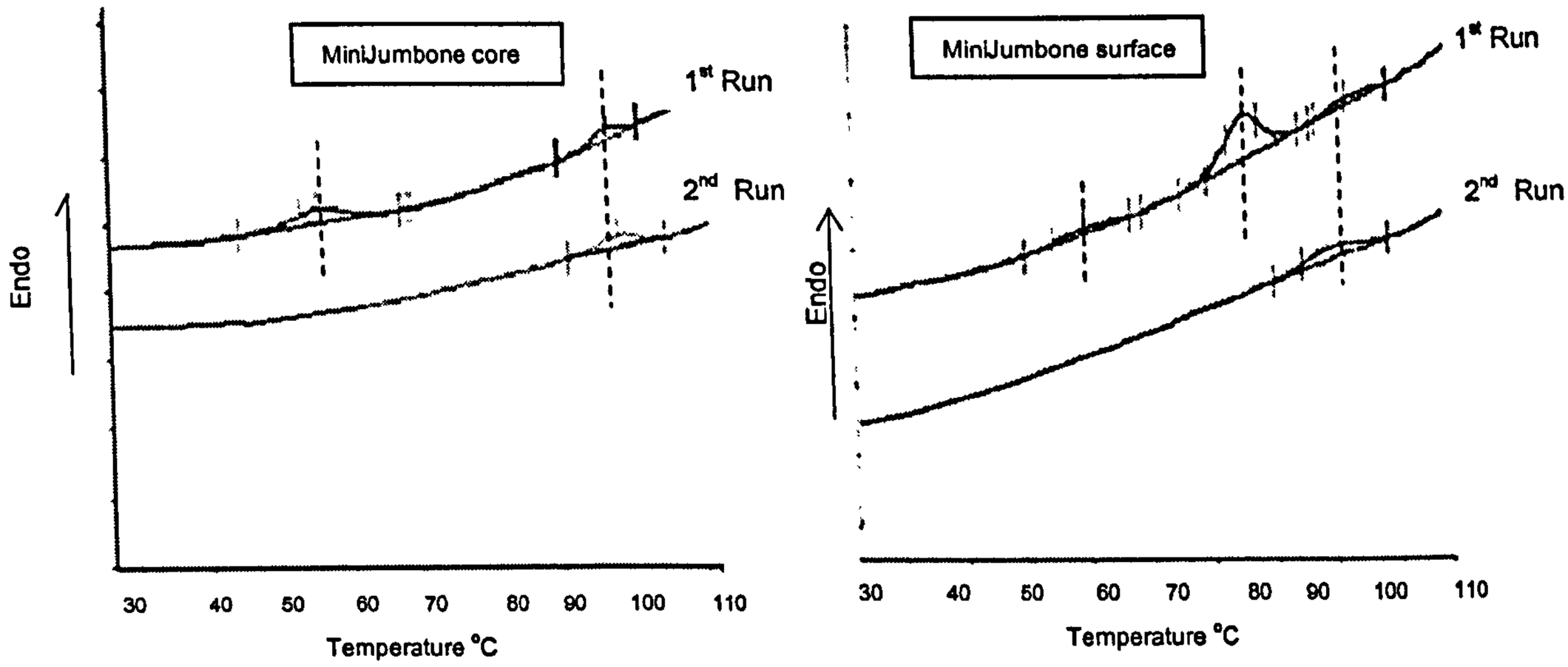

Figure 8.6. DSC scans (1st and 2nd runs) for "MiniJumbone", showing a different thermal profile between the core (left) and the surface (right) material.

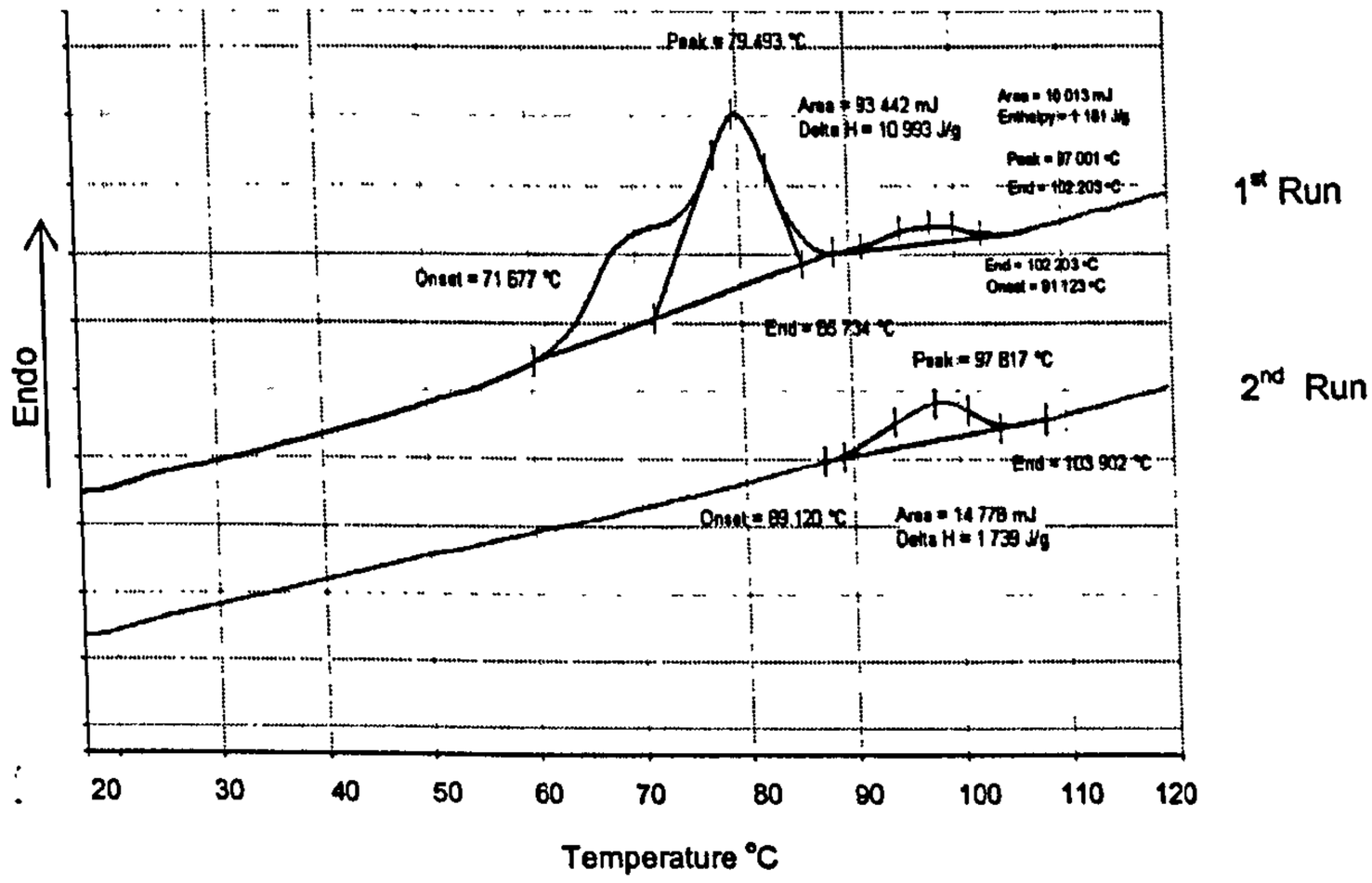

Figure 8.7. DSC scan (1st and 2nd runs) on "rice flour" used in the formulation of the commercial products.

A third endotherm peak was detected on the first run at ~ 102°C with a transition endotherm of ~ 0.43 J/g. This endotherm was also detected on the second DSC.

Although this peak on the second run was measured at similar temperature (~102°C), its area was greater giving an enthalpy value of ~ 1.0 J/g. It is possible that the amount of amylose available for lipid complexation was structurally immobilised as part of the unconverted fraction of starch. After the first DSC a complete gelatinisation was achieved freeing the amylose from the starch granules increasing its interaction with lipids.

Figure 8.8 depicts DSC scans for the commercial products "Keeble", "Rancho" and "Dentastix".

The first and second run for "Kibble" showed a irreversible endotherm detected at ~ 42°C with an endotherm of ~ 0.14 J/g which may suggest of the denaturation of protein component in the mixture. Another irreversible endotherm was detected at ~ 57°C with an enthalpy ~ 0.15 J/g. This enthalpy would suggest that most of the starch fraction in the mixture was converted during manufacturing of this product. Amylose-lipid complexes were not detected at higher temperatures (data not shown).

In the case of "Rancho" an endotherm was detected at ~ 84°C with an associated enthalpy of ~ 4.6 J/g. The DSC profile for this product looked very similar to the scan obtained for the pure rice flour. The difference in the endotherm peak temperature may be related to a presence of other hydrophilic compounds, which may affect the complete hydration of the starch prior to the measurment. The conversion enthalpy value for this product corresponds to ~ 40% of the conversion enthalpy for the rice flour used in this formulation, which is relatively close to the 50% of rice flour specified in this formulation. It is also possible that part of the rice flour had been gelatinised during manufacturing.

Similarly to "MiniJumbone" surface material, a small reversible endotherm was detected at ~ 100°C with an enthalpy of 0.36 J/g which would indicate the formation of an amylose lipid complex. As discussed before, the difference in the endotherm value between the first and second run may be related to the

increase in availability of amylose after the complete conversion of the starchy components during the first run.

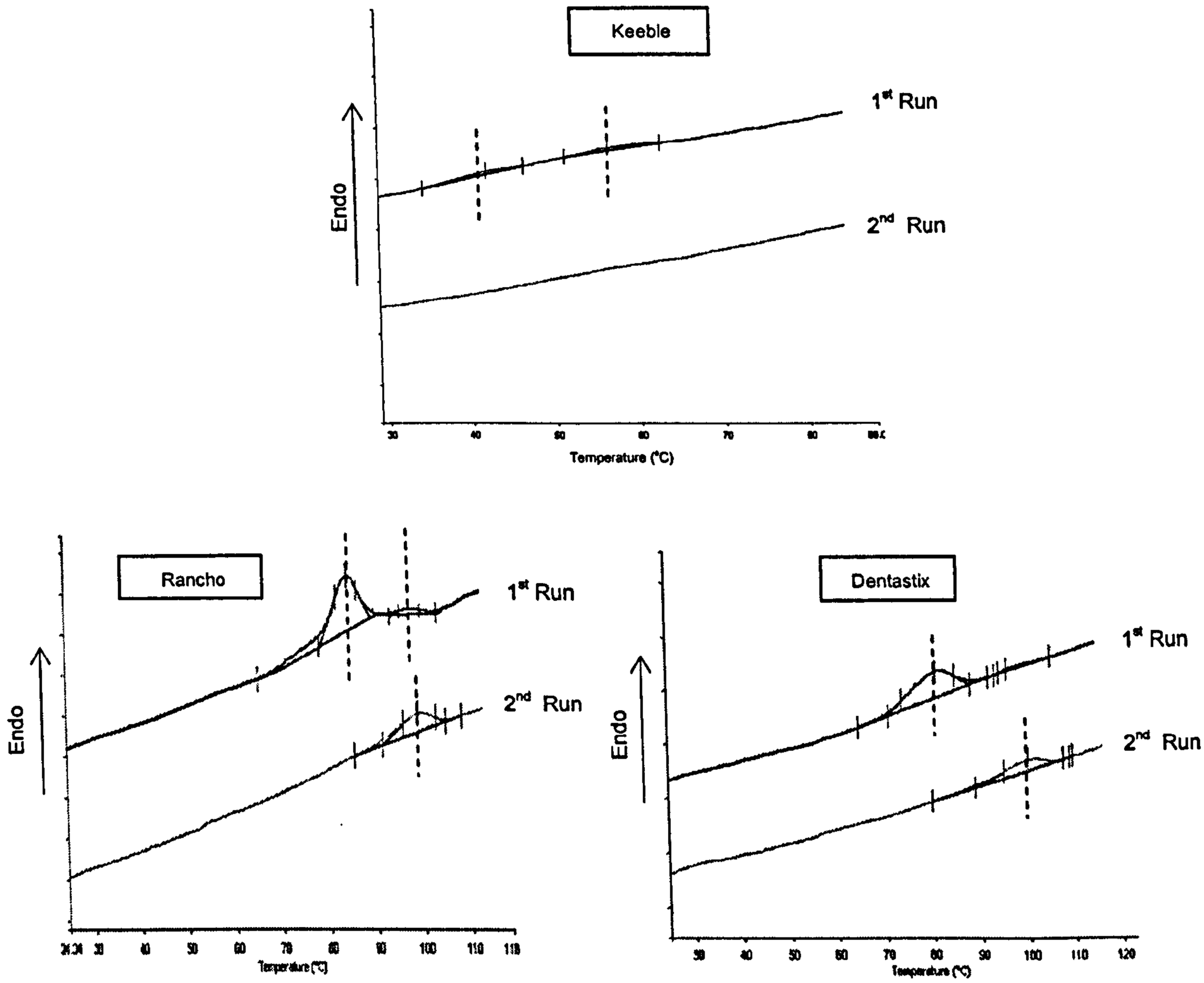

Figure 8.8. DSC scans (1st and 2nd run) for "Kibble", "Rancho" and "Dentastix"

In the case of Dentastix a single irreversible endotherm was detected at ~ 81°C with an associated enthalpy of ~ 2.1J/g. As before, this would suggest that the rice starch fraction was not fully converted during the manufacturing of this product.

The reversible endotherm detected at 96°C can be related to the amylose-lipid complex formation, which increased after the complete gelatinisation of the starch as shown in the second DSC run.

Table 8.4. Endotherm peak temperature and enthalpy for "MiniJumbone", "Kibble", "Rancho" and "Dentastix" obtained from DSC.

Product	Peak Temp. 1 (°C)	Enthalpy 1 (J/g)	Peak Temp. 2 (°C)	Enthalpy 2 (J/g)	Peak Temp. 3 (°C)	Enthalpy 3 (J/g)
MiniJumbone core 1st run	55.7 (2.2)	1.12 (0.25)	--	--	100.1 (3.3)	0.67 (0.06)
MiniJumbone core 2nd run	--	--	--	--	101.6 (2.9)	0.82 (0.08)
JMiniumbone surface 1st run	59.7 (2.5)	0.44 (0.08)	85.3 (2.2)	2.60 (0.26)	102.3 (3.1)	0.43 (0.05)
MiniJumbone surface 2nd run	--	--	--	--	102.7 (2.5)	1.08 (0.3)
Kibble 1st run	56.9 (1.5)	0.15 (0.04)	--	--	--	--
Kibble 2nd run	--	--	--	--	--	--
Rancho 1st run	--	--	84.7 (2.0)	4.56 (0.32)	100.1 (2.8)	0.36 (0.09)
Rancho 2nd run	--	--	--	--	99.0 (2.5)	1.08 (0.23)
Dentastix 1st run	--	--	81.0 (2.1)	2.44 (0.28)	96.0 (2.6)	0.15 (0.02)
Dentastix 2nd run	--	--	--	--	100.1 (3.3)	0.72 (0.15)

(*) Values in brackets represent the standard deviation of three measurements.
Peak Temp. 1: expected gelatinisation temperature for wheat/maize starch
Peak Temp. 2: expected gelatinisation temperature for rice starch
Peak Temp. 3: expected melting temperature of amylose-lipid complex

In the next section, X-ray diffraction performed for the same products is presented. The objective was to complement the DSC data by the assessment of the presence of structures with a high degree of molecular order.

8.3.1.3 X-ray Diffraction on Pet-Care Products

The preparation of the samples was as follow: samples were ground under cryogenic conditions and scanned from an angle $2\theta = 4^{\circ}$ to 38° at an angle step of 0.05° per minute. Due to the high reproducibility of this technique, the measurements were done in duplicates.

Figure 8.9 depicts the diffractograms for "MiniJumbone" core and surface. Marked differences were observed between these two components. For the core material a three distinctive peaks were detected at an angle of ~ 12.5°, ~ 19.5° and ~ 22.5°. The first two peaks are clearly related to the formation of amylo-lipids complex between the available amylose molecules and lipids. This ordered structure has been classified as V-type crystal (Buléon, Colonna et al. 1998; Kaur and Singh 2000; Becker, Hill et al. 2001). The third peak seems to be related to a fraction of unconverted starch which would eventually lead to the formation of A-type crystals for cereal starch type (top curves on figure 8.10). These findings correlates well with the DSC data, where

endotherms associated to unconverted starch and amylo-lipids complex were detected on the first run. Other smaller peaks detected at diffractive angles > 28° can be related to other additives included in the formulation of this product (e. g. salts).

In the case of the surface material (right curve in figure 8.9) a different profile was detected with approximately five distinctive peaks at diffractive angles < 28°. These were detected at ~ 15°, 18°, 19°, 20° and ~ 23 °. It is interesting to note that this diffractogram does not show the formation of amylo-lipid complex, just a very small peak at ~ 19°. The reduction in intensity of the peaks associated to these complexes seems to be overlapped by the presence of an important proportion of unconverted starch.

The presence of native starch is supported by the DSC data (right curve in figure 8.7) and by the similarities with the diffractogram for rice flour (top curves in figure 8.10).

The peak at ~ 29.5° has been identified as crystals of potassium carbonate (KCO_3), which was confirmed by the scanning of this salt (data not shown).

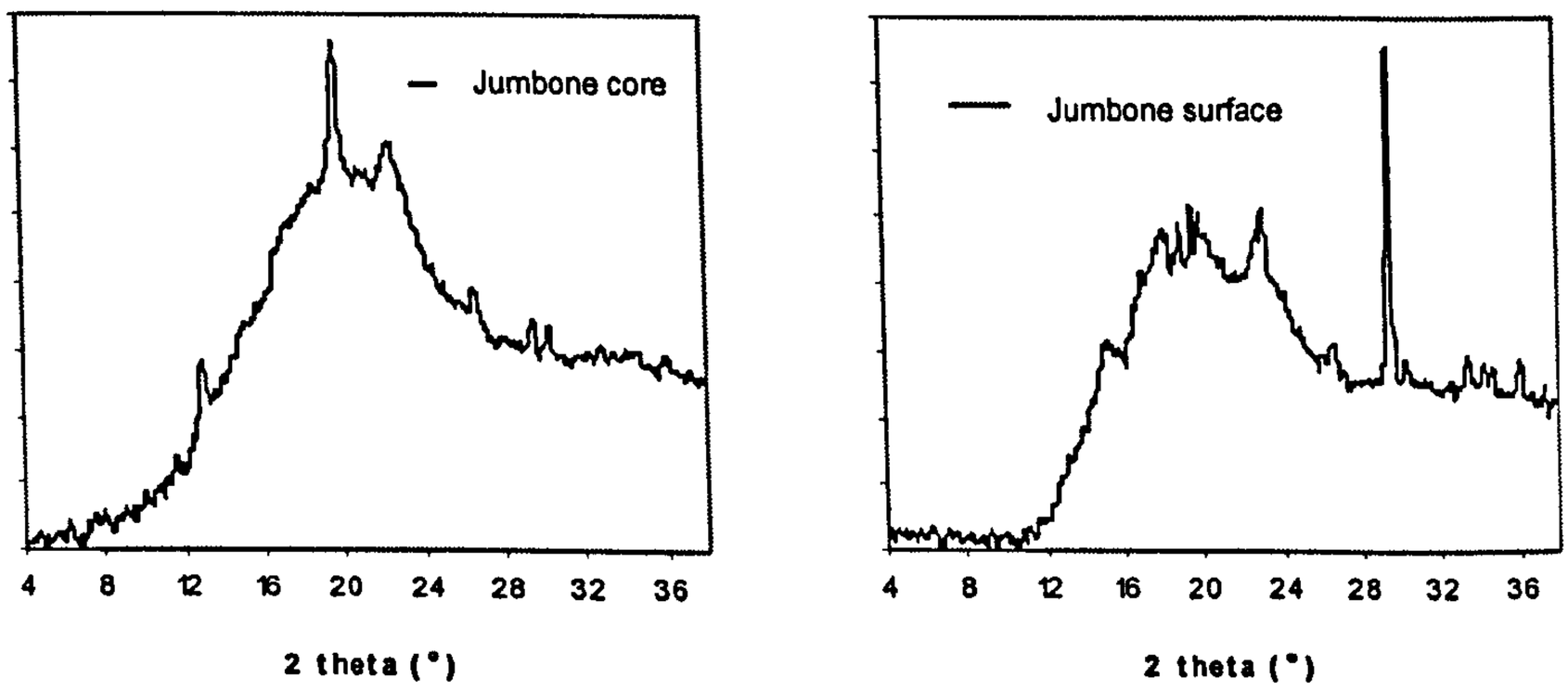

Figure 8.9. X-ray diffraction scans for "MiniJumbone" core (left) and "MiniJumbone" surface (right).

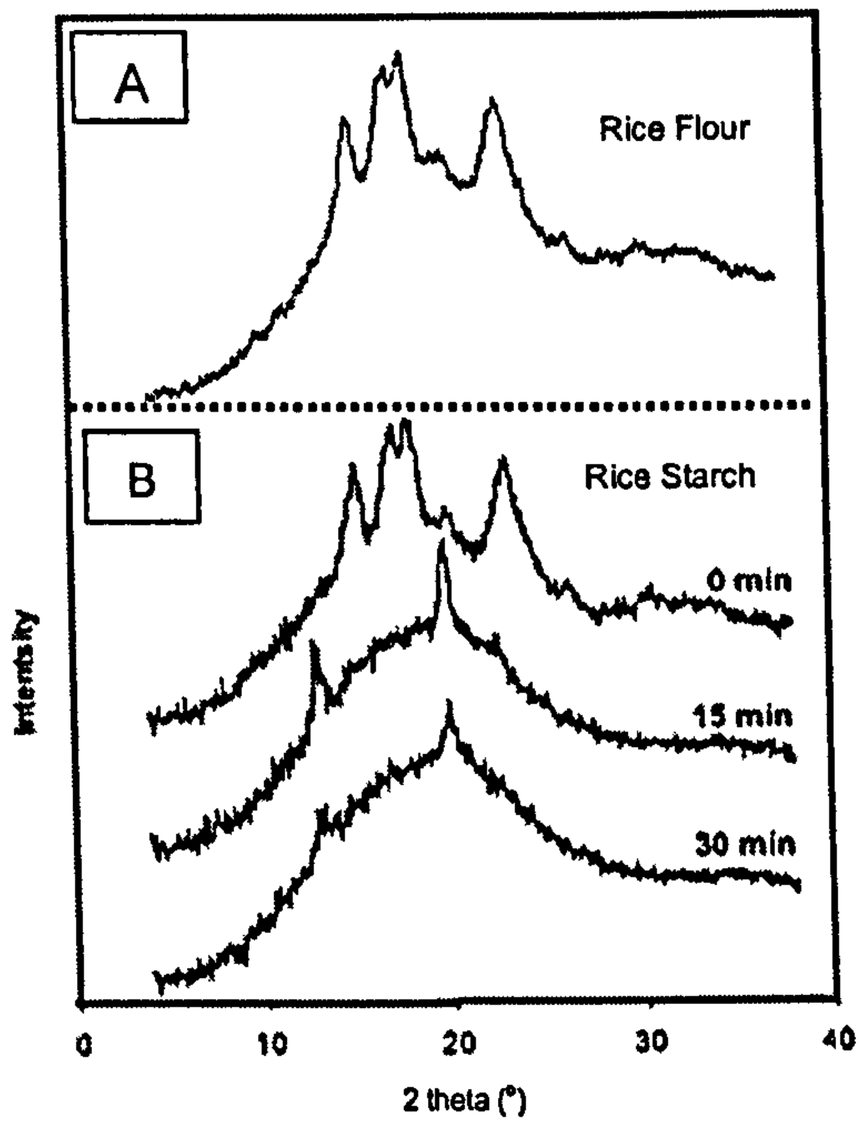

Figure 8.10. X-ray diffraction patterns for native rice flour used in these commercial products (A); native and processed rice starch cooked at different times (B) (modified from (Becker, Hill et al. 2001))

The diffractograms of "Kibble", "Rancho" and "Dentastix" are presented in figure 8.11.

In the case of "Kibble", an amorphous like pattern was obtained with no distinctive peak for diffractive angles < 30°. The amorphous structure of this product was also detected by DSC. Indeed, figure 8.8 shows a very small endotherm (enthalpy < 0.1 J/g) at the temperature expected for native wheat/maize starch (~ 56°C) suggesting that most of the starch present in this formulation was converted during manufacturing.
Just a small peak was detected at a diffractive angle ~ 32° which seems to be related to other minor components in the formulation.

The X-ray scan for Dentastix show three peaks at approximately 16°, 20° and 23°, associated to native rice starch (main starchy component in the formulation), two peaks at ~ 13° and ~ 19°, associated to the formation of some amylose-lipid complex and a major peak at 29° which is related to the presence on KCO_3. These findings were also supported the DSC data showing endotherms at temperatures similar to the endotherms detected for rice flour.

It is thought that the other peaks at diffractive angles > 30° are from other unidentified minor compounds added to the formulation.

"Rancho" shows a very similar profile compared to the material at the surface of "MiniJumbone" (with the exception of the peak at ~ 29.5°). The presence of native or unconverted starch in this formulation is supported by the DSC data showing an endotherm with an enthalpy value that would account of 80% of the total of rice flour used in the mixture.

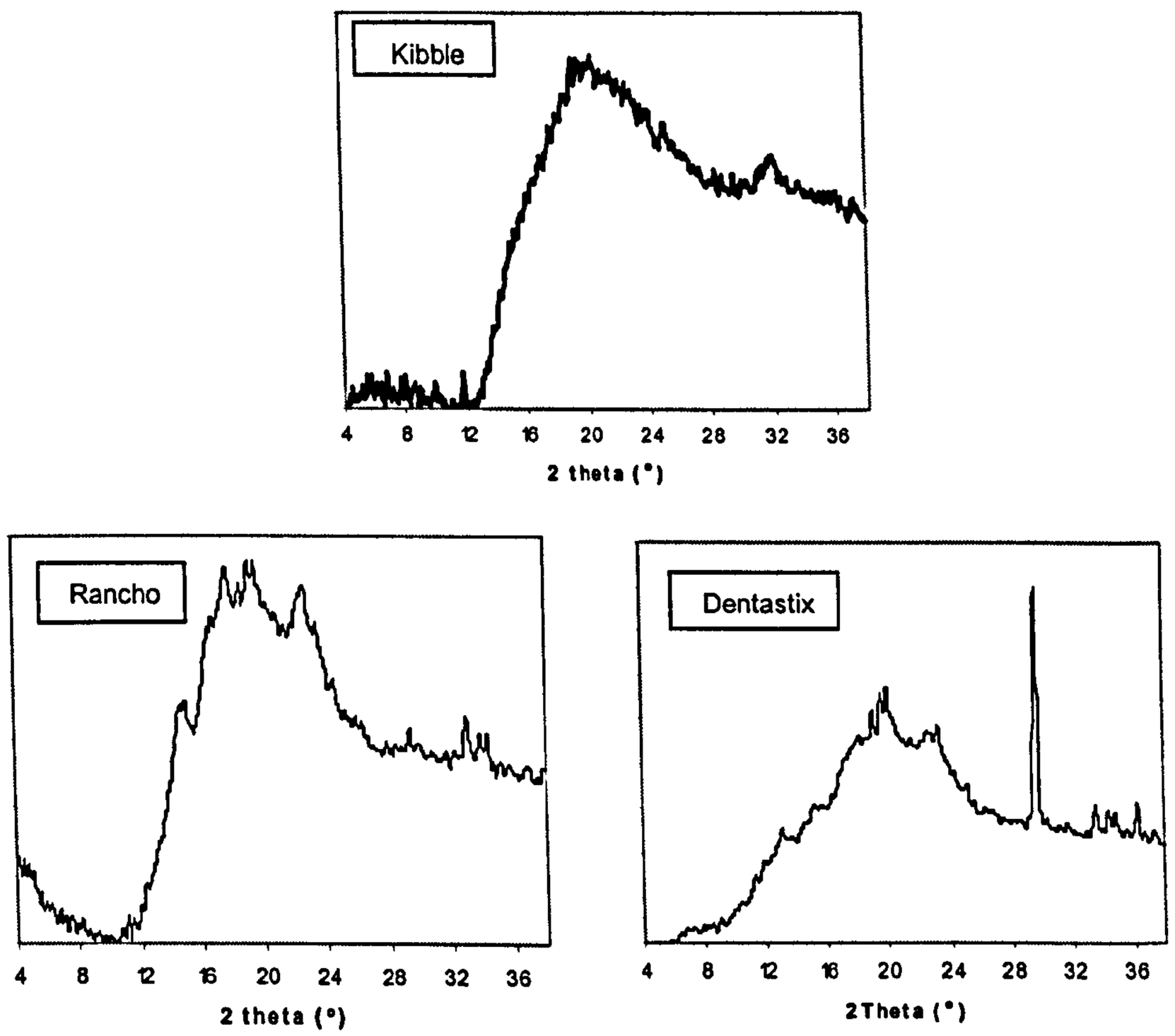

Figure 8.11. X-ray diffraction patterns for the products "Rancho", "Kibble" and "Dentatix"

Prediction of the physical state of these products can have a significant impact on the improvements of current formulation. It can help in the optimisation of different ingredients to achieve a desired mechanical attribute.

The next section aims to study the applicability of predictive and descriptive models on these systems.

8.3.2 Prediction of Mechanical Behaviour of Pet-Care Products

Some of the models that were already fitted on the extruded starch glycerol systems were applied to "Kibble" and "Dentastix". The formulation of these products is given in table 8.1.

The experimental work presented on the previous section showed that all of these products are in a rubbery state (at ~ 25°C) and a single Tg for the mixture could be obtained. This would suggest that changes in the plasticiser content can have a significant impact on the textural attributes of these materials.

To test this hypothesis, the moisture contents of "Kibble" and "Dentastix" were reduced by exposing these products to 0%RH (P_2O_5). The range of the equilibrated moisture varied from 17% to ~ 7% (wb) for "Kibble" and 14% to 6% wb for Dentastix. The changes in the texture (compression and penetration forces) and Tg versus moisture content were evaluated using texture analyser and DMTA (details of the force measurements methods are presented in section 8.3.3.1 and 8.3.3.2 of this chapter. For DMTA, the experimental protocol is presented in section 8.3.1.1).

Figure 8.12 (left) shows the changes in the force at various moisture contents. In the case of "Kibble" (A), a marked increase in the compression force was detected when the moisture content reached ~12% wb from ~ 70 N to of ~ 370 N for a moisture content of ~ 7.0 % wb.

A marked change in the penetration force was also detected for "Dentastix" (B) at different moisture contents. The major increase in force was measured at moisture contents < ~8.5% wb, reaching a value of ~ 260 N for a moisture content of ~ 6.5% wb.

This change in the hardness seems to be related to an increase in the glass transition temperature of the starchy component present in these two formulations. Indeed, figure 8.12 (right) depicts the tan δ curves obtained from DMTA for "Kibble" and "Dentastix" at four different moisture contents (circled values in figure 8.12 (left)). The tan δ peak temperature for both products increased when the water concentration present in the mixture was reduced. In the case of "Kibble" the tan δ peak temperature increased from ~ 17°C for a moisture content of 17% wb to ~ 45°C for 7% wb. "Dentastix"

showed a similar increase in tan δ peak temperature from ~30°C at 14% wb to 50°C for a moisture content of 6.5% wb.

Another distinctive feature observed on the Tg delta curves was the secondary peaked detected at ~ -40°C on both products. As it was discussed before, these secondary peaks may be related to short range movements on the main polymer and/or the main transition of a phase separate components present in the formulation. The decrease in the peak height for the products with moisture contents < 10% is thought to be related to the structure being more constrained due to the decrease in plasticiser concentration..

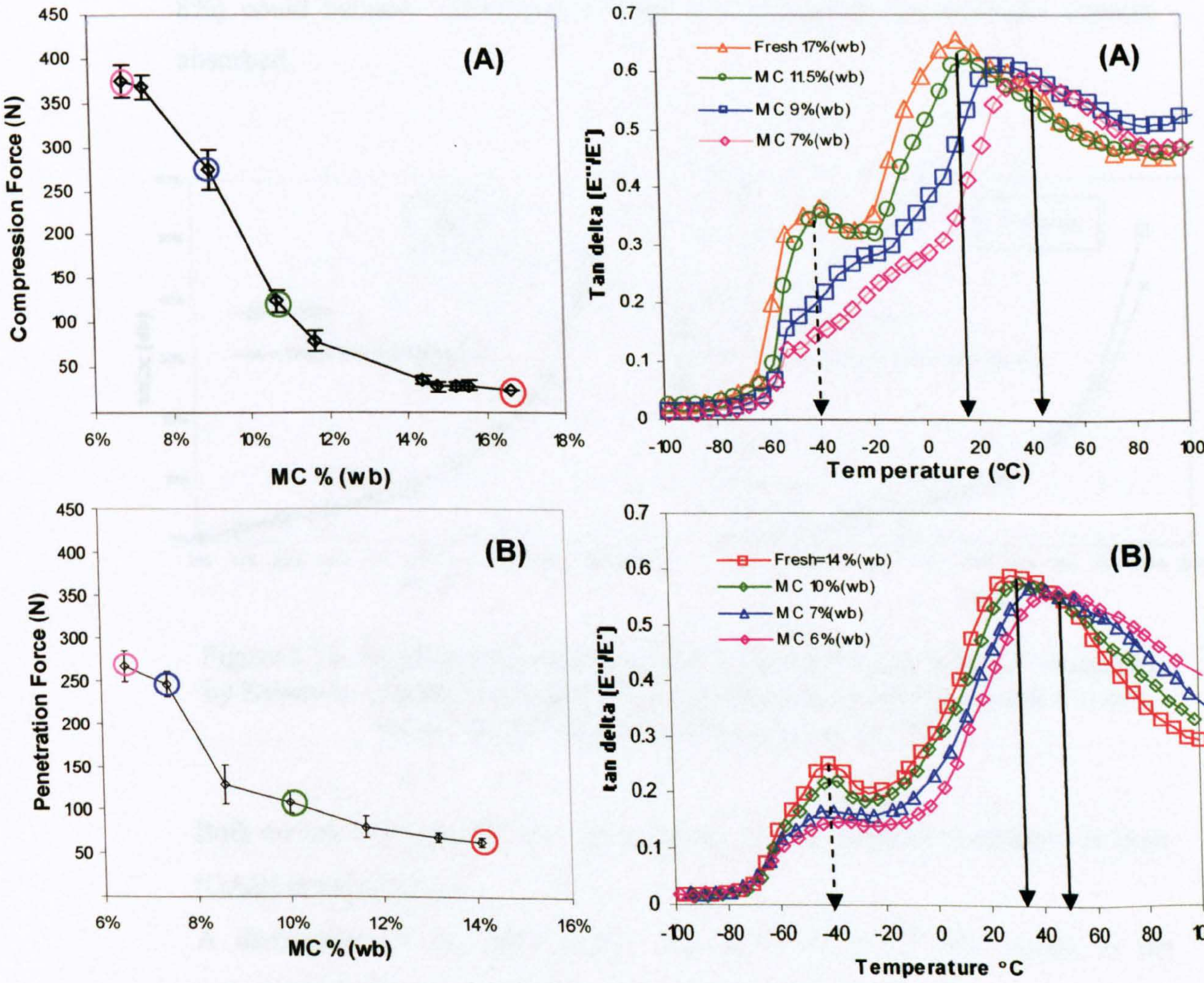

Figure 8.12. Effect of changes in moisture content on texture and the glass transition temperature (Tg) of "Kibble" (A) and "Dentastix" (B). DMTA settings were heating rate 3°C/min. at 10Hz and x 4 deformation (62 μm). Itwas carried out on the moisture contents corresponding to the circled values in (A).

From the discussion above it is clear that the texture of these materials is dependent on the changes in moisture, especially if reaches values < 10% wb. Therefore it is important to establish the moisture contents of products if they are stored at different relative humidities. Figure 8.13, shows the sorption isotherms for "Kibble" and "Dentastix" measured at 25°C by Dynamic Vapour Sorption (DVS). Overlapped on these curves is the sorption isotherm of one of the studied model systems (wheat starch) mixed with 20% glycerol (presented in chapter 4, section 4.1.1.2.1).

This comparison suggests that for RH ~ < 80% the sorption of water by these products is mainly driven by the starch -polyol (glycerol) components. At a RH > 80% differences were detected between the products and the model systems. It is possible that crystalline salts present in the commercial formulation (~ 6%-8%) could become solubilised at high RH increasing the moisture content absorbed.

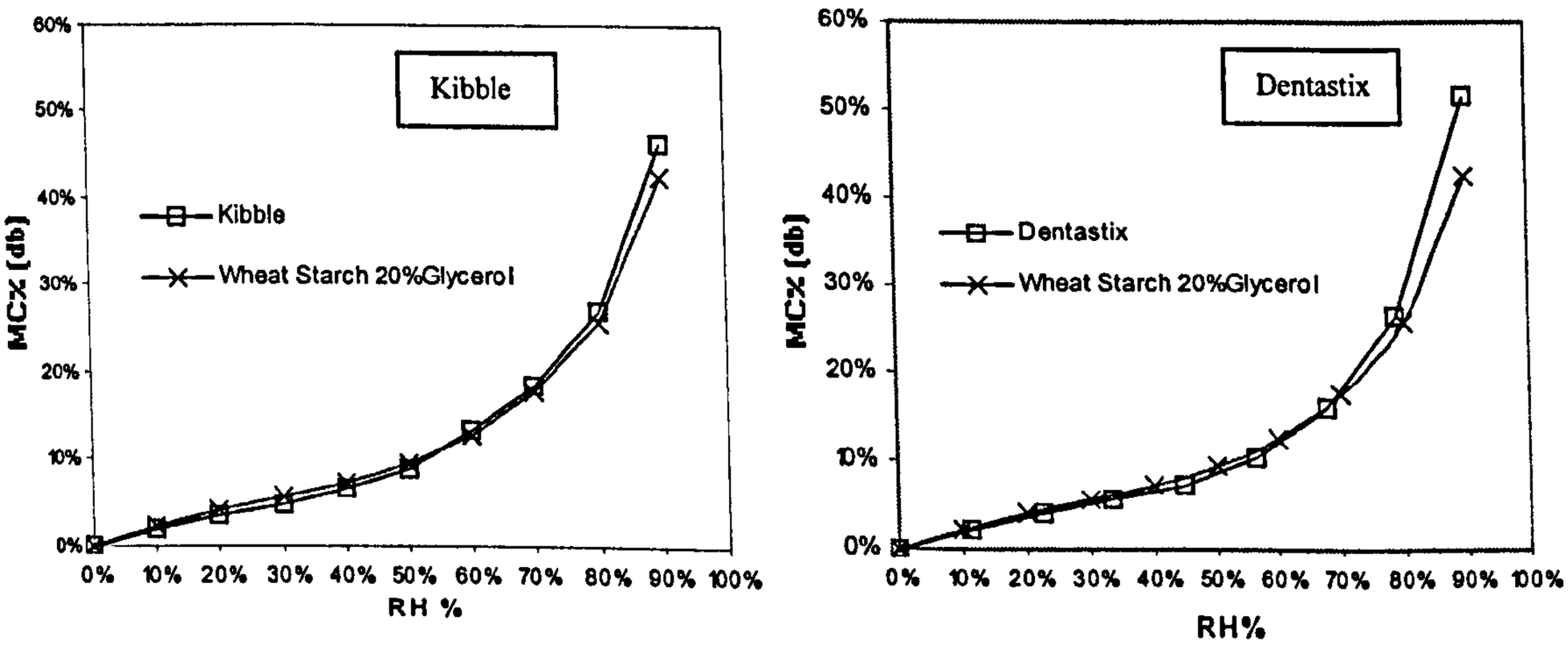

Figure 8.13. Sorption isotherm for ground "Dentasix" and "Kibble" measured by Dynamic Vapour Sorption (DVS). Equilibration reached at dm/dt < 0.002, values are the mean of two measurements (25°C).

Both curves were modelled by the equation of Guggenheim-Anderson-de Boer (GAB) (equation 8.1).

A discussion of the applicability and optimisation of this model to the experimental data can be found in chapter 4, section 4.1.2.1.2.

$$M = \frac{m_o C K a_w}{(1 - K a_w)(1 - K a_w + C K a_w)} \qquad \text{Equation 8.1}$$

Where:

m_o = monolayer value (all sorption sites occupied by one molecule)

C = constant (related to the net heat of sorption)

K = constant (related to the heat of sorption of the multilayer)

The final values after optimisation of the GAB model are presented in table 8.5. These values are compared against the values obtained for wheat starch 0% and 20% glycerol.

Table 8.5. GAB parameters for commercial products and wheat starch and wheat starch-glycerol systems after model optimisation.

	Mo	*K'*	*C*	R^2
Kibble	7.8%	0.93	2.13	0.98
Dentastix	6.0%	0.98	2.50	0.99
Wheat Starch 20% glycerol	6.9%	0.94	3.50	0.99
Wheat Starch	8.7%	0.73	6.41	0.99

Following the rationale discussed in chapter 3 for model systems, a *K'* value of ~ 0.97 (~ 0.73 for pure starch) would suggest an increase in the interaction energy between the multilayer and bulk liquid, due to the hygroscopic nature of the polyol.

For the case of *C*, with a value of < ~2.3 compared with ~ 6.4 obtained for wheat starch, it would indicated water molecules are less strongly bound to the monolayer (free absorption sites in the starchy matrix) due to the presence of polyols at low RH (<50%). It is believed that the hydroxyl groups present in these small molecules can occupy the sorption sites when the water vapour pressure of the surroundings is low (Sala and Tomka 1993).

After establishing the relation between moisture content at different relative humidities (RH) for these products, an empirical model can be used to represent the changes in texture when the storage RH is varied. This model

(Peleg 1994 a; Peleg 1994 b) has already been successful used to represent the flexural modulus at different moisture contents for three starch-based glycerol systems as presented in chapter 6, section 6.3.3 of this thesis.

$$Y(RH) = \frac{Y_S}{\left\{1 + \exp\left[\frac{RH - RH_C}{a'}\right]\right\}} \qquad \textit{Equation 8.2}$$

Where *Y(RH)* are the magnitudes of the mechanical parameter at the corresponding relative humidity (*RH*). Y_s is the magnitude of the mechanical parameter in the glassy state, RH_c is the relative humidity at which the curve inflection point occurs, a' is the empirical constant. The magnitude of a' describes the steepness of the region depicting decrease in modulus. Figure 8.14 shows the variation on force as a function of relative humidity (RH%). The parameters obtained after model optimisation are presented in table 8.6. Although both graphs depict the increase in hardness of thee products, a direct comparison between both set of data is not entirely correct. The penetration test data represents a combination of compressive and shear forces, increasing the surface area of the material to the applied force.

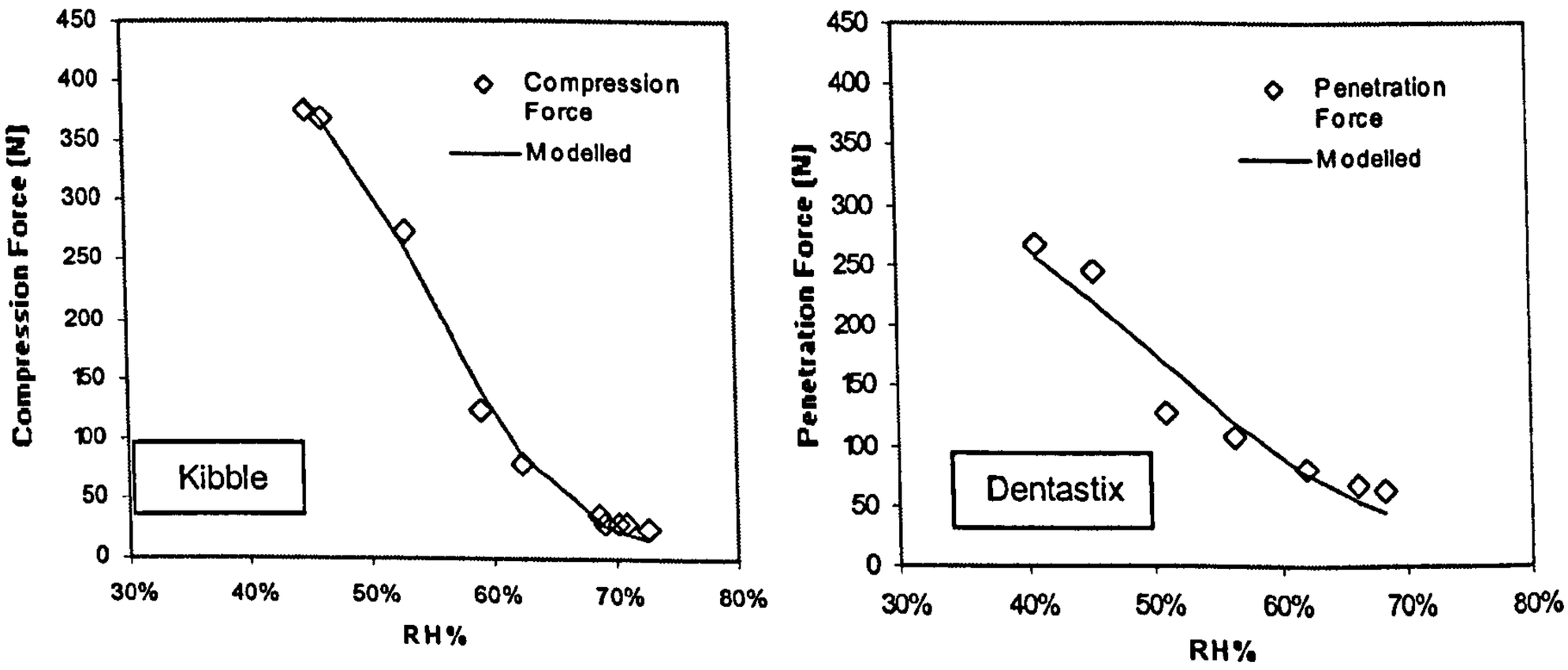

Figure 8.14. Products hardness as a function relative humidity at 25°C, modelled using equation 8.2.

Table 8.6. Model parameters for "Kibble" and "Dentastix" after optimisation

	Ys (N)	RH_c (%)	*a'* (%)	R^2
Kibble	439	55%	5.3%	1.00
Dentastix	350	50%	9.3%	0.93

Although it is difficult to interpret these values, due to the different mechanical properties evaluated and the lack of experimental points at low RH% (< 40%), it seems clear that "Dentastix" (*a'* = 9.3%) is less sensitive to changes in moisture compared to "Kibble" (*a'* = 5.3%). It is important to note that the obtained RH_c values are similar to the measured water activity for these products. This suggests that a small change in this parameter (e.g. storage conditions) can markedly affect the texture of these two products.

The following section focuses on the study of the mechanical stability of these products during storage. Although it was shown that the texture of these products change over time, the mechanism driving this process remained unclear. The objective here is to improve the understanding of this ageing process and be able to predict it by using models already tested on simpler model systems.

8.3.3 Mechanical Stability of Pet-Care Products on Storage

As already mentioned, the increase in hardness of these products during storage can have a negative effect on their commercial value. The following experimental work aimed to improve the understanding of the ageing mechanism affecting these products in order to reduce its effect and to extend their shelf life.

"Kibble" and "Dentastix" were selected for this study. In the case of "Kibble", sealed bags were stored at 25°C for up to 120 days. "Dentastix" were also stored for 120 days at 25°C but they were kept in their original package.

The analytical techniques used on this study were, DMTA, DSC and X-Ray diffraction (details of these methods are presented in section in chapter 3). In the case of Texture Analyser (TA) the experimental protocols used to analyse these products is presented in sections 8.3.3.1 and 8.3.3.2 of this chapter.

The first set of experimental data presented in this section is for "Kibble".

8.3.3.1 Semi-moist Kibble

Table 8.7 shows the moisture contents for fresh and aged samples.

Table 8.7. Moisture content (*) of fresh and aged "Kibble".

Storage Time	MC (wb)
Fresh	16.2% (0.25)
16 days	15.9% (0.21)
30 days	16.0% (0.18)
44 days	16.3% (0.15)
60 days	16.2% (0.22)
81 days	15.8% (0.12)
103 days	16.1% (0.13
120 days	15.2% (0.20

The presented values are the mean of 3 measurements. Values in brackets represent the standard deviation.
(*) vacuum oven at 70°C overnight

The first analysis was the assessment of the changes in the texture of this product with storage time. The selected method was the compression test where the maximum force to compress the product a determined strain is recorded. The experimental method was: compression plate diameter of 70 mm, compression strain was 30% and probe speed was 2 mm/s. The experiment was performed at ambient temperature (~ 25°C). 5 replicates were measured for each of the ageing times.

Figure 8.15 depicts a representation of the compression force measurements and a typical curved obtained for "Kibble" using the Texture Analyser.

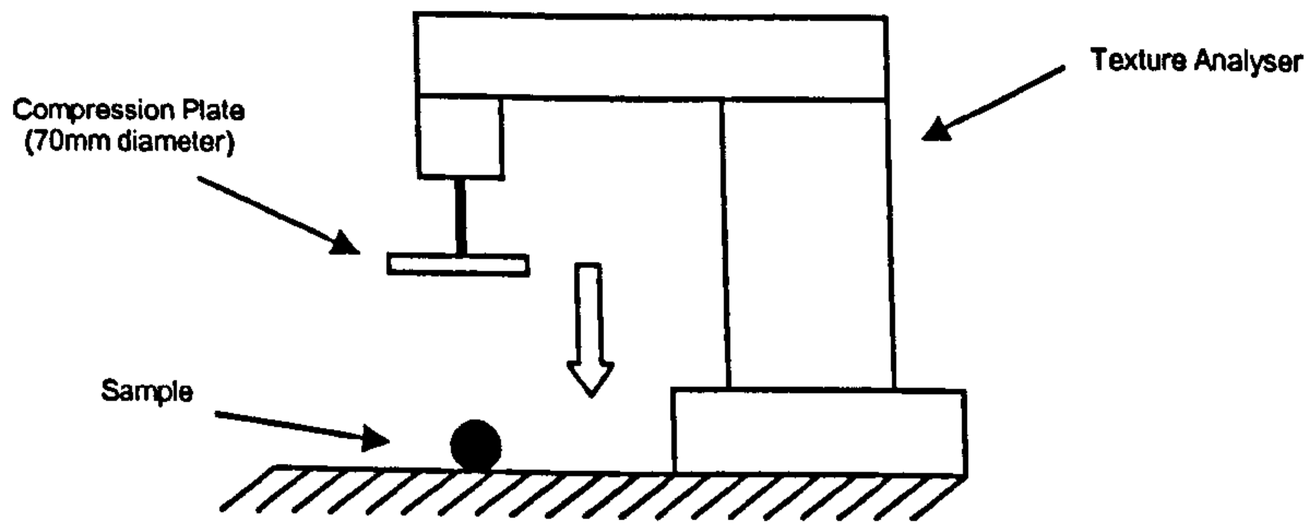

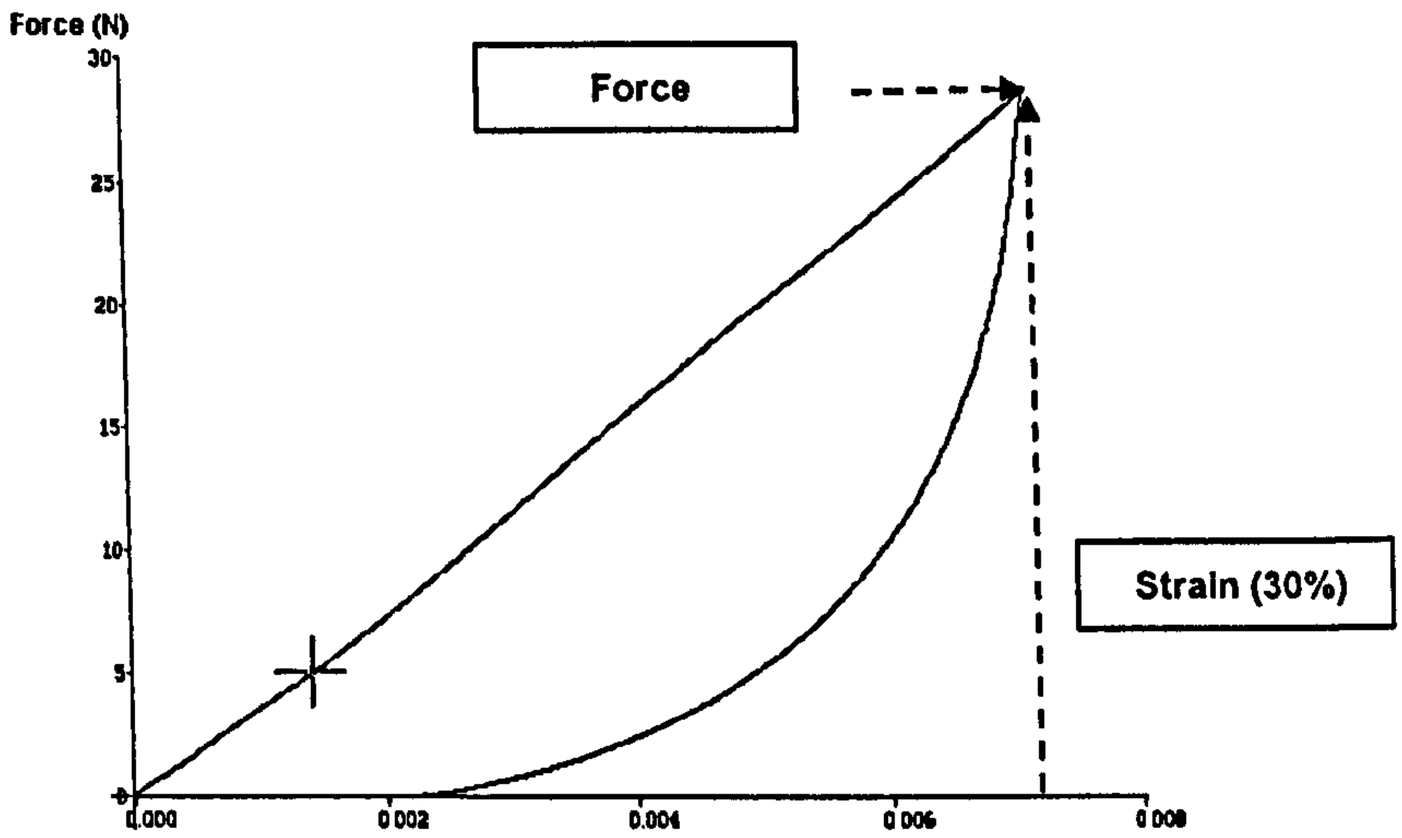

Figure 8.15. Diagram describing compression test and a typical compression curve of Kibble indicating the force value considered.

Figure 8.16 shows the changes in the compression force during storage at 25°C. For the first 30 days of storage there was a slight but significant increase ($P<0.05$) in this parameter, from ~ 25N to ~ 32N. After 30 days storage, a marked and significant increase ($P<0.05$) in the compression force was detected up to ~ 60 days storage, with an increase from ~ 32N to ~ 80N. At this point, the curve started to level off ($P>0.05$) with a final value of ~ 82N after 120 days of storage time.

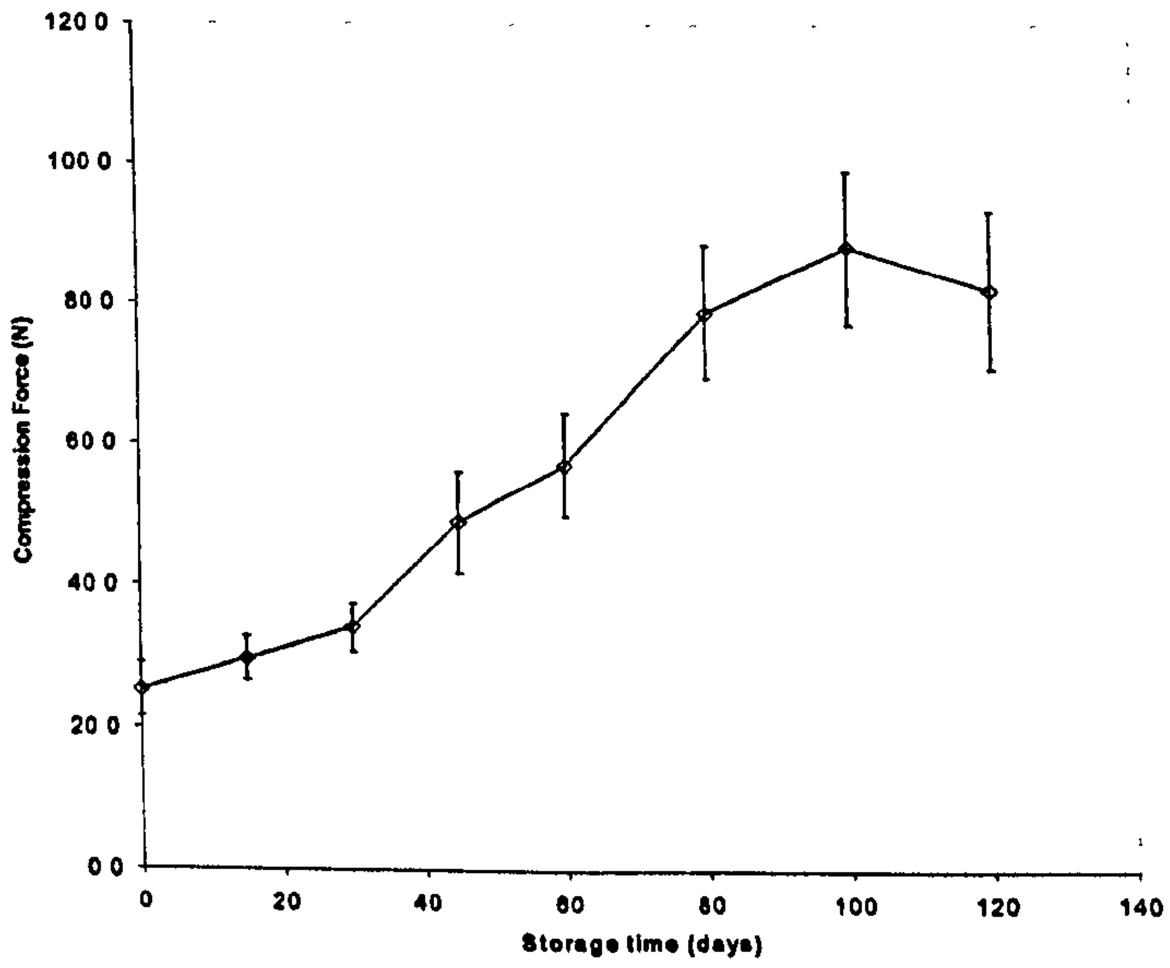

Figure 8.16. Changes in the compression force of Kibble with storage time at 25°C. Error bars represent the standard deviation of 5 measurements.

The experimental data presented on figure 8.17, was modelled using the Avrami equation (Farhat, Blanshard et al. 2000), which has already been used to model the retrograding of extruded starch-glycerol systems (chapter 7 of this thesis). The fitting optimisation was be done by independently adjustable adjusting Y_o, k and n.

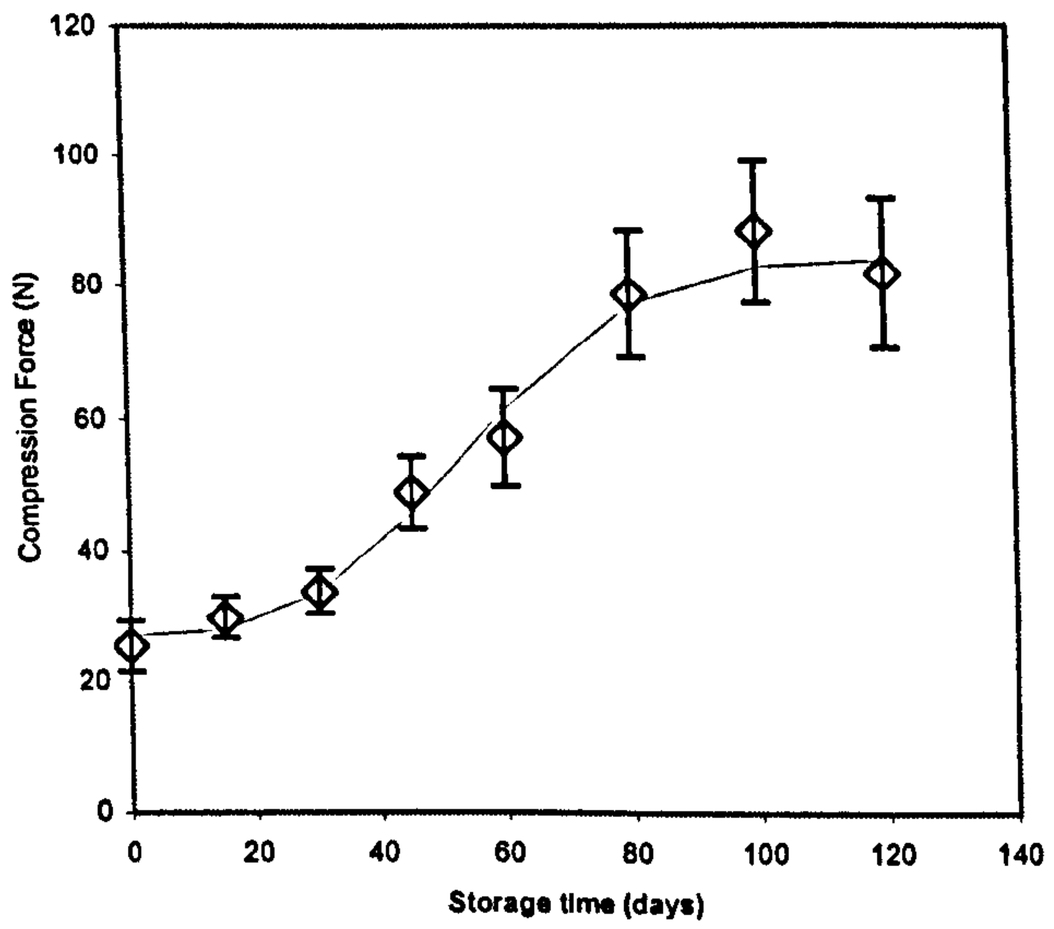

Avrami Model Parameters

n	2.90
G (h^{-1})	1.62E-02
k	6.35E-06
Y_{inf} (N)	84.0
Y_o (N)	27.0

Figure 8.17. Avrami modelled data fitted on the penetration force data (R^2 = 0.99). Modelling parameters were obtained after minimising the squared sum on the difference (Solver, Excel, Office 2003. Microsoft).

Figure 8.17 shows the Avrami model overlapped onto the experimental data. The obtained R^2= 0.99 proved a good fit between the model and the obtained data. The obtained retrogradation kinetic value (G) was 1.6E-02 (h^{-1}), was in a similar order of magnitude to the ~ 6.5E-03 obtained for the extruded wheat-20% glycerol and ~16% (db) moisture content as presented in chapter 7 of this thesis (table 7.3).

Next section investigates the effect of storage time on the stiffness and glass transition temperature measured by mechanical spectroscopy using DMTA.

For this experiment four storage times were evaluated; 0, 30, 60 and 120 days. The samples were shaped and clamped on single bending mode as described in section 8.3.1.1 of this chapter.

Figure 8.18 shows the elastic modulus (E') (left) and the tan δ (right) values versus temperature for the fresh and stored "Kibble". The tan δ curve showed no change (~ 15°C) on the main peak with storage time, suggesting that Tg of the mixture remained constant through ageing. This is consistent with the

measured moisture content of the fresh and aged samples, which remained relatively constant during storage (table 8.7).

On the other hand a decrease in the peak height was detected for the aged products. This decrease seems to be correlated with the storage time. Indeed, for the fresh product the peak value was ~ 0.65 and for the aged it decreased to ~ 0.40. The change in this value could be explained by a decrease in the molecular mobility of the amorphous component due to a possible molecular reassociation of the starchy polymer main chains during storage. Lionetto *et al.* (2005) showed a decrease on the peak height for aged wheat starch extrudates. They detected a reduction in tan δ from ~ 0.85 for the fresh sample to ~ 0.25 for the extrudate aged for 180 h.

In the case of the secondary transitions represented by the smaller peaks occurring at – 40°C, their height also seemed to decrease with storage time but not to the same extent as for the main peak transition. It is possible that reduction in long range molecular relaxation due to ageing contributed to restrict local short rotational movements of the starchy main chains.

Following the hypothesis that attributes the origin of this small peak on a phase separated component; it is possible that this polymeric structure may also become less mobile with storage time or an integration might occurred between the starchy component and other lower concentration polymers present in the mixture.

As expected, there were not differences in *E'* between the fresh and aged samples at temperature below their glass transition temperature (Tg ~ 5°C). Below this temperature, the amorphous fraction is in the glassy state, therefore difference in the stiffness were not detected. At temperatures over Tg, differences in *E'* were obtained. Indeed, if 25°C is taken as a reference temperature, differences in E' between the fresh and aged "Kibble" were clearly observed (figure 8.18 (left)). These results correlated well with the findings from the compression test (at ~ 25°C) were significant changes in the hardness were detected during storage. Despite the positive correlation between these two techniques, the extent of deformation and therefore their effect on the material structure is different. In the case of DMTA a small strain is applied minimising the changes in the structure of the sample. On the other hand, during compression test, the strain applied on the material reaches a point at

which, damage to the structure can be irreversible. Small deformation analysis such as DMTA is able to separate the viscous and elastic component of materials giving fundamental information of polymeric systems. In the case of compression measurements, it has been suggested that the obtained information can be correlated to the overall perception of texture in food systems. The differences in extent of the increase in hardness of the Kibbles (at 25°C) between DMTA and compression test can be attributed to oscillating the frequency used in mechanical spectroscopy. Indeed, the viscoelastic behaviour of polymeric materials are considered highly dependant on the experimental time scale.

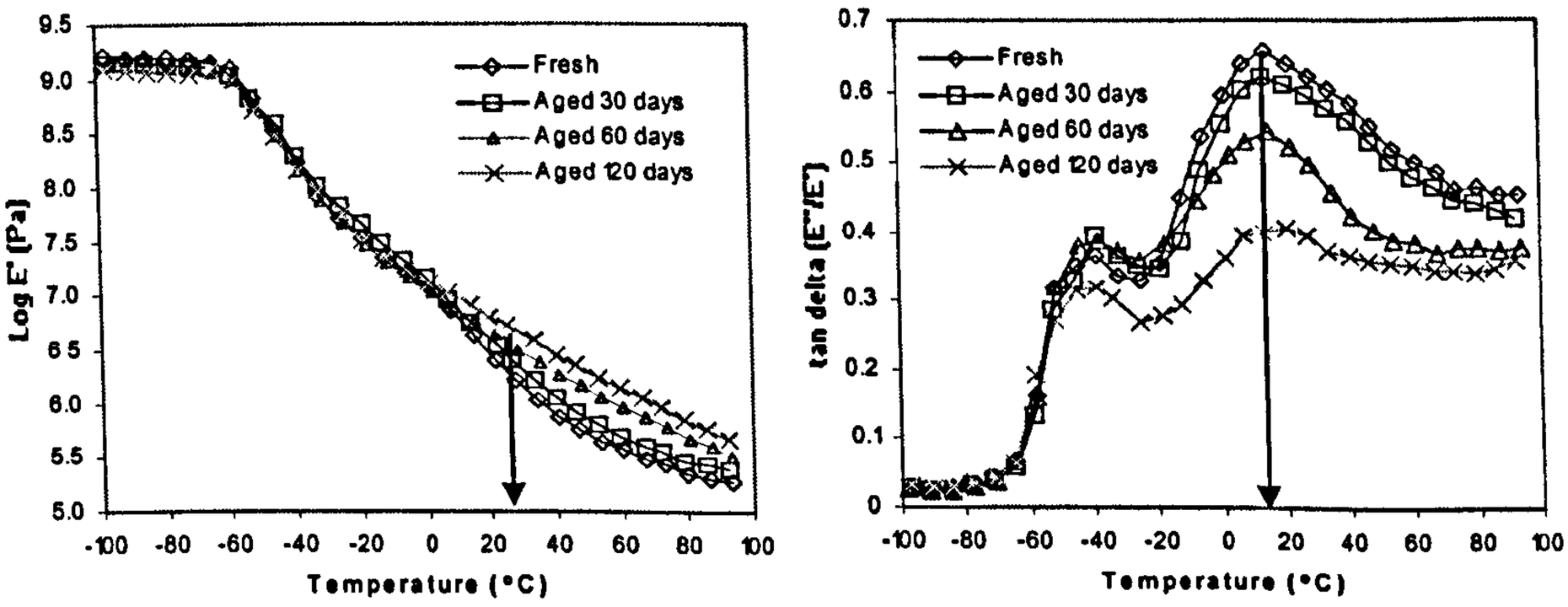

Figure 8.18. Elastic modulus (E') and tan δ versus temperature (10 Hz) for "Kibble" stored for 0, 30, 60 and 120 days at 25°C. Heating rate 3°C/min and strain x4 (amplitude 62*u*m).

The hypothesis relating the hardening of this product to a molecular re-ordering process during storage was tested by evaluating fresh and aged samples using differential calorimetry (DSC). The sample preparation (in excess water) and the experimental setting protocols is discussed in section 8.3.1.2 of this chapter.

Similarly to DMTA, four ageing times were evaluated: 0, 30, 60 and 120 days. Figure 8.19 depicts the 1st runs (left) and 2nd runs (right) for the fresh and aged "Kibbles". The first and second runs of the fresh and aged samples show a small endotherm at ~ 25°C with an enthalpy of ~ 0.3 J/g, which is associated with the melting of lipids included in the formulation. This was confirmed by a reduction in the associated enthalpy when the product was thoroughly washed

by an organic solvent (data not shown). As expected for lipids, the enthalpy of this endotherm did not change with storage time (table 8.8)

A second endotherm was detected at ~ 58°C for the "Kibbles" aged for 60 (enthalpy ~ 1.03 J/g) and 120 days (enthalpy ~ 2.10 J/g). For the fresh and stored for 30 samples the measured enthalpy was ~ 0.1 J/g.

The enthalpy, peak temperature and irreversible nature of second endotherms (table 8.8) suggests the presence of retrograded starch formed during storage (Ottenhof 2003).

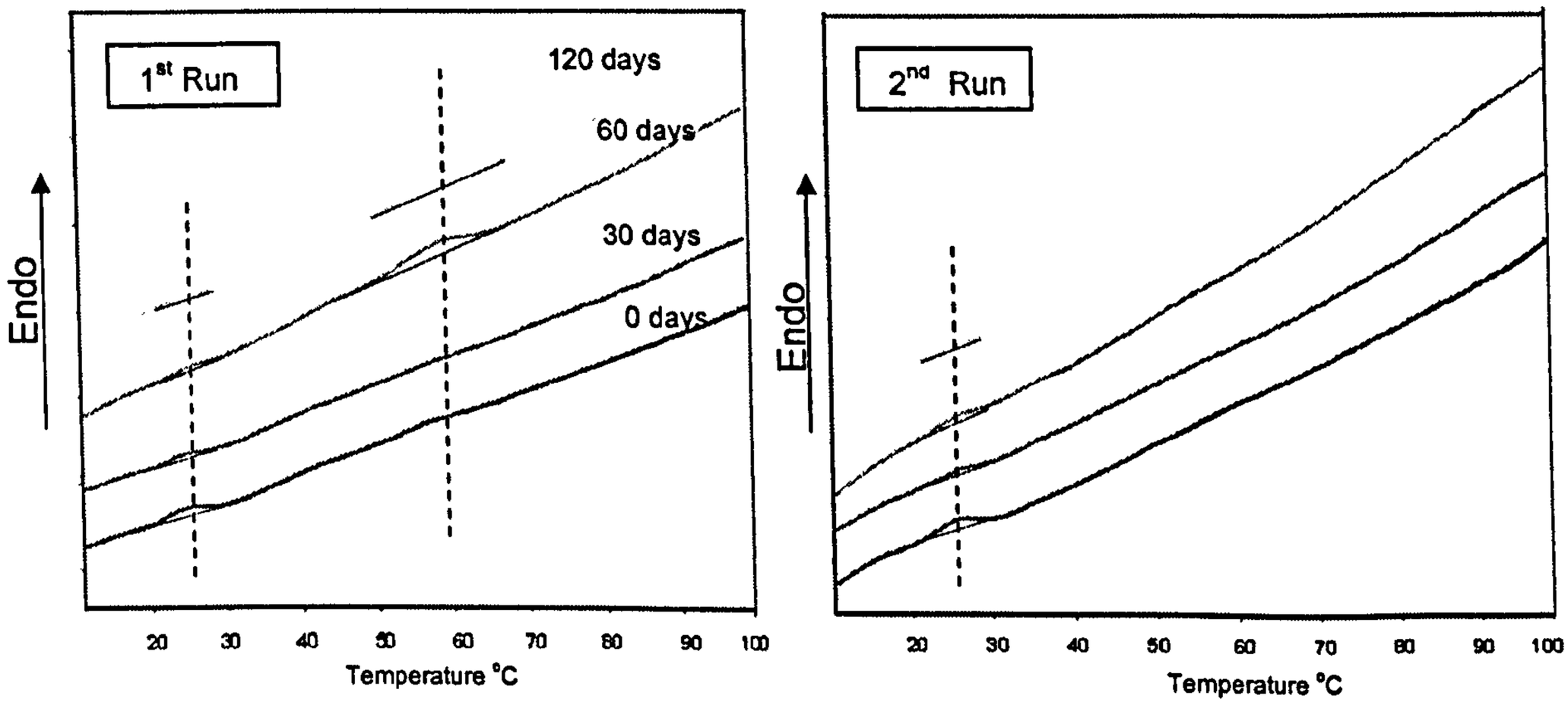

Figure 8.19. 1st and 2nd runs from DSC for fresh and 30, 60 and 120 days stored "Kibbles". Samples were prepared in excess water (solid:water = 1:3), heating rate 10°C/min.

Table 8.8. DSC endotherms and enthalpy for fresh and aged "Kibble" .

	1st Peak Temperature °C	1st Peak Enthalpy (J/g)	2nd Peak Temperature °C	2nd Peak Enthalpy (J/g)
Fresh 1st Run	25.4 (1.2)	0.33 (0.08)	56.1 (1.7)	0.12 (0.03)
Fresh 2nd Run	25.2 (1.8)	0.31 (0.06)		
Aged 30 days 1st run	24.1 (1.3)	0.28 (0.05)	57.4 (1.6)	0.11 (0.04)
Aged 30 days 2nd run	24.9 (1.6)	0.25 (0.07)		
Aged 60 days 1st run	25.5 (1.3)	0.26 (0.05)	57.1 (1.4)	1.03 (0.32)
Aged 60 days 2nd run	25.1 (1.1)	0.25 (0.09)		
Aged 120 days 1st run	25.3 (0.8)	0.28 (0.05)	58.6 (1.9)	2.10 (0.39)
Aged 120 days 2nd run	25.4 (1.2)	0.31 (0.03)		

(*) values in bracket represent the standard deviation from three DSC measurements.

X-ray diffraction was also used to measure the changes in molecular ordering of the stored samples. The experimental settings are presented in section 8.3.1.3 of this chapter

The diffractograms for the fresh and aged "Kibbles" are shown in figure 8.20. It was difficult to detect any significant differences between the fresh and aged products. A small peak was detected for all the samples at 32°, which is thought to occur from the presence crystalline additives (e.g. salts) included in the formulation.

The curves for the fresh and 30 days stored samples were very similar, showing an amorphous-like pattern. In the case of the samples stored for 60 and 120 days there was some indication of higher order structure being formed. Two peaks were detected, the first one at a diffractive angle of ~ 20° and the other at an angle of 23°. These peaks seem to be related to the formation of retrograded starchy structure

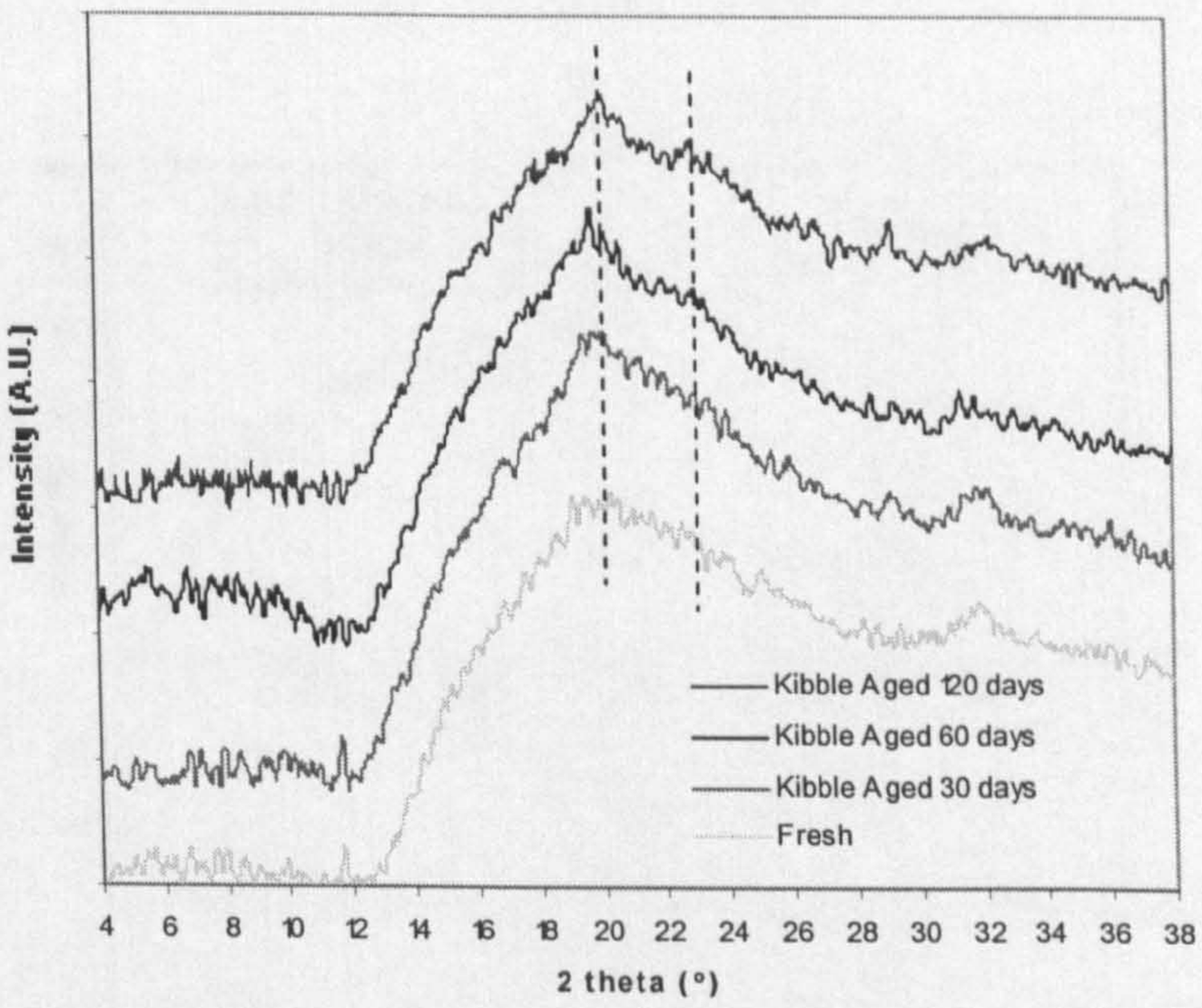

Figure 8.20. X-ray diffractograms for fresh "Kibble" and 30, 60 and 120 days storage.

Next section discusses the study of changes in mechanical and molecular stability on fresh and aged "Dentastix" using a similar analytical approach.

8.3.3.2 Dentastix

Dentastix products were stored as received (original package) for different times at 25°C. The changes in texture were evaluated using a penetration probe attached to the Texture Analyser (TA) (figure 8.21). The probe speed was set at 2 mm/s and the penetration distance was 5 mm. The selected probe had a diameter of 2 mm

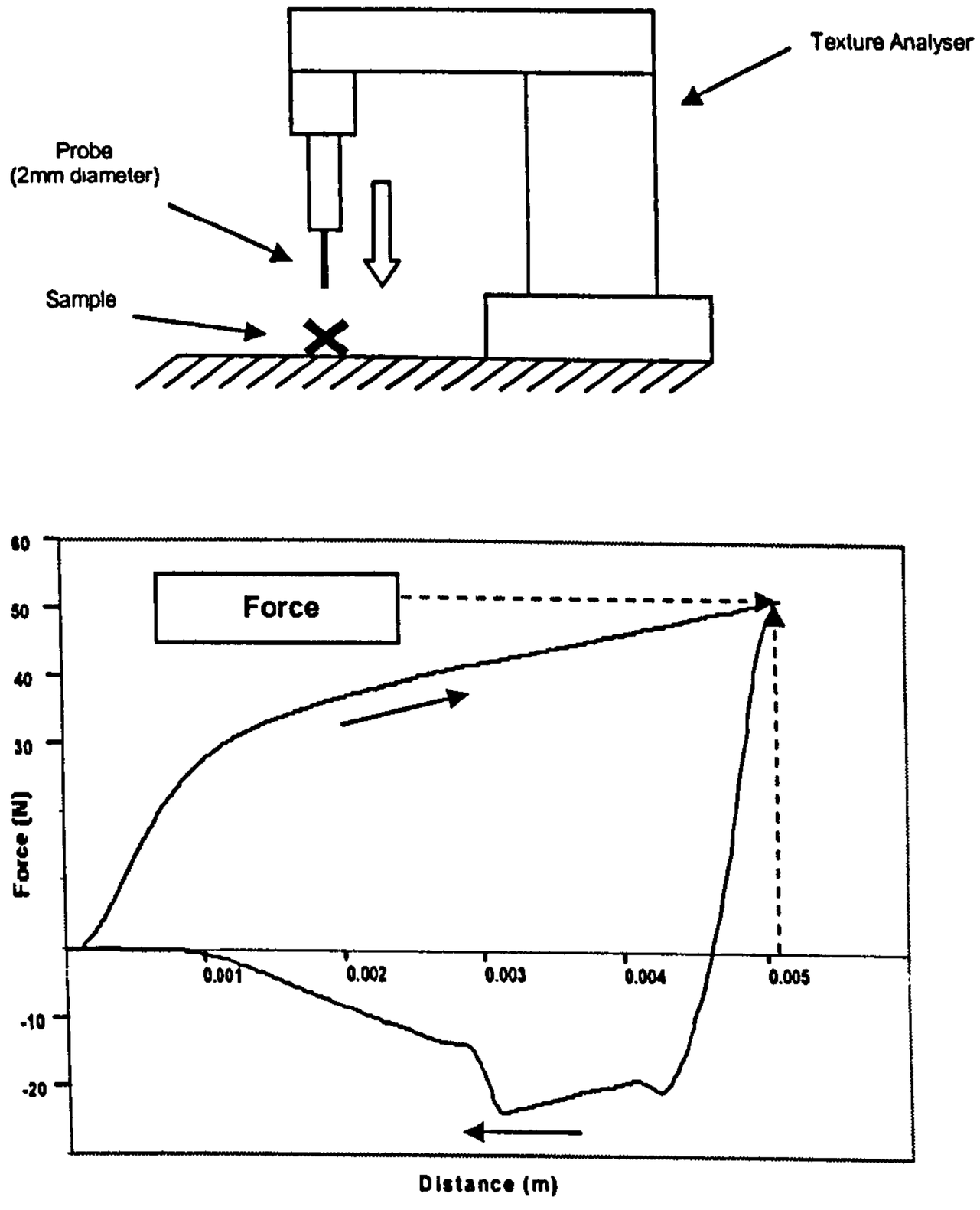

Figure 8.21. Diagram representing the penetration test and a typical curve obtained for Dentastix indicating the force value considered. Negative force values are generated from probe retuning to starting position.

The moisture content of all the samples was measured after storage. This data (mean of three measurements) is presented in table 8.9. A small decrease in the moisture content was detected for samples stored over 40 days. This indicates that the commercial packing used on this product was not effective in controlling moisture migration between the products and environment.

Table 8.9. Moisture content (*) of fresh and stored "Dentatix".

Storage Time	MC (wb)
Fresh	14.4%
15 days	14.5%
40 days	14.2%
70 days	13.7%
90 days	13.5%
100 days	12.9%
120 days	12.7%

The presented values are the mean of 3 measurements. Values in brackets represent the standard deviation..
(*) Vacuum oven at 70°C overnight

Figure 8.22 depicts the changes in penetration force with storage time at 25°C. Unlike "Kibble", there was a marked and significant increase ($P<0.05$) in this parameter for the first 40 days of storage, with increase from ~ 55N for the fresh sample to ~ 85N after 40 days. A continuous increase was detected up to 70 days of storage, point at which the curve started to level off. After 90 days storage no significant differences in the compression force were detected ($P>0.05$), with a final value of ~ 100N after 120 days.

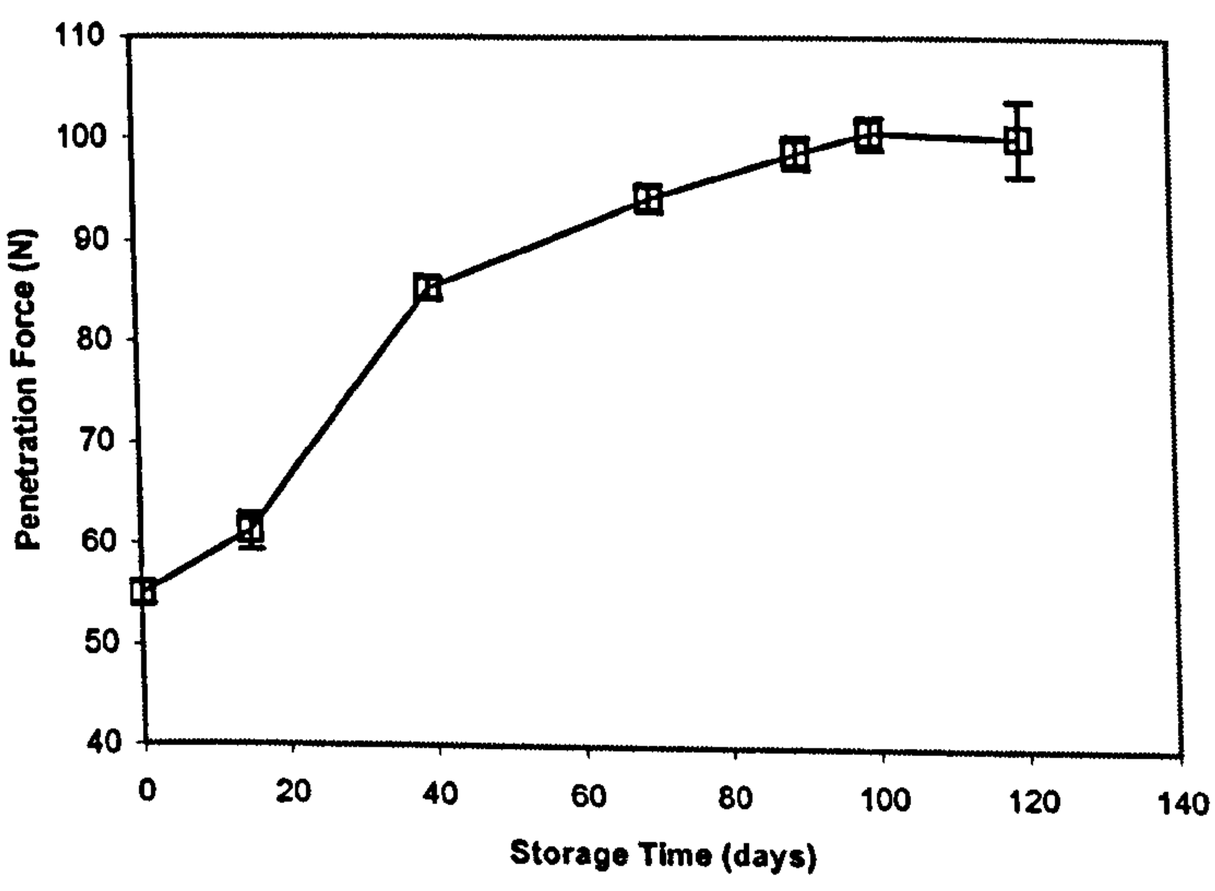

Figure 8.22. Penetration force (5 mm) on "Dentastix" versus storage time (days). Error bars represents the standard deviation of 5 measurements.

As for "Kibble", the experimental data was modelled using Avrami equation. Figure 8.23 show the modelled data and the Avrami parameters after model optimisation. Although obtained from different mechanical properties

(penetration force for commercial products and flexural modulus for model system), the final kinetic parameter *G* was ~ 2.5E-02 (h^{-1}) was comparable to the ~ 7E-03 (h^{-1}) obtained for wheat starch-20% glycerol and ~16% (db) moisture content (section 6.3.1.2 of chapter 6).

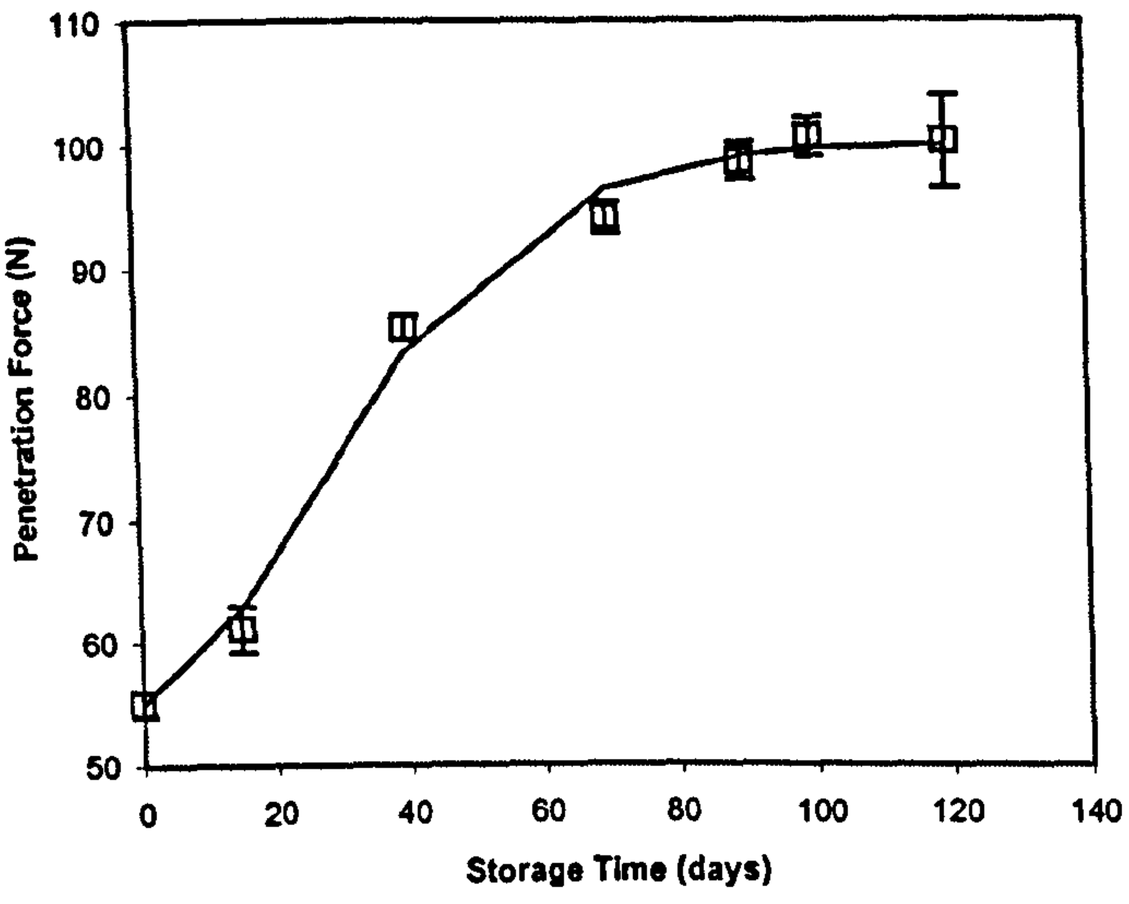

Avrami Parameters

n	1.69
G (h^{-1})	2.50E-02
k	1.97E-03
Y_{inf} (*V*)	100.0
Yo	69.0

Figure 8.23. Avrami modelled equation fitted on penetration force data for "Dentastix" ($R^2 = 0.99$). Modelling parameters were obtained after minimising the squared sum on the difference (Solver, Excel, Office 2003. Microsoft).

The following section of the experimental work investigates the validity of the approach that assumes the ageing process as a recrystallisation of the starchy component in these products

Figure 8.24 shows the elastic modulus (E') and tan δ curves from DMTA for fresh and aged "Dentastix". There were not marked differences in the elastic modulus (*E'*) at the reference temperature 25°C between the fresh and aged samples. The E' for the fresh "Dentastix" was ~ $10^{7.5}$ (Pa) and for the sample aged for 120 days was ~ $10^{7.7}$ (Pa). As mentioned before in this chapter, differences in the extent of increase in harness detected by large and small deformation tests can be attributed to higher frequency (measurements time-scale) used in mechanical spectroscopy (DMTA).

The small change in *E'* may also be explained as the storage temperature was similar to the obtained Tg values from DMTA (~ 20°C). As shown for starch-glycerol model system, when the T-Tg (T being storage temperature) decreases the retrogradation rate of the starchy component also decreases. Similarities between the fresh and aged products was also detected on the tan δ curve,

where only the sample aged for 120 days showed a marked decrease in the main transition peak. Another finding was the slight shift in the main tan δ peak to higher temperatures when the storage time increased from a peak temperature of ~ 25°C to ~ 45°C. This seems to be related to the reduction in the moisture content during storage, which would influence the obtained Tg values. This increase in tan δ, due to moisture loss during storage, would also have an impact on the increase on the hardness of these products (figure 8.12 in section 8.3.2).

From this data it seems that the changes in texture of this product during storage is not entirely related to a reduction on molecular mobility as in the case of "Kibble" for which tan δ peak showed a significant reduction after 120 days.

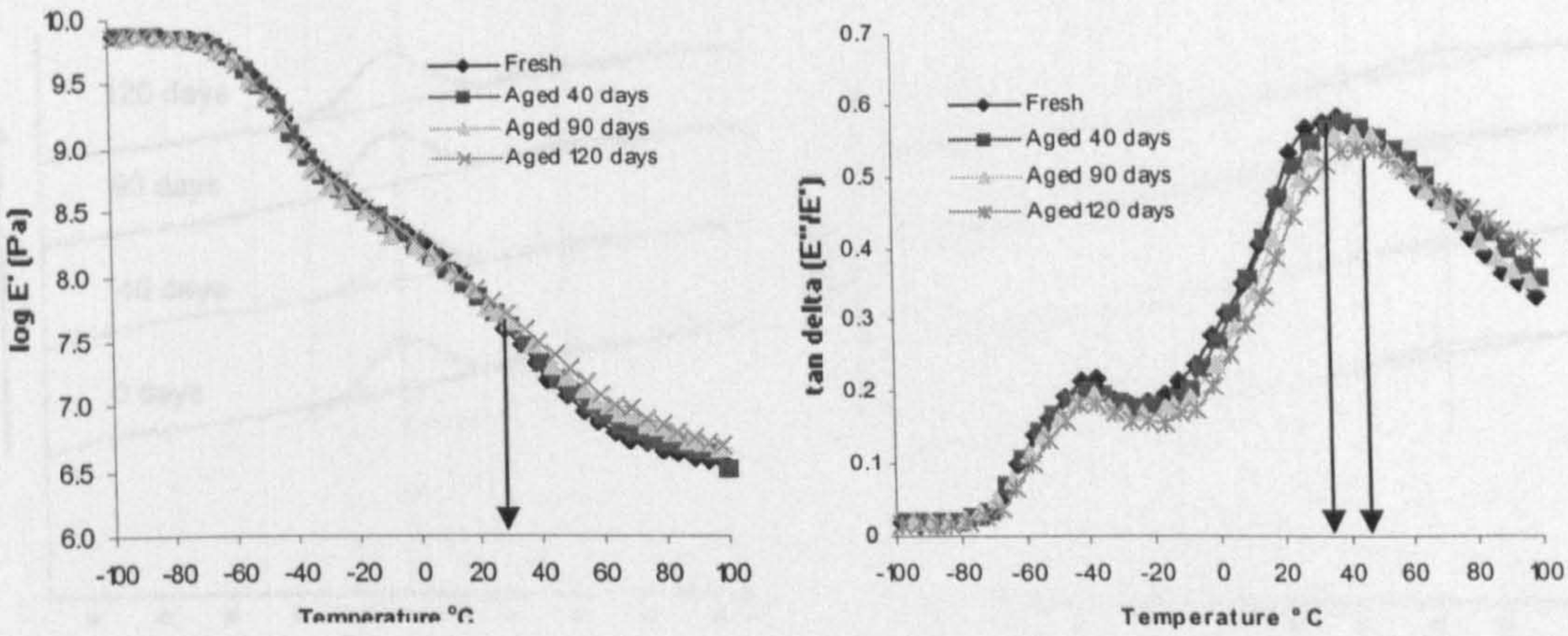

Figure 8.24. Elastic modulus (E') and tan δ (DMTA) for "Dentastix" aged for 0, 40, 90 and 120 days. 10 Hz, heating rate 3°C/min, strain x4 (60um).

"Dentastix" samples were also analysed by DSC using the experimental protocol specified in section 8.3.1.2. Figure 8.25 shows the first (left) and second (right) runs for the fresh and aged "Dentastix". The obtained scans for the fresh sample showed two endotherms, an irreversible transition at ~ 76°C with an enthalpy of ~ 2.1 J/g and a reversible transition at ~ 100°C with an associated enthalpy of 0.6 J/g. As discussed in the first section of this chapter, the first endotherm seems to be related to native rice starch, showing that only a partial conversion during the manufacturing of this product. The reversible endotherm detected at higher temperature has been identified as melting of amylose-lipid complexes formed possible from free lipids present in the

formulation and amylose available from the pregelatinised wheat starch added to the mixture. The aged samples showed a slight increase in the endotherm detected at ~ 76°C, from ~ 2.1 J/g for the fresh product to ~ 2.9 J/g for the products store for 120 days. Retrogradation peaks could be expected to occur at lower temperatures that native starch samples. Table 8.10 present the onset of the gelatinization peaks, where a small decrease in the onset temperature of this peak was detected, from 66.1°C for the fresh product to 63.3°C for the product stored for 120 days.

These findings would also suggest that the converted fraction of rice starch and pregelatinised wheat starch added to the formulation could have retrograded during ageing on existent native crystals of the unconverted fraction of rice starch in the mixture.

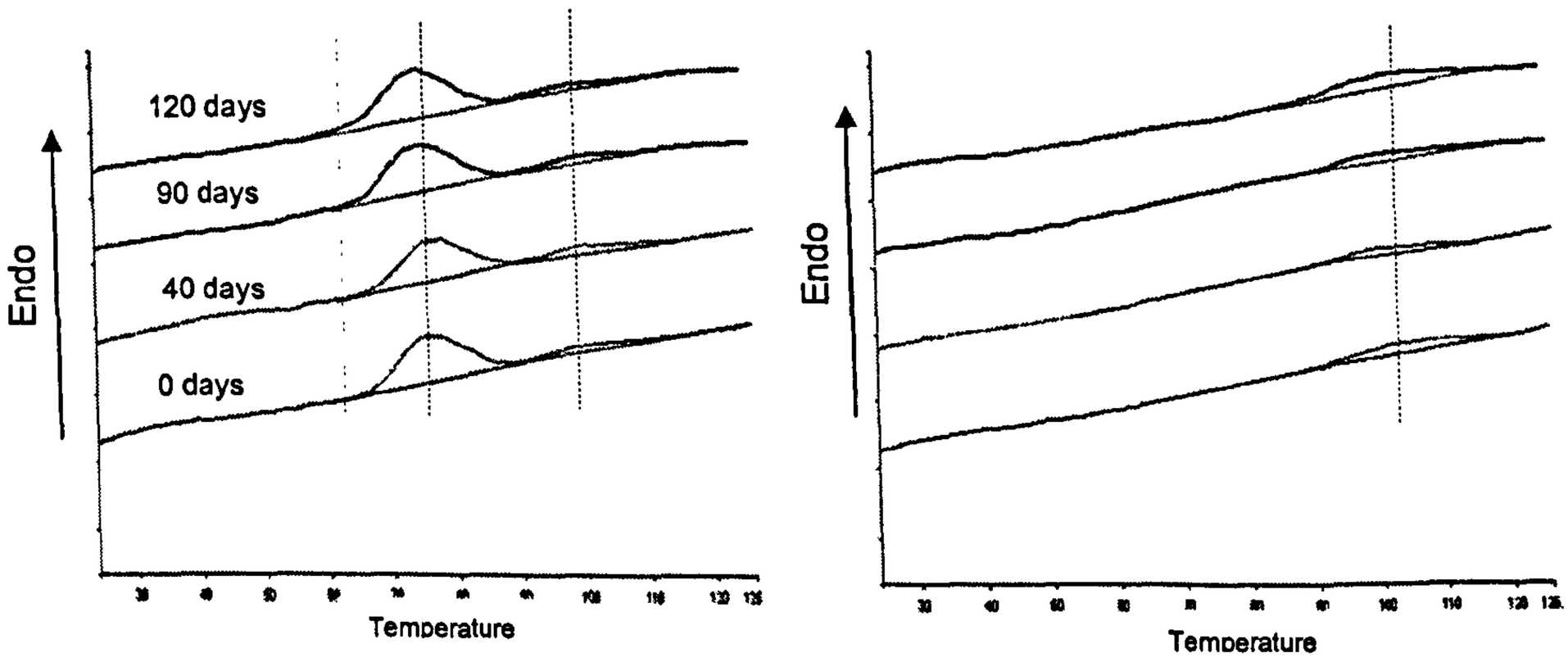

Figure 8.25. DSC 1st (left) and 2nd run for "Dentastix" aged for 0, 40, 90 and 120 days. Heating rate 10°C/min.

Table 8.10. DSC endotherms and enthalpy for fresh and aged "Dentastix"

	Onset 1st Peak °C	1st Peak Temperature °C	1st Peak Enthalpy (J/g)	2nd Peak Temperature °C	2nd Peak Enthalpy (J/g)
Fresh 1st Run	66.1 (0.7)	75.1 (1.1)	2.1 (0.31)	101.3 (2.3)	0.56 (0.09)
Fresh 2nd Run	--	--	--	100.1 (2.2)	1.01 (0.11)
Aged 40 days 1st run	66.0 (0.9)	76.1 (1.4)	2.23 (0.19)	102.1 (1.9)	0.77 (0.12)
Aged 40days 2nd run	--	--	--	101.4 (2.3)	1.11 (0.08)
Aged 90 days 1st run	64.6 (0.8)	76.8 (1.2)	2.80 (0.23)	101.6 (2.5)	1.32 (0.13)
Aged 90 days 2nd run	--	--	--	100.3 (2.3)	1.45 (0.14)
Aged 120 days 1st run	63.6 (0.5)	75.9 (0.8)	2.91 (0.33)	102.7 (2.1)	1.56 (0.13)
Aged 120 days 2nd run	--	--	--	101.6 (2.1)	1.65 (0.19)

Values in brackets represent the standard deviation of three DSC measurements

The DSC data was complemented by the analysis of the fresh and aged samples by X-Ray diffraction. The experimental settings and the protocol for samples preparation are presented in section 8.3.1.3 of this chapter.

Figure 8.26 showed not significant differences between the fresh and aged samples. The profile of all the samples were similar to partially converted starch with peaks at angles ~ 19° and ~ 23° which was supported by the findings from DSC. As indicated before, the peak at 29° has been identified as crystalline KCO_3 used as an additive in the formulation of this product.

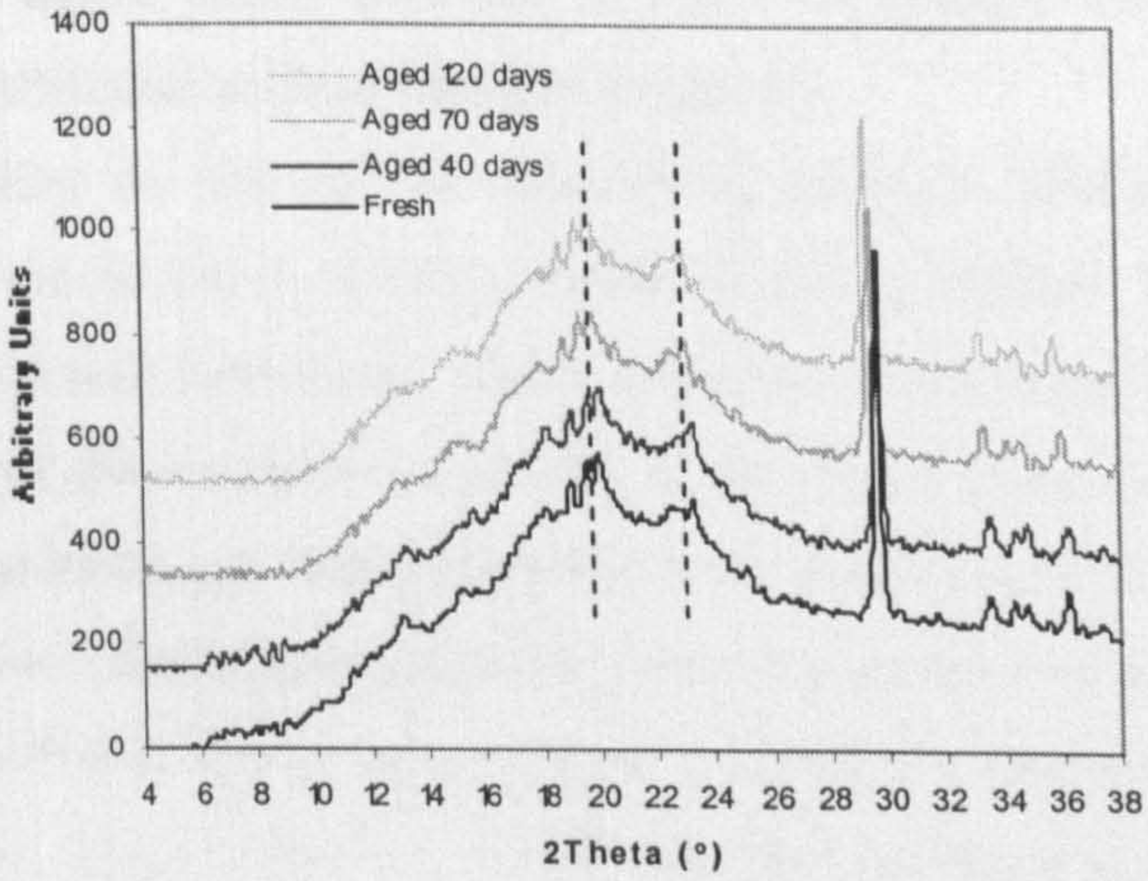

Figure 8.26. X-Ray diffraction for "Dentastix" for 0, 40, 90 and 120 days storage at 25°C

8.4 Conclusions

Mechanical spectroscopy (DMTA) showed that all the commercial products studied were in the rubbery state at ambient temperature (~ 25°C) with an overall glass transition temperature (Tg) of around ~ 10°C. It was also shown that variation in moisture content in these products had an effect on their mechanical properties (Texture Analyser), and these changes seemed to be related to a shift in the mixture Tg (DMTA).

It was estimated by calorimetry (DSC) and X-Ray diffraction that in most of the products evaluated, with exception of Kibble, the starchy component (e.g. rice flour) was not fully converted during manufacturing. It is believed that the presence of native starch structure in the final product could give desired mechanical attributes such as abrasive properties.

Ageing studies on two of the commercial products detected a significant increase in the hardness of these materials during storage. This data agreed with the proposed hypothesis, which attributed this change in texture to re-association of the amorphous structure of the starch component as confirmed by DSC. Another factor that contributed to the hardening in one of the products evaluated was a slight reduction in the moisture content during storage.

The retrogradation kinetic value (*G*) for the products studied was comparable to the values obtained from the model systems suggesting that the temperature differences T-Tg could influence this value *(G)*. Ageing studies at different Tg or storage temperatures are needed to test hypothesis that attributes *G* to T-Tg.

Overlapping the sorption isotherms of pure wheat starch and ~ 20% polyol on the commercial products data suggests that the water sorption is manly controlled be the starchy-polyol component in the product formulation.

8.5 Practical Implications

Based on the experimental work on the model systems and commercial products, several recommendations could be implemented to minimise the changes in texture of this product during storage.

- The first and simplest indication would be to consider an improvement in the packaging of these materials. This would reduce moisture loss of the products and its associated changes in texture during storage.
- Knowing that T-Tg (storage – glass transition temperatures) is an important factor affecting the retrogradation kinetic of the starch fraction, varying this difference by the addition of different plasticizers or storage temperatures would minimise its effect on the stiffness of these products.

  The impracticality of changing storage temperatures indicates that changes in concentrations of plasticizers, such as poly-ethylene glycol, glycerol and sorbitol, can be used to vary Tg. Choosing which of these compounds to use would depend mainly on the extent of Tg reduction (Mw dependent), product formulation -manufacturing and costs.
- Finally, changes in formulations such as the addition of antistaling agents (e.g. emulsifiers) could contribute to reduce the extent of retrogradation by complexation of the amylose fraction of the starch compoents in the mixture.

9 General Conclusions

Sorption studies on extruded starch-glycerol systems did not show differences in the sorption isotherms between waxy, rice, wheat. The successful modelling by the BET and GAB equations (R^2=0.99) showed that the presence of amylose decreased the availability of sorption sited by possibly by the increase in the proportion linear polymers and by the presence on amylose-lipid complexes. The addition of glycerol to the starch systems changed the sorption profile depending on the equilibrating relative humidities (RH). This polyol would interact with the starch polymer at low RH, increasing the water activity (Aw) at constant moisture. At high RH, this polyol would increase the molecular mobility of the polymer, increasing the absorption of moisture and decreasing the Aw of the system at constant moisture.

The sorption kinetic was also affected by the presence of glycerol, with an increase in the diffusion coefficient (*D*) at low RH. An interesting behaviour was detected at higher RH, where *D* values started to decrease. It was observed that this decrease was related to the glass transition temperature (Tg) of the systems. If the ambient temperature gets near Tg, it would indicate that the Fickian approach used was not applicable for the whole RH range influencing the final *D* values. Another factor that affected diffusivities was the change in particle geometry, as observed by optical microscopy. This behaviour was similar for all the extruded waxy maize, rice and wheat starches-glycerol system.

DSC measurements confirmed the plasticization effect of glycerol on the three studies starches. As expected, a sharp decrease in Tg was detected on the samples with low moisture contents. This decrease in Tg started to level off when the moisture concentration reached levels known to decrease this temperature to 25°C (~ 23% wb). The extent of plasticization of this polyol was very similar between waxy maize, rice and wheat starches. This may be explained by the well-known Tg dependence on molecular weight, which would remain relatively constant after certain degree of polymerisation is reached.

This decrease in Tg by water and glycerol were modelled using the Couchman-Karasz and ten-Brinke Karasz equiations. Although both models were accurate

in predicting the experimental data ($R^2 = 0.97$), the latter gave values for ΔCp starch, ΔCp water and ΔCp glycerol, which were more comparable with the literature. The difference in the two models may be related to ten-Brinke model accounting for different ΔCp in glassy and rubbery states and possible interactions between the polyol and the starchy matrix.

Comparable Tg values were obtained from DMTA and DSC analysis on wheat starch extrudates. This would indicate that calorimetry could be use to approximately predict the DMTA mechanical values under well-defined experimental conditions.

Large deformation tests on extruded starches showed no differences in the flexural modulus between the extruded rice and wheat samples. Differences were detected for waxy maize starch at low moisture contents (< ~ 15% wb) due to the brittleness of the material. This was explained by the branched nature of amylopectin, which would influence the mechanical compliance of the material compared to amylose-amylopectin co-polymers.

The presence of glycerol had a marked effect in reducing the flexural modulus at the low end of moisture contents (<15%wb). The softening effect of this polyol was not significant when the moisture present in the samples reached ~ 20% (wb), where these systems showed a rubbery behaviour. The plasticizing effect of this polyol reduced the moisture content at which the inflection point of the stiff to rubber transition occurred. The onset of the stiff to ductile transition was not related to the Tg as reported by DSC. Indeed, it was demonstrated that when T-Tg (T=25°C) approached 0°C, it coincided with the end point of this transition suggesting that this parameter is not the only factor influencing mechanical transitions of these materials.

Small (DMTA) and large (TPBT) deformation tests showed that the determination of Tg also proved to be an important factor in defining the kinetic of hardening of extruded starch-glycerol systems. In the glassy state the ageing mechanism seemed to be related to "physical ageing" where a slow increase in the hardness was detected. In the rubbery state, the increase in hardness was much faster and followed an exponential function. This phenomenon was attributed to starch "retrogradation". This ageing process was successfully modelled by the Avrami equation giving retrogradation rate values (G) that were dependent on polyol concentration. The positive correlation

between *G* and glycerol content was related to the T-Tg value, which varied by the plasticising effect of the polyol.

A similar analytical approach was used to study the mechanical stability of cereal based extruded pet-care products during storage. It was found that these materials were in a rubbery state at ambient temperature as shown by DMTA. Although all of the products analysed show similarities in terms of their formulations (e.g. cereals starches, proteins and polyols), the extent of conversion of the starchy component was different as shown DSC and X-Ray diffraction. Despite these differences, their mechanical behaviour was mainly influenced by the moisture present in the product. DMTA measurements on two of the products showed that this dependency seemed to be related to a change in the glass transition of starchy component in these formulations.

The increase in hardness of these products during storage was related mainly to a retrogradation process as shown by DSC. Nevertheless, the slight moisture loss detected during storage could also have a significant effect of the texture on this material.

It was shown that the material science approach applied to simpler model system was relevant to improve the understanding of the effect of glycerol on the sorption, mechanical properties and ageing stability of starch based materials. This helped to interpret analytical information obtained from more complex formulation such as pet-care products and be able to successful applied theoretical and empirical models to predict the effect of changing plasticiser concentration and storage time on textural properties of these materials.

Although, a better understanding of the functionally of glycerol in starch based systems was obtained from presented work, further study on this these systems is required. An important variable not covered was the effect of temperature on the sorption and mechanical properties as well as on the ageing kinetics during storage. This would complement the information related to the effect relative humidities during storage. Both factors could contribute to the development of more accurate predictive models.

The study of other plasticizers added to starch based systems, under different storage conditions, such as polyethylene glycol and sorbitol would also

contribute clarify the role of these compounds on the structural stability of starches.

Similar experimental approach on more complex systems, such as starch-protein-plasticisers, would also contribute to evaluate possible interaction between the polymeric components affecting the overall mechanical performances of these systems.

10 Bibliography

AACC (1999). "Starch, Practical Guide for Food Industry," American Association of Cereal Chemists.

Alfrey, A., E. F. Gurnee, et al. (1966). "Diffusion in Glassy Polymers." Journal of Polymer Science C12: 249-261.

Allen, G. (1993). A History of the Glassy State. In "The Glassy State in Foods" (J. M. V. Blanshard and P. J. Lillford, eds.), pp. 1-12. Nottingham University Press, Nottingham.

Al-Muhtaseb, A. H., W. A. M. McMinn, and T. R. A. Magee. (2002). "Moisture Sorption Isotherm Characteristics of Foods Products: A Review." Food and Bioproducts Processing 80(Part C): 118-128.

Al-Muhtaseb, A. H., W. A. M. McMinn and T. R. A. Magee (2004). "Water sorption isotherms of starch powders: Part 1: mathematical description of experimental data." Journal of Food Engineering 61: 297-307.

Anderson, R. B. (1946). "Modifications of the Brunauer, Emmett and Teller Equation." Journal of American Chemical Society 68: 686-691.

Arvanitoyannis, I. and C. G. Biliaderis (1999). "Physical properties of polyol-plasticized edible films made from methyl cellulose and soluble starch." Carbohydrate Polymer 38: 47-58.

Arvanitoyannis, I., Kalichevsky, M., Blanshard, J. M. V., and Psomiadou, E. (1994). Study of diffusion and permeation of gases in undrawn and uniaxially drawn films made from potato and rice starch conditioned at different relative humidities. Carbohydrate Polymers 24, 1-15.

Atkins, P. W. (1998). Physical Chemistry. Oxford, Oxford University Press.

Attenburrow, G. E. and A. P. Davis (1993). The mechanical properties of cereals based foods in and around the glassy state. The Glassy State in Foods. J. M. V. Blanshard and P. J. Lillford. Nottingham, Nottingham University Press: 317-331.

Attenburrow, G. E., R. M. Goodband, et al. (1989). "Structure, Mechanics and Texture of a Food Sponge." Journal of Cereal Science 9: 61-70.

Atwell, W. A., Hood, L. F., Lineback, D. R., Varriano-Martson, E., and Zobel, H. F. (1988). The terminology and methodology associated with basic starch phenomena. Cereal Foods World 33, 306-311.

Bader, H. and D. Goritz (1994). "Investigations of high amylose corn starch fimls. Part 2: Water Vapor Sorption." Starch 46: 149.

Baik, M.-Y., Kim, K.-J., Cheon, K.-C., Ha, Y.-C., and Kim, W.-S. (1997). Recrystallization Kinetics and Glass Transition of Rice Starch Gel System. Journal of Agricultural and Food Chemistry 45, 4242-4248.

Becker, A., S. E. Hill and J. R. Mitchell (2001). "Relevance of Amylose-Lipid Complexes to the Behaviour of Thermally Processed Starches." Starch 53: 121-130.

Belitz, H. D., Grosch, W., and Shieberle, P. (2004). "Food Chemistry," 3rd Edition/Ed. Springer.

Bell, L. N. and T. P. Labuza (2000). Moisture Sorption Practical Aspects of Isotherm Measurement and Use, American Association of Cereal Chemists.

Berlin, E., B. A. Anderson, M. J. Pallansc. (1968). "Comparison of water vapour sorption by milk powder components." Journal of Dairy Science 51: 1913-1915.

Biliaderis, C. G. (1990). Thermal analysis of food carbohydrates. Thermal analysis of foods. V. R. Harwalker and C. Y. Ma. London, Elsevier.

Biliaderis, *C. G., A. Lazaridou,* Arvanitoyannis I. (1999). "Glass transition and physical properties of polyol-plasticised *pullulan-starch blends at low* moisture." Carbohydrate Polymers 40: 29-47.

Biliaderis C. G, Page C. M, Maurice T. J, Juliano B. O (1986). Thermal characterisation of rice starches: A polymeric approach to phase transitions of granular starch. Journal of Agricultural and Food Chemistry 34: 6-14.

Bindzus, W., Livings, S. J., Gloria-Hernandez, H., Fayard, G., Lengerich, B. v., and Meuser, F. (2002). Glass Transition of Extruded Wheat, Corn and Rice Starch. Starch 54, 393-400.

Bizot, H., Bail, P. L., Leroux, L., Davy, J., Roger, P., and Buleon, A. (1997). Calorimetric evaluation of the glass transtion in hydrate, linear and branched polyanhyglucose compounds. Carbohydrate Polymers 32, 33-50.

Blanche, S., and Sun, X. (2004). Physical Characterisation of Starch Extrudates as a Function of Melting Transitions and Extrusions Condition. Advances in Polymer Technology 23, 277-290.

Blanshard, J. M. V. (1987). In "Starch: properties and potential". Edited by Galliard T. Society of Chemical Industry.

Borde, B., H. Bizot, Vigier G. and Buleon A. (2002). "Calorimetric analysis of the structural relaxation in partially hydrated amorphous polysaccharides. II. Phenomenological study of physical ageing." Carbohydrate Polymers 48: 111-123.

Brunauer, S., L. S. Deming, W.E. Deming and E .Teller. (1940). "On the Theory of the van der Waals Adsorption of Gases." Journal of American Chemical Society 62: 1723-1732.

Brunauer, S., P. H. Emmet, Teller E. (1938). "Adsorption of Gases in Multimolecular Layers." Journal of American Chemical Society 60: 309-319.

Buléon, A., Colonna, P., Planchot, V., and Ball, S. (1998). Starch granules: structure and biosynthesis. International Journal of Biological Macromolecules 23, 85-112.

Carvalho, A. J. F., Job, A. E., Alves, N., Curvelo, A. A. S., and Gandini, A. (2003). Thermoplastic starch/natural rubber blends. Carbohydrate Polymers 53, 95-99.

Carvalho, C., W. P (2001). Effect of sugar on the extrusion of wheat and maize. PhD, University of Nottingham, Nottingham.

Chen, Z. C., Mukarami, K. I., and Takeda, T. (2000). Effect of particle paking on extrusio nehavior of pastes. Journal of Material Science 35, 5301-5307.

Chinnaswamy, R., Hanna, M. A., and Zobel, H. F. (1989). Microstructural, physicochemical, and macromolecular changes in extrusion-cooked and retrograded corn starch. Cereal Foods World 34, 415-422.

Chirife, J. and H. Iglesias (1978). "Equations for fitting water sorption isotherms of foods: Part 1 - a review." Journal of Food Technology 13: 159-174.

Chung, H.-J. and S.-T. Lim (2004). "Physical Aging of Glassy Normal and Waxy Rice Starches: Thermal and Mechanical Characterisation." Carbohydrate Polymers 57: 15-21.

Collison, R. (1968). Starch Retrogradation. Starch and its Derivatives. J. A. Radley. London, Chapman and Hall Ltd.

Colonna, P., and Mercier, C. (1983). Macromolecular modification of manioc starch components by extrusion cooking without lipids. Carbohydrate Polymer 3, 87-108.

Colonna, P., Doublier, J. L., Melcion, J. D., de Monredon, F., and Mercier, C. (1984). Extrusion cooking and Drum drying of wheat starch I. Physical and macromolecular modification. Cereal Chemistry 61, 538-543.

Columbano, A., G. Buckon, P. Wikeley. (2002). " A study of the crystallisation of amorphous salbutamol sulphate using water vapour sorption and near infrared spectroscopy." International Journal of Pharmaceutics 237: 171-178.

Cooke, D. and M. J. Gidley (1992). "Loss of crystalline and molecular order during starch gelatinisation: origin of the enthalpic transition." Carbohydrate Research 227: 103-112.

Coultate, T. P. (1996). "Food: the chemistry of its components," 3rd Edition/Ed. The Royal Society of Chemistry.

Coupland, J. N., N. B. Shaw, F. J. Monahan, E. D. O'Riordan and M. O'Sullivan (2000). "Modelling the effect of glycerol on the moisture sorption behaviour of whey protein edible films." Journal of Food Engineering 43: 25-30.

Crank, J. (1993). The Mathematics of Diffusion, Oxford University Press.

Davidson, I. G., E. J. Langne, S.V. Plowman, J.A. Blair. (2003). "Release Mechanism of Insulin Encapsulated In Trehalose Ester Derivative Microparticles Delivered Via Inhalation". International Journal of Pharmaceutics 254: 21-222.

de Boar, J. H. (1953). The Dynamic Character of Adsorption. Oxford, UK, Clarendon Press.

de Muelenaere , H. J. H. and Buzzardm J. L. (1969). Cooker extruders in service of World feeding. Foof Technology 23: 345

Del Nobile, M. A., T. Martoriello, G. Mocci, E. La Notte (2003). "Modelling the starch retrogradation kinetic of durum wheat bread." Journal of Food Engineering 59: 123-128.

Dobraszczyk, B. and J. V. Vincent (1999). Measurement of Mechanical Properties of Food Materials in Relation to Texture: The Materials Approach. Food Texture. A. J. Rosenthal. Aspen Publishers, Inc.

Donovan, J. W. (1979). "Phase transitions of starch-water systems." Biopolymers 19: 263-275.

Farhat, I. A. (1996). Molecular Mobility and interactions in biopolymer-sugar-water systems. PhD Thesis. Food Sciences. Sutton Bonington, University of Nottingham.

Farhat, I. A., and J. M. V. Blanshard, (1997). On the extrapolation of the melting temperature of dry starch from starch-water data using the Flory-Huggins equation. Carbohydrate Polymer 32, 263.

Farhat, I. A., Blanshard, J. M. V., and Mitchell, J. R. (2000b). The retrogradation of waxy maize starch extrudates: Effects of storage temperature and water content. Biopolymers 53, 411-422.

Farhat, I. A., Blanshard, J. M. V., Decamps, M., and Mitchell, J. R. (2000a). Effect of sugars on retrogradation of waxy maize starch-sugar extrudates. Cereal Chemistry 77, 202-208.

Felder, R. M. and G. S. Huvard (1980). Permeation, Diffusion, and Sorption of Gases and Vapours. Methods of experimental physics. L. Marton, C. Marton and R. Fava. New York, London, Academic Press: 315-377.

Fennema, O. R. (1996). "Food Chemistry," 3rd Edition/Ed. Marcel Dekker, New York.

Fletcher, S. I., Richmond, P., and Smith, A. C. (1985). An experimental study of twin-screw extrusion-cooking of maiz grits. Journal of Food Engineering 4, 291-312.

Fontanet, I., S. Davidou, C. Dacremont, M. and Le Meste (1997). "Effect of Water on the Mechanical Behaviour of Extruded Flat Bread." Journal of Cereal Science 25: 303-311.

Forssell, P. M., J. M. Mikkiläa, G. K Moates, R. Parker (1997). "Phase and glass transition behaviour of concentrated barley starch-glycerol-water mixtures, a model for thermoplastic starch." Carbohydrate Polymers 34: 275-285.

Forssell, P. M., S. H. D. Hulleman, et al. (1999). "Ageing of rubbery thermoplastic barley and oat starches." Carbohydrate Polymer 39: 43-51.

Forssell, P., J. Mikkila, T. Suortti. (1996). "Platicisation of Barley Starch with Glycerol an Water." Journal of Pure Applied Chemistry 5: 703-715.

Franks, F. (1991). Hydration phenomena: an update and implications. Water Relations in Books. H. Levin and L. Slade. New York, Plenum Press.

Gal, S. (1972). "Expression of concentration of water vapor in water vapor sorption measurements". Helvetica Chimica Acta 55: 1752.

Gallant, D. J., Bouchet, B., and Baldwin, P. M. (1997). Microscopy of starch: evidence of a new level of granule organization. Carbohydrate Polymers 32, 177-191.

Garber, B. W., Hsieh, F., and Huff, H. E. (1997). Influence of particle size on the twin-screw extrusion of con meal. Cereal Chemistry 74, 656-661.

García, M. A., M. N. Martino, E. N. Zaritzky. (2000). "Microstructural Characterization of Plasticised Starch-Based Film." Starch 52(4): 118-124.

Gaudin, S., D. Lourdin, D. Le Botlan, J.L. Ilari, P. Colonna (1999). "Plasticisation and Mobility in Starch-Sorbitol Films." Journal of Cereal Science 29: 273-284.

Gelders, G. G., Vanderstukken, T. C., Goesaert, H., and Delcour, J. A. (2004). Amylose-lipid complexation: a new fractionation method. Carbohydrate Polymers 56, 447-458.

Gomez, H. M., and Aguilera, M. (1983). Changes in Starch Fraction During Extrusion-cooking of Corn. Journal of Food Science 48, 378-381.

Gomez, H. M., and Aguilera, M. (1984). A physicochemical model for extrusion of corn starch. Journal of Food Science 49, 40-.

Goodfellow, B. J. and Wilson, R. H. (1990). A Fourier Transform IR Study of Gelation of Amylose and Amylopectin. Biopolymers 30, 1183-1189.

Gordon, M. and J. S. Taylor (1952). "Ideal copolymers and the second order traditions of synthetic rubbers I. Non-crystalline copolymers." Journal of Applied Chemistry 2: 593-600.

Graaf, R. A. d., Karman, A. P., and Janssen, L. P. B. M. (2003). Material Properties and Glass Transition Temperatures of Different Thermoplastic Starches After Extrusion Processing. Starch 55, 80-86.

Guggenheim, E. A. (1966). Application of Statistical Mechanics, Clarendon Press, Oxford, UK.

Guo, J.-H. (1993). "Effects of plasticizers on water permeation and mechanical-properties of cellulose-acetate - antiplasticization in slightly plasticized polymer film". Drug development and industrial pharmacy 19: 1541-1555.

Guzman, L. B., T. C. Lee,., and C. O. Chichester. (1992). Lipid Binding During Extrusion Cooking. In "Food Extrusion Science and Technology" (J. L. Kiokini, C.-T. Ho and M. V. Karwe, eds.), pp. 427-436. Marcell Deker, Inc., New York.

Hagenimana, A., P. Pu, X.L. Ding (2005). "Study on thermal and rheological properties of native rice starches and their corresponding mixtures." Food Research International 38: 257-266.

Haines, P. J., Ed. (2002). Principles of Thermal Analysis and Calorimetry. RSC Paperbacks, The Royal Society of Chemistry.

Hallberg, L. M. and P. Chinachoti (1992). "Dynamic Mechanical Analysis for Glass Transitions in Long Shelf-Life Bread." Journal of Food Science 57: 1201-1204.

Harper, J. M. (1981). "Extrusion of Foods," CRC Press, Boca Raton (Florida).

Harper, J. M. (1992). A comparative analysis of single- and twin-screw extruders. In "Food Extrusion Science and Technology" (J. L. Kokini, C.-T. Ho and M. V. Karwe, eds.), pp. 139-148. Mec; Dekker, Iic., New York.

Harris, M. and M. Peleg (1996). "Pattern of Textural Changes in Brittle Cellular Cereal Foods Caused by Moisture Sorption." Cereal Chemistry 73: 225-231.

Hartley, L. (1996). Hydration of biopolymers to low water content. Division of Food Sciences. Loughborough, The University of Nottingham.
Healey, J. N. C., M. H. Rubistein, V, Walters (1974). "The Mechanical properties of some binders used in tableting." Journal of pharmacy and pharmacology 26: 41-46.

Heldman, D. R., and Hartel, R. W. (1997). Food Extrusion. In "Principles of Food Pocessing", pp. 253-283. Chapman and Hall.

Ho, C.-T., and Izzo, M. T. (1992). Lipid-Protein and Lipid-Carbohydrate Interactions During Extrusion. In "Food Extrusion Science and Technology" (J. L. Kiokini, C.-T. Ho and M. V. Karwe, eds.), pp. 415-427. Marcell Deker, Inc., New York.

Hoover, R., and Hadziyev, D. (1981). Chracterization of potato starch and its monoglycerides complexes. archSt 33, 290-300.

Hopfenberg, H. B. and H. L. Frisch (1969). Journal of Polymer Science Part B 7.

Hopkinson, I., R. A. L. Jones, S. Black, D.M. Lane, P.J. McDonald. (1997). "Fickian and Case II diffusion of water into amylose: a stray field NMR study." Carbohydrate Polymers 34: 39-47.

Hopkinson, I., R. A. L. Jones, P.J. McDonald, B. Newling, A. Lecat, S. Livings. (2001). "Water ingress into starch and sucrose:starch systems." Polymer 42: 4947-4956.

Hutchinson (1995). "Physical aging of polymers." Progress in polymer science 20: 703-760.

Iglesias, H. A. and J. Chirife (1982). Handbook of Sorption Isotherms: Water Sorption Parameters for Food and Food Components. New York, London, Academic Press.

Iglesias, H., J. Chirife, Boquet, R. (1980). "Prediction of water sorption isotherms of food models from knowledge of components sorption behavior." Journal of Food Science 45: 451-452 and 457.

Jagannath, J. H., Jayaraman, K. S., Arya, S. S., and Somashekar, R. (1998). Differential scanning calorimetry and wide-angle X-ray scattering studies of bread staling. Journal of Applied Polymer Science 67, 1597-1603.

Jiugao, Y., Songzhe, C., Jianping, G., Huawu, Z., Jie, Z., and Tong, L. (1998). A Study on the Properties of Starch/Glycerine Blend. Starch 50. 246-250.

Jouppila, K., Kansikas, J., and Roosa, Y. H. (1998). Factors affecting crystallization and crystallization kinetics in amorphous corn starch. Carbohydrate Polymers 36, 143-149.

Kalambur, S. B. (2004). Starch-Based Nano-Composites by Reactive Extrusion Processing. Polymer International 53, 1413-1416.

Kalichevsky, M., E. M. Jaroszkiewicz, et al. (1992). "The Glass Transition of Amylopectine Measured by DSC, DMTA and NMR." Carbohydrate Polymer 18: 77-88.

Kalichevsky, M. T., J. M. V. Blanshard, R. D. L. Marsh. (1993). Applications of Mechanical Spectroscopy to the Study of Glassy Biopolymers and Related Systems. The Glassy State in Foods. J. M. V. Blanshard and P. J. Lillford. Nottingham, Nottingham University Press.

Kalichevsky, M., E. M. Jaroszkiewicz and J. M. V. BLANSHARD. (1993). "A Study of the Glass Transition of Amylopectin-Sugar mixtures." Polymer 34: 346.

Kaminski, W. and M. Al-Bezweni (1994). "Calculation of water sorption for multicomponent protein-containing mixtures."International Journal of Food Science And Technology 29: 129-136.

Karel, M. and I. Saguy (1991). Effects of water on diffusion in food systems. Water Relationships in Foods. H. Levin and L. Slade. New York, Plenum Press.

Karim, A., M. Norziah, C. Seow. (2000). Methods for the study of starch retrogradation. Food Chemistry 71, 9-36.

Kaur, K., and Singh, N. (2000). Amylose-lipid complex formation during cooking of rice starch. Food Chemistry 71, 511-517.

Kearns, J. P., Rokey, G. J., and Huber, G. R. (2004). Extrusion of texturized proteins. American Soybean Association.

Kirby, A. R., S. A. Clark, R. Parker, A. C. Smith. (1993). "The deformation and failure behaviour of wheat starch plasticised with water and polyols." Journal of Material Science 28: 5937-5942.

Kokini, J. L., Ho, C.-T., and Karwe, M. V., eds. (1992). "Food Extrusion Science and Technology." Mrcel Dekker, Inc.

Kruiskamp, P. H., A. L. M. Smits, J. J. G. van Soest, J. F. G. Vliegenthart (2001). "The influence of plastisers on molecular organisation in dry amylopectin measured by differential scanning calorimetry and solid state nuclear magnetic resonance spectroscopy." Journal of Industrial Microbiology & Biotechnology 26: 90-93.

Kugimiya, M. and J. W. Donovan (1981). "Calorimetric determination of the amylose content of starches based on formation and melting of the amylose-lysolecithin complex." Journal of Food Science 46: 765-777.

Kugimiya, M., J. W. Donovan, R.Y. Wong (1980). "Phase Transitions of Amylose-Lipid Complexes in Starches a Calorimetric Study." Starch 32: 265-270.

Kuipers, N. J. M., H. F. Vervelde, E. J. Stamhuis, , A. A. C. M. Beenackers (2003). "Sorption and diffusion of ethylene oxide in semidry potato starch granules." Industrial and Engineering Chemistry Research 42: 6068-6079.

Kulp, K., and Ponte, J. G. J. (1981). Staling of white pan bread: fundamentals Causes. Critical Review in Food Science and Nutrition 15, 1-48.

Labuza, T. Creation of Moisture Sorption Isotherms for Hygroscopic materials. URL:http://faculty.che.umn.edu/fscn/Ted_Labuza/PDF_files/Papers/Creation_Moisture_Isotherms.PDF.

Labuza, T. P., J. Hawkes, D. Gallaghe, F. Hurtado, L. MCnally (1972). "Stability of intermediate moisture foods 1.Lipid oxidation." Journal of Food Science 37: 154.

Lai, L. S., and Kokini, J. L. (1990). The effect of extrusion operating variables on the on-line apparent viscosity of 98% amylopectin (Amioca) and 70% amylose (Hylon 7) corn starches during extrusion. Journal of Rheology 34, 1245-1266.

Lai, L. S., and Kokini, J. L. (1991). Physicochemical Changes and Rhelogical Properties of Starch during Extrusion (A Review). Biotechnol. Prog. 7, 251-266.

Lang, K. W. and M. P. Steinberg (1980). "Calculation of Moisture Content of a Formulated Food System to any Given Water Activity." Journal of Food Science 45. 1228-1230.

Laohakunjit, N. and A. Noomhorm (2004). "Effect of Plasticizers on Mechanical and Barrier Properties of Rice Starch Film." Starch 56: 348-356.

Lauritzen, J. I., and Hoffman, J. D. (1973). Extension theory of growth of chain-folded polymer crystals to large undercoolings. Journal of Applied Physics 44, 4340.

Leiras, M. C. and H. Iglesias (1991). "Water vapour sorption of two cake mixes and their components." International journal of food science and technology 26, 91-97.

Levine, H. and L. Slade (1986). "A polymer Physico-Chemical Approach to the Study of Commercial Starch Hydrolysis Products (SHPs)." Carbohydrate Polymer 6, 213-244.

Levoguer, C. L. and J. Booth Moisture Sorption of EC Standard Reference.

Lewis, G. N. (1901). "Das Gesetz physiko-chemischer Vorgange". Zeitschrift für Physikalische Chemie 38: 205-226.

Lewis, G. N. b. (1907). "Umriss eines neuen tsystems der chemischen thermodynamic". Zeitschrift für Physikalische Chemie 61: 129-165.

Lim, C. a. C. (2001). Thermal transition characteristics of heat–moisture treated corn and potato starches. Carbohydrate Polymers 46, 107-115.

Lionetto, F., A. Maffezzoli, M. A., Ottenhof, I. A. Farhat, and J. R. Mitchell (2005). "The Retrogradation of Concentrated Wheat Starch Systems." Starch 57: 16-24.

Liu, Y., Feng. (2001). Effects of glycerin and glycerol monostearate on performance of thermoplastic starch. Journal of Material Science 36, 1809-1815.

Lloyd, N. E. and L. C. Kirst (1963). "Some factors affecting tensile strength of starch films." Cereal Chemistry 40: 154.

Lopez, L. (2003). Impact of Processing Prior to Thermomechanical Extrusionof Starchy Materials. PhD, The University of Nottingham, Nottingham.

Lourdin, D., P. Colonna, G.J. Brownsey, T.R. Noel and S.G. Ring (2002). "Structural relaxation and physical ageing of starchy materials." Carbohydrate Research 337(9): 827-833.

Lourdin, C. P, T. R. Noel, R. Parker and S. G. Ring (2002). "The Influence of Starch Dynamics on Material Properties of Glassy Materials". 113-123

Lourdin, D., H. Bizot, P. Colonna. (1997). "Antiplasticization in Starch-Glycerol Films?" Journal of Applied Polymer Science 63: 1047-1053.

Lourdin, D., L. Coignard, H. Bizot and P. Colonna (1997). "Influence of equilibrium relative humidity and plasticiser concentration on the water content and glass transition of starch materials." Polymer 38: 5401-5406.

Lourdin, L., H. Bizot, P. Colonna. (1997). "Correlation between static mechanical properties of starch-glycerol materials and low-temperature relaxation." Macromolecules Symposium 114: 179-185.

Martin, S. (1962). "The Control of Conditioning Atmospheres by Saturated Salt Solutions." Journal of Scientific Instruments 39: 370-372.
Material RM 302 on a DVS-1 instrument. Surface Micro Systems Dynamic Vapour Sorption Aplications Notes.

Mathew, A. P. and A. Dufresne (2002). "Plasticized Waxy Maize Starch: Effect of Polyols and Relative Humidity on Material Properties." Biomacromolecules 3: 1101-1108.

Mercier, C., Charbonniere, R., Grebaut, D., and Dela Guerivene, J. F. (1980). formation of amylose-lipid complexes by twin-screw extrusion cooking of manioc starch. Cereal Chemistry 57, 4-9.

Mitchell, J. R., and Areas, J. A. G. (1992). Structural changes in biopolymers during extrusion. In "Food Extrusion Science and Technology" (J. L. Kokini, C.-T. Ho and M. V. Karwe, eds.). Marcell Dekker, Inc., New York.

Mitchell, J. R., Hill, S. E., Paterson, L., Valles, B., Barclay, F., and Blanshard, J. M. V. (1997). The Role of Molecular Weight in the Conversion of Starch. In "Starch: Structure and Functionality" (P. J. Frazier, A. M. Donald and P. Richmond, eds.), pp. 68-76. The Royal Society of Chemistry, Cambridge.

Mizuno, A., Mitsuiki, M., and Motoki, M. (1998). Effect of Crystallinity on the Glass Transition Temperature of Starch. Journal of Agricultural and Food Chemistry 46, 98-103.

Moates, G. K., Noel, T. R., Parker, R., and Ring, S. G. (2001). Dynamic mechanical and dielectric characterisation of amylose–glycerol films. Carbohydrate Polymers 44, 247-253.

Moraru, C. I., T.C. Lee, M.V. Karwe and J.L. Kokini, (2002). "Plasticizing and Antiplasticizing Effects of Water and Polyols on a Meat-Starch Extruded Matrix." Journal of Food Science 67: 3396-3401.

Morrison, W. R. (1995). Starch Lipids and How They Relate to Starch Granule Structure and Functionality. Cereal Foods World 40, 437.

Mousia, Z. (2000). Structural and Mechanical Propereties of Biopolymer and Biopolymer-Sugar Blends. Food Sciences. Sutton Bonington, University of Nottingham.

Mousia, Z., I. A. Farhat, J.F. Blachot and J.R. Mitchell (2000). "Effect of Water Partitioning on The Glass-Transition Behaviour of Phase Separated Amylopectin–Gelatin Mixtures." Polymer 41: 1841-1848.

Myllärinen, P., R. Partanen, J. Sépala and P. Forssell. (2002). "Effect of glycerol on behaviour of amylose and amylopectin films." Carbohydrate Polymers 50: 355-361.

Nashed, G., Rutgers, R. P. G., and Sopade, P. A. (2003). The Plasticisation Effect of Glycerol and Water on the Gelatinisation of Wheat Starch. Starch 55, 131-137.

Nguyen, X. Q., M. Sipek and G. T Nguyen (1992). "Permeation of Carbon-Dioxide and Water-Vapour in Plasticized Poly (VinylChloride) Starch Blends-Anomalous Behaviour." Polymer 33: 3698-3705.

Nicholls, R. J., A. J. Appelqvist, A. P. Davies, S.J, Ingman and P.J. Lillford (1995). "Glass Transition and the Fracture Behaviour of Gluten and Starches within the Glassy State." Journal of Cereal Science 21: 25-36.

Nielsen, S. S. (1998). Food Analysis. Second Edition. Maryland, Aspen Publishers, Inc.

Norton, C. (1998). Texture and hydration of expanded rice. Division of Food Sciences. Nottingham, The University of Nottingham.

Orford, P. D., R. Parker, S.G. Ring. (1990). "Aspects of the Glass Transition Behaviour of Mixtures of Carbohydrates of Low Molecular Weight." Carbohydrate Research 196: 11-18.

Orford, P. D., Parker, R., Ring, S. G., and Smith, A. C. (1989). Effect of water as a diluent on the glass transition behaviour of malto-oligosaccharides, amylose and amylopectine. International journal of biological macromolecules 11, 91-96.

Ottenhof, M. A. (2003). A multi-technique study of the retrogradation of concentrated starch systems. PhD, University of Nottingham.

Ottenhof, M.-A., S. E. Hill and I.A. Farhat. (2005). "Comparative study of the retrogradation of intermediate water content waxy maize, wheat, and potato starches." Journal of Agricultural and Food Chemistry 53: 631-638.

Owasu-Ansah, Van de Voort, F. P., and Stanley, D. W. (1983). Physico-chemical changes in constarch as a function of extrusion variables. Cereal Chemistry 60, 319-324.

Parker, R. and S. Ring (1995). "Diffusion in maltose-water mixtures at temperatures close to the glass transition." Carbohydrate Research 273: 147-155.

Parker, R. and S. Ring (2001). "Aspects of the Physical Chemistry of Starch." Journal of Cereal Science 34: 1-17.

Peleg, M. (1993). "Assessment of a semi-empirical four-parameter general model for sigmoid moisture sorption isotherms." Journal of Food Process Engineering 16: 21-37.

Peleg, M. (1993). "Assessment of a semi-empirical four-parameter general model for sigmoid moisture sorption isotherms." Journal of Food Process Engineering 16: 21-37.

Peleg, M. (1994 a). "A model of Mechanical Changes in Biomaterials at and around Their Glass Transition." Biotechnology Progress 10: 385-388.

Peleg, M. (1994 b). "Mathematical characterisatio and graphical presentation of the stiffness-temperatue-moisture relationship of gliadin." Biotechnol Progress 10: 652-654.

Peppas, N. A. and G. Sinclair (1983). Colloid Polymer Science 261: 404.

Peppas, N. A. and L. B. Peppas (1994). "Water diffusion and sorption in amorphous macromolecular systems and foods." Journal of Food Engineering 22: 189-210.

Price, D. M. (2002). Thermomechanical, Dynamic Mechanical and Dielectric Methods. Principles of Thermal Analysis and Calorimetry. P. J. Heines. Cambridge, The Royal Society of Chemistry.

Rahman, S. (1995). Food Properties Handbook, CRC Press. place of pbication
Raj, B. A., E. Raj, et al. (2003). "Modeling of Moisture Sorption Isotherms of Poly(vinyl alcohol)/Starch Films." Journal of Applied Polymer Science 89: 3874-3881.

Ribeiro, C., J. E. Zimeri, E. ILDIS and J.L. Kokini (2003). "Estimation of effective diffusivities and glass transition temperature of polydextrose as a function of moisture content." Carbohydrate Polymers 51: 273-280.

Rindlav-Westling, A., M. Stading, A M. Hermansson, and P. Gatenholm (1998). "Structure, Mechanical and Barrier Properties of Amylose and Amylopectin Films." Carbohydrate Polymers 36: 217-224.

Roman-Gutierrez, A. D., S. Guilbert and B. Cuq. (2002). "Distribution of Water between Wheat Flour Components: A Dynamic Water Vapour Adsorption Study." Journal of Cereal Science 36: 347-355.

Roos, Y. H. (1995). Phase Transitions in Foods. San Diego, USA., Academic Press.

Roos, Y. H. and M. Karel (1990). "Differential Scanning Calorimetry Study of Phase Transition Affecting the Quality of Dehydrated Materials." Biotechnology Progress 6: 159-163.

Roy, S., X. W. Xu, S.J. Park and K.M. Liechti. (2000). "Anomalous moisture diffusion in viscoelastic polymers: modelling and testing." Journal of Applied Mechanics 67: 391-396.

Rudin, A. (1999). The elements of polymer science and engineering. Academic Press. USA.

Russell, P. L. (1987). Gelatinization of starches of different amylose/amylopectin content. A study by differential scanning calorimetry. Journal of Cereal Science 6, 133–145.

Rutherford, J. L. and N. Brown, . (1980). Stress-Strain Yield Testing of Solid Polymers. Methods of Experimental Physics. R. A. Fava, Academic Press Inc. (London) Ltd. 16 Part C: 117-135.

Ryu, G. H., and Lee, C. H. (1988). Effect of moisture content and particle size of rice flour on the physical properties of the extrudate. Korean Journal of Food Science and Technology 20, 463-469.

Sala and Tomka (1993). Water uptake in partially frozen and plasticised starch. The Glassy State in Foods. J. M. V. Blanshard and Lilliford. Nottingham, University of Nottingham.

Salwin, H. and V. Slawson (1959). "Moisture transfer in combinations of dehydrated foods." Food Technology 13: 715-718.

Scandola, M., G. Ceccorulli and M. Pizzoli. (1991). "Molecular motions of polysaccharides in the solid state: dextran, pullulan and amylose." International Journal of Biological Macromolecules 13: 254.

Schenz, T. W. and E. A. Davis (1998). Thermal Analysis. Food Analysis Second Edition. S. S. Nielsen. Maryland, Aspen Publishers Inc.: 587-598.

Schields, P. J. (2002). Bragg's Law and Diffraction: How Waves Reveal the Atomic Structure of Crystals", Center for High Pressure Research. Department of Earth & Space Sciences. State University of New York at Stony Brook.

Shah, V. (1998). Mechanical Properties. Handbook of Plastics Testing Technology, John Wiley & Sons: 546.

Slade, L. and H. Levine (1991). A Food Polymer Science Approach to Structure-Property Relationship in Aqueous Food Systems: Non-Equilibrium Behavior of Carbohydrate-Water Systems. Water Relations in Foods. L. Slade and H. Levin. New York, Plenum Press: 29-101.

Slade, L. and H. Levine (1993). The Glassy State Phenomenon in Food Molecules. The Glassy State in Foods. J. M. V. Blanshard and P. J. Lillford. Nottingham, Nottingham University Press: 35-102.

Slade, L. and H. Levine (1988). "Non-Equilibium Melting of Native Granular Starch: Part I: Temperature Location of the Glass Transition Associated with Gelatinisation of A type Cereal Starches." Carbohydrate Research 8: 183.

Slade, L. and H. Levine (1991a). "Beyond water activity: recent advances based on an altenative approach to the assesment of food quality and safety." Critical Review in Food Science and Nutrition 30: 115-360.

Slade, L. and H. Levine (1995). "Water and the Glass Transition-Dependence of the Glass Transition on Composition and Chemical Structure: Special Implications for Flour Functionality in Cookie Baking." Journal of Food Engineering 24: 431-509.

Slade, L., and Levine, H. (1988b). Structural Stability of Intermediate Moisture Foods -- A New Understanding? In "Food Structure -- Its Creation and Evaluation" (J. M. V. Blanshard and J. R. Mitchell, eds.). Butterworths, London.

Smits, A. L. M., P. H. Kruiskamp, J. J. G. van Soest and J. F. G. Vliegenthart (2003). "Interaction between dry starch and plasticisers glycerol or ethylene glycol, measured by differential scanning calorimetry and solid state NMR spectroscopy." Carbohydrate Polymers 53: 409-416.

Smits, A. L. M., S. H. D. Hulleman, J. J. G., Van Soest, H. Feil and F. G. Vliegenthart (1999). "The influence of polyols on the molecular organization in starch-based plastics." Polymers for Advanced technologies 10: 570-573.

Soekarto, S. T. and M. P. Steinberg (1981). Determination of Binding Energy For the Three Fraction of bound Water. Water Activity: Influences on Food Quality. L. B. Rockland and G. F. Stewart. California, Academic Press.

Sombatsompop, N. and K. Chaochanchaikul (2004). "Effect of moisture content on mechanical properties, thermal and structural stability and extrudate texture of poly(vinyl chloride)/wood sawdust composites." Polymer International 53: 1210–1218.

Sperling, L. H. (1996). "Introduction to Physical Polymer Science," John Wiley & Sons, Canada.

Stading, M., Å. Rindlav-Westling and P. Gatenholm (2001). "Humidity-induced structural transitions in amylose and amylopectin films." Carbohydrate Polymers 45: 209-217.

Steebdam, R., W. Henderic, et al. (2001). "Plasticisation of amylodetrin by moisture. Consequences for compactaction behaviour and tablet properties." European Journal of Phamaceutical Sciences 14: 245-254.
Sudharsan, M. B., G. R. Ziegler and J.L. Duda (2004). "Modelling diffusion of moisture during stoving of starch-molded confections." Food and Bioproducts Processing 82(C1): 60-72.

Surface-Measurement-Systems (2000). DVS User Guide/Manual.

Suwonsichon, T. and M. Peleg (1998). "Instrumental and sensory detection of simultaneous brittleness loss and moisture toughening in three puffed cereals." Journal of Texture Studies 29: 255-274.

Swallowe, G. M. (1999). Relaxation in Polymers. Mechanical Properties and Testing of Polymers. G. M. Swallowe: 195-197.

Tadmor, Z., and Klein, I. (1970). "Engineering principles of plasticating extrusion," Van Nostrand-Reinhold, New York, London.

Takaya, T., Sano, C., and Nishinari, K. (2000). Thermal studies on the gelatinisation and retrogradation of heat–moisture treated starch. Carbohydrate Polymers 41, 97-1000.

Tattiyakul, J. (2004). Factors Affecting Extrusion Cooking. http://pioneer.netserv.chula.ac.th/~tjirarat/AdvFoodProcI/Extrusion%20Cooking%20Process7.htm

Teoh, H. M., S. J. Schmidt, G.A. Day andJ.F. Faller (2001). "Investigation of cornmeal components using dynamic vapor sorption and differential scanning calorimetry." Journal of Food Science 66: 434-440.

Tester, R. F. and X. Qi (2004). "Molecular basis of the gelatinisation and swelling characteristics of waxy barley starches grown in the same location during the same season. Part I. Composition and alpha-glucan fine structure." Journal of Cereal Science 39: 47-56.

Tester, R. F., Karkalas, J., and Qi, X. (2004). Starch--composition, fine structure and architecture. Journal of Cereal Science 39, 151-165.

The-UK-Glycerin-Producer's-Association (1975). Glycerin (for the paper industry). 45 Portman Square London.

Timmermann, E. O. (2003). "Multilayer sorption parameters: BET or GAB values?" Colloids and Surfaces A: Physicochem. Eng. Aspects 220: 235/260.
Triton-Technology (2003). Dynamic Mechanical Analysis Seminar Workshop Handout.

Tromp H, R., R. Parker, S. G. Ring (1997). "Water diffusion in glasses of carbohydrates." Carbohydrate Research 303: 199-205.

Valles, B. (2000). Hydration-Induced Textural Changes in Cereal Products. Division of Food Sciences. Nottingham, The University of Nottingham: 207.

Van den berg, C. (1981). Vapour sorption equilibria and other water starch interaction. Wageningen Agricultural University.

Van den Berg, C. (1985). Developement of BET-like models for sorption of water on foods, theory and relevance. Properties of Water in Foods. N. A. Series.

Van den Berg, C. (1991). Food-Water Relations: Progress and Integration, Comments and Thoughts. Water Relations in Foods. L. Slade and H. Levin. New York, Plenum Press: 21-28.

Van den Berg, C. and S. Bruin (1981). Water Activity and its Estimation in Food Systems:Theoretical Aspects. Water Activity: Influences on Food Quality. L. B. Rockland and G. F. Stewart. London, UK, Academic Press: 1-60.

Van Lengerich, B. (1990). Influence of extrusion processing on in-line rheological behaviour, structure and function of wheat starch. In "Dough Rheology and Baked Product Texture" (H. Faridi and J. Faubion, eds.), pp. 421-472. Van Nostrand Reinhold, New York.

Van Soest, J. J. G. and J. F. G. Vliegenthart (1997). "Crystallinity in starch plastics: consequences for material properties." Trends in Biotechnology 19: 208-213.

Van Soest , J. J. G., and Vliegenthart , J. F. G. (1997). Crystallinity in starch plastics: consequences for material properties. Trends in Biotechnology 19, 208-213.

Van Soest and N. Knooren (1997). "Influence of glycerol and water content on the structure and properties of extruded starch plastic sheets during aging." Journal of Applied Polymer Science 64: 1411-1422.

Van Soest, and N. Knooren (1997). Influence of glycerol and water content on the structure and properties of extruded starch plastic sheets during aging. Journal of Applied Polymer Science 64, 1411-1422.

Van Soest, J. J. G., D. de Wit, H. Tournois and J. F. G. Vliegenthart (1994). "The influence of glycerol on structural changes in waxy maize starch as studied by Fourier transform infra-red spectroscopy." Polymer 35: 4722-4727.

Van Soest, J. J. G., D. De Wit and J. F. G. Vliegenthart (1996). "Mechanical properties of thermoplastic waxy maize starch." Journal of Applied Polymer Science 61: 1927-1937.

Vora, K. L., G. Buckon and D. Clapham (2004). "The Use of Dynamic Vapour Sorption and Near Infra-Red Spectroscopy (DVS-NIR) to Study the Crystal Transition of Theophylline And The Report Of A New Solid-State Transition." European Journal of Phamaceutical Sciences 22: 97-105.

Vrentas, J. S. and J. L. Duda (1977). "Diffusion in Polymer-Solvent Systems. III. Construction of Deborah Number Diagrams." Journal of Polymer Science Physics Edition. 15: 441-4453.

Waigh, T. A., M. J. Gidley, B. U. Komanshek and A.M. Donald (2000). "The phase transformations in starch during gelatinisation: a liquid crystalline approach." Carbohydrate Research 328: 165-176.

Walker, P. M. B., ed. (1995). "Larousse Dictionary of Science and Technology." Larousse.

Ward, I. M., and Hardly, D. W. (1993). "An introduction to the Mechanical Properties of Solid Polymers," John Wiley & Sons, England

.

Wetton, R. A. (1986). Theory, Practice and Application of Dynamic Mechanical Analysis.

Wetton, R. b. (1986). Dynamic Mechanical Thermal Analysis of Polymers and Related Systems. Development in Polymer Characterisation - 5. J. Dawkins, V, Elsevier Applied Science Publishers.

William, M. L., R. F. Landen and J. D. Ferry. (1955). "The temperature dependence of the relaxation mechanism in amorphous polymers and other glass forming liquids." Journal of American Chemical Society 77: 3701-.

Zeleznak, K. J. and R. C. Hoseney (1987). "The glass transition in Starch." Cereal Chemistry 64: 121.